The design and operation of a membrane photobioreactor using *Rhodopseudomonas palustris* for simultaneous wastewater treatment and biohydrogen production

by

Christi Gepke Kriek

Thesis presented in partial fulfilment

of the requirements for the Degree

of

MASTER OF ENGINEERING

(CHEMICAL ENGINEERING)

in the Faculty of Engineering

at Stellenbosch University

The financial assistance of the Water Research Commission (WRC) towards this research is hereby acknowledged. Opinions expressed and conclusions arrived at, are those of the author and are not necessarily to be attributed to the WRC.

Supervisor

Professor RWM Pott

Co-Supervisor

Professor VL Pillay

April 2022

DECLARATION

By submitting this thesis electronically, I declare that the entirety of the work contained therein is my own, original work, that I am the sole author thereof (save to the extent explicitly otherwise stated), that reproduction and publication thereof by Stellenbosch University will not infringe any third party rights and that I have not previously in its entirety or in part submitted it for obtaining any qualification.

Date: April 2022

AKNOWLEDGEMENTS

I would foremost like to thank my husband, my parents, siblings and friends for their unfailing support and encouragements during this period.

I would also like to thank Professor Robbie Pott and Professor Lingam Pillay, for support, guidance, and critical discussions during the course of my degree. Your support was invaluable in my development as an engineer.

Lastly, I would like to thank my fellow researchers. I could always count on your advice, support, and jokes in the lab, the last two years wouldn't have been the same without you.

ABSTRACT

Biological hydrogen production has significant potential as a replacement for current hydrogen production methods employed in the industry, although stumbling blocks remain, such as economic viability and environmental sustainability. A promising photosynthetic bacterium named *Rhodopseudomonas palustris* (*R. palustris*) has been demonstrated to produce biological hydrogen via photofermentation under certain growth conditions. Additionally, the organism is able to use wastewater components to fuel its hydrogen production metabolism, allowing for the potential integration of hydrogen production and wastewater treatment.

While some systems have been designed for the implementation of *R. palustris* as a method of waste valorisation in wastewater treatment systems with the added goal of biological hydrogen production, there is still much work needed investigating optimal reactor configurations to achieve this. In this project the use of a membrane photobioreactor (MPBR), as a method to separate the hydraulic and solids retention time of the photofermentative system, was investigated for use as waste valorisation for the treatment of glycerol-rich wastewater and simultaneous hydrogen production.

The goal of this study was to investigate the performance of the MPBR in both batch and continuous mode operations. The important investigated parameters for this study were: biomass concentration, glycerol conversion and biohydrogen production. Additionally, due to anticipated significant physical factors in the membrane system a 'pathology map', was constructed to determine the effe6cts of shear, temperature, nutrient limitations, and pressure on the bacterial cells.

The pathology map was developed using scanning electron microscopy (SEM) and flow cytometry (FCM), and it was observed that pressure, shear stress and elevated temperatures had significant effects on cell integrity, as visually observed by SEM, and supported by the percentage of cells reported alive in the cultures by FCM. It was also observed in this investigation that the time that the cells were exposed to each physical factor also had a significant effect on the cellular integrity, which was a concerning result as the cultures were simultaneously subjected to these conditions for extended periods of time in the MPBR.

The design and build of the MPBR was successfully conducted to ensure system sterility and sustainable use of the membrane during system setup and operation. The batch mode operation of the MPBR resulted in good bacterial growth with a final glycerol conversion of ~88% although with only 106±29.06mL cumulative hydrogen production over 240hours, which compared poorly to literature, for similar operational conditions. Poor hydrogen production may be attributable to photo-limitation, stress conditions on the cells or a combination of the two. Continuous mode operation of the MPBR was unsuccessful due to the limitations of the reactor fabrication and operation.

In conclusion, the MPBR was successful in displaying growth and glycerol conversion efficiency in batch mode operation. Although poor hydrogen production rates indicate that this reactor configuration is likely to not be the ideal one for use in photofermentative hydrogen production. As the continuous mode operation of the MPBR was unsuccessful in this investigation, the industrial application of this process requires further refinement, should work in this area continue.

OPSOMMING

Biologiese waterstofproduksie het beduidende potensiaal as ’n plaasvervanger vir huidige waterstofproduksiemetodes gebruik in die industrie, al is daar struikelblokke soos ekonomiese lewensvatbaarheid en omgewingsvolhoubaarheid. ’n Belowende fotosintetiese bakterium byname *Rhodopseudomonas palustris* (*R. palustris*) het al gedemonstreer dat dit biologiese waterstof via fotofermentasie onder seker groeikondisies produseer. Daarby, kan die organisme afvalwaterkomponente gebruik om sy waterstofproduksiemetabolisme aan te dryf, wat die potensiële integrasie van waterstofproduksie en afvalwaterbehandeling toelaat.

Terwyl sommige sisteme ontwerp is vir die implementasie van *R. palustris* as ’n metode van afvalvalorisasie in afvalwaterbehandelingsisteme met die toegevoegde doel van biologiese waterstofproduksie, is daar steeds baie werk aangaande ondersoek van optimale reaktorkonfigurasies benodig, om hierdie te bereik. In hierdie projek is die gebruik van ’n membraanfotobioreaktor (MPBR) as ’n metode om die hidroulise en vaste stowwe se retensietyd van die fotofermentatiewe sisteem te skei, ondersoek vir gebruik as afvalvalorisasie vir die behandeling van gliserolryke afvalwater en gelyktydige waterstofproduksie.

Die doel van hierdie studie was om die doeltreffendheid van die MPBR in beide lot- en deurlopende wyse bedrywe te ondersoek. Die belangrike parameters ondersoek vir hierdie studie was: biomassakonsentrasie, gliserolomsetting en biowaterstofproduksie. Boonop, as gevolg van die beduidende fisiese faktore in die membraansisteem, is ’n ‘patologiekaart’ gebou om die effek van skuifkrag, temperatuur, nutriënbeperkinge, en druk op die bakteriese selle, te bepaal.

Die patologiekaart is ontwikkel deur skandeerelektronmikroskopie (SEM) en vloeisitometrie (FCM) en dis waargeneem dat druk, skuifspanning en verhoogde temperature beduidende effekte op selintegriteit gehad het, soos visueel waargeneem deur SEM en ondersteun deur die persentasie van selle as lewendig in die kulture deur FCM gerapporteer. Dit is ook waargeneem in hierdie ondersoek dat die tyd wat die selle aan elke fisiese faktor blootgestel is, ’n beduidende effek op sellulêre integriteit gehad het, wat ’n kommerwekkende resultaat was omdat die kulture gelyktydig aan hierdie kondisies blootgestel was vir uitgerekte tye in die MPBR.

Die ontwerp en bou van die MPBR is suksesvol uitgevoer om sisteemsteriliteit en volhoubare gebruik van die membraan gedurende sisteemopstel en -bedryf te verseker. Die lotwysebedryf van die MPBR het in goeie bakteriële groei ontwikkel met ’n finale gliserolomsetting van ~88%, hoewel met slegs 106 29.06 mL kumulatiewe waterstofproduksie oor 240 ure, wat swak vergelyk met literatuur vir soortgelyke bedryfskondisies. Swak waterstofproduksie kan toegeskryf word aan fotobeperkinge, streskondisies op die selle of ’n kombinasie van die twee. Aanhoudende wyse van bedryf van die MPBR was onsuksesvol as gevolg van die beperkinge van die reaktorfabrikasie en bedryf.

Ter slotte, die MPBR was suksesvol om groei en gliserolomsettingdoeltreffendheid in lotwysebedryf ten toon te stel. Hoewel, swak waterstofproduksietempo's dui aan dat hierdie reaktorkonfigurasie nie die ideale een vir gebruik in fotofermentatiewe waterstofproduksie is nie. Omdat die aanhoudende wyse van bedryf van die MPBR onsuksesvol in hierdie ondersoek was, het die industriële toepassing van hierdie proses verdere verfyning nodig, sou werk in hierdie area aangaan.

TABLE OF CONTENTS

LIST OF FIGURES

LIST OF TABLES

NOMENCLATURE

Symbols		
a	Area	m^2
G	Velocity gradient	1/s
I	Thickness	mm
n	Biomass concentration	g/L
N	Mass velocity	kg/m.s
P	Pressure	Pa
V	Volume	m^3
Greek symbols		
Δ	Change	-
$\in$	Voidage	-
μ	Viscosity	Pa.s
ρ	Density	kg/m^3
Subscripts and superscripts		
M	Membrane	
Acronyms		
ANOVA	Analysis of variance	
ATP	Adenosine triphosphate	
ATPase	ATP synthase	
ATR	Autothermal reforming	
BChl-α	Bacteriochlorophyll-α	
CBB	Calvin-Benson-Bassham	
CDW	Cell dry weight	
FCM	Flow cytometry	
GC	Gas chromatograph	
GLA	Glutaraldehyde	
HPLC	High-performance liquid chromatography	
HRT	Hydraulic retention time	
Hup	Hydrogenase	
IPCC	Intergovernmental Panel on Climate Change	
MF	Microfiltration	
MPBR	Membrane photobioreactor	
NF	Nanofiltration	

N_2ase	Nitrogenase
NADP	Nicotinamide adenine dinucleotide phosphate
OD	Optical density
OFAT	One-factor-at-a-time
PNSB	Purple non-sulfur bacteria
POX	Partial Oxidation
RC	Reaction centre
RO	Reverse osmosis
SEM	Scanning electron microscopy
STEM	Scanning transmission electron microscopy
SR	Steam reforming
TCA	Tricarboxylic
UF	Ultrafiltration
VFA	Volatile fatty acid

1 INTRODUCTION

Global warming and the energy crisis are two concerning threats to humanity today; global warming is a result of the excessive burning of fossil fuels for both transportation and electricity generation. Today, the global energy infrastructure is highly dependent on fossil fuels which has resulted in an increase in global temperature, ocean acidification, and disruption of natural system. Due to these shortcomings, there has been an international move towards more renewable energy options. Despite this, no distinct viable solution has been provided to curb the effects of the shortcomings of the current energy cycle. The only solution would be to adopt an energy cycle that is both clean and carbon-neutral; this is essential to ensure sustainable energy usage and generation in the future (Mazloomi and Gomes, 2012).

Some renewable energy technologies that have been applied to the energy sector are biomass energy, geothermal energy, solar power, wind energy, and hydropower. However, due to unpredictable environmental conditions like sun or wind, as well as a lack of the required infrastructure or funding, these renewable energy sources have only been able to generate a minority of 11% of the energy supply (*Sources of energy - U.S. Energy Information Administration (EIA)*, no date).

As a solution to both the energy crisis and global warming, hydrogen is strong contender as an alternative to fossil fuels, as it is a promising energy carrier or fuel source due to excellent energy storage properties and high energy density. Energy density is a measure of the amount of energy that is stored per unit of volume, hydrogen has an energy density of 120MJ/kg in comparison to coal which has about 24 MJ/kg(Vezirocjlu and Barbir, 1992). However, using hydrogen as an energy carrier was first actively considered only after the global energy crisis of 1973; after the energy crisis, it was realized that the fossil fuels being used to generate energy for fuel and electricity are only available in finite amounts and an alternative energy source must be developed (Vezirocjlu and Barbir, 1992). In addition to this, Vezirocjlu and Barbir (1992) stated that hydrogen is considered to be “the best transportation fuel, the most versatile fuel, the most efficient fuel, the environmentally most compatible fuel, the safest fuel, and the most cost-effective fuel to society”.

Waste valorisation is the process of using organic waste materials and through processing turning this waste into a useful final product such as energy or chemicals that can be used in industrial processes (Kabongo, 2013). The application of waste valorisation in industry would be an ideal application to curb global warming and simultaneously provide energy.

Renewable methods of hydrogen production today include thermo-chemical hydrogen production, water splitting using renewable energy or biological hydrogen production. In the latter, organic matter is degraded by biomass to produce hydrogen. A promising organism for biological hydrogen production was identified to be a genetically modified photosynthetic bacterium named *Rhodopseudomonas palustris (R. palustris).* This robust organism has the ability to produce hydrogen from a variety of organic sources and can grow in a variety of operating conditions. The particular advantage of this organism is to produce this valuable biohydrogen from an identified industrial

wastewater stream, specifically a glycerol-rich wastewater stream identified in biodiesel production. Hence contributing to the valorisation of this wastewater stream.

R. palustris has been widely studied in the literature and characterized in laboratory batch cultures as a source of biological hydrogen. As the next stage in this investigation, suitable continuous bioreactors must be developed to upscale the usefulness of this technology. A new proposition in this field is the use of a membrane bioreactor, where the membrane is used continuously to retain biomass in the system as the wastewater is continuously treated. Membrane bioreactors have demonstrated several advantages in other applications although for this photosynthetic organism, very little has been reported.

Hence, in this investigation the focus lies on developing and evaluating a membrane bioreactor that can be used for waste valorisation to generate a reliable source of hydrogen energy and provide a new alternative for wastewater treatment. Specifically, the aim of the investigation was to develop a membrane photobioreactor that could operate both during batch and continuous mode operation and observing the resulting hydrogen production, substrate utilisation and cell growth for the investigative period.

1.1 Motivation for research

The aim of this investigation was to develop technology that serves as a possible source of renewable energy, in order to reduce the need for fossil fuels resulting in cleaner emissions and a more energy-secure future. The motivation for this research stems from observing the lack of literature on the use of membrane bioreactor to continuously produce biohydrogen, as a renewable energy source, by valorisation of an organic wastewater stream. As a method to attain this a membrane bioreactor was identified as a possible method to retain *R. palustris* biomass and continuously treat a glycerol-rich wastewater stream and simultaneously deliver a source of renewable energy.

1.2 Thesis Overview

Chapter 2, Literature review, is a summation of what has been found in the literature to develop understanding of *Rhodopseudomonas palustris* and identify the gaps in the literature that formed the basis of this study.

Chapter 3, Research scope, is the aims and objectives of this study, stemming from the gaps in the literature identified in Chapter 2. Key questions are identified to answer the objectives set by this study.

Chapter 4, Methodology, is a description of the experimental research that was conducted for this study. In this chapter, the specific materials and methods used are discussed that were required to achieve the set objectives and key questions from Chapter 3.

Chapter 5, Results and discussion, a detailed discussion of the experimental results and the implications they provide. A pathology map of *R. palustris* is provided and discussed along with reactor design choices and the observed performance of the bacteria in a batch and continuous mode

membrane photobioreactors. The performance of the culture is measured by observing growth, substrate utilisation and hydrogen production parameters.

Chapter 6, Conclusions, brings together the objectives of this investigation along with the summarized conclusions from the experimental investigation.

Chapter 7, Recommendations, outlines some recommendations for future work that can stem from this work and the intended contributions to the literature.

2 LITERATURE REVIEW

2.1 Energy production and global climate change

With an increasing population comes a greater demand for energy. According to Kumar Khanal et al., (2008), the energy demand is expected to increase by 50% by the end of 2025. Kumar Khanal et al., (2008) also mentions that the energy consumption in developing countries will increase by over 90% at the same time due to industrialisation. This means that with dwindling energy reserves in the fossil fuel sector in combination with the damaging effects of global climate change, the future of energy security is looking rather inauspicious. The effects of climate change have even been perceived to take a toll on the fossil fuel sector; due to increased extreme weather conditions that further increase energy sector costs, global climate change has started to significantly affect transportation of energy and infrastructure within the energy sector according to Schaeffer *et al.*, (2011).

2.1.1 Current energy practices

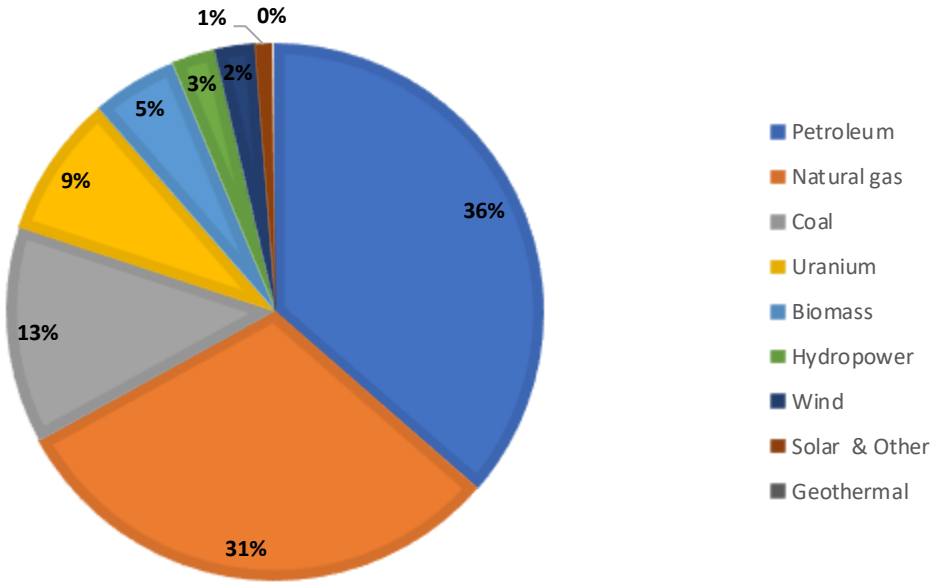

Figure 1: A pie chart displaying the source of energy worldwide. Figure adapted from Sources of energy - U.S. Energy Information Administration (EIA) (n.d.).s

From Figure 1, it can be seen that only roughly 11.3% of the energy produced can be considered a renewable energy from a renewable energy source. In comparison to the non-renewable sources such as petroleum, natural gas and coal make up roughly 88.7% of the energy worldwide. When these fossil fuels are combusted, carbon dioxide is released into the environment; this has been identified as the leading cause of global climate change. The abundant emission of anthropogenic greenhouse gasses poses a threat to not only the environment but the human race itself.

2.1.2 Challenges with current practices

The Intergovernmental Panel on Climate Change (IPCC), states that the net damage costs of global climate change will be momentous, and the cost thereof will increase over time as the extent of climate change on earth is observed. Global climate change results in disruption of natural systems, ocean acidification, global temperature increase, etc. The IPCC also estimates that the global temperature has increased by approximately 0.74°C over the last 100 years (IPCC, 2001). The increase in global temperature has catastrophic consequences on natural habitats and ecosystems such as coral bleaching, ice caps melting and species extinction due to habitat loss. According to McMichael (2013), the effect of global climate change poses a significant threat to global food security due to the negate effects of climate change on the agriculture sector. Global temperatures are expected to increase by 3 to 4°C by 2100, solely due to anthropogenic emissions (McMichael, 2013).

2.1.3 Alternative energy sources

The answer to this would be a sustainable energy source, being defined as a source of energy that is not depleted with continued use and does not results in significant emissions and other environmental threats (Baykara, 2018). The need for a reliable renewable energy source is thus highlighted in recent global warming events, to lower emissions and provide a more secure future. Multiple renewable energy solutions have been provided and investigated although fossil fuels still remain the primary source of energy production in the energy sector. Multiple studies have discussed the aspects of using hydrogen technology and provide rationale for hydrogen energy systems (Baykara, 2018). Thus from an investigative point of view, hydrogen is seen as part of the answer to the energy crisis, due to its' high energy density and is considered to be a clean fuel source (Vezirocjlu and Barbir, 1992), the only stumbling blocks that remain is the industrial application of this technology.

2.2 Hydrogen as an energy source

2.2.1 Overview of hydrogen as an energy source

As discussed in section 1, hydrogen is seen as one of the most promising fuels of the future. However, for hydrogen energy to be utilised for both energy generation and transportation, significant changes in infrastructure need to occur. When hydrogen is combusted, the hydrogen reacts with oxygen to form water with sudden energy release as seen in Equation 1 below.

$$2H_2 + O_2 \rightarrow 2H_2O + Energy \qquad [1]$$

This is the case if hydrogen is combusted with pure oxygen, although if this is carried out in atmospheric air, the reaction yields minor amounts of various nitrogen oxides as displayed in Equation 2 below. This would mean that the resulting hydrogen gas yield would be lower than desired for this application.

$$H_2 + O_2 + N_2 \rightarrow H_2O + NO_X + N_2 + Energy \qquad [2]$$

Because the eventual goal of applying hydrogen fuel technology is to minimize harmful emissions, modern engines often make use of exhaust gas recirculation to reduce nitrogen oxide emissions to only trace amounts and make hydrogen energy practically emission free (Heffel, 2003).

2.2.2 Hydrogen fuel cell

A fuel cell is an electrochemical cell that converts the chemical energy of hydrogen and an oxidising agent into electricity by means of a pair of redox reactions (Sarangi, Nanda and Mohanty, 2018). The use hydrogen fuel cells are a critical part of energy security and sustainable development; fuel cells provide a clean and efficient mechanism for energy conversion. Fuel cells operate in a static manner meaning no noise or vibrations are present while the fuel cell is operating. This also means that these fuel cells are more efficient, cleaner and can be used in a variety of transport or power generation applications (Sharaf and Orhan, 2014). Sharaf and Orhan (2014) also mention that if a fuel cell is operated using pure hydrogen, rather than with reformation-based hydrogen (reformation-based hydrogen contains CO_x), the fuel cell is significantly more durable and reliable. In Table 1 below, some fuel cell types that are operated using hydrogen are mentioned.

Table 1: Typical fuel cells that utilize hydrogen as a fuel with some key characteristics (Sharaf and Orhan, 2014)

Fuel cell type	Typical anode/cathode catalysts	Major contaminants	Advantages	Disadvantages
Low-temperature proton exchange membrane	Platinum supported on carbon (anode & cathode)	Carbon monoxide and hydrogen sulphide	High power density & compact structure	Sensitive to contaminants & expensive catalysts
High-temperature proton exchange membrane	Platinum-Ruthenium supported on carbon (anode & cathode)	Carbon monoxide	High tolerance to contaminants & simple water and heat management	Accelerated degradation & expensive catalysts
Phosphoric acid	Platinum supported on carbon (anode & cathode)	Carbon dioxide	Reliable technology & good tolerance to contaminants	Low power density & expensive catalysts
Alkaline	Nickel (anode) & silver supported on carbon (cathode)	Carbon monoxide	Wide range of operation & relatively low costs (including inexpensive catalysts)	Pure hydrogen and oxygen required for operation & extremely high sensitivity to contaminants

From this table a major drawback to fuel cell technology can be deduced, it's very expensive. Contaminants from reformation-based hydrogen degrade the catalysts in the fuel cell and catalysts are one of the most expensive parts to the fuel cell itself. Although as the industry develops, costs of these fuel cells can decrease with an increase in the required infrastructure; development of these technologies have the potential to significantly cut global emissions and lead to a more secure future for the energy sector (Sharaf and Orhan, 2014).

An attractive characteristic of the considered organism in this investigation is the purity of hydrogen gas produced. From du Toit and Pott (2021) it was observed that the hydrogen gas was composed of roughly ~96% with the remainder carbon dioxide, which would mean that this gas is unlikely to poison the catalyst in a fuel cell making this an attractive source of energy.

2.2.3 Hydrogen production methods

Hydrogen is the most abundant chemical element in the universe, although pure hydrogen in scarce on the Earth's surface and in the atmosphere (Kalamaras *et al.*, 2013; Baykara, 2018). Hydrogen energy can be used as a replacement for fossil fuels which would result in decreased carbon emissions and delay the estimated effects of global warming on earth. Thus, hydrogen has the promise of being both environmentally friendly and being a sustainable energy source. However, this is entirely dependent on the initial source of hydrogen in question. Hydrogen is an attractive energy source due to a high energy density and an increased efficiency in conversion to usable power (Hallenbeck and Ghosh, 2009). Hydrogen is currently being produced in both a non-renewable manner (using fossil fuels) or other renewable (mostly biological) processes.

Currently, the majority of hydrogen gas is produced from the fossil fuel sector with sources such as coal, oil and natural gas. According to Department of Energy USA (2020), 95% of hydrogen energy currently being produced in the USA is made by natural gas reforming. With the reforming of fossil fuels the major issue is the emission of carbon dioxide and despite hydrogen being a clean, carbon emissions are just shifted upstream to the production of hydrogen. As discussed in Section 2.1, the need for renewable energy is immense, to meet the energy demand and simultaneously to curb carbon emissions and halt global climate change. This section discusses the production of hydrogen as a solution to the renewable energy requirement.

2.2.3.1 Non-renewable hydrogen production

Non-renewable hydrogen is obtained from fossil fuels that contain abundant hydrogen such as coal, natural gas, alcohols, and hydrocarbons. Through fossil fuel processing technologies, as named in Figure 2 below, a hydrogen-rich gas can be produced (Kalamaras *et al.*, 2013). Currently, the most inexpensive and the most utilised methods of hydrogen production are steam reforming (SR), partial oxidation (POX) and autothermal reforming (ATR) (Kalamaras *et al.*, 2013).

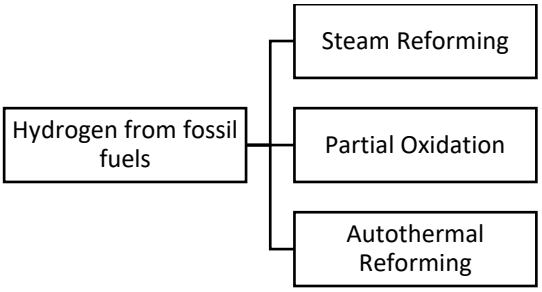

Figure 2: Breakdown of methods used for hydrogen production from fossil fuels. Figure adapted from Kalamaras et al. (2013).

Fossil fuels all contain sulphur, which means that for each of these production methods, significant downstream processing is required. Hydrogen and sulphur in the product gas stream can react to from hydrogen sulphide which is a corrosive and poisonous gas. Thus, to remove sulphur from the product gas mixture, desulphurisation technologies are required. Anoteher downside of fossil fuel processing technology is the production of poisonous carbon monoxide (CO) gas alongside hydrogen in the product gas stream. Thus, to further purify the gas stream, the water-gas shift reaction is used to convert CO to the inert carbon dioxide (CO_2).

As mentioned in section 2.3.2, this is why using fossil fuels to produce hydrogen does not eliminate greenhouse gas emissions but simply shifts the production downstream to hydrogen production. With renewable energy there is limited treatment necessary as the hydrogen gas is already a relatively pure product. The absence of sulphur is another benefit of using renewable energy, no desulphurisation technology is required, and no greenhouse gasses are emitted.

2.2.3.2 Renewable hydrogen production

From what has been mentioned in previous sections, the need for renewable energy is immense. Due to the high energy density of hydrogen, this seems like an obvious energy source to focus on, although with a renewable perspective. Current methods for renewable hydrogen production will be discussed in this section with a focus on biological hydrogen production in agreement with the aim of this investigation. This is because *R. palustris* is a PNSB which uses photofermentation to produce hydrogen. In the figure below, various methods of renewable hydrogen production are shown. Below in Figure 3, renewable methods for hydrogen production are mentioned and in Table 2 the main advantages and drawbacks of these methods are discussed.

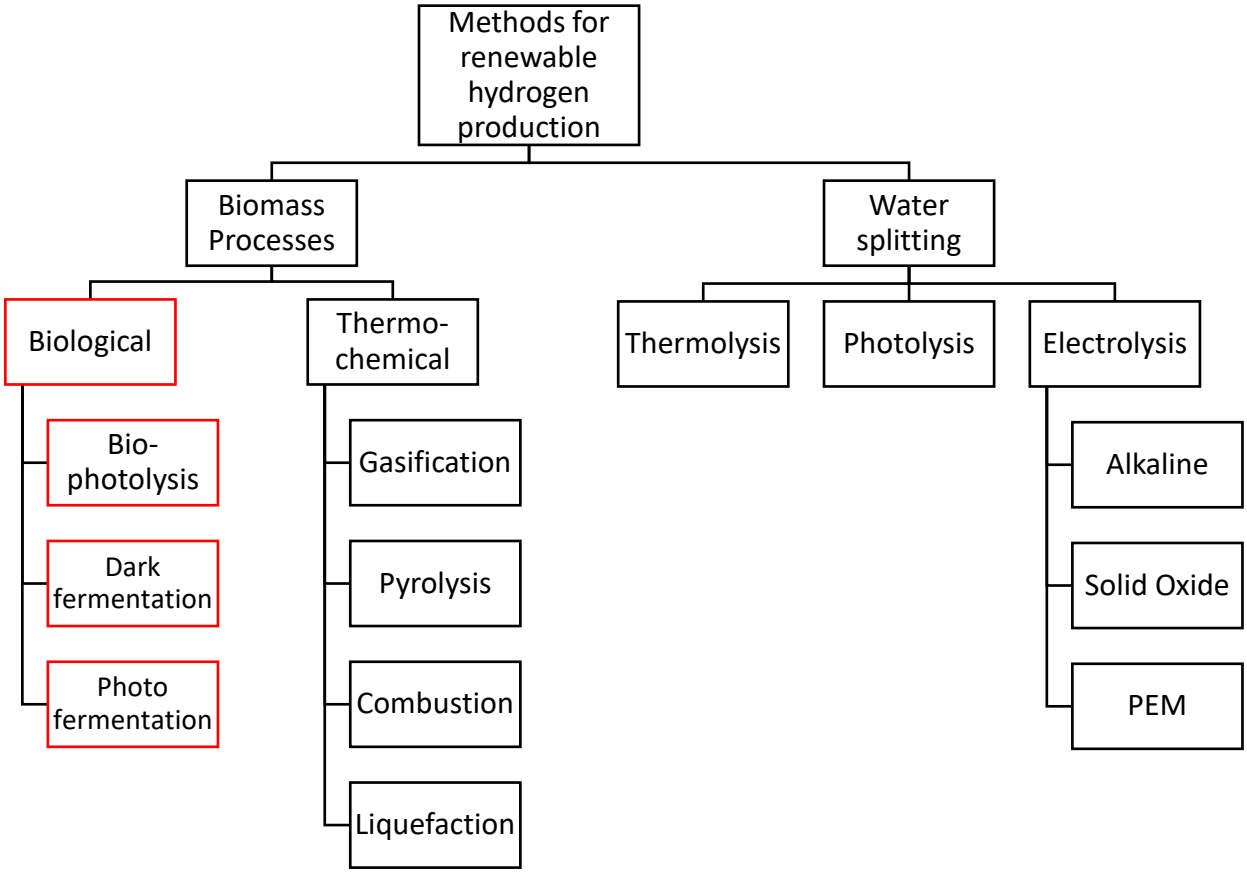

Figure 3: Renewable hydrogen production methods. Figure adapted from (Shiva Kumar and Himabindu, 2019)

Table 2: A list of renewable hydrogen sources with main advantages and disadvantages (Hallenbeck and Ghosh, 2009; Shiva Kumar and Himabindu, 2019)

Renewable hydrogen source	Advantages	Disadvantages
Direct biophotolysis	Water (abundant) as a substrate and produces only H_2 and CO_2.	Light conversion efficiency is low, hydrogenase is oxygen-sensitive and expensive photobioreactors are required (hydrogen impermeable).
Dark fermentation	No direct sunlight required, a variety of waste stream or energy crops can be used, and simple bioreactor technology is required.	Does not result in good H_2 yield and a large quantity of by-products are formed.

Renewable hydrogen source	Advantages	Disadvantages
Photo fermentation	Organic waste has a high conversion efficiency to H_2 and CO_2 (high substrate conversion efficiency). Technology can be used in wastewater treatment.	Light conversion efficiency is low, nitrogenase enzyme has a high energy demand and hydrogen impermeable photobioreactors are required (expensive).
Gasification	Abundant waste streams from municipality or animal waste as a feedstock.	Fluctuating H_2 production due to fluctuations of substrate in waste stream, seasonal availability, presence of feedstock impurities and formation of tar. Some emission of CO_2.
Pyrolysis	Abundant waste streams from municipality or animal waste as a feedstock. CO_2-neutral.	Fluctuating H_2 production due to fluctuations of substrate in waste stream, seasonal availability, presence of feedstock impurities and formation of tar.
Thermolysis	Clean and sustainable with O_2 as a by-product. Abundant feedstock.	High capital costs due to toxicity of elements. Corrosion occurs in the system.
Photolysis	Clean and sustainable with O_2 as a by-product. Feedstock is abundantly available and no sulphur emissions.	Low efficiency, requires sunlight and non-effective photocatalytic material.
Electrolysis	No sulphur emissions, O_2 as a by-product, infrastructure is already in place and technology has been established.	Storage and transportation issues and capital cost is very high (almost 25 times higher than current fossil fuel technologies)

There are three different methods for biological hydrogen production: direct bio-photolysis, dark fermentation and photofermentation (Hallenbeck and Ghosh, 2009; Shiva Kumar and Himabindu, 2019). In each of these processes the nitrogenase and hydrogenase enzymes within the bacterium are utilized for hydrogen production using energy produced by the cell from either light or carbon energy sources. The process of hydrogen production by these enzymes is discussed in further detail in Section 2.3.3.1 . The three different methods for biological hydrogen production are discussed in the following subsections.

a) Direct bio-photolysis

Direct bio-photolysis is the process in which an organism photosynthesizes (plant-type photosynthesis) using captured solar energy to produce hydrogen. Organisms that utilize direct bio-photolysis for hydrogen production include photosynthetic green algae or cyanobacteria; these organisms obtain their energy through photosynthesis (Hallenbeck and Ghosh, 2009). These organisms have the ability to split water molecules, which act as a substrate, using captured solar energy to release oxygen and captured electrons; released protons are then used by the organism for the production of adenosine triphosphate (ATP). The electrons, derived from oxidation of organic substrates, then reduce ferredoxin and nicotinamide adenine dinucleotide phosphate ($NADP^+$) to result in NADPH; the presence of the hydrogenase enzyme in some these organisms catalyses the reduced products and ATP to result in hydrogen gas (Hallenbeck and Ghosh, 2009; Lee, Vermaas and Rittmann, 2010).

Direct bio-photolysis is considered to be such an attractive method of hydrogen production because the energy production cycle does not involve carbon. When looking at the net reaction of direct bio-photolysis, it indicates the simple conversion of water into oxygen and hydrogen gas, using the most renewable energy source at our exposal, solar energy (Lee, Vermaas and Rittmann, 2010). Some of the biggest challenges of using direct bio-photolysis are low light conversion efficiencies and the presence of oxygen; the hydrogenase enzyme is sensitive to the presence of oxygen and the enzyme is deactivated at low concentrations of oxygen (Kim and Kim, 2011). From an evolutionary viewpoint, this reaction makes sense because it would be counter-productive for the cells to utilize valuable reducing equivalents for production of hydrogen rather than ATP (Lee, Vermaas and Rittmann, 2010).

b) Dark fermentation

Dark fermentation is a process where microbes anaerobically utilize substrates that are rich in carbohydrates to produce hydrogen and other by-products, mostly acids (butyric, acetic, lactic, etc.) and alcohols (butanol, ethanol, etc.) in the absence of light. For dark fermentation, a variety of microbes can be used, although product distribution will differ with each microbe depending on the fermentation pathway (Levin, Pitt and Love, 2004). Product distribution can also differ due to the oxidation state of the substrate and environmental conditions such as pH or hydrogen partial pressure (Hallenbeck and Ghosh, 2009). A benefit of using dark fermentation for hydrogen production is the wide variety of organic material that can be used as a substrate: municipal waste, food waste, cellulose etc. In dark fermentation, the organic substrate acts as an electron donor to reduce pyruvate-ferredoxin-hydrogenase or pyruvate-formate lyase to produce hydrogen (Lee, Vermaas and Rittmann, 2010).

Hydrogen production is also influenced by the by-products formed by different microbes. According to Levin, Pitt and Love (2004), the highest theoretical yields of hydrogen were achieved with microbes that result in acetate as the fermentation end-product although high hydrogen yields have also been observed with the presence of acetate and butyrate. Another critical factor for hydrogen production

is the metabolic balance of the system which is affected by factors such as: hydrogen partial pressure, pH and hydraulic retention time (HRT)(Levin, Pitt and Love, 2004). The HRT has a significant effect on the microbial growth rate thus the HRT must be longer than the maximum growth rate of the organism (Hallenbeck and Ghosh, 2009). To maximize the yield of hydrogen in the system, the metabolic activity of the microbe must be directed to reducing acids to volatile fatty acids (VFA's) rather than alcohols. (Levin, Pitt and Love, 2004)The partial pressure of hydrogen is important because the concentration of hydrogen affects hydrogen-synthesis metabolic pathways; as hydrogen concentration increases the metabolic pathways change to the production of more reduces substrates (ethanol, lactate, acetone etc.) (Levin, Pitt and Love, 2004).

Hallenbeck (2009) investigated the use of dark fermentation for the production of hydrogen using glucose and a maximum conversion efficiency of only 33% was achieved. This means that only 33% of the available electrons are utilized to produce hydrogen and the remaining electrons are utilized to produce alcohol and acid waste products. Hallenbeck (2009) then introduces the Thauer limit, explaining the limit of the chemotrophic metabolism which is the reason for these low hydrogen yields. The Thauer limit and theoretical limit of hydrogen production is displayed in Equation 3 and 4 respectively.

Thauer limit: $$C_6H_{12}O_6 + H_2O \rightarrow 4H_2 + 2CO_2 + 2CH_3COOH\ [acetate] \quad [3]$$

Theoretical limit: $$C_6H_{12}O_6 + 6H_2O \rightarrow 12H_2 + 6CO_2 \quad [4]$$

From these equations it can be seen that in practice, only 4 moles of hydrogen can be produced in comparison with the expected 12 moles as described in theory. In this case, when glucose is used as a substrate the formation of acetate inhibits hydrogen production and results in the low conversion efficiencies observed.

c) Photofermentation

Photofermentation can take place in a variety of photosynthetic bacteria; one class of photosynthetic bacteria and the focus of this investigation is the use purple non-sulphur bacteria (PNSB). PNSB photosynthesize anaerobically by using captured solar energy to produce high energy electrons and ATP; these products then reduce ferredoxin. The combination of ATP and reduced ferredoxin result in hydrogen production through proton reduction by nitrogenase (Hallenbeck and Ghosh, 2009). Organic substances are used as substrate for these organisms because they have the ability to drive electrons from water (Hallenbeck and Ghosh, 2009). The ability of this bacteria to produce hydrogen and carbon dioxide from organic waste streams, makes it a valuable method for industrial waste valorisation.

To calculate the maximum theoretical hydrogen yield via photofermentation, McKinlay *et al.* (2014) provides a reaction network for acetate (as an organic substrate). Ross (2019) developed a general reaction network that can be used to determine the maximum theoretical moles of hydrogen that can be produced for different organic substrates; the reaction network can be seen from Equation 5, 6 and 7.

$$C_mH_nO_o + (2m - o)H_2O \rightarrow mCO_2 + (4m + n - 2o)H^+ + (4m + n - 2o)e^- \quad [5]$$

$$(4m + n - 2o)H^+ + (4m + n - 2o)e^- \rightarrow \left(2m + \frac{n}{2} - o\right)H_2 \quad [6]$$

$$C_mH_nO_o + (2m - o)H_2O \rightarrow mCO_2 + \left(2m + \frac{n}{2} - o\right)H_2 \quad [7]$$

The following stoichiometric reactions compare the performance of dark fermentation and photofermentation when utilizing the same organic substrate, glycerol. It is known that with photofermentation the carbon dioxide emission will be greater when compared to dark fermentation; this is because acids and alcohols are formed during dark fermentation. The stoichiometric reactions for dark fermentation and photofermentation are displayed in Equations 8 and 9.

Photofermentation: $$C_3H_8O_3 + 3H_2O \rightarrow 3CO_2 + 7H_2 \quad [8]$$

Dark fermentation: $$C_3H_8O_3 + H_2O \rightarrow CH_3COOH\ (acetic\ acid) + CO_2 + 3H_2 \quad [9]$$

From these equations it can be seen that with photofermentation, an additional 4 theoretical moles of hydrogen can be produced when compared to dark fermentation. The additional hydrogen production indicates that during photofermentation, substrate utilization is more efficient which makes it a more favourable method for hydrogen production when compared to dark fermentation.

2.2.4 Practical aspects of hydrogen production

According to a blog post by S&P Global (Tom DiChristoher, 2021), hydrogen prices for reformation of natural gas is currently at about $2.40 /kg and fossil fuel-based hydrogen is around $1.80 /kg. In comparison, green hydrogen, from renewable sources, the price varies between $3 /kg and $6.55 /kg. Although the price of hydrogen sourced from renewable sources is more expensive than that of fossil fuels, the price of renewable hydrogen is becoming significantly more affordable in comparison to what the prices were in 2013 as reported by Kalamaras *et al.* (2013).

Although this price is likely to increase due to greenhouse gas emissions that must be captured and stored. Hydrogen from fossil fuels is much cheaper to produce in comparison with renewable energy sources due to the maturity of fossil fuel technology; with the development of renewable technology the dependency on fossil fuels for a reliable energy supply will decrease.

With hydrogen being such a commonplace element on earth, the feedstock for hydrogen technology is everywhere. This means that every region around the world will eventually be able to generate most of their own power with the availability of appropriate infrastructure for hydrogen production (Kalamaras *et al.*, 2013). The production of biological hydrogen is still in the introductory phases and the stumbling blocks must first be overcome before these technologies can be applied to industry.

Another major stumbling block for the application of hydrogen technology is high capital costs; hydrogen fuel cells require expensive catalysts and required infrastructure. When considering water - splitting as a source of hydrogen energy, the capital costs and energy intensity associated with these

processes is immense due to corrosive materials and high operating temperatures. The price for this source of hydrogen reaches up to $11.3/kg (Ball and Weeda, 2016). With thermochemical and biological hydrogen production, the main stumbling block is capital cost (Acar and Dincer, 2014).

Recent developments in renewable energy technology have resulted in an increase in fermentative hydrogen production with real wastewater and under real conditions hydrogen production has started to reach practical levels for implementation in industry. Although a major stumbling block remains, incomplete substrate conversion that results in low hydrogen yields (Hallenbeck and Ghosh, 2009).

2.3 Rhodopseudomonas palustris

Rhodopseudomonas palustris (*R. palustris*) is a PNSB with the ability to produce hydrogen using organic waste as a substrate, which is why this bacterium has been selected for this investigation. This organism is known for its ability to grow by any of the four metabolisms to support life: photoautotrophic, photoheterotrophic, chemoautotrophic and chemoheterotrophic (Larimer *et al.*, 2004). In the following text the taxonomy, metabolic pathways, photosystems, hydrogen production and current industrial use of *R. palustris* will be discussed.

2.3.1 Taxonomy

As mentioned previously, *R. palustris* is known for its metabolic versatility and ability to grow in various environments; this can be seen by its wide distribution in nature: marine coastal sediments, swine wastewater lagoons and earthworm droppings to name a few (Larimer *et al.*, 2004). The taxonomical classification of *R. palustris* is displayed in Table 3 below.

Table 3: Taxonomical classification of *R. palustris* (Larimer *et al.*, 2004)

Domain	Bacteria
Phylum	Proteobacteria
Class	Alphaproteobacteria
Order	Rhizobiales
Family	Bradyrhizobiaceae
Genus	*Rhodopseudomonas*
Species	*Rhodopseudomonas palustris*

R. palustris (seen in Figure 4) is a gram-negative bacteria, which is why it is classified under the order 'Rhizobiales' (Auling *et al.*, 1988). *R. palustris* Is classified under the 'Bradyrhizobiaceae' and the genus *Rhodopseudomonas*; palustris comes from the Latin word 'marsh-loving' which is understood to be a common habitat for the organism (Smith, 1963; Imhoff, Hiraishi and Süling, 2005).

Figure 4: A full, general representation of *R. palustris.* Figure and permission for use obtained from American Society for Microbiology (ASM) (Welander *et al.*, 2009).

Imhoff, Hiraishi and Süling (2005) state that the bacteria size is mostly in the range 0.6-0.9μm with a rod to ovoid shape although the shape, size and opacity of the cells can differ significantly. Whittenbury and McLee (1967) state that these differing characteristics of the cells can be useful in the identification of the species. This variety is caused by the "life cycle" of the cell; the smallest cell is the daughter (swarmer) cell that is produced during budding when released from a short tube produced by the mother cell. From this it was also observed that at division the smaller daughter cells were motile by polar flagella whereas the mother cell is immotile (Whittenbury and McLee, 1967; Imhoff, Hiraishi and Süling, 2005). The colour of the bacterial cells can also differ greatly, varying between a pink, red, brown-red and brown shade (Imhoff, Hiraishi and Süling, 2005). A diagram depicting the budding in the cell cycle can be seen in Figure 5 below.

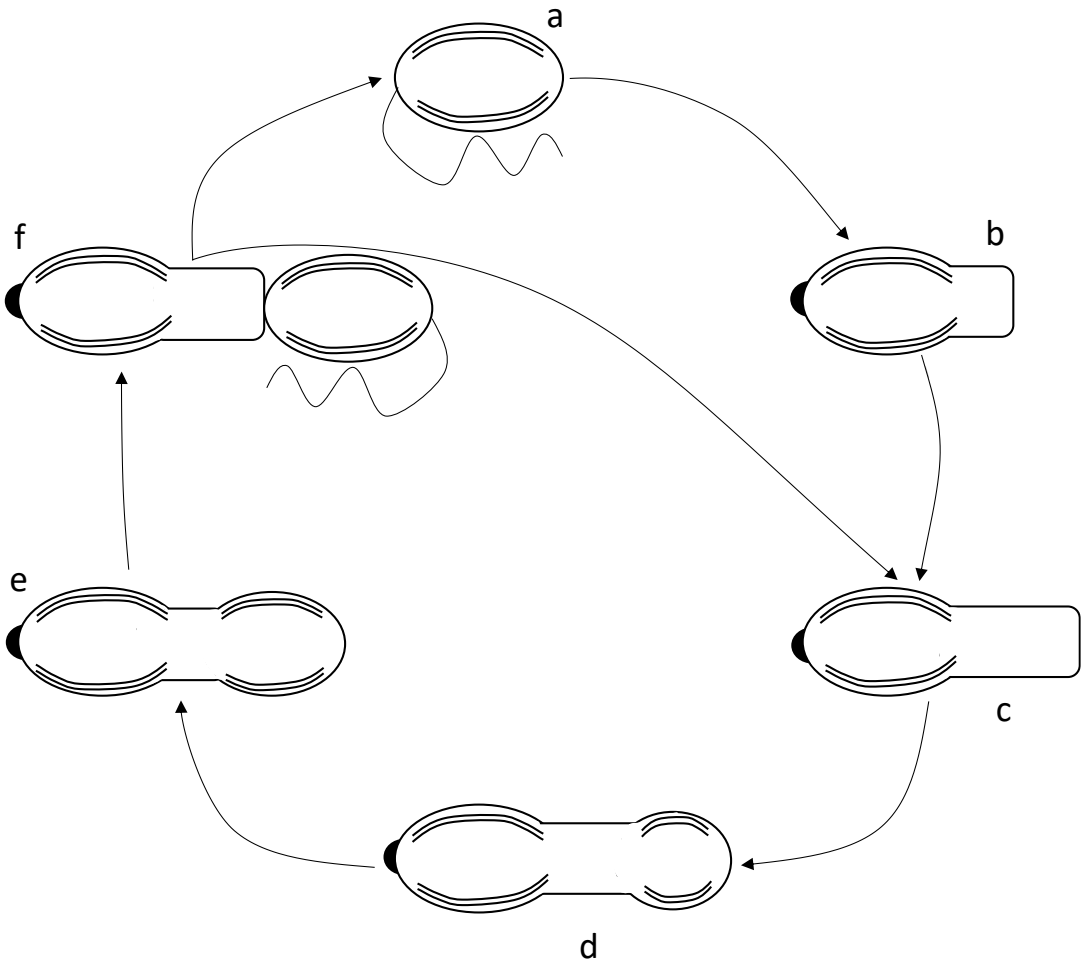

Figure 5: Developmental cycle of *R. palustris.* Figure adapted from Westmacott and Primrose (1976)

Following the process in Figure 5, at point (a), the daughter cell is displayed; from point (a) to (b) the daughter cell develops a short phase contrast-translucent tube with a blunt end which can be seen at (b,c). This tube is only slightly narrower than the original daughter cell. At point (d) of the cycle, a bud develops at the end of the tube which then increases in size to point (e) and the shape of a dumbbell can be observed. Between point (e,f), the mother cell and newly developed daughter cell are divided. The daughter cell is now motile and the mother cell that is non-motile has a sticky 'holdfast' at the opposite pole to the tube (Whittenbury and McLee, 1967; Westmacott and Primrose, 1976).

2.3.2 Metabolic pathways

As mentioned in the introduction of Section, *R. palustris* has the ability to operate within all four main metabolisms that sustain life: photoautotrophic (carbon dioxide as carbon source and energy from light), photoheterotrophic (organic compounds as carbon source and energy from light), chemoautotrophic (carbon dioxide as carbon source and energy from inorganic compounds) and chemoheterotrophic (organic compound as both carbon and energy source) (Larimer *et al.*, 2004). The different growth modes are summarised in Table 4 below.

Table 4: The four different modes of *R. palustris* growth with their main aspects (Larimer *et al.*, 2004; Pott, 2013).

Growth mode	Light source (Yes/No)	Carbon source	Energy source	Anaerobic or aerobic	Hydrogen production?
Chemoautotrophic	No	Carbon dioxide	Hydrogen, thiosulfate & inorganic compounds	Aerobic	Hydrogen consumed as an energy source
Chemoheterotrophic	No	Organic carbon	Organic carbon	Aerobic	None
Photoautotrophic	Yes	Carbon dioxide	Hydrogen, thiosulfate & inorganic compounds & light	Anaerobic	Hydrogen consumed as an energy source
Photoheterotrophic	Yes	Organic carbon	Organic carbon & light	Anaerobic	Hydrogen production in the absence of ammonia

2.3.3 R. palustris and hydrogen production

From Table 4 it was deduced that hydrogen production only takes place with *R. palustris* growth under photoheterotrophic conditions in the absence of ammonia. In this investigation, the eventual goal is the production of hydrogen using *R. palustris*. To develop a better understanding of hydrogen production from this organism, it is required to look deeper into the metabolism of hydrogen production.

2.3.3.1 Enzymes vital to hydrogen production

Nitrogenase and hydrogenase play a critical role in hydrogen production through *R. palustris*. The sum of hydrogen produced by nitrogenase, and hydrogen produced by hydrogenase is the total of hydrogen produced by *R. palustris*. The hydrogenase and nitrogenase enzymes are inhibited by the presence of oxygen; to maximize hydrogen production, *R. palustris* must grow anaerobically to ensure optimal hydrogen production (Burris, 1991; Hallenbeck and Ghosh, 2009; Shiva Kumar and Himabindu, 2019). Before the metabolism of hydrogen production in *R. palustris* is discussed, more background will be given on the two major enzymes that play a critical role in the hydrogen production process.

a) Nitrogenase

The ability of *R. palustris* to produce hydrogen is completely associated with the use of nitrogenase enzymes. The nitrogenase enzyme is best-known for its part in nitrogen fixation; the conversion of atmospheric nitrogen (N_2) into ammonia (NH_4^+) with hydrogen as a by-product of this irreversible reaction (McKinlay *et al.*, 2014); this is an energy-intensive process driven by ATP in the cell. Nitrogenase has three different isozymes, dependant on the metal cofactor; Molybdenum (Mo) is most commonly observed, although vanadium (V) and iron (Fe) are also encoded by *R. palustris* (McKinlay *et al.*, 2014). The three different isozymes are: Mo-nitrogenase, V-nitrogenase and Fe-nitrogenase. The final ATP usage and hydrogen production are dependent on the metal cofactor as can be seen in Equations 10, 11 and 12 below.

Mo-nitrogenase: $$N_2 + 8H^+ + 8e^- + 16ATP \rightarrow 2NH_3 + H_2 + 16ADP \quad [10]$$

V-nitrogenase: $$N_2 + 8H^+ + 8e^- + 24ATP \rightarrow 2NH_3 + 3H_2 + 24ADP \quad [11]$$

Fe-nitrogenase: $$N_2 + 8H^+ + 8e^- + 42ATP \rightarrow 2NH_3 + 7.5H_2 + 42ADP \quad [12]$$

From these equations it can be seen that Mo-nitrogenase is the least energy intensive but also does not produce as much hydrogen as the other metal cofactors; this isozyme also has the lowest conversion efficiency and a large enzyme concentration is required to produce a good hydrogen yield (Pott, 2013; McKinlay *et al.*, 2014).

In the absence of molecular nitrogen, however, nitrogenase has the ability to reduce protons into hydrogen (Burris, 1991; Koku *et al.*, 2002), which would mean an increase in hydrogen production. This is because if nitrogen in the system is limited, the reducing equivalents are redirected solely to hydrogen production; hydrogen production under the inhibition of molecular nitrogen and oxygen can be seen in Equation 13 below.

$$8H^+ + 8e^- + 16ATP \rightarrow 4H_2 + 16ADP \quad [13]$$

By comparing the theoretical hydrogen produced by nitrogenase in a nitrogen limited environment versus an environment where molecular nitrogen is not inhibited, an extra 3 mole of hydrogen were produced in a nitrogen limited environment. Thus, it can be deduced that maximum hydrogen production will be achieved if *R. palustris* is grown under anaerobic photoheterotrophic conditions. To remove atmospheric oxygen and nitrogen from the photobioreactor system, an inert gas such as argon (Ar) can be used (McKinlay *et al.*, 2014) or as an inexpensive alternative carbon dioxide can be used.

b) Hydrogenase

The production of hydrogen through the hydrogenase enzyme is a reversible reaction; the direction of the reaction is dependent on the culturing conditions. The reaction is given in Equation 14 below.

$$2H^+ + 2e^- \leftrightarrow H_2 \quad [14]$$

Ross (2019) explains that due to the conditions used for photofermentation, the reverse reaction is favoured and instead of producing hydrogen, hydrogenase then consumes hydrogen. Thus, the maximum hydrogen that can be produced by *R. palustris* during anaerobic photofermentation is the amount of hydrogen produced by nitrogenase, subtracted by the amount of hydrogen consumed by hydrogenase. In certain *R. palustris* strains, the hydrogenase enzyme is inactive to prevent the consumption of hydrogen, such as with the strain *R. palustris* CGA009. The genome for *R. palustris* CGA009 is fully sequenced, meaning that the strain is easy to manipulate, and desired characteristics, such as enhanced hydrogen production, of the strain can be expressed. In comparison to this, a wild type, for example *R. palustris* NCIMB11774, would perhaps not achieve such high hydrogen yields but may be more robust in terms of temperature variation. The modified strains are thus with certain advantages, like enhanced hydrogen production, but with a decrease in adaptability to environmental conditions. Kim, Ito and Takashi (1980) also reiterated that the rate of hydrogen production of *R. palustris* was almost proportional to nitrogenase activity and no correlation between hydrogen and hydrogenase activity was observed.

2.3.3.2 Metabolism of hydrogen production

R. palustris has the ability to produce hydrogen under photoheterotrophic growth conditions in the absence of molecular oxygen (anaerobic conditions) and limitation of molecular nitrogen with an organic substrate for utilisation and sufficient illumination. As mentioned previously in Section 2.3.3.1(a), the growth of *R. palustris* must take place in an environment where nitrogen is limited to prevent the production of ammonia that inhibits the production of hydrogen; this is because ammonia inhibits the nitrogenase enzyme which is primarily responsible for hydrogen production (Burris, 1991; Koku *et al.*, 2002). Because the inhibition of nitrogenase is reversible when all ammonia in the system is consumed the nitrogenase enzyme activity can fully recover. Although this is the case for all nitrogen-containing compounds, meaning that the bacteria must be grown under nitrogen limited conditions to ensure hydrogen production. Pott (2013) and Koku *et al.* (2002) state that the use of glutamate as the sole nitrogen source in the system can stimulate the activity and synthesis of the nitrogenase enzyme to enhance hydrogen production. If used industrially, glutamate would be required to only to grow the culture, and is not necessary during standard plant operations and would thus not be too costly to include in process operation.

Under these conditions the hydrogen production metabolism of *R. palustris* consists of several key components: The Calvin-Benson-Bassham (CBB) cycle, the photosystem, the nitrogenase and hydrogenase enzyme and the storage compounds (Pott, 2013). An illustration of the metabolism of hydrogen production under these specified conditions can be seen in Figure 6.

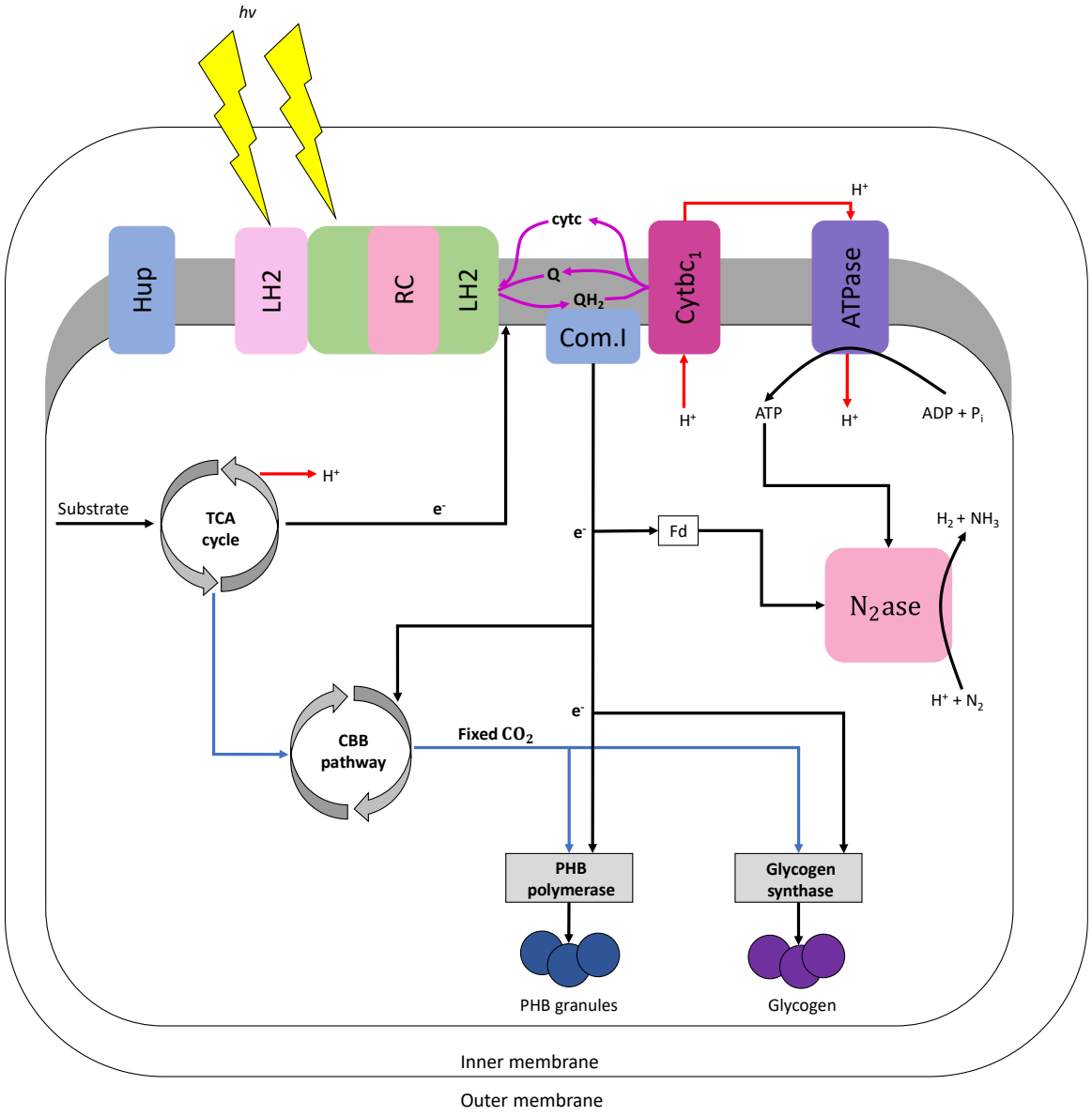

Figure 6: This figure is an adaptation from Pott (2013), representing the metabolic pathway of hydrogen production by *R. palustris* during photoheterotrophic, anaerobic and nitrogen fixing conditions. Light excitation is represented by the yellow lightning bolts. The outermost thin black line represents the outer membrane of the cell and the thicker grey line represents the inner cell membrane. The straight, thick black arrows represent the flow of electrons in the cell, red lines indicate proton (H^+) flow and the thick blue lines represent the flow of CO_2. Curves black arrow indicate that a reaction is occurring and curved purple arrows represent the cyclic electron transport system that is part of the photosynthetic apparatus.

In Figure 6, light harvesting complexes (LH1 and LH2) absorb light photons and the energy is rapidly transferred to the photosynthetic reaction centre (RC). The cyclic electron transport between the RC and the cytochrome b/c_1 ($Cytbc_1$) is then initiated by this energy. Ubiquinone (Q) transports reducing equivalents (e^-) here. A proton gradient is then produced, and ATP synthase (ATPase) can then utilise

this to produce the ATP required. Reducing equivalents then leave the ubiquinone pool and through ferredoxin are transported to nitrogenase (N_2ase). Ferredoxin is a mediator for electron transport as can be seen in the figure. The responsibility of the nitrogenase enzyme is to fix nitrogen to ammonia with hydrogen as a by-product. Hydrogenase (Hup) is found in photosynthetic microalgae and cyanobacteria and is used during bio-photolysis to produce hydrogen. In the case of PNSB however, hydrogenase is responsible for the conversion of hydrogen to protons and electrons used by ATPase; although there is a possibility that an active hydrogenase enzyme is not present, for example with *R. palustris* CGA009 which is a commonly used laboratory strain, as explained in section 2.3.3.1 b). Reducing equivalents are also utilized in the Calvin cycle (CBB pathway). In this cycle e^- are used to fix carbon dioxide and store carbon as glycogen and poly(hydroxybutrate). Another source of electrons is the tricarboxylic cycle (TCA cycle), otherwise known as the Krebs cycle. In this cycle, organic substrates are metabolized to produce protons and electrons. The electrons are then used as reducing equivalents in the photosystem and the protons are used in the formation of hydrogen (Roszak *et al.*, 2003; Pott, 2013).

2.3.4 Photosystems

Photosynthesis is a process critical to life as we know it; photosynthesis is the conversion of light energy to chemical energy by the action of a light driven proton pump coupled to electron transfer within complex organic molecules (Hu *et al.*, 2002; Okamura and Feher, 2006). Photosynthesis occurs in a variety of organisms: algae, plants and photosynthetic bacteria (Hu *et al.*, 2002). According to Roszak *et al.* (2003), under these photosynthetic organisms, purple photosynthetic bacteria have been prime model systems to study light reactions of photosynthesis; this is due to the relatively simple photosystems of purple photosynthetic bacteria that resemble photosystem II in higher order plants. Although both purple photosynthetic bacteria, algae and plants can all photosynthesize, there is difference between the type of photosynthesis that takes place in purple photosynthetic bacteria in comparison with plants and algae. In purple photosynthetic bacteria, there is only a photosystem II, whereas in plants and algae both a photosystem I and photosystem II are present. This means that photosynthetic bacteria do not have the ability to split water to evolve oxygen (Pott, 2013). For each photosynthetic bacterium, in this case *R. palustris,* the oxygen concentration needs to be below a specific threshold which can trigger the formation of photosynthetic pigments and pigment-binding proteins (McEwan, 1994).

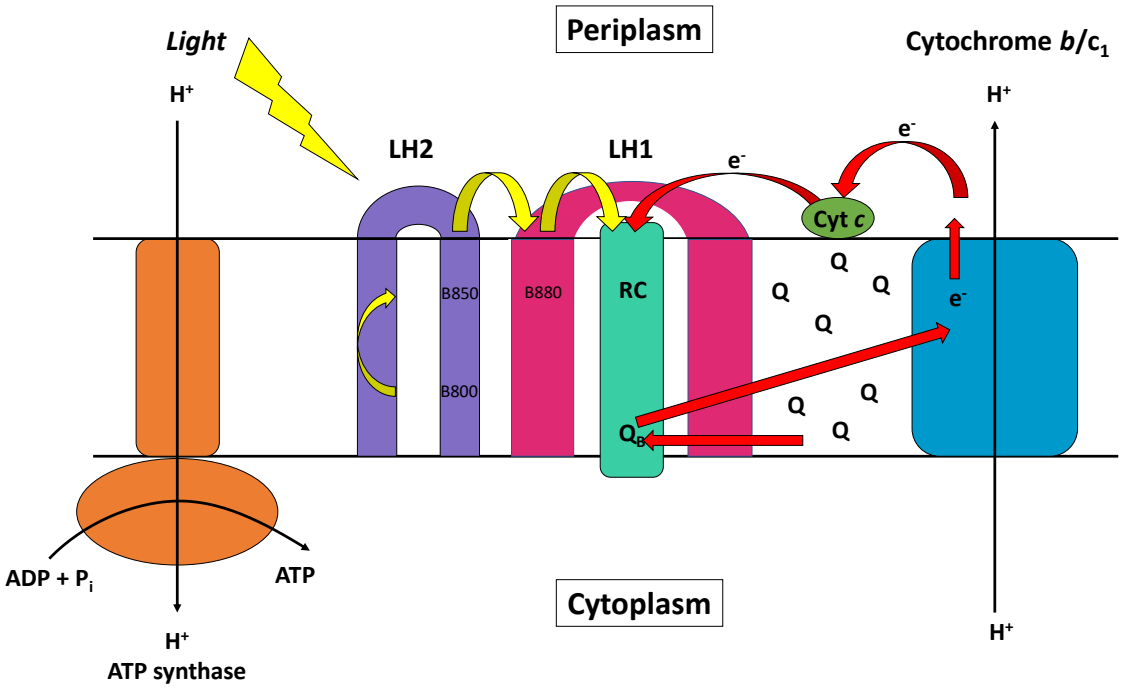

Figure 7: The figure was adapted from Hu *et al.* (1998) and Roszak *et al.* (2003). This is a schematic representation of the major membrane proteins involved in the light reaction of PNSB. The yellow arrows represent photon energy. The purple complex represents L2, the wavelength of maximum absorption is represented by the values B800 and B850. The dark pink complex is L1, the wavelength of maximum absorption is represented by the value B880. The reaction centre is seen in the green section and represented by RC. Electron flow is represented by the thick red arrows and curved black arrows represent a reaction taking place. The blue block represents cytochrome b/c_1 complex. ATP synthase is represented by the orange block and oval, where ATP is synthesized in the membrane.

In Figure 7, the major membrane proteins in photosynthetic bacteria are represented; these proteins are involved in the light reaction of purple photosynthetic bacteria. The photosynthetic process starts with photon energy as represented by the yellow arrows. Photon energy is captured by the bacteriochlorophyll-α (BChl-α) pigments in antenna LH2 represented by B850 and B800; this is because the approximate wavelength of maximal absorption is between 800 and 850nm in the LH2 complex. The absorbed photon energy is then passed to BChl-α in LH1 represented by B880, which also acts as a light-harvester (Roszak *et al.*, 2003). The approximate wavelength of maximal absorption is between 870 and 890nm in the LH2 complex. Finally, the absorbed photon energy is transported to two BChl-α in the reaction centre (RC). In the RC, charge separation then occurs and the lipid soluble electron carrier (ubiquinone (Q)) is reduced, from here the aqueous phase cytochrome *c* (Cyt *c*) then reduces the RC. A second photon is then absorbed and the twice reduced Q then diffuses into the cytochrome bc_1 complex. The electrons are then passed from the Q by cytochrome bc_1 to reduce the water phase in Cyt *c* (Pott, 2013). The cyclic electron transport chain is then closed due to a generated

chemical potential preserved as a proton (H^+) gradient. This can then be used by ATP synthase to produce ATP from ADP and an inorganic phosphate.

In the LH complexes, there are various pigments present such as billin pigments, bacteriochlorophylls (BChl's) and carotenoids. For *R. palustris*, two main pigments are present in the LH complexes namely carotenoids and BChl-α (Imhoff, Hiraishi and Süling, 2005). As mentioned previously, the major function for BChl-α pigments is light-harvesting. Carotenoids have three functions in this process: light harvesting at lower wavelengths (the blue-green wavelength range, photoprotection and stabilising LH's as structural components (Damjanović, Ritz and Schulten, 1999; Paulsen, 1999).

From an engineering perspective, this translates to the wavelengths required from illumination and how this can be applied in a real reactor system. The specific illumination requirement for this system is discussed in section 2.6.1.3.

2.3.5 Current use in industry

The ability of *R. palustris* to produce hydrogen from an organic wastewater stream makes it an attractive option for application in wastewater treatment. Larimer *et al.* (2004) states that currently many PNSB are used in microbial populations for digestion of wastewater in wastewater treatment facilities. The conditions that *R. palustris* thrives in are common in the wastewater treatment industry, which makes the application of this bacteria to wastewater treatment a reasonable option.

R. palustris can metabolise fatty acids and dicarboxylic acids, lignin monomers, animal fats, seed oils and other organic compounds commonly found in wastewater treatment. Certain chlorinated compounds can also be dehalogenated and degraded using *R. palustris*. Certain nitrogen-containing compounds (amino acids and some aromatic compounds) can also be degraded by *R. palustris*.

The wide range of abilities of *R. palustris* make this bacterium a valuable asset in the wastewater treatment industry, which is why it is the focus of this investigation.

2.3.6 R. palustris growth substrate

Due to the metabolic versatility of *R. palustris,* this organism has the ability to utilize various organic substrates. Therefore, in the literature, multiple organic substrates had been investigated; each of these substrates resulting in varying hydrogen yield through photofermentation. In Table 5 below, the specific hydrogen production rates via photofermentation of various substrates were compared.

Table 5: Comparison of various substrates and resulting hydrogen production

Organic substrate	Specific hydrogen production rate ($mL/g_{dw}/h$) (STP)	Source
Glycerol	~31	(Pott, Howe and Dennis, 2013)
	~32	(Sabourin-Provost and Hallenbeck, 2009)
Treated crude glycerol	~30	(Pott, Howe and Dennis, 2013)
Glucose	~27	(Pott, Howe and Dennis, 2013)
	~37	(Tian *et al.*, 2010)
Sucrose	~35	(Pott, Howe and Dennis, 2013)
Crude glycerol	~25	(Pott, Howe and Dennis, 2013)
	~11	(Ghosh, Tourigny and Hallenbeck, 2012)
Lactate	~25	(Pott, Howe and Dennis, 2013)
	~38	(Vincenzini *et al.*, 1982)
Acetate	~24	(Pott, Howe and Dennis, 2013)
	~38	(Barbosa *et al.*, 2001)
Butyrate	~21	(Pott, Howe and Dennis, 2013)
	~24	(Wu *et al.*, 2010)
Malate	~15	(Pott, Howe and Dennis, 2013)
	~38	(Fißler, Kohring and Giffhorn, 1995)

As discussed in previous sections, the goal of this investigation is the application of biological hydrogen production using crude glycerol for waste valorisation. With the production of biodiesel comes the by-product crude glycerol, for each 1 m^3 of biodiesel produced about 0.1m^3 of crude glycerol is produced; initially this was considered a benefit to increase the economics of the process (Pott, Howe and Dennis, 2013). Although with the expansion of the biodiesel industry this has resulted in a significant increase in crude glycerol availability which has become a burden for the industry; the sheer excess of this by-product requires significant costs to dispose of. To counter-act this, crude glycerol can be used as a substrate in photofermentation of photosynthetic bacteria to partake in waste valorisation and result in useable hydrogen gas.

An investigation by Hallenbeck and Liu (2015) reported when using glycerol as the carbon source during photofermentation, a yield of 6.9 mol hydrogen per mole of crude glycerol was achieved in

comparison with the theoretical maximum hydrogen of 7 mol. This signifies that 96% of the theoretical hydrogen production could be attained as seen in Equation 15 below.

$$C_3H_8O_3 + 3H_2O \rightarrow 3CO_2 + 7H_2 \quad [15]$$

Similarly, in an investigation by Pott, Howe and Dennis (2013), a hydrogen yield of 80-85% the theoretical maximum (7 mol) could be achieved. Sabourin-Provost and Hallenbeck (2009) also reported a hydrogen yield of 75% the theoretical maximum. This repetitive promising result makes crude glycerol an attractive substrate during photofermentation for biological hydrogen production.

When considering the use of this system for long-term application, it would be necessary to ask, if hydrogen production were to become stable, would we still need to produce biodiesel? In Table 5, it was seen that multiple organic substances could act as a carbon source for biohydrogen production and many of these carbon sources can be found in multiple waste streams within several industries. As an example, sucrose is a demonstrated substrate for biohydrogen production and can be found in sugar production wastewater.

2.3.7 Typical behaviour of R. palustris in a batch free cell system

From the literature, this section provides typical profiles over time for the important parameters in this investigation: cell concentration, substrate utilisation and cumulative hydrogen production. These profiles represent the performance of *R. palustris* in a batch free cell system, meaning little to no physical strain and sufficient growth nutrients under anaerobic nutrient limitation conditions, i.e., ideal conditions for hydrogen production.

The goal is to compare these profiles to profiles from experimentation, to draw some conclusions regarding comparative cell growth, hydrogen production and substrate utilisation. The profiles presented were obtained and adapted from du Toit and Pott (2021) as the growth conditions were similar at conditions controlled at 35°C and an irradiance intensity of 200 W/m^2 using the same strain of *R. palustris*.

2.3.7.1 Expected profile for R. palustris cell growth

Similar growth rates were obtained from (Pott, Howe and Dennis, 2013a), with the stationary phase occurring at a cell concentration of roughly 5 g/L. As observed in Figure 8, a steady increase in biomass concentration can be expected until a relatively constant biomass concentration is observed, which is labelled as the stationary growth phase, where hydrogen production is expected, as mentioned in section 2.2.3.2.

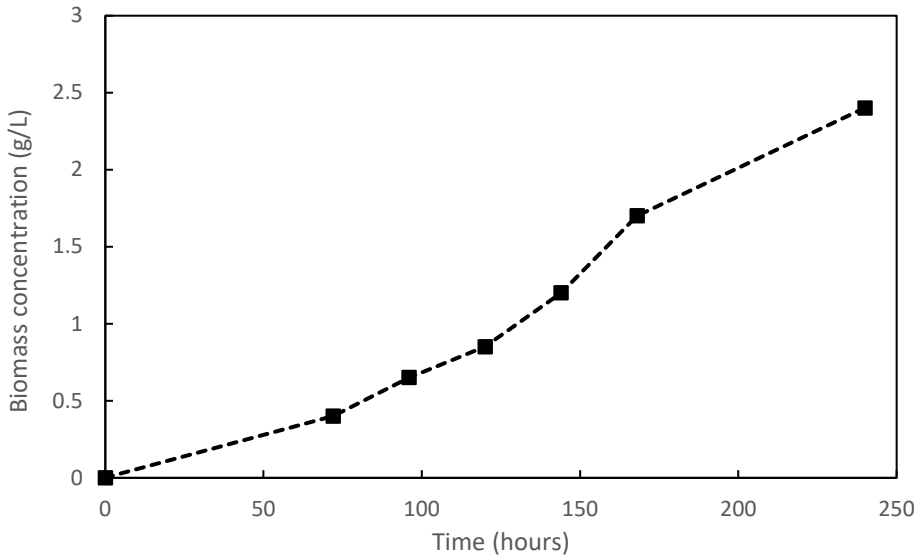

Figure 8: Typical growth curve for R. palustris in minimal medium, cultured at 35°C. Figure adapted from du Toit and Pott (2021)

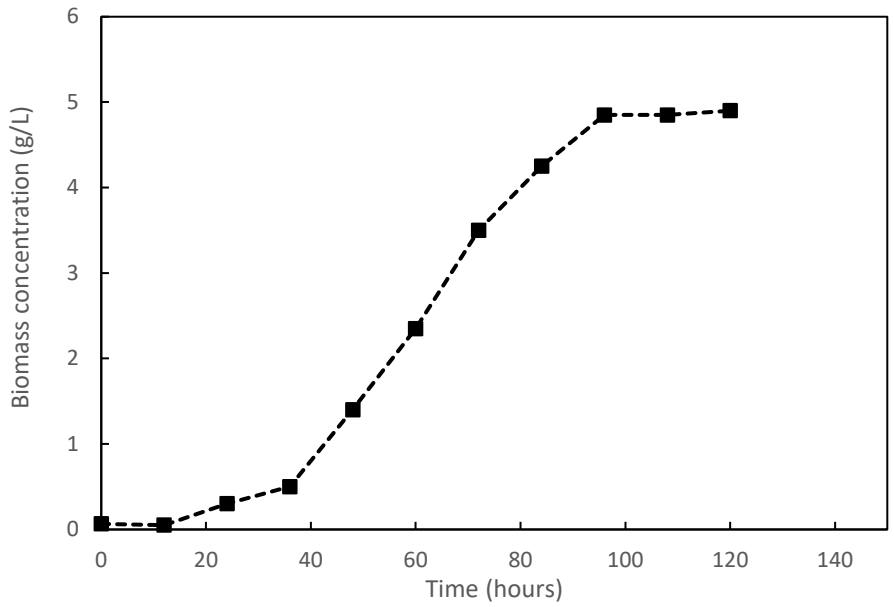

Figure 9: Growth curve of R. palustris 11774 in van Niels medium, cultured at 35°C. Figure adapted from Ross (2019)

When comparing the two growth curves (Figure 8 and Figure 9), the growth rate observed for van Niels medium is significantly faster than that of minimal medium due to a higher concentration of yeast extract. As mentioned in section 2.3.3, however, *R. palustris* does not produce hydrogen in this medium due to the presence of molecular nitrogen.

2.3.7.2 Expected profiles for substrate utilization

Substrate utilisation is a key consideration to the feasibility of both hydrogen production and efficiency of wastewater treatment. As the basis of this investigation is wastewater treatment and delivering a wastewater stream with a low substrate concentration is an important requirement. Considering an industry standard for a greasy effluent, as crude glycerol would be, the industrial effluent requirement would be 10mg/L (National Water Act 36 of 1998, 2013; Krishnan and Balasubramanian, 2014).

In a study by du Toit and Pott (2021) it was found that the optimum temperature for glycerol conversion efficiency was 35°C, for this specific strain of *R. palustris,* from the literature, final substrate concentrations after experimentation (see Figure 10) were observed be below 0.1g/L (Ross, 2019). Values below 0.1 g/L were not reported in the literature, due to HPLC detection limits.

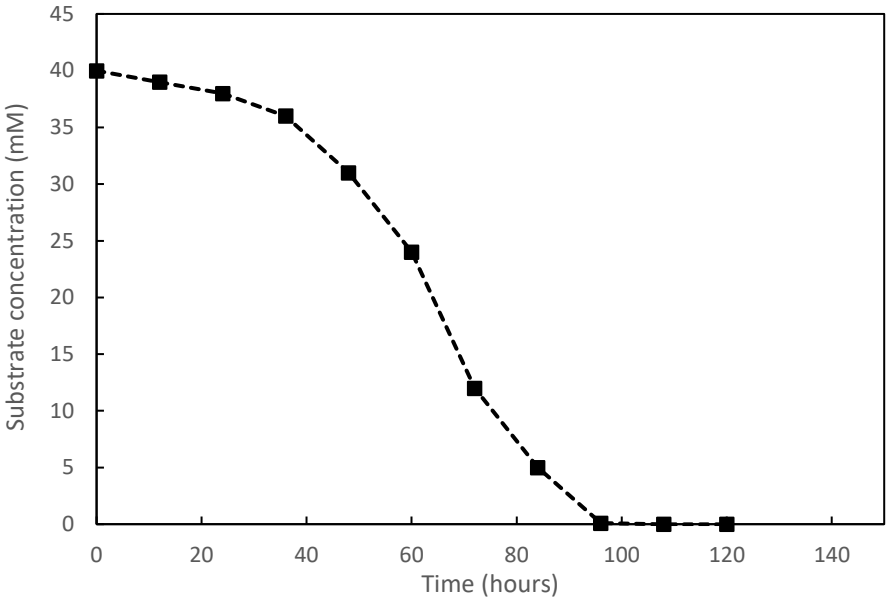

Figure 10: Substrate (glycerol) utilisation of *R. palustris* 11774 cultured in van Niels medium at 35°C. Figure adapted from Ross (2019)

2.3.7.3 Expected profile for hydrogen production

In Figure 11, the observed hydrogen production from the literature for *R. palustris* when growing in a simple Schott bottle setup, which is described later in Section 4.1.4.2 (du Toit and Pott, 2021). From the figure for the time period investigated in this study (240 hours), cumulative hydrogen production was expected to reach 1200 mL under optimal culturing conditions.

For this study to be considered a viable solution for waste valorisation, it was expected that efficient substrate utilisation in combination with sustainable hydrogen production must take place.

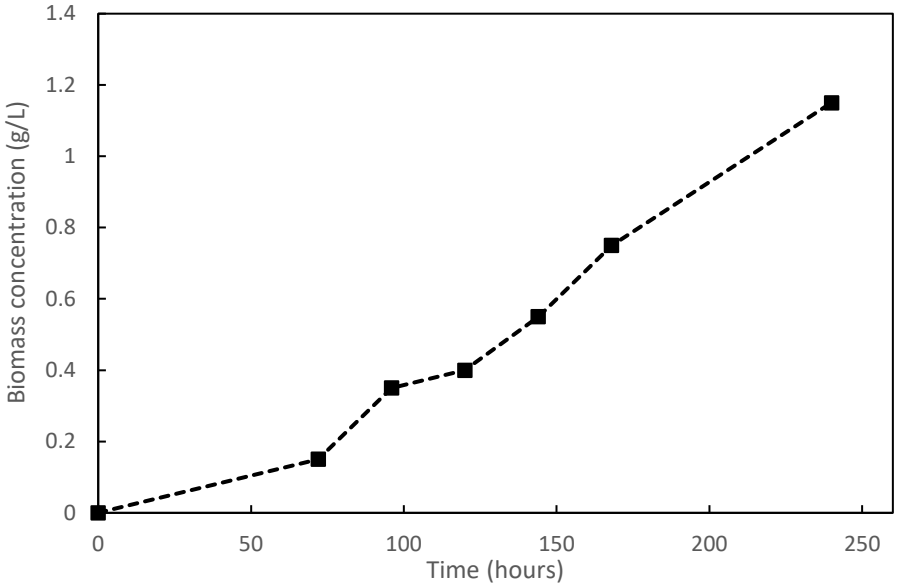

Figure 11: Cumulative hydrogen production by *R. palustris* 11774 under anaerobic conditions at 35°C with a starting glycerol (organic substrate) concentration of 50mM. Figure adapted from du Toit and Pott (2021)

2.4 Bioreactors

This study focuses on the development and implementation of a new photobioreactor configuration that can be used for the simultaneous treatment of a glycerol-rich waste stream and be used as a source of renewable energy. In order to understand how to go about designing a new type of reactor, it was necessary to work through the design and operation criteria required to deliver the desired outcomes of this investigation. There are multiple aspects to consider with bioreactor design for *R. palustris* such as illumination, agitation, physical reactor dimensions or the choice between immobilised or a free cell system.

The following subsections will discuss the various background information required to appropriately design the desired bioreactor. Going into detail the requirements to efficiently operate a bioreactor supported with what has been observed in the literature with regards to efficient bioreactor design to produce optimal growth results.

2.4.1 What is a bioreactor

The definition of a bioreactor, according to Wang and Zhong (2007), is vessel in which a biological change or reaction takes place. The goal of a bioreactor is to provide an optimal external environment to meet the needs of the biological reaction system to achieve a high yield of the desired product from the biological process. In order to design an appropriate bioreactor, to optimize the desired product yield and biological reactions, intensive knowledge is required about the requirements for the physical and chemical environments for the bacterial cell (Wang and Zhong, 2007). In this case, the desired

yield is hydrogen gas, and the desired reaction is the production of hydrogen by the nitrogenase enzyme in *R. palustris* bacteria.

In the case of *R. palustris,* in order to theoretically optimize hydrogen production, photoheterotrophic conditions are utilized for bacterial growth. Under these conditions and in the absence of molecular oxygen and nitrogen (anaerobically), photofermentation occurs to produce hydrogen. During photofermentation, photon energy is responsible for the production of hydrogen in *R. palustris*. Thus, when considering these requirements in the design of a bioreactor, it highlights the importance of light in this process; a photobioreactor must be designed in order to optimize the environment inside the reactor for biohydrogen production.

2.4.2 Types of bioreactors

Currently, the most developed photobioreactor technology is designed for the application of algae culture and generation of hydrogen. Some of the most commonly found designs include: tubular reactors, vertical column reactors and flat panel reactors (Xu, 2007). Due to the difference in the metabolic pathways and photosystems of algae versus photosynthetic bacteria, these reactor designs cannot be interchangeably used for both algal and bacterial cultures. Thus, to make use of *R. palustris* during photofermentation, many novel photobioreactors have been designed. Chen, Lee and Chang (2006) designed a novel optical fibre-illuminating photobioreactor, Carlozzi and Sacchi (2001) designed a tubular underwater photobioreactor and Wang *et al.* (2010) designed a packed-bed reactor using immobilized bacteria.

Wang and Zhong (2007) classify biological reaction systems into two groups: immobilization systems and suspension systems. Suspension systems, otherwise known as free-cell systems, are a reactor condition where the cells are in suspension in the system, in other words, not contained in a matrix or growing in a biofilm. The advantage to this system is the increased efficiency of mass-and-heat transfer as the cells can freely interact with the medium in which it is growing. Disadvantages of these systems are the mutual shading effect, observed when the cells shade each other from the source of illumination due to a higher culture concentration or a loss of biomass when operating the system continuously. Suspension systems commonly use membrane-, stirred-tank- or bubble column bioreactors to ensure sufficient mixing and are commonly operated in batch mode configuration to limit the loss of biomass during operation.

Immobilized systems are mostly found in two different ways, either a biofilm or cells immobilised in a matrix. A major advantage to these systems is the elimination of biomass loss in continuous process operation, as the culture is not in free suspension and is stopped from exiting the system. In a biofilm system, culture is attached to suspended structures within the bioreactor, although disadvantages include mutual shading as the cells at the bottom of the biofilm receive no light exposure, and the associated capital costs for biofilm bioreactors (Hülsen *et al.*, 2020).The other type of immobilisation is the immobilisation of cultures in a matrix, the matrix material varies significantly in multiple studies as the matrix is still being optimised for efficient mass-and-heat transfer along with sufficient light

exposure. Although, the immobilization of bacteria is a laborious process and not currently widely researched making this an unattractive option. Immobilised bacteria are mostly used in stirred-tank-, packed bed- and fluidised bed bioreactors. The main problem with stirred tank photobioreactors is the lack of homogeneity with regards to illumination from outside the photobioreactor (Chen, Lee and Chang, 2006). From this perspective, a packed bed- or fluidised bed photobioreactor might be a viable solution.

As a simpler alternative, for free-cell systems the membrane photobioreactor (MPBR) can be used. To combine both the advantages of a free cell system and the advantage of keeping biomass in the system with the use of a membrane. At the time of this study, no research has been done on the dual purpose of wastewater treatment and hydrogen production using *R. palustris.*

2.4.3 Characteristics for an ideal bioreactor for Rhodopseudomonas palustris

The reactor in this investigation is a combination of the benefits of both the immobilized and suspension systems by separating the hydraulic retention time (HRT) and solids retention time (SRT) of the system; the goal is to increase the SRT and decrease the HRT. Simply put, the bacteria must ideally not exit the system and the wastewater must enter and exit the system in continuous manner. By using a free cell system, the bacterial exposure to light and substrate is improved, along with limited dead volume inside the reactor in comparison to immobilized systems. This means that the substrate is more efficiently utilized, and hydrogen production can proceed. A major drawback to free cell systems is however a shorter solids retention time and as the treated water exits the system, so does the bacteria. This is where the separation of HRT and SRT comes into consideration; by using a membrane to filter the exiting stream, the bacteria can be recycled back into the bioreactor and the wastewater can exit the system sans bacteria. This is the benefit of an immobilized system, the bacteria simply remain in the system and the wastewater can flow in, the substrate is utilized and the water flows from the system.

The following section discusses a basic background into membranes, efficient membrane bioreactor design and a short summary of what has been observed in the literature.

2.5 Membrane bioreactors

The use of membranes in industry only started gaining popularity much later in the wastewater treatment industry, as the unattractive characteristics that made membranes so unpopular in the past were only recently eliminated; membranes were too unselective, expensive, unreliable, fouled easily, and they were slow.

A membrane bioreactor is simply, as the name suggests, a bioreactor in combination with membrane separation (Judd, 2008). As discussed in the previous section, the advantage of a membrane in combination with a free cell system, delivers both the benefits of a separate HRT and SRT with increased substrate utilisation efficiency as the cells are in suspension.

To design this specific membrane bioreactor, it is necessary to take a deeper look into what a membrane is, challenges experienced with membranes and how membrane bioreactors look today. In the following subsections, this will be discussed as a basis for membrane bioreactor design.

2.5.1 Membrane technology basics

2.5.1.1 What is a membrane?

A membrane is simply defined as a selective barrier that allows some substances to pass through easily, whilst preventing or restricting the passage of other substances. This is achieved by multiple different driving forces to separate the inlet fluid to both a permeate and a retentate, as simply illustrated in Figure 12.

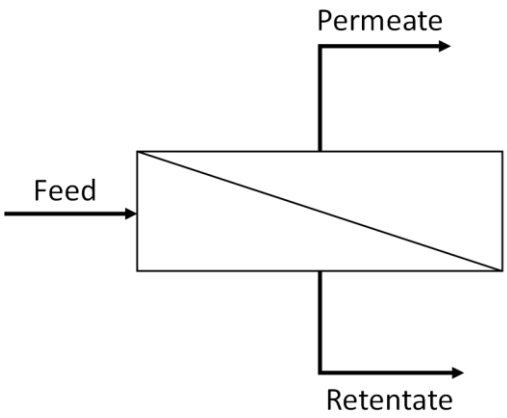

Figure 12: Simplified representation of a membrane

In the following figure (Figure 13), the different categories of synthetic membranes are classified. These types are membranes can be produced with a large variety of pore sizes by simply changing either the polymer, solvent or precipitating agent making them an attractive option for industry. According to Porter (1990), due to the large internal surface of these membranes they have a high absorption rate to ensure that a complete removal of components takes place during separation.

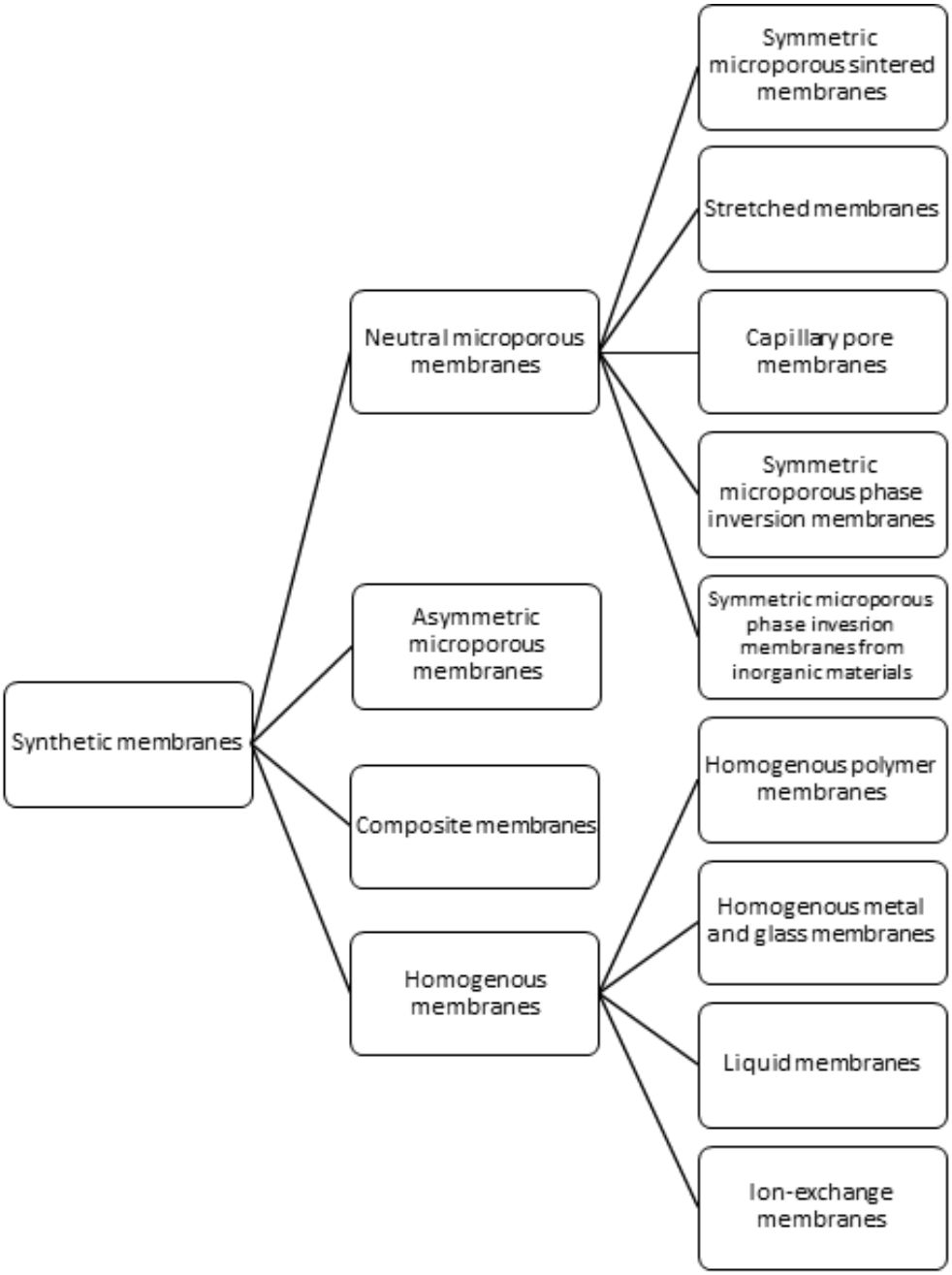

Figure 13: Classification of different types of synthetic membranes (Porter, 1990)

2.5.1.2 Types of membranes

The pore size of a membrane is the basis on which the degree of selectivity of a membrane is classified into one of the following groups: microfiltration (MF), ultrafiltration (UF), nanofiltration (NF) or reverse osmosis (RO) as seen in Figure 14. Within these pore size groups membranes can be further distinguished based on charge, method of particle transport or synthesis. The driving force behind particle transport can vary with membrane modules; pressure, concentration, chemical and electron gradient or temperature driven processes have investigated, used and developed in both research and industry (El-Ghaffar and Tieama, 2017).

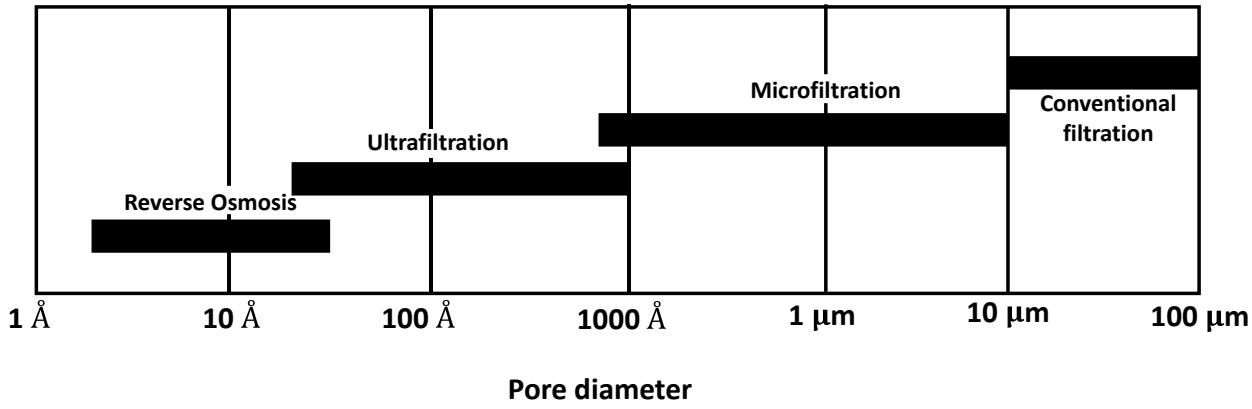

Figure 14: Classification of membranes according to pore diameter (Figure adapted from Baker (2012))

The design of the MPBR in this investigation facilitates the use of pressure to induce particle transport of the membrane and the classification of selectivity can be seen in Table 6 below.

Table 6: Membrane classification according to pore size for pressure driven membranes (Baker, 2012; El-Ghaffar and Tieama, 2017)

	Selectivity	**Pressure range**
Microfiltration (MF)	50-10^4 nm	5-5000 kPA
Ultrafiltration (UF)	5-100 nm	<1 MPa
Nanofiltration (NF)	1-10 nm	<4 MPa
Reverse osmosis (RO)	<2 nm	>5-10 MPa

2.5.1.3 Membrane terminology

In the table below are a few terms that will be used throughout this investigation and are required in order to understand the workings of a membrane system. Refer to Figure 12, for a basic schematic of a membrane as a background for the following terminology.

Table 7: Membrane terminology (Koros, Ma and Shimidzu, 1996; Baker, 2012)

Term	**Definition**
Critical flux	Flux value where fouling is not observed and decline with time is does not occur and the same with flux values below this. Above this flux value, fouling is observed.
Cross-flow velocity	The linear velocity of the fluid that is flowing tangential to the surface of the membrane

Term	Definition
Feed	Stream entering membrane for desired filtration
Flux	Mass, volume, or number of moles of a component that passes through the membrane per unit of time normal to the thickness direction
Fouling	Deposition of particles/substances on the surface of the membrane or lodged in the pores or at the pore openings of the membrane. Results in a decreased performance. Could be either reversible or irreversible or a combination of the two.
Membrane module	Membrane or membranes assembly to separate feed, permeate and retentate streams.
Permeate	Exiting stream from a membrane containing penetrants from the membrane.
Retentate	Exiting stream from a membrane containing compounds rejected by the membrane, void of penetrants. Otherwise known as the raffinate.

2.5.1.4 Modes of operation

There are two different modes used for membrane filtration: cross-flow and direct-flow (otherwise known as dead-end flow). Cross-flow is a filtration mode, seen in Figure 15, where the feed is flowing parallel to the membrane surface. A benefit of this mode of operation is the high fluid velocity prevents the rapid accumulation of solids (fouling) on the membrane surface. A drawback to this method is the high energy costs associated with this operation as high fluid velocities are required over the membrane surface.

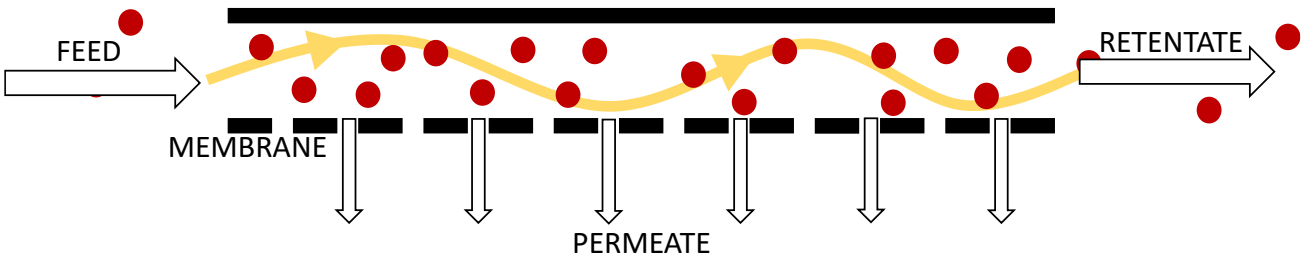

Figure 15: Illustration of the cross-flow filtration mode of operation. Figure adapted from AsahiKASEI (2021).

Direct-flow, otherwise known as dead-end flow, can be seen in Figure 16, is a filtration mode where the feed is directly fed into the membrane. This method is less energy intensive in comparison to cross-flow although the membrane requires regular cleaning due to cake formation on the membrane surface. Regular cleaning requirement means that this mode of operation is generally limited to batch systems.

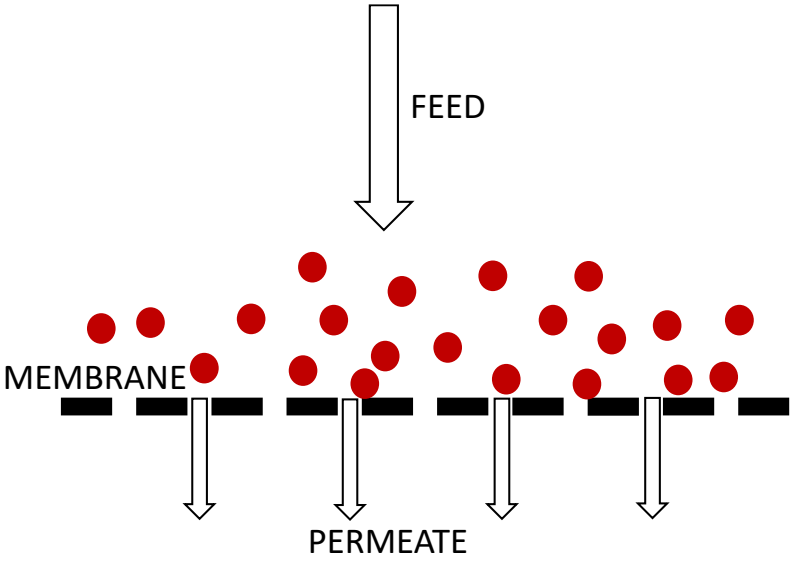

Figure 16: Illustration of the direct-flow filtration mode of operation. Figure adapted from AsahiKASEI (2021).

2.5.1.5 Membrane performance parameters

When considering a mass balance over a membrane, it is important to first consider the reaction by which hydrogen is produced from the glycerol substrate as seen in the equation below (Equation 16). This accounts for the glycerol still in the permeate stream and the glycerol that has been converted to gaseous products.

$$C_3H_9O_3 + 3H_2O \rightarrow 3CO_2 + 7H_2 \qquad [16]$$

During the continuous operation of the MPBR, it is critical to ensure that no fluid is lost, to do this a mass balance is conducted, the mass of gas produced is assumed to be negligible. This is an important mass balance which ensures that the liquid level inside the reactor does not fluctuate (Equation 17).

$$\dot{m}_{in} = \dot{m}_{out} = \dot{m}_{permeate} \qquad [17]$$

The most important parameter when working with membranes is flux, as this is the final filtered product from the system and can be calculated using the equation (Equation 18) below.

$$J = \frac{V_p}{t} \qquad [18]$$

Where V_p is the volume of permeate that passed through the membrane in time t.

2.5.1.6 Membrane fabrication options

In order to employ the use of membranes in industry, a significant area of membrane is required to achieve the desired scale of operation. For this, membrane modules were developed; there are currently four membrane modules that are frequently used in industry, namely the plate-and-frame module, tubular module, spiral wound module and hollow fibre modules, which will be briefly covered

in this section. Other less common types are vibrating or rotating modules, submerged membranes, membrane contactors and counter-flow sweep modules (Baker, 2012).

A plate-and-frame membrane module (Figure 17) was the first design of a membrane module that was seen in industry. In this module, feed spacers, product spacers and flat membranes are stacked together with two end plates. As the feed is pushed through the membrane the permeating fluid passes to a central permeate collection manifold and exits the module. These modules are unpopular due to their high costs and maintenance associated with gasket leaks. They are used mainly for small scale applications such as electrodialysis and pervaporation systems or feed that are highly fouling (Baker, 2012; Balster, 2013a).

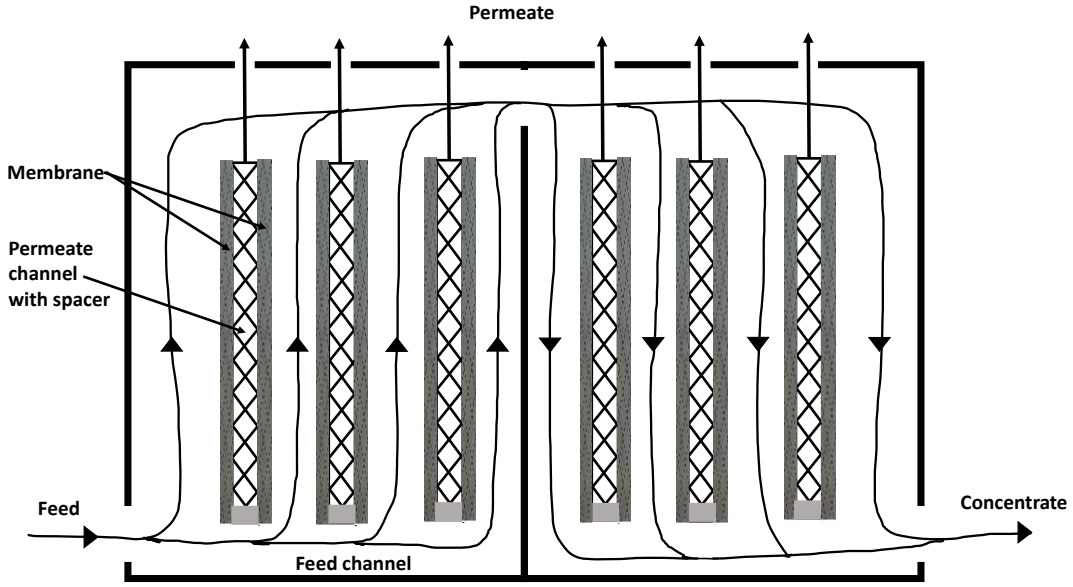

Figure 17: Plate-and-frame membrane module. Figure redrawn from Balster (2013a).

Tubular membranes (Figure 18) are built by placing multiple tubular membranes inside a larger tube that serves as a pressure vessel which creates a larger filtration surface area. These membranes are operated at a high fluid velocity to resist fouling. Tubular membrane modules come with a hefty price tag although their benefit of resistance to fouling due to superior fluid hydronamics can usually justify their cost; these modules are therefor almost exclusively used for ultrafiltration applications (Baker, 2012).

Figure 18: An image of a tubular membrane module. Image reproduced with permission from PALL (no date).

The spiral wound membrane module (Figure 19) is one of the most used modules currently used due to its prevalent use in nanofiltration (reverse osmosis). It is essentially a plate-and-frame module that has been wrapped around a permeate collection tube; the module is constructed by stacking membranes and feed spacers and winding this around a perforated permeate collection tube. The feed then passes axially down the module and permeate ends up at the centre in the collection tube. In industrial applications, around 4 to 6 of these modules are placed in series inside a single pressure vessel. This is because had the module been one large unit the permeate collection pipe would naturally also be several meters long which would lead to significant pressure drop over the collection pipe. This is a less favourable option for high pressure applications due the pressure vessel capital and operation costs. Although initially designed for RO, these modules have also been used in UF and gas permeation (Baker, 2012; Balster, 2013b).

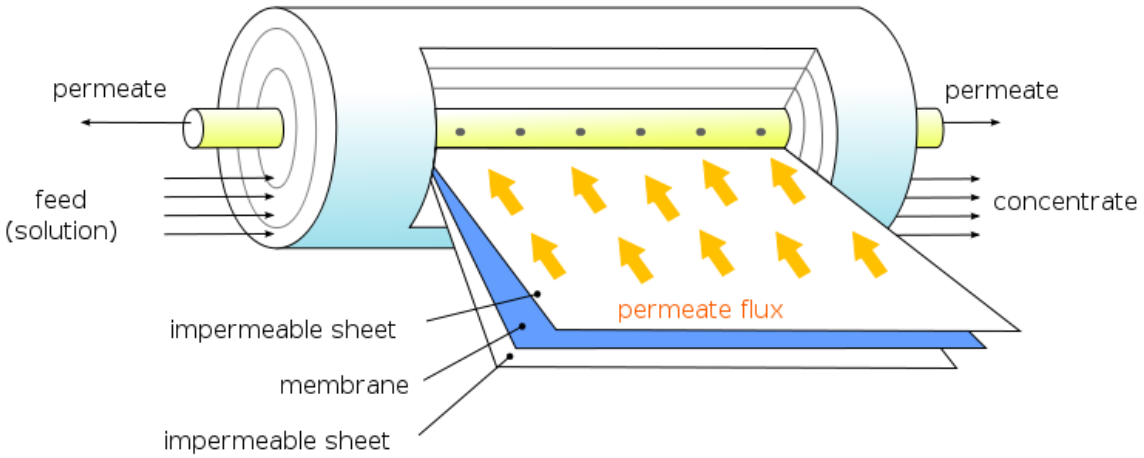

Figure 19: Spiral wound membrane module. Image reproduced with permission from Pugliesi (2008).

The final module to be discussed is the hollow fibre module (Figure 20); there are two basic geometries of this module. The first module assembles in a similar manner as a shell and tube heat exchanger, a bundle of fibres are contained inside a pressure vessel with a shell side feed and pressurised from shell side. The second module is constructed in the same manner although with a bore-side feed and the fluid can be circulated through the bore of the fibres. Hollow fibre modules have a very simple design and the great benefit of simply having the best surface area in comparison with any other module. However this technology comes at a very high cost with limited availability of the hollow fibre membranes due to the cost of module fabrication equipment (Baker, 2012; Balster, 2014).

Figure 20: Hollow fibre membrane module, figure reproduced with permission from Druz (2008)

2.5.2 Challenges with membranes

2.5.2.1 What is fouling?

When first considering the use of a pressure driven membrane photobioreactor system, or in fact any membrane system at all, the first thing that must be considered is the effect of fouling. Fouling is the main physical limitation with the use of pressure-driven membranes and if not properly managed can lead to severe under performance of membrane technology; fouling is defined as the reduction of flux to a value that is significantly below the theoretical capability of the membrane (Field *et al.*, 1995). On a smaller scale, the fouling is a phenomenon observed when a membrane is systematically clogged, either by a deposition layer on the surface on the membrane or blockage of membrane pores with particles in the system. Over time, this leads to a change in pore size distribution (Field *et al.*, 1995) leading to a dramatic decrease in flux. Membrane fouling could be caused by adhesion or accumulation of microorganisms, deposition of colloidal particles, crystallization of dissolved inorganic compounds and deposition and adsorption of macromolecular organic compounds or a combination of these (Touati *et al.*, 2017).

The correct operational conditions for membranes have a significant effect on membrane fouling due to the effects of regular membrane cleaning. It was mentioned in Baker (2012) that membranes that were cleaned less regularly tended to have a significantly longer lifetime. Which makes sense, as membranes that are regularly subjected to abrasive chemicals, surface scouring and flushing, display diminished performance over a period of time. This is not to mention the effect of irreversible fouling, which permanently alters membrane selectivity and degrades performance.

2.5.2.2 Different types of fouling

a) Inorganic fouling

Inorganic fouling, otherwise known as scaling, is caused by the accumulation of inorganic precipitates such as metal hydroxides. As the solution in the system grows more concentrated around the feed side of the membrane, the solution surpasses the solution saturation point and these dissolved constituents precipitate from solution. The phenomenon of a concentration increase on the feed side surface of the membrane is known as concentration polarisation. This results in the crystallised particles to either bind to the membrane surface or lodge in the membrane pores (SAMCO, 2018).

RO and NF membranes are particularly susceptible to concentration polarisation as these membranes reject inorganic species, especially with feeds containing calcium or magnesium constituents. Scaling can be minimized by application of chemical scale inhibitors, or acid softening or injection taking care to use chemical treatments that are compatible with the membrane material (SAMCO, 2018).

b) Organic fouling

When natural organic matter (NOM) collects on a filtration membrane, this is referred to as organic fouling. NOM is a result of decomposing plant and animal material and consists of carbon-based

compounds found in soil, surface and groundwater. As organic matter is quite reactive, it poses several risks as a fouling, the affinity for a membrane material being one of them (SAMCO, 2018).

In surface water treatment, NOM was observed to be the most significant contributor to flu decline. Organic fouling can be mitigated to an extent by raw water treatment or by using a membrane material that is resistant to adsorption of NOM(SAMCO, 2018).

c) Particulate/colloidal fouling

When suspended solids and/or colloidal materials, specifically non-biological and inorganic particle, either clog or adhere to the membrane surface, this is referred to as colloidal fouling. As the particles accumulate on the surface of the membrane, a 'cake' layer is formed, which obstructs flow through the membrane pores. This results in an increase in pressure over the membrane which significantly increases energy consumption of the system (SAMCO, 2018).

To measure the risk of colloidal fouling, the Slit Density Index (SDI) of the feed stream is measured. With the utilisation of RO, this is particularly important, and these membranes have the smallest pore size, making them particularly susceptible to pore clogging by particulates (SAMCO, 2018).

d) Biological fouling

Biological fouling is caused by the growth of algae, microorganisms, or other contaminants on the surface on the membrane resulting in the formation of a biofilm. As the culture grows on the surface of the membrane, it produces extracellular polymetric substances (EPS) and starts to present as a biofilm in the form of a viscous, slimy, hydrated gel. EPS have a high negative charge density and typically consist of heteropolysaccharides which protects these microorganisms from hydraulic shearing or attack by biocides (e.g. chlorine) (SAMCO, 2018).

Similar to colloidal fouling, flow through the membrane will be restricted by the biofilm layer resulting in a pressure increase over the membrane, reduction in flux and in increase in energy consumption. Membranes fouled by biological matter are very difficult to clean and often require replacement (SAMCO, 2018).

2.5.2.3 Options to overcome fouling

a) Backflushing

Backflushing, otherwise known as backwashing, is an increasingly popular way of controlling membrane fouling in a system. This type of cleaning can only be conducted with membrane modules that are able to withstand a flowrate from the permeate side without causing damage to the membrane such as capillary or ceramic membrane modules. During backwashing a slightly pressurised (usually 0.2-0.5bar) solution is forced from the permeate side to the feed side of the membrane, to lift deposited solids from the feed side (Baker, 2012).

b) Chemical cleaning

Chemicals used for membrane cleaning are selected based on the interactions between foulants, the membrane material and the cleaning chemical, this is to ensure that no reactions take place inside the system that could damage either the system or the membrane. Chemical cleaning can be done in three different ways: immersing fouled membranes directly in the chemicals, soaking the membrane in a separate tank with cleaning chemicals or cleaning in conjunction with system flushing (either forward or backflushing) (Liu *et al.*, no date; Lin, Lee and Huang, 2010).

Cleaning chemicals are classified in six different groups and are used for different types of fouling. In the table below (Table 8), the categories are mentioned, and some examples of chemicals are given along with some major functions of each category.

Table 8: Categories of cleaning chemicals along with typical chemicals used under each category and the major functions of each (Liu *et al.*, no date; Lin, Lee and Huang, 2010).

Category	Typical chemicals	Major functions
Caustic	NaOH, KOH, NH_4OH	Hydrolysis, solubilisation
Acidic	HCl, HNO_3, H_2SO_4, H_3PO_4, citric, oxalic	Solubilisation
Surfactants	Surfactants, detergents	Emulsifying, dispersion, and surface conditioning
Chelating agents	EDTA, Citric acid,	Chelation
Enzymes	α-CT, CP-T, peroxidase	Protein, lipid degradation
Oxidative/disinfectants	NaOCl, H_2O_2, $KMnO_4$	Oxidation, disinfection

c) Air scouring

Air scouring is the process of sparging a membrane with pressurised air, which moves parallel to the membrane surface and rapidly scrapes collected compounds on the feed side surface of the membrane. The air used for scouring of commonly pressurised to between 1 and 2 bar and the flowrate of air controlled to between 0.1 and 1.5 m^3 per m^2 of membrane per hour (thewayMembranes, 2020).

If air scouring is not conducted at sustainable air flowrates and pressures specific to different membranes, scouring could result in severe abrasion of the membrane surface, significantly shortening membrane lifetime (thewayMembranes, 2020). In some literature studies it was found that in situ sparging during reactor operation increase membrane filtration efficiency, as it prevents the formation of a cake layer on the membrane surface (Li *et al.*, 1998).

d) Operation below critical flux

Field et al. (1995) first introduced the concept of critical flux as applied to yeast cells in an investigation that was aimed at pinpointing the relationship between pressure, flux, and the resulting fouling in an attempt to reduce the ever-present crippling characteristic of a membrane. This investigation yielded that at a certain flux value, named the critical flux, there is a marginal point where there is no fouling by a cake deposition layer. In conjunction to this, when operating at a flux higher than this critical flux, severe fouling was observed; remembering that the flux and critical flux value are directly dependent on the hydronamics of the system and other variables. This investigation was concluded by stating that the effect of fouling is solely related to the flux and per se not dependent on the applied transmembrane pressure (TMP) only the flux it yields.

Using the following equation (Equation 19), the flux of a membrane can be calculated:

$$J = \frac{TMP}{\mu(R_m+R_f)} = \frac{TMP}{\mu(R_m+R_{ir}+R_r)} \quad [19]$$

Where J is the permeation flux, TMP refers to transmembrane pressure and μ is the viscosity of the fluid being filtered. The R values refer to resistance by the membrane, the subscript 'm' refers to the clean membrane hydraulic resistance, 'f' refers to fouling which can be divided into two types: 'r' refers to refers to reversible fouling including polarisation effect and 'ir' refers to irreversible fouling which is a value that is not reserved to zero as the pressure the released from the system. The units of flux is $m^3/m^2{\cdot}s$ which translates to m/s. However, conventionally in membranes, units of $L/m^2{\cdot}h$ (otherwise written as LMH) $L/m^2{\cdot}d$ are used.

Critical fouling is referred to as J^* where the values of R_{ir} and R_r are equal to zero as seen in the equations (Equations 20 and 21) below.

$$R_f = R_{ir} + R_r = 0 \quad [20]$$

$$J^* = \frac{TMP}{\mu(R_m)} \quad [21]$$

From the literature, it was deduced that an ideal operational flux point is roughly 80% of the critical flux as seen in the equation (Equation 22) below (Jeison and van Lier, 2007; Navaratna and Jegatheesan, 2011)

$$J_{operation} = 0.8 \times J^* \quad [22]$$

During the lifetime of a membrane there is unavoidable degradation due to fouling, this could be mitigated by operating the membrane at a sustainable flux and employing appropriate cleaning procedures. A parameter used to compare the performance of a membrane at any point in its lifetime to the performance of the membrane when it was brand new is the pure water flux value, otherwise known as water permeation flux. The pure water flux is the flux value at which pure water (meaning no other dissolved components) flows through the membrane for a given TMP value. Pure water flux is used during experimentation to observe the extent of fouling and the efficiency of the cleaning

regime, to make sure that the resulting flux for each experimental setup is similar to that used in prior experimentation.

In order to better explain how this relates to membrane fouling, the figure below contains two simplified curves where flux is displayed as a function of TMP. Using the flux-stepping protocol, these curves can be determined for each different membrane and fluid system (Choi *et al.*, 2005; Miller *et al.*, 2014).

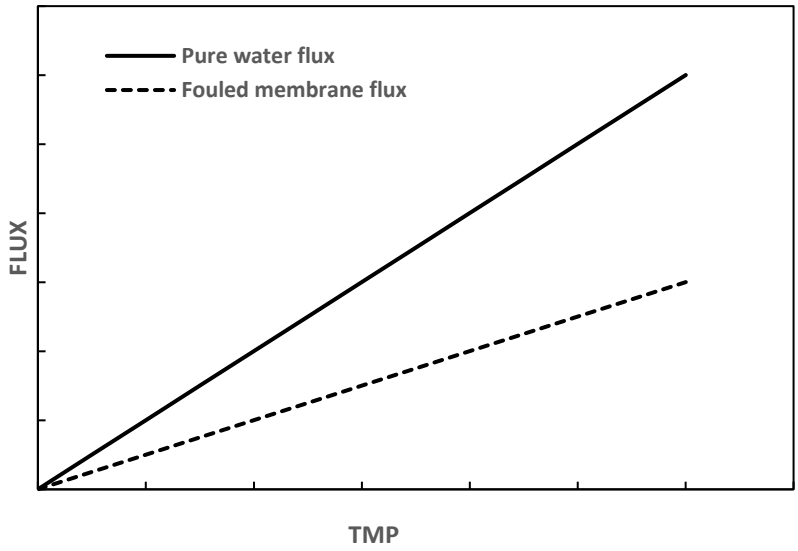

Figure 21: Basic representation of the pure water flux of a completely unfouled membrane for a range of pressures in comparison to the pure water flux for a range of pressures for a membrane with fouling. The solid line represents a completely unfouled membrane and the striped line represents a membrane with fouling. Figure adapted from results found in Choi et al. (2005).

The figure above (Figure 21) is a basic representation of the effect that fouling has on the performance of a membrane as proved by the pure water flux. The solid black line in (Figure 21) represents the best possible attainable flux for this membrane at any given TMP, while keeping the fluid velocity constant. As discussed previously, when fouling occurs in a membrane, the pore size distribution changes; this leads to the change in the pure water flux for each TMP (operating at the same fluid velocity) when conducting the same experiment after fouling has occurred. When considering the dotted line, the possible attainable flux is significantly less for the same TMP; to put it simply, the membrane is now less effective in yielding filtered fluid for the same operating conditions.

In summary, when designing a membrane system and develop operating parameters, it is critical to consider the critical flux of the system and consequently ensuring that the operating flux for the membrane remains at sustainable levels. To ensure that the membrane conditions remain comparable to one another during experimentation, the pure water flux should routinely be tested after the cleaning regime.

2.5.3 Membrane photobioreactors (MPBR) today and a summary of current knowledge

In this section a table (Table 9) summarizing the use of membrane photobioreactors in the literature is given. From this investigation it is clear that literature pertaining to the use of photosynthetic organisms, other than algae, used in membrane photobioreactors is practically non-existent.

As mentioned previously, there are multiple reactor designs for the use of photosynthetic algae that cannot be used for the photosynthetic bacteria *R. palustris* due to the difference in organism metabolism and the need for gas sparging with *R. palustris*. Limited investigation has been done on using membrane photobioreactors with photosynthetic bacteria for wastewater treatment, not to mention membrane photobioreactors that can be used both for wastewater treatment and hydrogen production. Membranes are currently widely employed in the wastewater industry, although mostly with the goal to remove solids from the process stream.

Membrane photobioreactors are currently mostly used on a laboratory scale within research, this is owing to the difficult nature of membranes due to the requirement of precise operating conditions, membrane fouling and high capital costs. Laboratory scale rarely exceeds a 25L capacity and reactor design could change drastically on a larger scale due to photo-limitation in large reactors.

A membrane photobioreactor system offers multiple advantages over the currently used chemical or biological processes. According to González *et al.* (2017), some more benefits are that system only requires a light source and an ambient temperature. Due to the great metabolic versatility of *R. palustris* and the high possible yield of hydrogen, this bacterium is theoretically ideal for the application in wastewater treatment. Although some major stumbling blocks with the use of photosynthetic bacteria in a bioreactor remain, such as that photoheterotrophs have poor settling properties and exhibit slow growth. The use of a membrane reduces the effect of certain stumbling blocks, however, pose some new challenges of their own. Some other disadvantages of membranes are photoheterotrophic growth (biofilm formation) resulting in fouling of the membrane, significantly decreasing separation efficiency. Another drawback is the unknown effect of the membrane on *R. palustris* cells, which may result in accelerated cell death in the system.

This section was created to be used as a guideline during the design process to ensure that design flaws observed in other experimentation were kept to a minimum in this investigation. Otherwise just to serve as a guideline to keep improving and building on what was observed in the literature to deliver a project with new insight into the provided scientific question.

Table 9: Summarization of membrane photobioreactors found in the literature

Investigation	Organism used	Scale	Typical duration	Type of membrane	Problems experienced	Solutions presented	Perceived advantages	Reference
Cultivation for harvesting	*Chlorella vulgaris*	25 L	60 days	Silica sheets	Difficulty ensuring a homogenous solution inside the reactor	Immersed agitator	Increased growth rates	(Bilad *et al.*, 2014)
Cultivation for secondary effluent treatment	*Chlorella vulgaris*	25 L	20 days	PVDF[1] hollow-fiber in MF membrane module	Light intensity limitations due to biofilm formation resulted in insufficiently treated effluent	Immobilisation of organism in biofilm on designated surfaces	Biofilm MPBR resulted in better algal growth in comparison to free cell system	(Gao *et al.*, 2015)
Water reclamation and biomass production	Wild type[2] PNSB[3]	8 L x2	433 days	Polyethylene hollow-fiber membrane module	High COD concentration in effluent due to loss of biomass in sludge	Sequencing batch membrane to prevent significant loss of biomass in sludge		(Chitapornpan *et al.*, 2012)

[1] Polyvinylidene flouride

[2] Defined by Merriam-Webster dictionary, wild type refers to 'a phenotype, genotype, or gene that predominates in a natural population of organisms or strain of organisms in contrast to that of a natural or laboratory mutant forms' (Merriam-Webster, no date)

[3] Purple non-sulfur bacteria

Investigation	Organism used	Scale	Typical duration	Type of membrane	Problems experienced	Solutions presented	Perceived advantages	Reference
Optimisation of sewage wastewater treatment, separating HRT and SRT[4]	Microalgal-bacterial combination	550 L x 2	15 days	Hollow-fiber membrane module PURON® Koch Membrane Systems (PUR-PSH31)	Photo-limitation due to high culture concentrations and contamination from other organisms	Design adaptation for flat plate reactor and operation under sterile conditions	No loss of biomass,	(González-Camejo *et al.*, 2019)

[4] Hydraulic retention time and solids retention time

2.6 Bioreactor condition requirements for hydrogen production

To ensure optimal growth of *R. palustris* and ultimately hydrogen production within the photobioreactor system, certain production conditions need to be maintained. Some important operational parameters include temperature, pH, illumination, and feedstock as they greatly affect the operation of the bioreactor system and will be discussed in the subsections below. To ensure the optimal environment for the bacteria, these conditions must be met throughout experimentation.

2.6.1 Operating conditions

2.6.1.1 pH

The optimal pH for bacterial growth varies between bacterial groups; according to optimum pH conditions, bacteria can be classified into three groups: neutrophiles(pH 7±2), acidophiles (pH <5.55) and alkaliphiles (pH 8-10.5).

According to (Pott, 2013), *R. palustris* is a neutrophilic organism. *R. palustris* can tolerate a pH between 5 and 9 although minimal growth and limited hydrogen production was observed for a pH below 5 and a pH above 9. The maximum growth rate and hydrogen production are at an optimum at a pH of 7 when observing performance in a range of pH 5 to 9 (Pott, Howe and Dennis, 2013). In the following Table 10, the pH used in multiple investigations of *R. palustris* are indicated.

Table 10: pH utilized in multiple investigations using *R. palustris* in photofermentation

***R. palustris* strain**	**pH**	**Source**
***R. palustris* NCIMB 11774**	7	(Pott, Howe and Dennis, 2013)
***R. palustris* HCC 2037**	7	(Barbosa *et al.*, 2001)
***R. palustris* CQK 01**	7	(Tian *et al.*, 2010)
***R. palustris* W004**	6.8	(Wu *et al.*, 2010)
***R. palustris* CQK 01**	7	(Guo *et al.*, 2011)
***R. palustris* 42OL**	7 ± 0.05	(Carlozzi and Sacchi, 2001)
***R. palustris* DSM 123**	6.7±0.1	(Basak, Kumar Jana and Das, 2016)

From this it can be concluded that independent of the *R. palustris* strain, the optimal operating pH varies only slightly around pH 7. In investigations where the optimum pH was sought after, the optimum pH for *R. palustris* was found to be exactly pH 7 (Tian *et al.*, 2010; Pott, Howe and Dennis, 2013).

2.6.1.2 Temperature

The optimal temperature for bacterial growth differs significantly; according to optimum temperature conditions bacteria can be classified according to the following groups: mesophiles, psychrotrophs, psychrophiles, thermophiles and hyperthermophiles.

Table 11: Temperature utilized in multiple investigations using *R. palustris* in photofermentation. Temperatures marked by an asterisk (*), indicate that for that specific investigation, the goal was to search for an optimal temperature.

***R. palustris* strain**	**Temperature (°C)**	**Reactor**	**Source**
***R. palustris* NCIMB 11774**	Room temperature	0.1 L Conical flasks/ 0.5L Bottles	(Pott, Howe and Dennis, 2013)
***R. palustris* ATH 2.1.37**	35	0.5 L Bottles	(du Toit and Pott, 2021)
***R. palustris* HCC 2037**	30	0.25 L Rubber-stopper vessels	(Barbosa *et al.*, 2001)
***R. palustris* CGA 009, wild type**	30	0.125 L Serum bottles	(Sabourin-Provost and Hallenbeck, 2009)
***R. palustris* W004**	32	0.35 L Photobioreactors	(Wu *et al.*, 2010)
***R. palustris* CQK 01**	30*	0.125 L Sealed vessel[5]	(Guo *et al.*, 2011)
***R. palustris* 42OL**	30±1	53 L Tubular photobioreactor (partly shaded)	(Carlozzi and Sacchi, 2001)
***R. palustris* DSM 123**	33±1	Triple jacketed vertical annular photobioreactor	(Basak, Kumar Jana and Das, 2016)

From the values seen in Table 11, it can be seen that the average temperature for optimal growth of *R. palustris* varies around 30°C, this is however different from the temperature for optimal hydrogen production. This means that *R. palustris* falls within the mesophilic bacterial growth and grows optimally in the 20 to 45°C range. According to Basak, Kumar Jana and Das (2016), during photofermentation the temperature varies significantly (between 15 and 40°C), which can significantly reduce hydrogen production. Thus, if the goal is to optimise hydrogen production, the temperature of the system must be kept relatively constant. If the culture is exposed to higher temperatures than what is mentioned in the literature, this would result in cell death although if a temperature of the system is below than desired, only hydrogen production will be affected.

In a specific investigation by du Toit and Pott (2021), the growth, hydrogen production and substrate utilisation of *R. palustris* ATH 2.1.37 (also known as NCIMB 11774), which is the strain utilised in this study, was investigated at the range of temperatures observed in the literature (as seen in Table 11). It was found that optimal hydrogen production and cell growth was observed at a temperature of 35°C

[5] In this study, a biofilm photobioreactor was utilized thus the bacterial cells were immobilized (Guo *et al.*, 2011).

2.6.1.3 Illumination

As discussed in previous sections, a secure supply of ATP in bacterial cells is required for efficient hydrogen production during photofermentation. Because ATP synthesis is dependent on light in photosynthetic bacteria, the illumination of the environment the bacteria are growing in is imperative (Chen, Lee and Chang, 2006b). Chen, Lee and Chang (2006) also mention that the wavelength of the light-energy provided is within a specific wavelength between 500 and 1100 nm; the lamps used in the experimentation must suit the required wavelength. An issue that was mentioned, is the poor light conversion efficiency of conventional illumination in photobioreactors; this is because the illumination cannot be situated close to the bacterial culture due to the generation of heat (Chen, Lee and Chang, 2006b). Thus, the two most important characteristics of illumination are both the intensity and the source.

The first, most obvious light source that can be utilised is the sun. The sun is an abundantly available energy source that covers the entire light spectrum and is considered a 'free' light source in terms of cost. Thus, sunlight is commonly used as the light source for photobioreactors that contain photosynthetic bacteria or algae in an industry setting (Chen, Lee and Chang, 2006b). Within lab-scale experiments, incandescent lights are used to mimic sunlight; this is because they are the closest representation of sunlight because the light-emission spectrum of these bulbs are similar to that of sunlight, with an emission wavelength between 800 and 1200 nm as seen in the image below Figure 22.

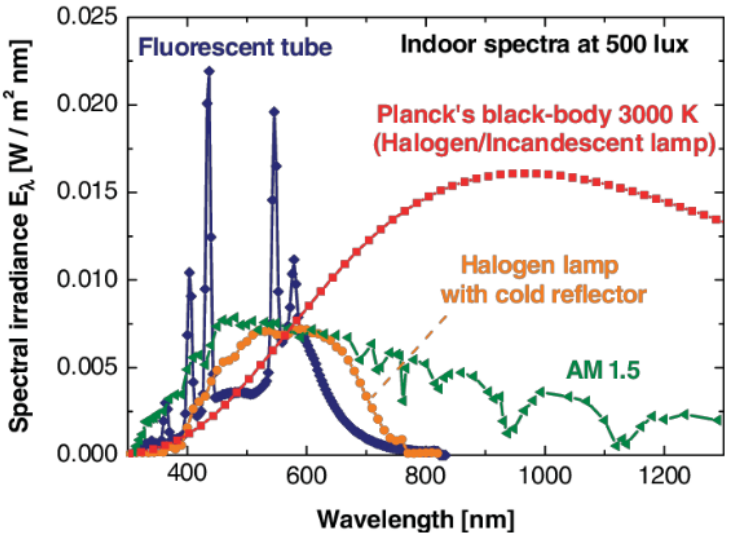

Figure 22: The comparison of emission spectrums for common light sources and those encountered in an outdoor environment. Figure reproduced from Virtuani, Lotter and Powalla (2006).

The light intensity and emission spectrum play a significant role on the bacterial growth and hydrogen production of *R. palustris* (Carlozzi and Sacchi, 2001; Chen, Lee and Chang, 2006b). The intensity of the light source can either be too low, which is known as photo-limitation or the light intensity can be too high, which is known as photoinhibition. During photo-limitation not enough ATP is generated in the bacterial cell and results in poor growth and hydrogen production. During photoinhibition, however,

singlet oxygen (a highly reactive chemical) causes damage to PS II electron transport and the degradation of the D 1 and D 2 reaction centre (Tandori *et al.*, 2001). Visible light can result in damage to protein subunits and/or electron transport within anaerobic organisms due to photoinhibition (Tandori *et al.*, 2001). Although with PNSB water splitting does not occur and photoinhibition is not a concerning factor.

Xiao (2017) stated that for *R. palustris,* photo-limitation occurred with a light intensity ranging from 10.6 to 65.4 W/m^2, deduced from poor hydrogen production. The photo-saturation region occurred between an intensity of 65.4 to 228.9 W/m^2 with a significant increase in hydrogen production. It has also been observed in an investigation by Carlozzi (2009) that when the light intensity surpasses 500 W/m^2, hydrogen production decreases; this is most likely due to photoinhibition.

For this investigation it was decided to operate at a light intensity of 200 W/m^2 as it was observed to be the optimal point for *R. palustris* growth and hydrogen production as it emits the correct wavelength of light, between 800 and 890 nm, for the photosystem of the bacterium (Pott, Howe and Dennis, 2013a; Ross, 2019)

2.6.1.4 Biomass density

As discussed in the previous section 2.6.1.3, an important factor that affects hydrogen production is photo-limitation. Photo-limitation can either occur if the light source is not emitting sufficient illumination and can also occur with mutual shading in the bioreactor (du Toit and Pott, 2021). As the culture concentration increases, the effects of mutual shading increase and the average cell light exposure decreases. The effects of mutual shading can be moderated through reactor design and operating cell concentrations.

An important parameter to verify before experimentation is the starting concentration of the culture to ensure that there is enough bacterial biomass in the system to bypass the lag phase of growth (Section 2.7.3) and start grow in the exponential growth phase. This is to ensure that experimentation does not see stagnant results in the first few days in the lag phase but rather shows bacterial growth and later hydrogen production in the stationary growth phase. This means that during experimentation both the growth of the bacteria in the system can be observed and the point at which hydrogen production starts in the stationary phase can be identified and monitored as the substrate is sequentially utilized.

2.6.2 Potential Stressors

When considering potential physical stressors in the system, the final desired use of this system was considered, the use of the membrane system to treat wastewater continuously while retaining biomass in the reactor system. This also means that, realistically, there would be variation in the inflow stream to the bioreactor such as temperature or glycerol (the acting substrate) concentrations. Other than this, it must be considered that the bacterial cells would be under varying shear and pressure conditions within in the system due to the continuous circulation of the bacteria within the system. In the following paragraphs each potential effect and observations from the literature will be discussed.

One major drawback to the use of a membrane in combination with a photobioreactor is the shear stress induced on bacterial cells as the medium is filtered and the bacteria circulated in the system. Shear stress

does not only come from the membrane but also other physical parts of the membrane system, such as the valve to control backpressure, the pump to circulate the fluid and the mixer to ensure a homogenous mixture inside the reactor. Pressure is another form of stress induced on the bacteria on the system, as the backpressure is required to ensure flow through the membrane. These physical effects may result in morphological variations, cell lysis or changes in metabolism in the cells (Lange, Taillandier and Riba, 2001). Despite this, the exact effect of shear or pressure stress on bacteria is still not well understood. In the investigation by Lange et al. (2001), it was confirmed that the tolerance to shear stress greatly differs between organisms and depends on the composition of the cell wall and the size of the cell. From the (Equation 23) below, it is obvious that resulting shear is a function of viscosity, although there is no literature to support this for use in membranes in combination with bacteria, it was assumed that an increase in viscosity would aid in decreasing resulting shear on bacterial cells.

Significant shear stress was expected to influence the bacterial cells which will most like directly affect cell growth and/or hydrogen production. To decrease the shear stress on the bacteria, many design alterations were considered for instance the choice in valve, pump or the viscosity of the fluid. In order to increase the viscosity of a fluid an inert substance is required, and guar gum was observed to be a commonly used inert in the literature. Thus, it was assumed that the gum would have limited to no effect on the bacteria in the system while increasing the viscosity in the system to decrease the effect of shear. But the compound was not utilised as a substrate for growth in the system. The effect of guar gum on a membrane, however, remains unknown.

It was important to consider the ability to replicate these results in another laboratory, as not all laboratories would use the same mixer. The velocity gradient, otherwise known as the G-value, is a suitable indication of the combination of shear stress and mixing intensity as supplied by a mixer. Which means that the conditions can be replicated without requiring an identical mixer. Thus, the G-value was identified as a good parameter to act as an indication of shear and mixing intensity.

$$G = \sqrt{\frac{P}{\mu \cdot V}} \qquad [\,23\,]$$

Where G(s^{-1}) is the velocity gradient for rapid mixing, P(W) is dissipated power, μ($N \cdot s/m^2$) is dynamic viscosity and V(m^3) is the volume of the mixing tank. Equation 23 was obtained from Stechemesser and Dobiáš (2005).

Another physical factor that might affect cells within the system is temperature, as mentioned in section 2.6.1.2, unfavourable temperatures result in cell lysis or a significantly stunted growth rate as suggested by du Toit and Pott (2021). Also mentioned is the tendency of cultures, that have experienced prolonged exposure to similar conditions, and the resulting lack of adaptability of the same culture to different temperatures (du Toit and Pott, 2021). This would mean that if there were a sudden change in temperature of an inflow stream, this would result in decreased efficiency in hydrogen production and growth rate of the organisms.

The final physical parameter considered is a possible change in available glycerol in the wastewater, a sudden decrease in available nutrients could directly affect the hydrogen production and cell growth in

the system. In an investigation conducted by Pott et al. (2013b), different glycerol concentrations and the resulting cell growth were observed. It was seen that although the cell growth is significantly affected, the bacterial cells did not appear to be severely stressed and simply presented a poor growth rate which would in turn significantly affect hydrogen production(Pott, Howe and Dennis, 2013a).

Due to the significant lack of literature regarding the effect of these physical parameters on the bacterial cells only assumptions could be made regarding their effects. It was assumed that shear and pressure would greatly affect cell death whereas the effect of temperature variation and nutrient deficiencies will have a limited effect on the cells.

2.6.3 Hydrogen productivity

du Toit and Pott (2021) present results indicating the drastic effect of temperature on the specific hydrogen production rate of this specific strain of *R. palustris* (NCIMB 11774). The specific hydrogen production rate provided to be the most efficient at the selected operating temperature of 35°C, as seen in the table summary below (Table 12). 35°C is considered optimal as it's the middle ground between temperatures observed for optimal growth at 30°C and temperatures observed for optimal hydrogen production at around 40°C.

Table 12: Hydrogen production rates at different temperatures, adapted from du Toit and Pott (2021)

Temperature (°C)	**Hydrogen production rate (mL/h)**
30	2.8 ± 0.5
Temperature (°C)	Hydrogen production rate (mL/h)
35	7.7 ± 1.3
40	11.0 ± 0.9

2.7 Performance parameters for bioreactors

2.7.1 Substrate conversion yield

The substrate conversion yield of a carbon source is the ratio between the amount of hydrogen obtained in reality and the theoretical hydrogen yield that is attainable from the amount of substrate available for consumption (Adessi and De Philippis, 2014). When using glycerol as a substrate the following maximum hydrogen yield can be achieved as seen in Equation 24.

$$C_3H_8O_3 + 3H_2O \rightarrow 3CO_2 + 7H_2 \quad [24]$$

Equation 25 displays the equation that can be used to calculate the substrate conversion yield.

$$substrate\ conversion\ (\%) = \frac{H_2 mol\ obtained}{H_2 mol\ theoretical} \times 100 \quad [25]$$

One of the major stumbling blocks in the application of biological processes for hydrogen production is incomplete substrate conversion (Hallenbeck and Ghosh, 2009; Adessi and De Philippis, 2014). Thus, the value of this parameter is critical toward the application of process technology in industry. During the design of photobioreactors, this is considered to be one of the most important parameters.

2.7.2 Specific hydrogen production rate

The specific hydrogen production rate of the system defines the hydrogen production per gram of cell dry weight (CDW) for an hour. The specific hydrogen production ratee can be calculated using Equation 26 below.

$$Specific\ hydrogen\ production\ rate\ \left(\frac{\frac{mL}{g_{CDW}}}{h}\right) = \frac{\left(\frac{H_{2,t_2} - H_{2,t_1}}{\left(\frac{CDW_{t_2} + CDW_{t_1}}{2}\right)}\right)}{t_2 - t_1} \qquad [\ 26\ ]$$

2.7.3 Maximum specific growth rate

The maximum specific growth rate of the bacteria in the system is at the point where the cell division is at a maximum and corresponds to the exponential growth phase of the bacteria according to the growth curve. The maximum specific growth rate can be determined graphically using a plot of the natural logarithm of the biomass concentration (n) versus the time of the experimental run (t) (Clarke, 2013). An example of a bacterial growth curve can be seen in Figure 23 below.

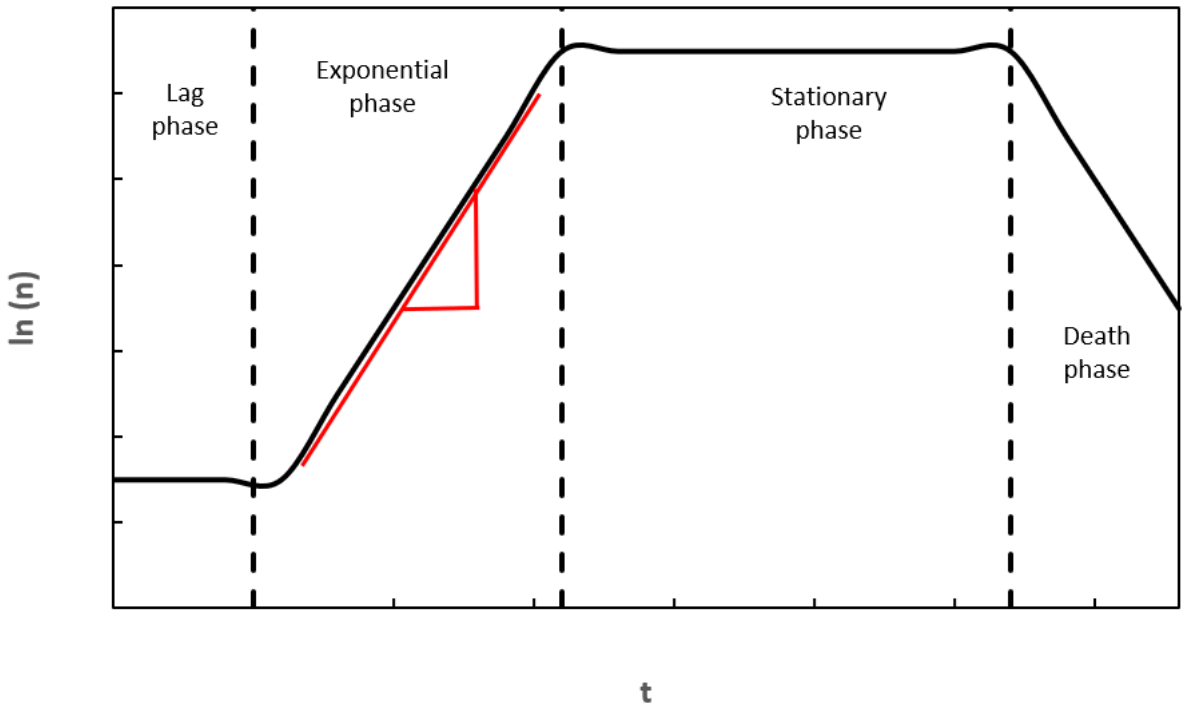

Figure 23: A typical bacterial growth curve

By looking at Figure 23, the maximum growth rate is equal to the slope of the linear section of the growth curve within the exponential growth phase as indicated by the red lines on the graph. Using linear

regression on MS Excel for the linear part of the exponential growth phase, the parameters for the straight line can be obtained and from this the maximum specific growth rate is known.

3 RESEARCH SCOPE

3.1 Aims

The aim of this investigation was to develop and evaluate a membrane photobioreactor (MPBR) for the simultaneous treatment of a glycerol rich wastewater stream, from biodiesel production, and the production of biohydrogen using purple non-sulfur bacteria (PNSB). This thesis will cover the design, fabrication, and operation of a MPBR. As the use of a MPBR is rarely reported in the literature, additional investigations were required to study the interaction of the membrane bioreactor system on the organism, which was defined in this investigation as the 'pathology map'. This membrane photobioreactor was designed to be used for wastewater treatment using the photosynthetic non-sulfur bacteria (PNSB) *Rhodopseudomonas palustris* (*R. palustris*). The wastewater investigated was a synthesized biodiesel waste stream and consisted mainly of glycerol which acted as a substrate for the bacteria. As *R. palustris* has the ability to produce biohydrogen, the photobioreactor was designed in such a way that the glycerol could be metabolised to hydrogen under anaerobic conditions.

In summary, the MPBR was designed to simultaneously support the physical conditions that favour the growth of *R. palustris* by substrate utilisation and conditions that stimulate hydrogen production, which was the eventual goal of the system to act as both a method of wastewater treatment and a source of biohydrogen. This was done by operating the system anaerobically at optimal substrate concentrations, external illumination, and temperature conditions as observed in the literature.

3.2 Objectives

1. Construction of a 'pathology map'

Today, membranes are mostly used in the wastewater industry to separate suspended solids from a wastewater stream or removing biomass from the waste stream. Therefore, in the literature, investigations pertaining to membranes in wastewater treatment are more focused on the fouling of membranes rather than the effect of the membrane on the bacterial cell itself, for example the effect of shear stress, pressure, or nutrient limitations. Due to the ability *of R. palustris* to produce biohydrogen, cell growth, and sufficient accumulation of cells in the reactor are essential for efficient hydrogen production, thus, the effect of the membrane on the cells is a critical factor that must be investigated.

Prior to the operation of the system, certain physical effects of the experimental setup on the bacterial cells were identified that may have a distinct effect on the growth rate of the organism within the system; namely pressure and shear inside the membrane itself, the shear over the valves, possible temperature fluctuations or nutrient limitations in the system. Due to the novel nature of the membrane photobioreactor system in combination with the unknown effect of the physical components of the membrane system, it was necessary to ascertain the extent of these physical parameters on the organism. To do this a 'pathology map' was constructed, where each effect was isolated and the effect on the bacteria observed, in other words we could then answer the question 'did the isolated physical parameter greatly affect the bacterial cell?'. The observations were conducted both visually using scanning electron microscopy (SEM) and by counting the live cells after manipulation, using flow

cytometry (FCM); from this, preliminary conclusions could be made with regards to the effect each specific manipulation had on the bacteria.

2. Design and fabricate a membrane photobioreactor system for use in wastewater treatment using a glycerol rich synthetic wastewater stream and the photosynthetic bacterium *Rhodopseudomonas palustris*

Limited literature is available that considers the use of a membrane photobioreactor system. To bridge this gap in the literature, a membrane photobioreactor was designed, fabricated, and operated with a biological culture in combination with glycerol rich wastewater. Due to the ability of *R. palustris* to produce biohydrogen under anaerobic conditions, the reactor was designed to operate anaerobically, with a light source and a system to measure the hydrogen gas produced. The glycerol rich wastewater was synthesized to ensure the substrate conditions remained consistent throughout experimentation. Under this design objective, considering the main component of the system is a membrane, it was necessary to further investigate appropriate operating conditions to ensure efficient membrane performance.

3. Evaluation of membrane photobioreactor performance in the batch (closed loop) operation mode

As mentioned previously, literature investigating the use of a membrane photobioreactor is very limited. In the case of *R. palustris*, there is no literature available discussing the effect of the membrane on bacterial cell growth and consequently no literature on the effect of the membrane on hydrogen production. This objective investigated the effect of a batch configuration on the cell growth and hydrogen production of *R. palustris*.

Prior to batch mode operation a control run where the culture is recirculated through the membrane and back into the reactor without permeation observing the selected performance parameters (growth, hydrogen production and substrate utilisation). This acts as a 'base case' for the eventual evaluation of both the continuous and batch mode membrane photobioreactors. In the batch operation mode, the culture is recirculated through the membrane and back into the reactor and all permeate is also recycled back into the reactor and the selected performance parameters are observed.

4. Evaluation of membrane photobioreactor performance in the continuous operation mode

Next, the performance of *R. palustris* hydrogen production was investigated under a continuous operation reactor configuration. The difference between the batch and continuous operation was that the substrate concentration did not decrease over time, but rather stayed relatively constant due to new wastewater being fed into the system at a constant rate. The effect of this on cell growth and hydrogen production was observed.

If this membrane technology is to be applied in industry, the system would have to perform well under continuous condition operation to be considered economically viable (Hallenbeck and Ghosh, 2009). Thus, it was critical to observe the growth, substrate utilisation efficiency of bacterial cells and resulting hydrogen production under continuous operation to draw a conclusion regarding the viability of this system for use in industry.

3.3 Key questions

1. What is the effect on cell growth and cell death when *R. palustris* is used in a membrane photobioreactor system? Which factors must be considered?
2. In what way is *R. palustris* affected by shear, temperature, pressure and nutrient limitations?
3. Is there a simple way to decrease shear in a MPBR system?
4. What is the comparison between the growth rate, substrate utilisation and hydrogen production of *R. palustris* when passed through the membrane and recycled back into the reactor and the performance of *R. palustris* cultured in a batch setup?
5. Does the use of a membrane affect hydrogen production? If so, why would the membrane affect hydrogen production?
6. Can the membrane photobioreactor system be run continuously with effective hydrogen production and cell growth?

4 METHODOLOGY

4.1 Bacterial culturing

4.1.1 Materials

In the table below (Table 13), the chemical reagents that were used in experimentation are listed. Alongside each chemical the respective chemical formula, purity and supplier is list provided.

Table 13: List of all chemicals used during experimentation along with purity and source

Chemical	Formula	Purity	Source
Acetone	$(CH_3)_2CO$	≥99.5	Merck
Bacteriological agar	-	-	Biolab Diagnostics Laboratory Inc.
Boric acid	H_3BO_3	99	Unilab
Calcium chloride	$CaCl_2 \cdot 2H_2O$	99	Merck
Cobalt (II) chloride	$CoCl_2.6H_2O$	97	Merck
Copper (II) chloride	$CuCl_2.6H_2O$	97	Merck
Cyanocobalamin	$C_{63}H_{88}CoN_{14}O_{14}P$	≥98	Sigma-Aldrich
Dipotassium phosphate	K_2HPO_4	98	Merck
Ethanol	C_2H_6O	99.9	Science World
Ferric citrate	$C_6H_5FeO_7$	TG[6]	Sigma-Aldrich
L-Glutamic acid monosodium	$C_5H_8NNaO_4$	≥98	Sigma-Aldrich
Glycerol	$C_3H_8O_3$	99	Science World
Magnesium sulfate	$MgSO_4 \cdot 7H_2O$	≥99	Kimix
Manganese(II) chloride	$MnCl_2.4H_2O$	≥99	Sigma-Aldrich
Methanol	CH_3OH	≥99	Science World
Monopotassium phosphate	KH_2PO_4	≥99	Sigma-Aldrich
Nickel (II) chloride	$NiCl_2.6H_2O$	≥97	Sigma-Aldrich
Para-aminobenzoic acid	$C_7H_7NO_2$	≥99	Sigma-Aldrich
Potassium chloride	KCl	98	Sigma-Aldrich
Sodium chloride	NaCl	99	Merck

[6] TG – Technical Grade

Chemical	Formula	Purity	Source
Sodium hydroxide	NaOH	98	Merck
Sodium molybdate	$Na_2MoO_4.2H_2O$	≥99.5	UnivAR
Sodium thiosulfate	$Na_2S_2O_3$	99	Science World
Thiamine hydrochloride	$C_{12}H_{18}Cl_2N_4OS$	AG[7]	Sigma-Aldrich
Yeast Extract	-	-	Biolab Diagnostics Laboratory Inc.
Zinc Chloride	$ZnCl_2$	≥97	Merck

4.1.2 Culture

In this investigation, the specific strain of *R. palustris* used was NCIMB 11774 (otherwise known as ATH 2.1.37) and was obtained via a lyophilized culture purchased from the NCIMB.

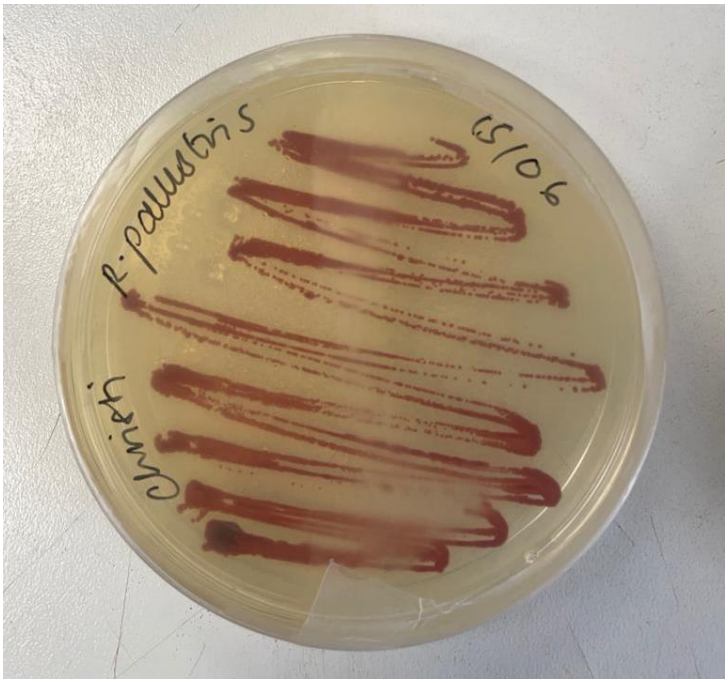

Figure 24: *Rhodopseudomonas palustris* NCIMB 11774 streaked on fast growing van Niels nutrient agar

4.1.3 Culture medium

4.1.3.1 Liquid medium

a) Minimal medium

The nutrient components and concentrations of the liquid minimal medium for bacterial growth were obtained from Pott (2013). There are three main components of the liquid minimal medium: bulk

[7] AG – Analytical Grade

nutrients, buffers, and sterile additions. In the following Table 14, the concentrations are given to make a litre of minimal medium.

Table 14: The nutrient components and concentrations required to make 1 litre of liquid minimal medium according to Pott (2013).

Solution	Components	Concentration (g/L)
Buffers	KH_2PO_4	1.7
	K_2HPO_4	1.7
Bulk nutrients	Yeast extract	0.2
	$MgSO_4 \cdot 7H_2O$	0.2
	$CaCl_2 \cdot 2H_2O$	0.05
	NaCl	0.4
	$Na_2S_2O_3$	0.15
	Ferric citrate	0.005
	Para-aminobenzoic acid	0.002

To the bulk nutrients, the sterile additions need to be added to complete the minimal medium. The sterile additions consist of three different solutions: trace element solution, vitamin solution and the carbon and nitrogen sources. To the 1 litre of solution, 1 ml of the trace element solution and 1 ml of the vitamin solution must be added. For the carbon and nitrogen sources, a glycerol stock solution was made and 10 mL was added to achieve a glycerol concentration of 50mM; similarly for glutamate, a stock solution was made and 4mL was added to achieve a glutamate concentration of 10 mM. The components and concentrations required for the sterile additions to minimal medium can be seen in Table 15 below.

Table 15: Components and concentrations required for sterile additions to the minimal medium as observed in Pott et al. (2013a)

Solution	Components	Concentration (g/L)
Trace elements	$ZnCl_2$	0.07
	$MnCl_2.4H_2O$	0.1
	H_3BO_3	0.06
	$CoCl_2.6H_2O$	0.2
	$CuCl_2.2H_2O$	0.02
	$NiCl_2.6H_2O$	0.02
	$Na_2MoO_4.2H_2O$	0.04

Solution	Components	Concentration (g/L)
Vitamin solution	Thiamine HCl	1.2
	Cyanocobalamin	0.001
Carbon source	Glycerol	50mM
Nitrogen source	Glutamate	10mM

The medium was prepared by the addition of the bulk nutrients and the buffers to deionized water. To ensure a sterile solution, the buffers and bulk nutrients were autoclaved at a temperature of 121°C and a pressure of 101kPa for 40 minutes. The vitamin solution was filter sterilized and after complete sterilisation, the sterile additions were added to the liquid medium aseptically in a sterile laminar flow cabinet.

b) Van Niels medium

Another liquid medium that was used in this investigation is an adjustment of the Van Niels Yeast Broth (ATSS Medium 112) with the addition of glycerol as a carbon source. In Table 16 below, the concentrations and components for the adjusted Van Niels yeast broth is given. This liquid medium was later also used to identify contamination during experimentation.

Table 16: Components and concentrations required for the preparation of Van Niels Yeast Broth

Solution	Component	Concentration (g/L)
Van Niels Yeast Broth	K_2HPO_4	1
	$MgSO_4.7H_2O$	0.5
	Yeast Extract	10
Carbon source	Glycerol	40mM

The medium was prepared by the addition of the Van Niels yeast broth components to deionized water and then mixing. The pH of the mixture was then adjusted to 7 ± 0.2 with NaOH (Pott, Howe and Dennis, 2013). After this the solution was sterilised by autoclaving at a temperature of 121°C and a pressure of 101kPa for 40 minutes. The glycerol solution was autoclaved separately and added to the Van Niels yeast broth aseptically prior to sterilization of both solutions. A 10 mL of the 4 M glycerol stock solution was added, aseptically in a laminar flow cabinet, to 1 L van Niels medium to achieve a final concentration of 40 mM glycerol.

4.1.3.2 Solid media

In this investigation, two different types of solid media were used. The first is a fast-growing medium, to check for contamination during experimental runs, to ensure the growth of *R. palustris* alone is being observed. The second is a long-term storage medium which is required for master plates.

a) Fast-growing medium to check for contamination

For the entire experimental procedure, it was critical to work completely sterile, to avoid contamination by any other bacteria which would result in variation of results. Thus, to ensure reliable results, each experimental run was tested for contamination using a solution made of Van Niels yeast broth with no additions (as seen in section 4.1.3.1(b)).

For a litre of Van Niels yeast broth, 20 g of bacteriological agar was dissolved at an elevated temperature (80°C) using a magnetic stirrer. The solution was then sterilised by autoclaving at a temperature of 121°C and a pressure of 101 kPa for 40 minutes. All undissolved agar was dissolved at the high temperature in the autoclave. The liquid agar was left to cool to a temperature of roughly 60°C after which 10 mL of a 5 M glycerol solution was added aseptically in a laminar flow cabinet. Also in this sterile environment, 25 mL liquid agar was then pipetted onto the agar plates and left to solidify.

b) Long term storage medium

The long-storage medium was prepared with a method similar to the preparation of fast-growing medium. To prepare this medium, 15 g of bacteriological agar was dissolved in 1 L minimal media (as seen in section 4.1.3.1(a)) using a magnetic stirrer operating at an elevated temperature (80°C). From here the solution was sterilized by autoclaving at a temperature of 121°C and a pressure of 101 kPa for 40 minutes. Similarly, when the solution had cooled to roughly 60°C, 10 ml of a 5 M glycerol solution was added aseptically in a laminar flow cabinet. In the same sterile environment, 25 mL of the liquid agar was then pipetted onto the agar plates and left to solidify.

4.1.4 Bacterial culturing

4.1.4.1 Inoculum

To decrease the time required for bacterial cultures to attain the stationary growth phase (the growth phase in which hydrogen production takes place), the membrane photobioreactor was loaded with an inoculum at the start of experimentation. Thus, the bacterial cultures that were used for the inoculation of the photobioreactor were grown in an airtight glass reagent bottle prior to inoculation. Figure 25 below, is a schematic of the setup required to grow the inoculum.

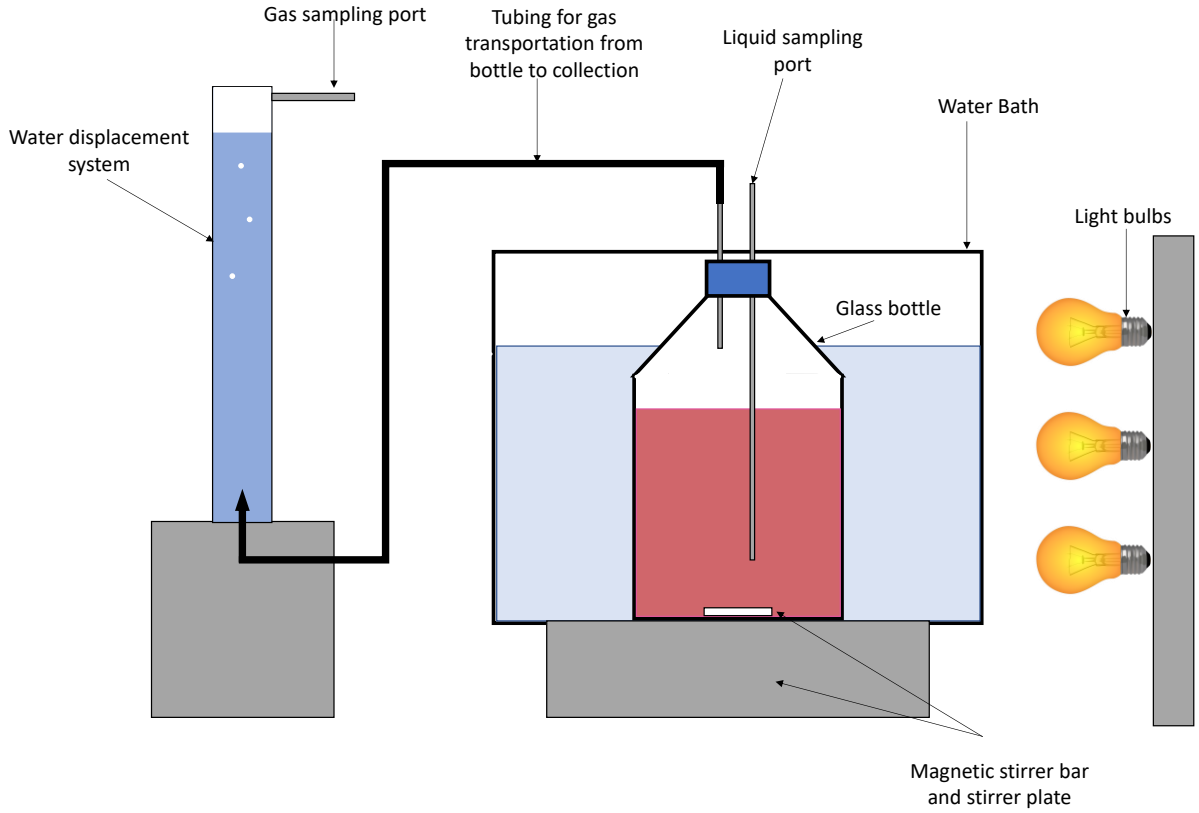

Figure 25: A schematic of the setup required to culture inoculum.

To prepare the inoculum, the liquid medium (minimal medium) was added to the glass reagent bottle aseptically (in a laminar flow cabinet) and *R. palustris* was added by scooping a loop of bacteria off an agar plate, into the liquid medium. After 48 hours of growth in a 35°C water bath, the liquid medium could then be aseptically transferred from the inoculum to the desired culture for growth. For the duration of growth, the culture was agitated using a magnetic flea and stirrer.

A tube was connected from the Schott bottle to the gas collection point. The gas collection point was a water displacement system; as the gas flows into the water-filled cylinder, the water was displaced downward, and a volumetric gas measurement can be read off the cylinder. Also present on this cylinder was gas sampling port, to analyse the composition of the produced gas.

All tubing specifications can be observed in Appendix B - Specifications of design choices.

4.1.4.2 Glass bottle (Schott bottle) bioreactors

As mentioned previously, the photobioreactors used in experimentation were inoculated using the cultured inoculum from the system described in section 4.1.4.1. To ensure the starting concentration was above a certain threshold, requiring only short-term growth within the reactor until stationary phase hydrogen production was attained. A sufficient volume (depending on the concentration of the inoculum and liquid culture volume) of the inoculum was added to ensure that the starting concentration was approximately 0.75 g/L when measuring the OD at a wavelength of 660 nm.

4.2 Membrane photobioreactors

In the following subsections, the fabrication of the MPBR, experimental procedure used to obtain the operational parameters and operation of various modes of the MPBR will be discussed. The reasoning behind certain design choices is discussed in in the results and discussion (section 5.2).

4.2.1 Fabrication

In the following table (Table 17), the equipment used to conduct experimentation is displayed. The same equipment was used for the control, batch and continuous mode operation of the MPBR.

Table 17: A list of the equipment used in the investigation and specification

Unit	Specification	Link to specific detail
Piping main reactor network	Tygon A-60-G	Table 41
Piping hydrogen gas collection	Tygon S3 B-44-3	Table 42
Reactor	500 mL Schott bottle	-
Membrane	Ceramic (Al_2O_3), 100 kDa, 50 cm^3	Table 46 & Figure 88
Valve	Stainless steel diaphragm valve, ND[8] of 6mm	Table 40 & Figure 85
Pressure gauge	0-250 kPa	Figure 90
Membrane feed pump	Peristaltic, Runze fluid	Table 44 & Figure 86
Dosing pump	Peristaltic, CR pump	Table 45 & Figure 87

4.2.2 Determination of operating parameters

4.2.2.1 Flux determination procedure

a) Pure water flux

As mentioned in (Section 2.5), the pure water flux is required to observe the fouling of the membrane during its' use to ensure that the membrane at the starting point of experimentation is similar to other experiments to reduce experiment related error. The method used to develop the pure water flux curve for the desired operating conditions were obtained from Choi et al. (2005) and Le Clech et al. (2003). A graph illustrating the flux-step method can be seen in the figure (Figure 26) below.

The flux was recorded with increasing pressure up to a selected point and similarly decreased back to a pressure of 0. This was to ensure that the water used was pure and salts commonly present in water has not fouled the membrane; if the flux values observed are lower for each set pressure value this is an

[8] ND – Nominal diameter

indication that the water used has fouled the membrane. The resulting flux changes as the pressure and fluid velocity change thus it was important to maintain a constant fluid velocity throughout experimentation to ensure a comparable flux at each given temperature. It is critical to use pure water as most sources of water contain salts which foul the membrane.

The operating conditions chosen was a fluid velocity of 5.6 ml/min (0.34 L/h), meaning a turnover rate of once every two hours. The pump speed of 100 rpm was chosen to ensure this fluid velocity.

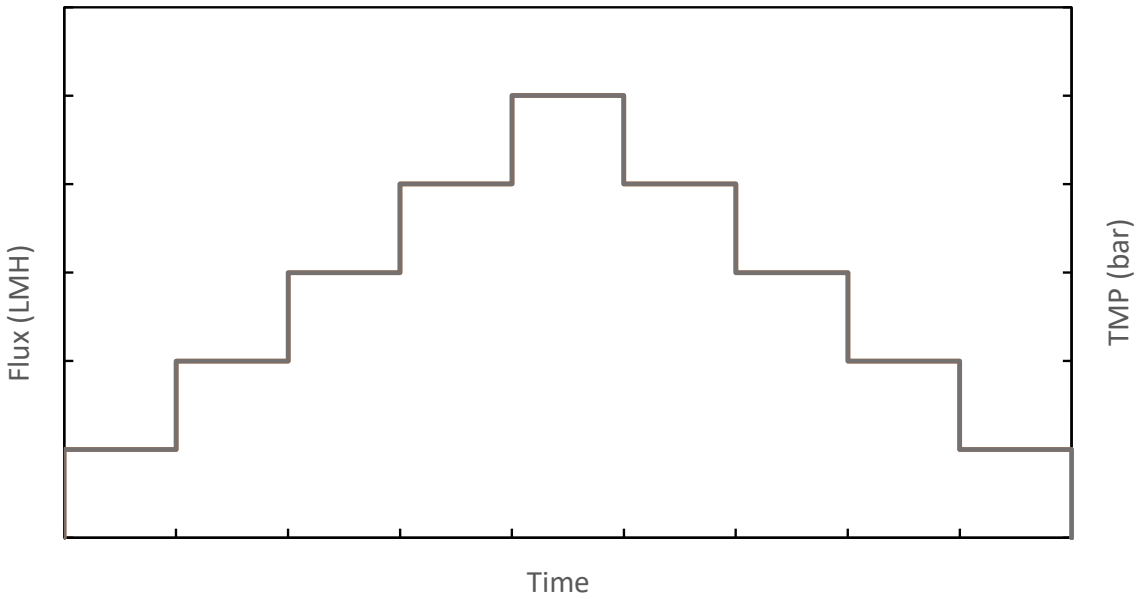

Figure 26: Graphic illustration of the flux-step method, adapted from Le Clech et al. (2003)

To set up the experimentation (as seen in Figure 27 below) pure water was placed the glass Schott bottles, these are the same glass bottles that were also utilized in experimentation as photobioreactors. The pump was turned on to the desired pump speed and the water started circulating through the system. From here a stepwise increase in the pressure was executed in increments of 0.1 bar by partially closing the diaphragm valve (see Appendix B - Specifications of design choices for valve specifications) and observing the resulting pressure change in the pressure gauge. After a pressure increase was made, the flux would increase until reaching a constant value after a few minutes (roughly 3 minutes), this was monitored by using the measuring cylinder and a stopwatch; the resulting constant flux value is then recorded for each pressure value. The pressure was increased up to a value of 0.7 bar. The flux values at higher pressures were not investigated because the final operating flux would be lower than this to ensure the turnover rate of the system is not too high.

Once the flux values for up to 0.7 bar were obtained, a step decrease in pressure was conducted in a similar fashion up to 0 bar. From here, a curve was constructed that related flux as a function of pressure for a constant fluid velocity. These figures can be seen in the Appendix B - Specifications of design choices.

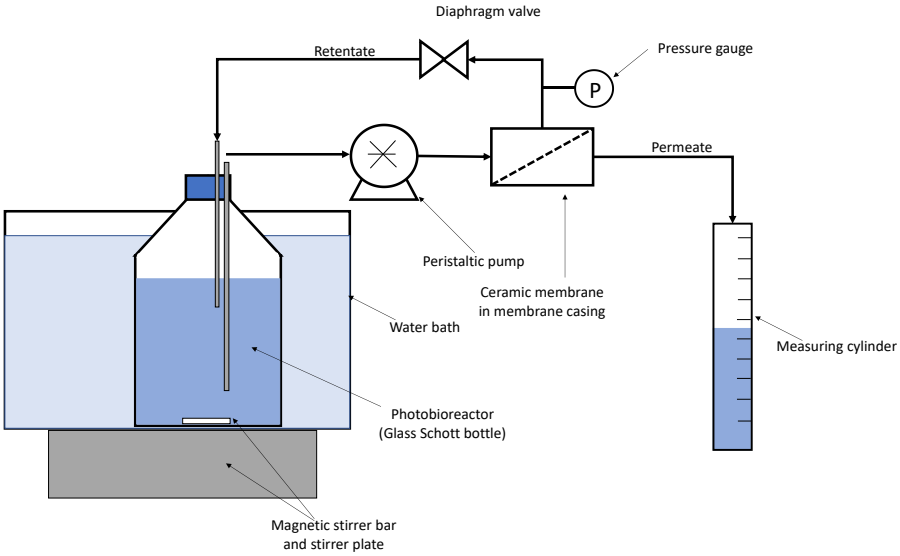

Figure 27: Experimental setup for the determination of the pure water flux for the membrane system using the 'bucket and stopwatch method' to measure flux and manipulation of the diaphragm valve.

b) Critical flux

To determine the critical flux of the system, an identical experimental setup was used Figure 26 and a similar experimental procedure was followed. Instead of pure water, a stationary phase culture of *R. palustris* was used at a biomass concentration of 3.8 g/L and the setup can be seen in Figure 28. The difference however between the use of pure water and the culture containing biomass is that a certain pressure value, the critical flux would be reached. Thus, when doing the stepwise increments, it was necessary to ensure that the flux had reached a steady state value before increasing the pressure again.

A stepwise increase in the pressure was executed in increments of 0.1 bar by partially closing the diaphragm valve and observing the resulting pressure change in the pressure gauge. After a pressure increase was made, the flux would increase until reaching a constant value after a few minutes, this was monitored by using the measuring cylinder and a stopwatch; the resulting constant flux value is then recorded for this pressure value.

This procedure was followed up to the pressure value where it was observed that the flux value does not reach a steady state value but instead, with prolonged operation under these pressure conditions the flux started to decrease, and pressure increased. This correlates to the definition of critical flux (section 2.5.1.3), when a membrane is operated with a flux at or above the critical flux, fouling occurs in the membrane resulting in progressively poorer filtration.

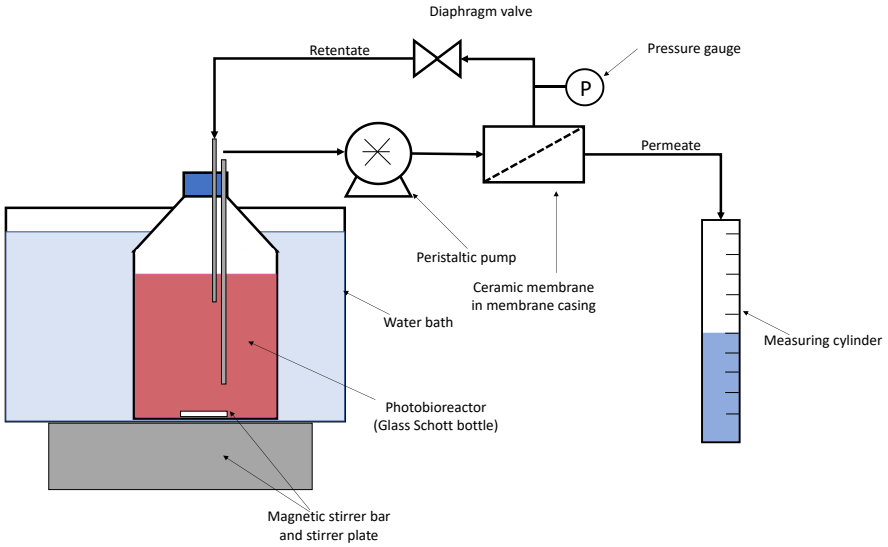

Figure 28: Experimental setup for the determination of the critical water flux for the membrane system

4.2.2.2 Operating flowrate

The operating flowrate of the system is dependent on the desired turnover rate of the culture in the system. Turnover rate is the time in which the entire volume inside the reactor has circulated once in the system. A slower turnover rate would result in decreased reactor capacity, slower delivery of a permeate although a faster turnover rate would result in increased stress on the cells and significantly reduced exposure to the light source which is essential for efficient hydrogen production. There was no literature available on ideal turnover rates and it was assumed that a turnover rate of once every six hours is appropriate.

The operating flowrate chosen was a fluid velocity of 0.113 L/h, meaning a turnover rate of once every six hours. The pump speed was chosen based on the resulting turnover rate to ensure that the residence time of the bacteria in the reactor bottle is increased and that the cells are not constantly in circulation in the piping network.

4.2.3 Control (closed loop) mode operation of the MPBR

For control mode operation, the goal was so isolate the effect of the circulation on the culture. For this experimental setup, the valve in the retentate network was removed, meaning that there was no backpressure in the system and there was no permeate stream. The retentate was recycled back into the reactor.

A schematic of the control mode membrane photobioreactor (MPBR) setup can be seen in Figure 30 below. Similar to the schematic seen in Figure 25 for bacterial culturing, a water displacement system was used to collect the gas produced in the photobioreactor. The same 100 W incandescent light bulbs were also used for illumination in the experimental setup. To achieve a 200 W/m^2 light intensity, a handheld lap photometer was used to ensure measure light intensity, which ensured the distance from illumination source was correct and accounting for interference from the reactor glass wall, water bath

wall and water. Temperature was controlled for the photobioreactor through submersion in a water bath, the temperature of the water bath was maintained at 35°C using a temperature controlled at all times to ensure the photobioreactor operates at the ideal temperature for *R. palustris* growth. Mixing in the reactor is achieve using a magnetic flea; the photobioreactor was placed in the water bath on top of a magnetic stirrer plate.

A peristaltic pump (see Appendix B - Specifications of design choices for pump specifications) was used to pump culture from the glass reactor bottle, through the membrane as permeate or as retentate back into the reactor. The membrane was stored inside stainless-steel housing so that the entire reactor system can be autoclaved to ensure complete sterility. Sampling ports were present in the gas collection cylinder (water displacement system), the retentate and membrane feed piping. The fluid velocity was maintained at 0.113 L/h with a pump speed of 100 rpm for experimentation during batch and continuous operation, meaning a turnover rate of once every six hours. Several factors influenced piping selection and a more detailed discussion of the design decisions can be seen in section 5.2.

To set up the MPBR, an inoculum was prepared as discussed in section 4.1.4.1, and a medium was inoculated, in a sterile laminar flow cabinet, to have a starting biomass concentration of 0.75 g/L. Prior to connecting the reactor to the glass bottle containing the culture, the entire reactor system was completely assembled (as depicted in Figure 29) and autoclaved at a temperature of 121°C and 101 kPa for 40 minutes to ensure complete sterility. An additional 180 mL of minimal media was added to the reactor aseptically to account for the volume of fluid in the piping and have sufficient liquid volume in the reactor. The total liquid volume in the reactor was then 680 mL. The reactor cap was aseptically connected to the inoculated medium in the glass bioreactor and the bioreactor was placed in the temperature-controlled water bath. The pump was switched on with a speed of 100 rpm, the system was allowed to flood with fluid. The reactor cap was connected to the hydrogen collection port and the system was left for the duration of the experiment.

Sampling was conducted daily through the sampling ports located in the retentate and feed piping network using 2mL sterile syringe. To determine the cell concentration, the OD of the sample was measured at 660nm (the procedure is described in section 4.4.1). The samples were then centrifuged (Eppendorf Minispin Plus) for 5 minutes at 13900 x *g* rpm. The supernatant was removed and placed in a storage vial and frozen at -20°C, until glycerol concentration analysis by HPLC (section 4.4.3) was conducted.

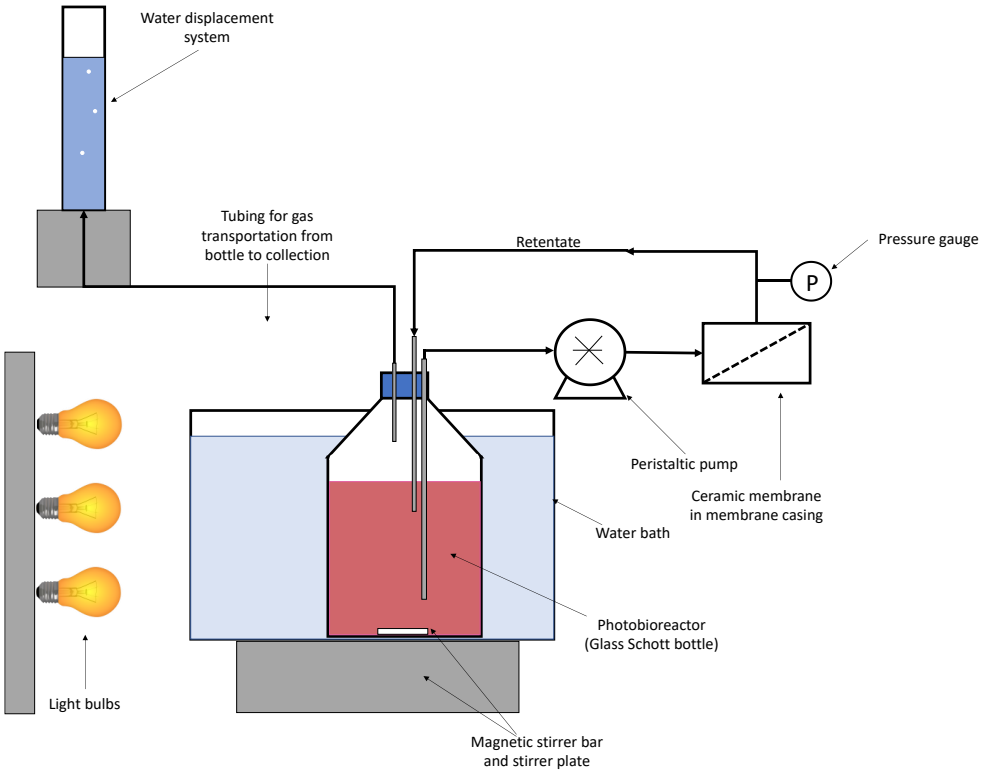

Figure 29: Diagram of experimental setup used to operate the MPBR under control mode operation

4.2.4 Batch (closed loop) operation mode of the MPBR

A schematic of the batch membrane photobioreactor (MPBR) setup can be seen in Figure 30 below. Similar to the schematic seen in section 4.1.4 for bacterial culturing, a water displacement system was used to collect the gas produced in the photobioreactor. The same 100 W incandescent light bulbs were also used for illumination in the experimental setup. To achieve a 200 W/m^2 light intensity, a handheld lap photometer was used to ensure measure light intensity, which ensured the distance from illumination source was correct and accounting for interference from the reactor glass wall, water bath wall and water. Temperature was controlled for the photobioreactor through submersion in a water bath, the temperature of the water bath was maintained at 35°C using a temperature controlled at all times to ensure the photobioreactor operates at the ideal temperature for *R. palustris* growth. Mixing in the reactor is achieve using a magnetic flea; the photobioreactor was placed in the water bath on top of a magnetic stirrer plate.

A peristaltic pump (see Appendix B - Specifications of design choicesfor pump specifications) was used in this investigation due to both the ease of use and non-invasive nature; the most important factor that was considered for experimentation was maintaining completely sterile conditions inside the reactor system. From the glass reactor bottle, the culture was pumped through the membrane. The membrane used was an Atech single-channel ultrafiltration (UF) ceramic (Al_2O_3) membrane element with an active surface area of 50 cm^3 and a selectivity of 100 kD; specifications can be seen in Appendix B - Specifications of design choices. The membrane is stored inside stainless-steel housing so that the entire reactor system can be autoclaved to ensure complete sterility. After the membrane, a diaphragm valve is used to

increase the pressure to ensure sufficient flow through the membrane. Valve specifications can be observed in Appendix B - Specifications of design choices. Between the membrane and the valve, a pressure gauge was placed to read to backpressure applied by the valve in the membrane to ensure the system is operating at the desired flux value.

For the batch experimentation runs, both the permeate and the retentate were recycled back into the reactor. Sampling ports were present in the gas collection cylinder (water displacement system), the retentate, permeate and membrane feed piping. The fluid velocity was maintained at 0.113 L/h with a pump speed of 100 rpm for experimentation during batch operation, meaning a turnover rate of once every six hours. Several factors influenced piping selection and a more detailed discussion of the design decisions can be seen in (section 5.2).

To set up the MPBR, an inoculum was prepared as discussed in section 4.1.4.1, and a medium was inoculated, in a sterile laminar flow cabinet, to have a starting biomass concentration of 0.75 g/L. Prior to connecting the reactor to the glass bottle containing the culture, the entire reactor system was completely assembled (as depicted in Figure 30) and autoclaved at a temperature of 121^{o}C and 101 kPa for 40 minutes to ensure complete sterility. An additional 180 mL of minimal media was added to the reactor aseptically to account for the volume of fluid in the piping and have sufficient liquid volume in the reactor. The total liquid volume in the reactor was then 680 mL. The reactor cap was aseptically connected to the inoculated medium in the glass bioreactor and the bioreactor was placed in the temperature-controlled water bath. The pump was switched on with a speed of 100 rpm, the system was allowed to flood with fluid. When it was assumed that the piping was flooded the valve was slowly closed until the pressure gauge indicated the pressure reading of 0.35 bar. The reactor cap was connected to the hydrogen collection port and the system was left for the duration of the experiment.

Sampling was conducted daily through the sampling ports located in the permeate, retentate and feed piping network using 2mL sterile syringe. To determine the cell concentration, the OD of the sample was measured at 660 nm (the procedure is described in section 4.4.1). The samples were then centrifuged (Eppendorf Minispin Plus) for 5 minutes at 13900 x *g* rpm. The supernatant was removed and placed in a storage vial and frozen at -20^{o}C, until glycerol concentration analysis by HPLC (section 4.4.3) was conducted.

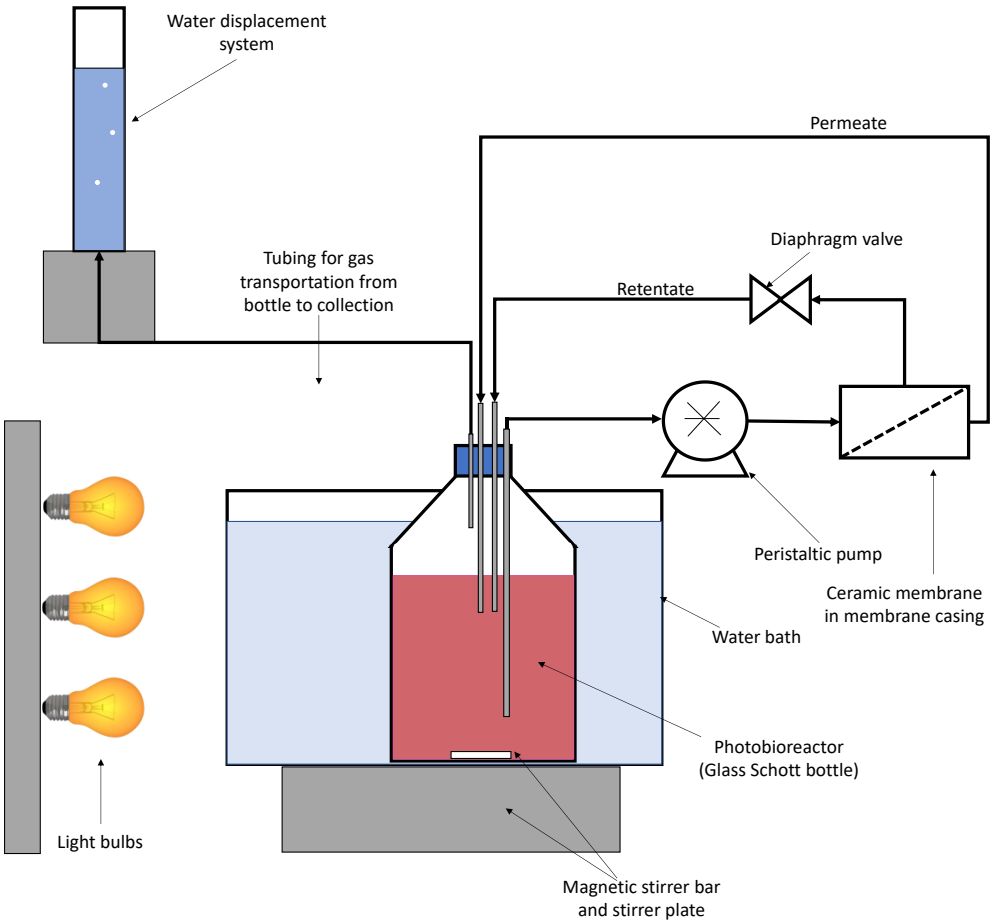

Figure 30: Schematic of a closed loop (batch) membrane photobioreactor setup

4.2.5 Continuous operation mode of the MPBR

A schematic of the continuous membrane photobioreactor (MPBR) setup can be seen in Figure 30 below. Similarly, a water displacement system was used to collect the gas produced in the photobioreactor. The same 100 W incandescent light bulbs were also used for illumination in the experimental setup. To achieve a 200 W/m^2 light intensity, a handheld lap photometer was used to ensure measure light intensity, which ensured the distance from illumination source was correct and accounting for interference from the reactor glass wall, water bath wall and water. Temperature was controlled for the photobioreactor through submersion in a water bath, the temperature of the water bath was maintained at 35^{o}C using a temperature controlled at all times to ensure the photobioreactor operates at the ideal temperature for *R. palustris* growth. Mixing in the reactor is achieve using a magnetic flea; the photobioreactor was placed in the water bath on top of a magnetic stirrer plate.

A peristaltic pump (seeAppendix B - Specifications of design choicesfor pump specifications) was used to pump the culture from the glass reactor bottle through the membrane (see Appendix B - Specifications of design choicesfor pump specifications). The membrane is stored inside stainless-steel housing so that the entire reactor system can be autoclaved to ensure complete sterility. After the membrane, a diaphragm valve is used to increase the pressure to ensure sufficient flow through the membrane. Valve

specifications can be observed in Appendix B - Specifications of design choices. Between the membrane and the valve, a pressure gauge was placed to read to backpressure of 0.35 bar.

For the continuous experimentation runs, the retentate was recycled back into the reactor and the permeate was fed to a different collection bottle. Sampling ports were present in the gas collection cylinder (water displacement system), the retentate, permeate and membrane feed piping. The fluid velocity was maintained at 0.113 L/h with a pump speed of 100 rpm for experimentation during operation, meaning a turnover rate of once every six hours. Several factors influenced piping selection and a more detailed discussion of the design decisions can be seen in (section 5.2).

To set up the MPBR, an inoculum was prepared as discussed in section 4.1.4.1, and a medium was inoculated, in a sterile laminar flow cabinet, to have a starting biomass concentration of 0.75 g/L. Prior to connecting the reactor to the glass bottle containing the culture, the entire reactor system was completely assembled (as depicted in Figure 31) and autoclaved at a temperature of 121^{o}C and 101 kPa for 40 minutes to ensure complete sterility. An additional 180 mL of minimal media was added to the reactor aseptically to account for the volume of fluid in the piping and have sufficient liquid volume in the reactor. The total liquid volume in the reactor was then 680 mL. The reactor cap was aseptically connected to the inoculated medium in the glass bioreactor and the bioreactor was placed in the temperature-controlled water bath. The pump was switched on with a speed of 100 rpm, the system was allowed to flood with fluid. When it was assumed that the piping was flooded the valve was slowly closed until the pressure gauge indicated the pressure reading of 0.35 bar. The reactor cap was connected to the hydrogen collection port and the system was left for the duration of the experiment.

Sampling was conducted daily through the sampling ports located in the permeate, retentate and feed piping network using 2 mL sterile syringe. To determine the cell concentration, the OD of the sample was measured at 660 nm (the procedure is described in section 4.4.1). The samples were then centrifuged (Eppendorf Minispin Plus) for 5 minutes at 13900 x *g* rpm. The supernatant was removed and placed in a storage vial and frozen at -20^{o}C, until glycerol concentration analysis by HPLC (section 4.4.3) was conducted.

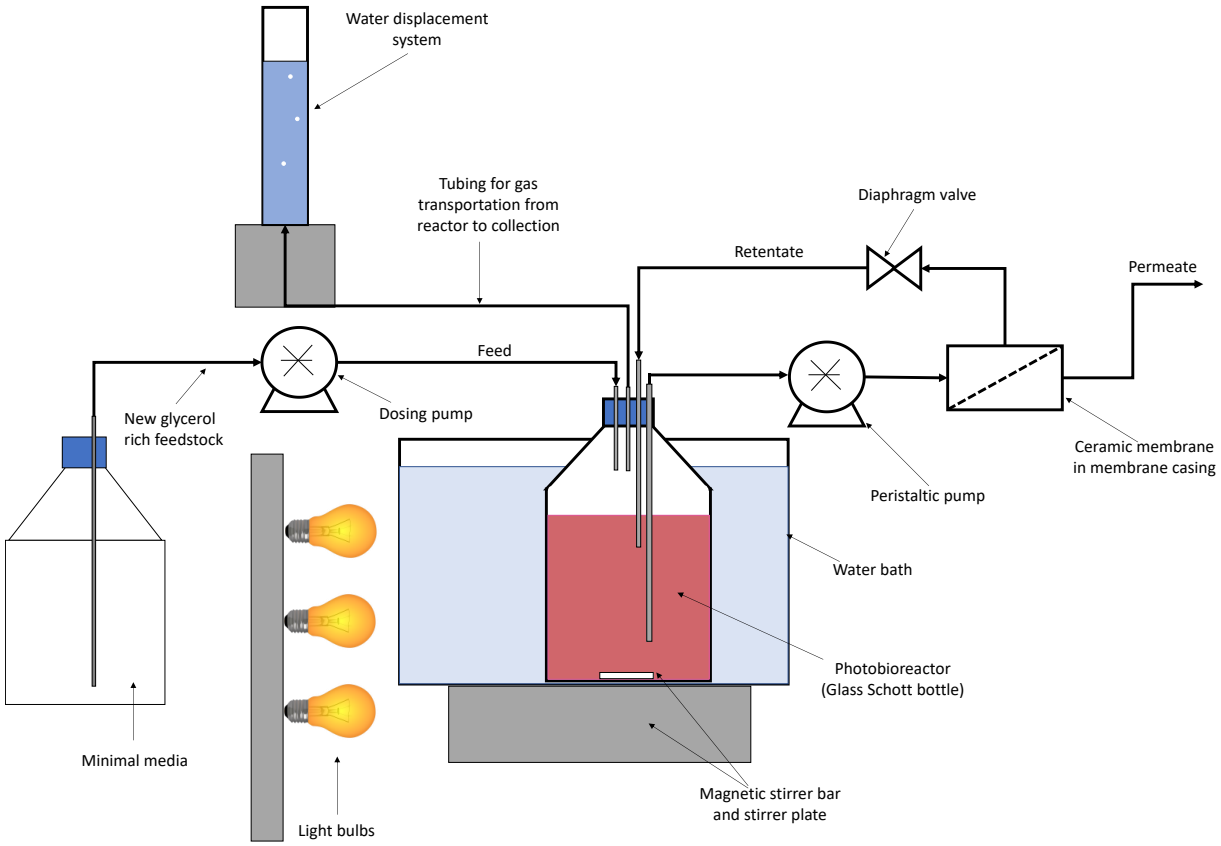

Figure 31: Schematic of the continuous membrane photobioreactor setup

4.3 Pathology map

4.3.1 Overview

In this section the experimental procedure that was followed to isolate the grown cultures under different desired physical conditions using the one-factor-at-a-time method (OFAT method) are discussed. This experimentation was conducted to obtain results that indicate the effect of each physical condition on the culture. Background information regarding the analytical technique can be seen in Appendix A – Analytical Techniques.

All cultures used for the pathology map experimentation were grown in van Niels medium for about 3-4 days, and experimentation was conducted when the biomass concentration was roughly $\pm$3 g/L.

4.3.2 Temperature

A large batch of culture was grown until the culture attained the stationary phase and a cell concentration of ~3 g/L (see 'Typical behaviour of R. palustris in a batch free cell system'). The culture was then separated into four 250 mL glass Schott bottles for each temperature investigation: 35°C, 40°C, 45°C and 50°C. For each sample the following procedure was followed:

The sample container was placed inside a glass bottle along with a magnetic flea and sealed. The sealed bottle was placed inside a water bath with a water heating element that had been preheated to the

desired temperature, the bath temperature was controlled throughout experimentation to remain at the desired temperature of each investigation. The culture is adequately agitated (Eins Sci (E-MS3-H2-D) mixer) throughout this time to ensure for efficient mass and heat transfer. The sample was left for 30 minutes under these conditions, then removed from the water bath and a 2 mL sample was taken from the culture and placed in a sample vial.

The samples were then centrifuged (Eppendorf Minispin Plus) at 13900 x *g* rpm for 5 minutes, and the supernatant removed. The cell pellet was then kept in the sample vial to be prepared for further analysis. Preparation for different types of analysis is discussed in section 4.4.4.

4.3.3 Pressure

Pressure on bacterial cells was achieved by using a Büchner vacuum filter. Culture in the stationary phase was used to conduct this experiment, the same as the culture in the previous experiment with a similar cell concentration of ~3 g/L.

A sample volume of 10mL was pipetted onto the moistened 0.22μm nylon filter paper. A vacuum line with a negative pressure of 190 mbar was attached to the flask and the entire sample volume was filtered. An additional 10 mL of deionised water pipetted onto the filter paper onto the cells and the water was completely filtered through. This resulted in total induced pressure of 82.3 kPa on the cells.

Once all liquid was completely filtered through, the cells on the filter paper were scraped off using a cell scraper into a sample vial and prepared for analysis. Preparation for different types of analysis is discussed in section 4.4.4.

4.3.4 Shear

4.3.4.1 Constant shear for varying time

A similar procedure to the temperature experiment was used in the preparation for the shear experiments. A large culture volume was prepared with a cell concentration of ~3 g/L and transferred into three 250 mL baffled Erlenmeyer flasks, each for a different time that will be tested: 5, 10 and 15 minutes. The following procedure was followed for each of the time intervals. With this experiment it was critical to ensure that the same culture was used for the experimentation to reduce error between varying cultures.

100 mL of culture was placed into the baffled flasks along with a magnetic flea and sealed, then placed in a temperature-controlled water bath at 30^{o}C. The reason for the baffled flask was to prevent the fluid forming a vortex that would counteract induced shear on the cells. The culture was agitated a constant mixing speed of 760 rpm using an Eins Sci (E-MS3-H2-D) mixer, for which the resulting velocity gradient (or G-value) for this mixing speed was calculated to be 5108.16 s^{-1}.

The sample was mixed for the designated amount of time, either 5, 10 or 15 minutes and a sample was taken from the culture and centrifuged (Eppendorf Minispin Plus) at 13900 x *g* rpm for 5 minutes and prepared for analysis. Preparation for different types of analysis is discussed in section 4.4.4.

4.3.4.2 Varying shear for a constant time

A similar procedure for the shear experimentation was be followed. A large culture volume was prepared with a cell concentration of ~3 g/L and transferred into five 250 mL baffled Erlenmeyer flasks each for a different induced shear with each mixing speed that will be tested. The following table (Table 18) contains the resulting G-value for each mixing speed, (section 2.6.2) can be referred to for the calculation of the G-value. An assumption of 90% efficiency for power dissipation was assumed using a mixer (Eins Sci (E-MS3-H2-D) mixer) with a power of 515 W.

Table 18: G-value to quantify the energy imparted to the cells during the test to determine the effect of shear

Shear setting	Mixing speed (rpm)	G-value (s^{-1})
1	100	1852.93
2	200	2620.43
3	300	3209.36
4	400	3705.85
5	500	4143.27

The following procedure was followed for each of the mixing speeds: 100 mL of culture was placed into a 250 mL baffled glass bottle along with a magnetic flea and sealed. The flask was then placed in a temperature-controlled water bath at 30°C. The sealed bottle was placed on a magnetic stirrer each with the desired mixing speed, for which the resulting mixing energy will be calculated.

The sample was mixed for 15 minutes, and a 2 mL sample was taken from the culture and centrifuged (Eppendorf Minispin Plus) at 13900 x *g* rpm for 5 minutes and prepared for analysis. Preparation for different types of analysis is discussed in section 4.4.4

4.3.5 Nutrient limitations

To investigate nutrient limitations, the glycerol added to the liquid medium was regulated. The following glycerol concentrations were tested: 5, 12.5, 25 and 37.5mM. In comparison to during all experimentation where the starting glycerol concentration was 50mM.

For each the minimal medium was prepared as specified by (section 4.1.4) although after autoclaving with the glycerol addition step, lower volumes of glycerol were added to attain the desired final glycerol concentrations. To ensure that all the cultures started with an identical starting concentration, a culture at the stationary growth phase with a cell concentration of ~3 g/L was used to inoculate the media. Into each media with a known glycerol concentration, 10 mL of the inoculum was added.

The media was placed in a temperature-controlled water bath and illuminated 100 W incandescent lightbulbs, the process exactly follow the same steps as standard bacterial culturing. As observed in the

literature (section 2.3.7), after 10 days the culture was assumed to have reached the stationary growth phase, thus at this time point 2 mL samples were taken from each different culture. The OD of the sample was measured at 660 nm to determine the cell concentration. The samples were then centrifuged (Eppendorf Minispin Plus) at 13900 x *g* rpm for 5 minutes and the supernatant was discarded. The cell pellet was then prepared for different types of analysis is discussed in section 4.4.4.

4.3.6 Viscosity

In an attempt to determine if an increase in viscosity would aid in a reduction of induced shear on the bacterial samples, samples were prepared that have an increasing viscosity from 0.9 cP to 22.32 cP.

A large culture volume was prepared with a cell concentration of ~3 g/L and transferred into three 250 mL baffled Erlenmeyer flasks, each for a different viscosity that was tested. Guar gum was used in the samples to increase the viscosity, this was chosen because the guar gum would not interact with the bacteria or the other components in the media.

The large culture volume was separated into different containers and the guar gum in varying masses were added to achieve the desired concentrations. The samples were each placed on the magnetic stirrer under 760 rpm mixing speed and left for 15 minutes. A 2 mL sample from each container was taken, placed into a sample vial then centrifuged at 13900 x *g* rpm for 10 minutes and prepared for further SEM analysis (section 4.4.4.1). FCM could not be used for these samples due to the negate effects the guar gum would have on the FCM column. The remainder of the sample was sent for rheology analysis to determine the viscosity of each sample. Specifications of the equipment used can be seen in section 4.4.5. The guar gum and resulting viscosity of the fluid can be seen in the table (Table 19) below.

Table 19: Concentration of guar gum and resulting viscosity of the medium containing ~3 g/L of *R. palustris*

Concentration of guar gum (g/L)	Viscosity (cP)
0	0.9
0.543	1.9
0.714	2.5
1.14	4.1
1.4	5.9
1.66	7.5
1.86	10.2
2.29	15
2.86	22.2

4.4 Analytical techniques

4.4.1 Cell concentration

In order to observe the change in cell concentration over time, it can either be quantified by the number of cells or the cell dry weight (CDW) in the system. As the simpler alternative, the CDW was used in this investigation where all moisture is removed from the sample to determine the mass of the cells remaining.

However, due to the exhaustive nature of the method used to determine the CDW, this method could not be used to analyse each sample. Thus, as an alternative, a standard curve (Figure 32 and Figure 33) was developed to relate the optical density to the cell dry weight in the system assuming that the optical properties and cell size stay constant throughout experimentation. The optical density of a sample can be considered an indirect measurement of the cell density, which confirms the use of the standard curve to determine the CDW from the optical density.

4.4.1.1 Cell concentration standard curve procedure

In order to develop a standard curve, bacteria in the late exponential phase was used. To determine the CWD, the filter paper (0.22 μm nylon filter paper) was dried in an oven at 60^{o}C for 24 hours and cooled in a desiccator to ensure all moisture had been removed, then the mass of the filter paper was noted using a lab scale (Sartorius AG BP 61S 5 decimal lab scale). A series of dilutions, each with a volume of 10 mL, were performed using the bacterial sample. Each diluted bacterial sample was filtered using a vacuum filter to remove as much moisture as possible; during filtration the samples were washed with deionized water the ensure all media and salts were washed off the cells. After using the same drying method as for the filter paper(60^{o}C oven for 24 hours), the paper loaded with bacterial cells was weighed again, noted and the resulting difference between the mass of the two, divided by the volume of the filtered sample, is the CDW value. These CDW's were then used for the construction of the standard curve.

When looking at the absorbance of *R. palustris* bacterial cells in the late exponential growth phase there are peaks present approximately at 500, 590, 870 and 970 nm (Pott, 2013). Thus, the wavelength to measure the optical density at was selected as 660 nm because no pigment absorption (identified as a peak), occurs at this wavelength. In order to determine the optical density, the late exponential culture was centrifuged (Eppendorf Minispin Plus) at 13900 x *g* for 5 minutes, and the supernatant removed from the solid cell pellet. The solid cell pellet was then resuspended in 1mL deionized water and the OD was measured at 660nm. Dilutions were made when necessary to ensure the optical density remains in the linear region of the CDW standard curve, namely an optical density of less than 1.5.

Lastly, the cell concentration standard curve was constructed; the optical density (OD) plotted against the respective CDW. Using the linear relationship of the data points, linear regression was performed to obtain an equation for the line of best fit to represent the standard curve over a range of data points. Thus, from this point by measuring the optical density and using the standard curve, the CDW was obtained as seen in Figure 32 and Figure 33 below for each different medium used in this investigation.

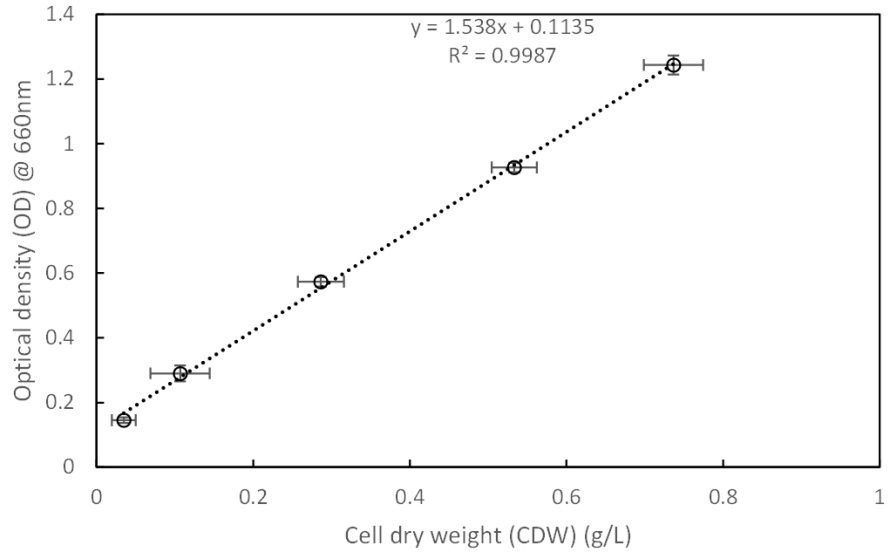

Figure 32: Standard curve that relates the optical density of the sample at a wavelength of 660 nm to the cell concentration in the sample when Minimal medium was used. Error bars are presented by means of standard error in the CDW and OD measurements.

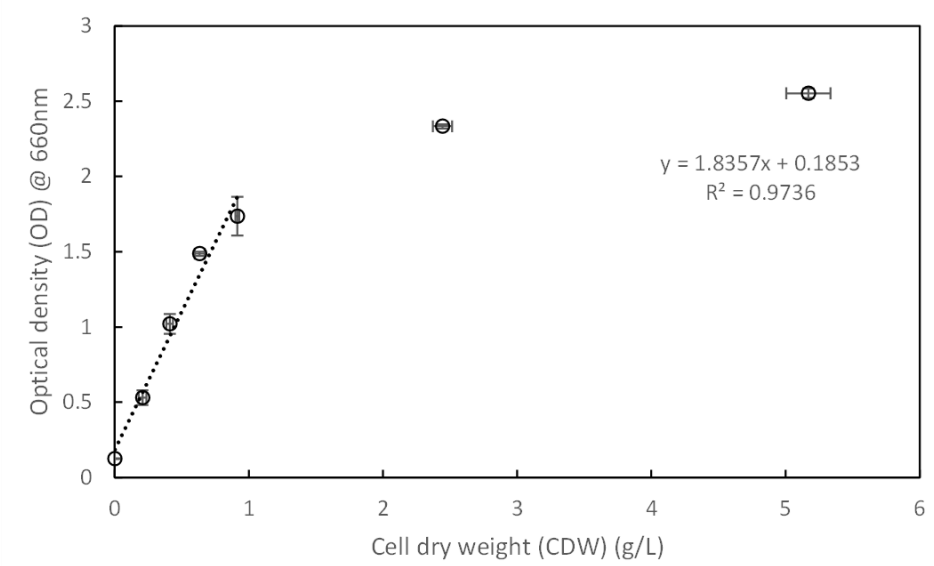

Figure 33: Standard curve that relates the optical density of the sample at a wavelength of 660 nm, to the cell concentration in the sample when the van Niels growth medium was used. Error bars are presented by means of standard error in the CDW and OD measurements.

4.4.2 Hydrogen concentration

As mentioned in the literature review (seen in section 2.3.3), the gas produced is a mixture of both hydrogen and carbon dioxide. To analyse the gas samples, a glass syringe was used to extract 200 mL of gas produced from the water displacement system into gas sampling bags for analysis.

Global Analyser Solutions CompactGC was used with an argon carrier stream and a thermal conductivity detector, in the results the content hydrogen and carbon dioxide were reported as relative percentages.

4.4.3 Glycerol concentration

Using high-performance liquid chromatography (HPLC), the glycerol concentration remaining in the media was determined. The sample was centrifuged to separate the liquid supernatant and the solid cell pellet, the supernatant was then filtered using a 0.22 μm syringe filter to ensure no remaining solids that could possibly clog the HPLC column.

To acquire the glycerol concentration from HPLC results, a standard curve was constructed that relates the glycerol concentration to the area under the curve. The standard curve was constructed by preparing a series of dilutions with known glycerol concentrations and injecting these dilutions into the HPLC. The area under the absorption peaks is plotted against respective glycerol concentration. At this point, linear regression was applied to obtain and equation for the line of best fit.

In the (Table 20) table below, specifications for the equipment used can be seen.

Table 20: A summary of the specifications of HPLC equipment used for analysis

Instrument	Component	Description
Doinex Ultimate 3000	Mobile phase and flowrate	0.005 M H_2SO_4 at 0.6 mL/min
	Sample volume	30 µL
	Column temperature	65°C
	Column	Aminex HPX-87H column, 250 x 7.8 mm with guard cartridge
	Detector	RI detector at 45°C (For glycerol)

The standard curve to determine glycerol concentration can be observed in Figure 34 below.

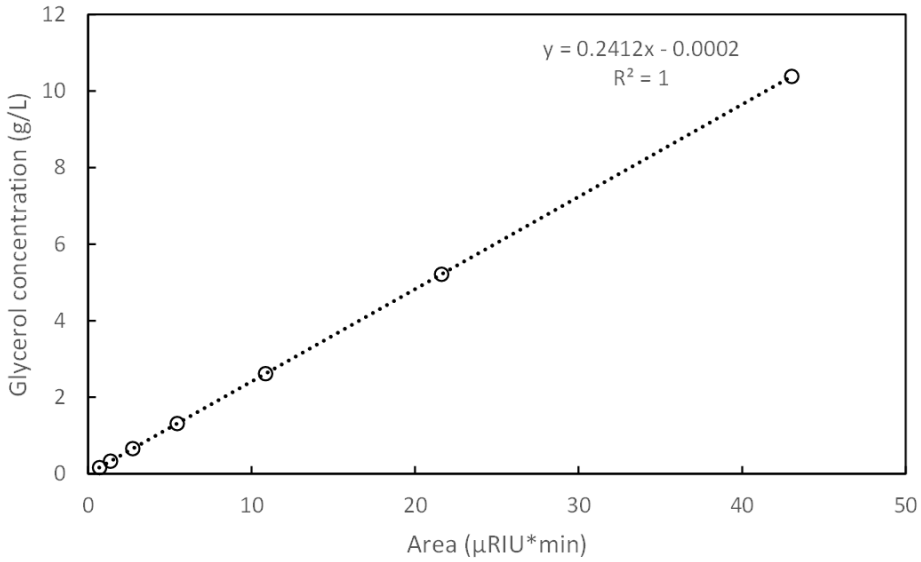

Figure 34: Standard curve developed from HPLC analysis that related the area under the absorbance peaks to the glycerol concentration in the sample.

4.4.4 Microscopy cell analysis

In this section the sample preparation for microscopy will be discussed, refer to section (Appendix A – Analytical Techniques) that discusses the operation of the equipment used.

4.4.4.1 Scanning electron microscopy (SEM) and Scanning transmission electron microscopy (STEM)

Sample preparation for SEM and STEM follow an identical procedure. A 2mL culture sample from each experiment was centrifuged for 10 minutes at 13900 x *g* rpm high speed to aid in the separation of the supernatant and a cell pellet. The supernatant was removed from the sample and 1 mL of 2.5% glutaraldehyde (GLA) solution was added. This is to ensure stability of the samples in storage (2-8^{o}C) until analysis. All STEM and SEM analysis was conducted by the Central Analytical Facilities at Stellenbosch University (CAF) using the Zeiss Merlin SEM.

4.4.4.2 Flow cytometry (FCM)

Sample preparation for flow cytometry follows a similar procedure. A 2mL culture sample from each experiment was centrifuged for 10 minutes at a high speed to aid in the separation of the supernatant and a cell pellet. The supernatant was removed from the sample and 1mL of phosphate buffered saline (PBS) solution (pH 7.4) was added. The concentration of each component in the PBS solution is in the table below (Table 21), these components were added to deionized water and sterilised in the autoclave for 30 minutes at 121^{o}C and 101 kPa. These samples had to be prepared as closely as possible to the submission and analysis of the samples to ensure the results are as accurate as possible. All FCM analysis was conducted by the Central Analytical Facilities at Stellenbosch University (CAF), the cells were stained using propidium iodide (PI) and Syto9 (Luo, Le-Clech and Henderson, 2018). Equipment used was the BD FACSMelody.

Table 21: Concentrations of components in 1L of phosphate buffer solution (PBS)

Component	**Concentration (g/L)**
NaCl	8
KCl	0.2
Na_2HPO_4	1.44
KH_2PO_4	0.245

4.4.5 Viscosity quantification

The equipment used to determine the varying viscosity of the samples was a Paar Physica MCR501 Rheometer from Anton Paar with a double gap (DG26.7) measuring system. No prior sample preparation was required and the sample after analysis could simply be submitted for analysis.

4.5 Statistical analysis

The only statistical parameter that was used to analyse triplicate data point was uncertainty, which was used for all experimental data. The equation used to determine the uncertainty parameter can be seen in the equation (Equation 27) below.

$$\Delta = \pm t(\alpha, n-1)s_n \quad [27]$$

Where, α is the relevant significance level (with 95% confidence this gives an α value of 0.05), n is sample size and $t(\alpha, n-1)$ is the two-tailed inverse students t distribution and finally s_n is the standard error which can be calculated using the equation (Equation 28) below.

$$s_n = \frac{s}{\sqrt{n}} \quad [28]$$

Where s is the standard deviation and can be calculated using Equation 29 below.

$$s = \sqrt{\frac{1}{n-1}\sum_{j-1}^{n}\left(x_{i,j} - \bar{x}_i\right)^2} \quad [29]$$

5 RESULTS AND DISCUSSION

As a start to the results and discussion of this study, the 'pathology map' discussion covers the investigation into the effect of different physical factors such as shear stress, pressure, or temperature on the bacterial culture. This was used later in the investigation to link the physical system to the internal growth, substrate utilisation and hydrogen production of the culture during operation of the membrane photobioreactor.

The system design and fabrication were based on a combination of the results from the pathology map and observations from the literature to create an environment for the culture to grow. The operation of the membrane photobioreactor for batch and continuous mode operation is discussed and the implications thereof for industrial application.

5.1 Pathology map

This section is a discussion of the effect on *R. palustris* when stressed, using the OFAT method, under multiple physical conditions, including: shear stress, pressure, nutrient limitations, and temperature. In membrane bioreactor literature it was found that physical conditions, either environmental or physically induced by the system, do affect the biological cultures inside them. As literature pertaining to PNSB was limited, for this investigation it was required to first observe the effect of these physical conditions. This could later, during operation of the MPBR, perhaps explain why certain parameters look the way they do.

The analysis of these samples was conducted by the Central Analytical Facilities (CAF) at Stellenbosch University. Samples were analysed using scanning electron microscopy (SEM), scanning transmission electron microscopy (STEM) and flow cytometry (FCM). After reviewing results from the analysis, it was decided that the results from STEM will not be displayed in this discussion but can be seen in Appendix A – Analytical Techniques. In this discussion, as suggestions regarding the physical effect of these conditions are based on the visual appearance of the cells, a clearer image of the cells were used to draw these assumptions. Therefor only SEM results will be displayed as they provide a more enhanced picture of the physical appearance of the organism.

A comparison can be seen in the two figures (Figure 35) displayed next to each other below. The SEM images provide a visual representation of the effect of the physical manipulation of the cells providing part of the conclusions drawn by the pathology map and supported by results from flow cytometry.

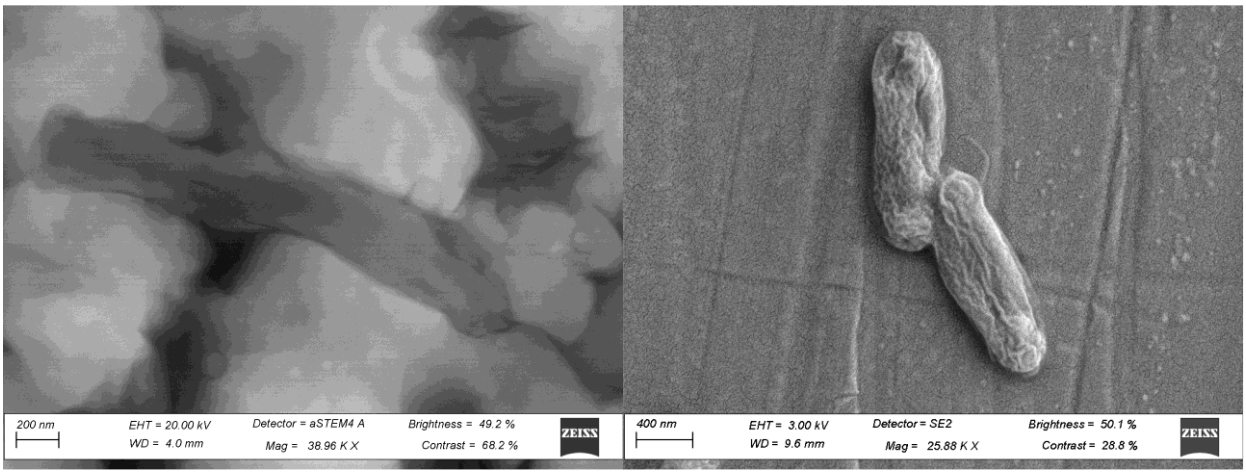

Figure 35: Comparison of *R. palustris* at 35 °C using STEM (image on the left) and SEM (image on the right)

The main difference between SEM and STEM comes down to the electron beam focused over the samples to generate images. With STEM, there is a strong signal from transmitted electrons which due to its' high intensity, reveals not only the surface of the sample, but can probe into internal structures of the sample. SEM on the other hand uses a stream of secondary and backscattered electrons with which the strongest signal is from the surface of the sample (Liao, 2006). Refer to Appendix A – Analytical Techniques, for a more detailed discussion on SEM technology. Thus, for the purpose of this investigation, SEM results paint a clearer picture of the physical external appearance of the organism.

In order to support assumptions made from visual observation of SEM results, flow cytometry was used. Flow cytometry (FCM) is a technique used to detect, identify and count specific cells, in this case damaged, dead or live cells. Different dyes are used that permeate cell membranes and emit fluorescent light, in this study SYTO9 and propidium iodide (PI) were used. PI is able to permeate compromised cells and emits a red fluorescence whereas live cell membranes are permeable to SYTO9 which binds to DNA and RNA emitting a green fluorescence (du Toit and Pott, 2020). In the flow chamber, cells are counted and sorted based on the light emitted and a direct number of cells reported in the system is obtained. The number of live cells will be reported as a percentage of the total counted cells from FCM. An illustration of how FCM works can be seen in Appendix A – Analytical Techniques.

In Figure 36 below, the final graphic output from FCM is displayed. As the singular cells pass the laser, the detectors count the cells based on the colour of fluorescence emitted, in this case red (from PI) and green (from SYTO9). The signals from the detectors either indicate a red fluorescence (for dead), a green fluorescence (for live), dual-fluorescence (indicating a compromised cell) or the cell is unstained. These signals are then divided into quadrants seen on the graph: Q1, Q2, Q3 and Q4. Each dot on the graph indicates a singular cell (in FCM referred to as an 'event') and the colour change on the graph indicates a higher concentration. On this graph, it is clear that the highest concentration of events was reported to Q3, as indicated by the red colour. The percentage of each quadrant that makes up the total of events is reported in the outermost corner of each quadrant. For example, quadrant 3 displays a value of '74.5',

which translates to 74.5% of all the events were in this quadrant. In the table below (Table 22), is a summary of what each quadrant indicates for this specific combination of dyes.

To produce clear data, outlier events are not considered and removed during the process of 'gating' the data. Gating is a process where the cellular population data is refined to remove outlier scatter events from the dataset.

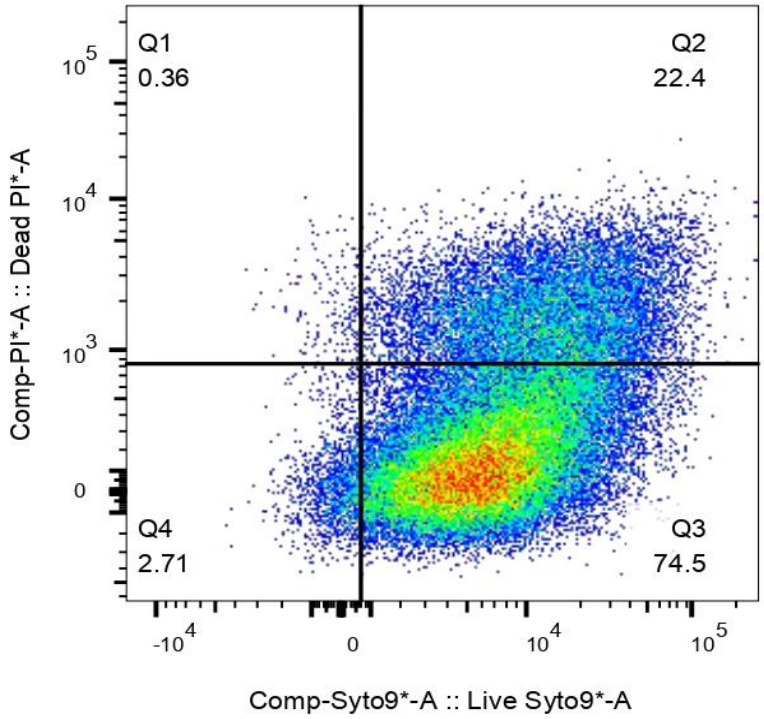

Figure 36: Example of final graphic results from FCM when analysing a healthy culture. 'Comp' indicates that the data has been compensated to ensure no false positives.

Table 22: Simplification of FCM results to improve understanding of results.

Quadrant	Cell status	Percentage of sample (%)
Q1	Dead	0.36
Q2	Compromised	22.4
Q3	Live	74.5
Q4	Unstained	2.71

The establishment of a pathology map was a vital part of understanding the effect of the designed MPBR system, or possible eventual use of the system on a larger scale, on the organism, at a microscopic level. This is because if the cells show signs of distress at a microscopic level, this can directly be associated with potential changes in biomass concentration, changes in substrate conversion efficiency or unreliable

hydrogen gas yields within the MPBR. When considering the membrane in the system, if cell lysis occurs in the system, cell debris could result in increased membrane fouling (Czekaj et al., 2000).

5.1.1 Control

With the intention of comparing the effect of the physical factors on the *R. palustris* cells a control sample was analysed alongside the manipulated cells. An *R. palustris* cell that is considered 'normal' or 'healthy' can be seen in Figure 37. From several images of the control group, this image was selected, as it provides the clearest close up visual representation of the culture. A comparative image from the same culture can be observed in Appendix C – SEM control images.

As the experimentation was operated at 35 °C, this culture was grown at this temperature with optimal illumination and substrate conditions obtained from the literature (Pott, Howe and Dennis, 2013a; du Toit and Pott, 2021), with no additional stress imposed on the cells. The culture they were taken from showed optimal growth, substrate conversion efficiency, and hydrogen production, when compared to the literature (du Toit and Pott, 2021). This meant that these cells are supposed to be a representation of an 'ideal' or a 'healthy' cell and can be used to compare the appearance of a normal cell to other manipulated and perhaps 'unhealthy' cells.

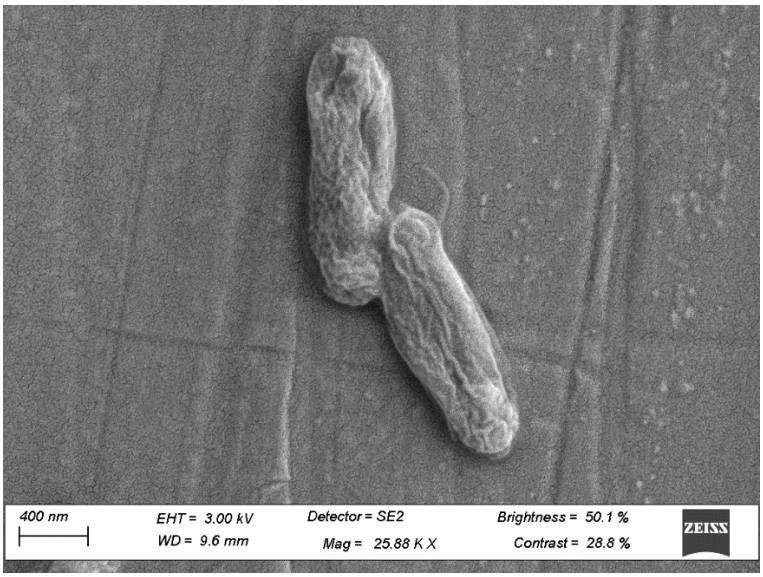

Figure 37: SEM image of an 'Optimal' *R. palustris* cell cultured at 35°C for showing efficient cell growth, substrate utilisation and hydrogen production. This figure is to be used as a control to compare other manipulated cells to for the pathology map investigation.

At this temperature, for a healthy culture, flow cytometry indicated that 74.5±1.76 %[9] of the sample contained uncompromised cells (Table 23), indicating that they are healthy, live cells. This value corresponds to what was observed in the literature, for control cultures the percentage of live cells was seen to be between 70 and 80% (Faber *et al.*, 1997; Cunningham *et al.*, 2008). This low percentage is due to an additional percentage of cells that exhibited dual-fluorescence, they are considered to be

[9] Experimental variation provided by means of standard error of triplicate runs

physiologically compromised, neither healthy nor dead, as depicted in Figure 36 This figure and percentage of healthy cells obtained from flow cytometry will be used to compare the effect of each physical factor on the bacterial cells.

Table 23: Composition of sample events as found by FCM, of a 'healthy' *R. palustris* culture at 35°C after 30 minutes of exposure.

Quadrant	Cell status	Percentage of sample (%)
Q1	Dead	0.36
Q2	Compromised	22.4
Q3	Live	74.5
Q4	Unstained	2.71

5.1.2 Temperature

From the literature, it was seen that the different strains of *R. palustris* have a wide range of optimal temperatures for bacterial growth, ranging from 25°C to 45°C. Specifically for the strain of *R. palustris* used in this investigation (*R. palustris* NCIMB 11774), the optimal temperature for an enhanced growth rate and specific hydrogen production is 35°C, as suggested by du Toit and Pott (2021). Also important to note, and stated in this investigation, is that although these cultures can grow at varying temperatures, an acclimatisation period is required for the organism to adapt to the new temperature conditions, which would result in a periodic slump in growth rates and hydrogen production (du Toit and Pott, 2021). As a standard, cultures require roughly two to three weeks, depending on temperature difference, to acclimatise to new temperature conditions. Thus, if the culture is acclimatised to a given temperature, a change in temperature would result in changed parameters (growth, substrate utilisation and hydrogen production), despite the famed temperature resilience of the organism.

However, it was expected that this strain of *R. palustris* could still, to an extent, withstand a wide range of temperatures due to this wide range of temperature operation within the species. The cultures were expected to experience a slump in cell growth, but not completely die out. The temperature range selected aimed to investigate whether the cells exhibit significant cell death, which would result in a significant loss in active biomass.

This investigation was conducted using *R. palustris* that is acclimated to growing at 35°C and it is expected that the cells would experience stress due to the sudden temperature change, as it would possibly occur in a continuous industrial system. For application in industry when considering an outdoor bioreactor, due to the combination of warm ambient temperatures and direct sunlight, culture temperatures tend to rise to unfavourable temperatures. Under section 5.1.2.4, temperature variation that could be expected in bioreactors in this context is discussed. The temperatures investigated were 40 °C, 45 °C and 50 °C and the results are displayed in the following subsections.

5.1.2.1 Investigation at 40°C

Seeing as 40°C is still within a reasonable range for R. palustris to grow at, and is close to the acclimatised temperature of 35°C, it was initially assumed that the cells would not experience significant cell death at this temperature. In the figure below (Figure 38), it can be observed that this assumption held true and that the cells still appear to maintain cell integrity, and the image compares well to the established control in section 5.1.1 (Figure 37).

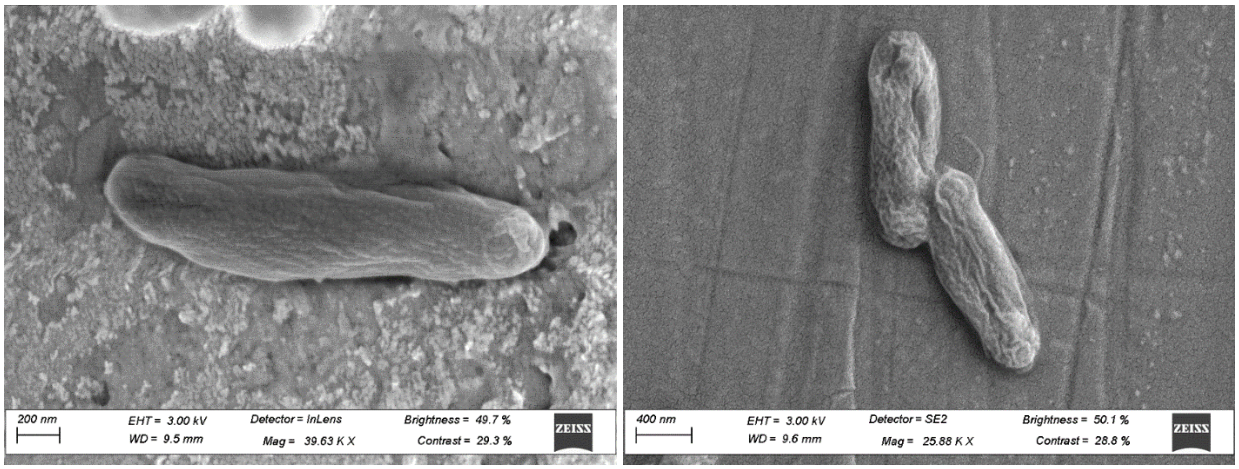

Figure 38: ON THE LEFT: SEM image of an *R. palustris* cell for the investigation on the effect of a temperature of 40°C imposed on the cells for 30minutes. ON THE RIGHT: a 'healthy' *R. palustris* cell

Similarly, FCM (Table 24) showed that 69.2±1.02 % of this sample had a large number of cells that remained uncompromised; there was only a ~10% decrease in the amount of live biomass. This difference in the percentage of healthy cells can be due to this specific strain of *R. palustris* that has shown ideal performance at exactly 35°C in the literature and is acclimatised to growing at this temperature close to this. The percentage decrease is mostly accounted for by the amount of unstained culture, and not a visible increase in dead or compromised cells.

Table 24: Composition of sample events as found by FCM, of an *R. palustris* culture at 40°C after 30 minutes of exposure.

Quadrant	Cell status	Percentage of sample (%)
Q1	Dead	1
Q2	Compromised	22.5
Q3	Live	69.2
Q4	Unstained	7.25

5.1.2.2 Investigation at 45°C

As previously stated, *R. palustris* can grow within a relatively wide temperature range, with 45°C being the point where this range ends. In other words, if the desired action for a study was for *R. palustris* to grow, temperatures above 45°C were rarely utilised. It was assumed that some cells would still present

alive with FCM analysis due to the temperature resilience of this specific strain, although some compromised cells were expected as the culture is acclimatised to temperatures 10°C below this specific study.

In the figure below (Figure 39) it is clear that the cells are starting to visually exhibit signs of physical strain from the higher temperatures, and cells appear to have collapsed to some degree, suggesting that the peptidoglycan cell wall has been compromised. This indicates that the state of cell electrolytes has been disrupted and death pathways have been activated.

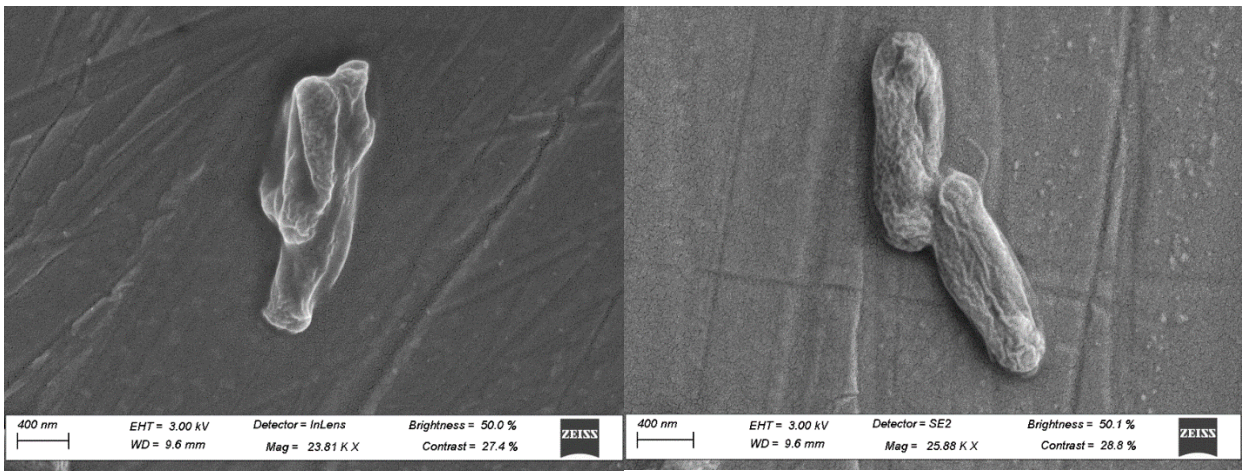

Figure 39: ON THE LEFT: SEM image of an *R. palustris* cell for the investigation on the effect of a temperature of 45°C imposed on the cells for 30minutes. ON THE RIGHT: A 'healthy' *R. palustris* cell

This again coincides with the results obtained from FCM (Table 25) which indicated that only 49.5±0.53% of the cells were alive. This already signifies a large difference between the healthy control cell and the effect of a 10°C temperature difference with a ~35% decrease in live biomass. For this temperature investigation there is a visible increase in the number of compromised cells in comparison to what was observed at 35°C or 40°C (referring to Table 23 and Table 24), which indicates that at this temperature, the cells were starting to exhibit signs of stress.

Table 25: Composition of sample events as found by FCM, of an *R. palustris* culture at 45°C after 30 minutes of exposure.

Quadrant	Cell status	Percentage of sample (%)
Q1	Dead	1.57
Q2	Compromised	35.9
Q3	Live	49.5
Q4	Unstained	13

5.1.2.3 Investigation at 50°C

Finally in order to observe the effect of a more extreme temperature on the bacterial cells, beyond the range of previously investigated temperatures in the literature; the cells were exposed to a temperature of 50°C. It was expected that a majority of the cells would perish under these conditions due to the unfavourably high temperature that would result in significant cell lysis are large temperature from the acclimatised temperature of this specific culture. In the figure below (Figure 40), it is clear that at this temperature most of the cells are mis formed and the cell wall is severely damaged.

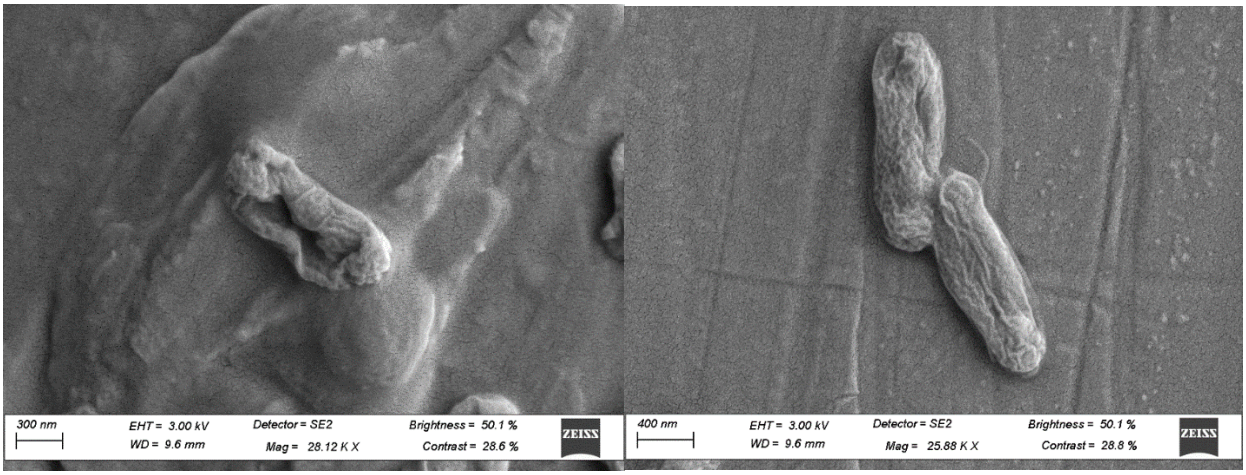

Figure 40: ON THE LEFT: SEM image of an *R. palustris* cell for the investigation on the effect of a temperature of 50°C imposed on the cells for 30minutes. ON THE RIGHT: a 'healthy' *R. palustris* cell

Again, the results from flow cytometry support this suggestion, it was seen that after exposure to this temperature for 30 minutes, only 37.4±1.1% of the cells were alive. This is a ~50% decrease from a healthy culture with only a 15°C temperature difference for 30 minutes of exposure. Similar to the effect observed at 40°C and 45°C, there is a large increase in the number of compromised cells, and not the dead cells as expected. This suggests that as the time of exposure is prolonged the state of the cell might progress from compromised to dead.

Table 26: Composition of sample events as found by FCM, of an *R. palustris* culture at 50°C after 30 minutes of exposure.

Quadrant	Cell status	Percentage of sample (%)
Q1	Dead	3.12
Q2	Compromised	45.9
Q3	Live	37.4
Q4	Unstained	13.6

Consequently, it was assumed that if the cells were exposed to this temperature for a longer period, it is likely that a larger percentage of the cells were to be compromised. This assumption was confirmed when

the same biomass sample was exposed to this temperature for more than an hour, and FCM reported (Table 27) that only 18.1±0.02% of the culture remained alive, which is a ~75% decrease in live biomass from a healthy culture. This was expected, as in laboratory practice, higher temperatures are sometimes utilised to ensure the culture is dead before disposal.

Table 27: Composition of sample events as found by FCM, of an *R. palustris* culture at 50°C after 60 minutes of exposure.

Quadrant	Cell status	Percentage of sample (%)
Q1	Dead	4.3
Q2	Compromised	74.5
Q3	Live	18.1
Q4	Unstained	2.92

5.1.2.4 Implications of temperature investigations

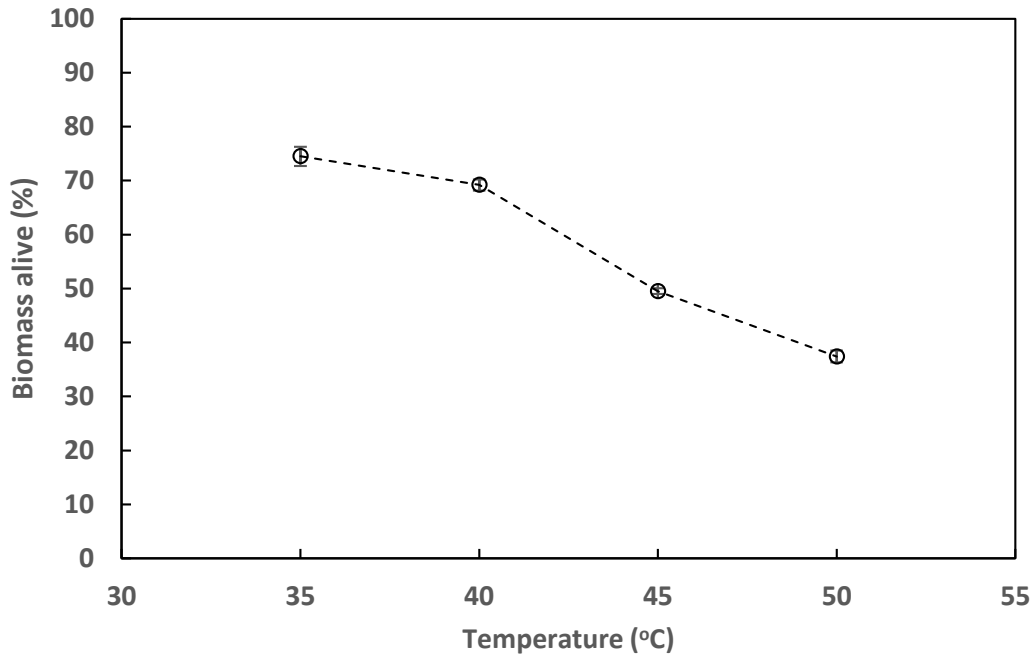

Figure 41: Percentage of *R. palustris* biomass reported alive after 30 minutes of elevated temperature exposure from flow cytometry results for a range of temperatures (35°C to 50°C) during the pathology map investigation. Error is presented by means of standard error of triplicate results.

In Figure 41, there is a strong suggestion that with increasing temperature, a decreasing percentage of biomass in the culture is observed after a period of 30 minutes. This highlights the importance of temperature control within the bioreactor, especially when considering use of this bioreactor in outdoor environments.

If considering the use of *R. palustris* in an industrial setting within South Africa, the required illumination for sufficient hydrogen production or biomass growth would have to be from solar illumination in an outdoor setting. This implies that illumination from the sun in combination with outdoor ambient temperatures must be sufficient for efficient substrate utilisation and hydrogen production. If as an example, the Western Cape, was considered to be the location of this technology, the climate is classified as humid subtropical with seasonal temperatures summarized in the table (Table 28) (Britannica, no date). In this table (Table 28), it can be observed that the culture temperature inside the bioreactor temperature is warmer than the ambient temperature, more so with direct solar illumination. For cultures with direct solar illumination, cultures could be more than 20°C warmer than the ambient temperature (Zhang, Kurano and Miyachi, 1999).

Table 28: Average seasonal temperatures for Cape Town, Western Cape, RSA (Climate-Data.org, 2019) along with estimated culture temperatures based on (Zhang, Kurano and Miyachi, 1999)

Season	Months	Average Temperature range (°C)	Estimated culture temperature (°C)	Sun hours
Autumn	March – May	18.9 – 15.1	~35	8.8 – 6.7
Winter	June – August	13.6 – 13	~20	6.4 – 6.8
Spring	September – November	14 – 17.1	~37	7.7 – 10.1
Summer	December – February	19 – 20.1	~45	10.8 – 9.9

From these estimated culture temperatures and sun hours during the day, preliminary assumptions can be made regarding the effect of the conditions on the culture. As *R. palustris* requires illumination for ATP generation which is then converted to hydrogen by the nitrogenase enzyme, thus the amount of sun hours the culture is exposed to is a critical parameter. From these outdoor conditions, the optimal reactor performance can be expected in the spring months, as there are several sun hours during the day, and near optimal temperatures in the reactor. In summer, despite several sun hours during the day, the higher ambient temperatures would result in bioreactor temperatures that are fatal to the culture.

During winter months, poor solar illumination in combination with low ambient temperatures would result in significantly stunted growth of the culture which would result in poor glycerol conversion efficiency and hydrogen production. Poor hydrogen production would also be a result of insufficient illumination. At temperature conditions well below 30°C in winter months, literature has not described the exact effect on the organism, but it can be assumed that both cellular growth and hydrogen production would not exhibit the efficiency seen in lab-scale conditions, as these conditions were designed to optimise these parameters. In Autumn months the sun hours are more, to result in increased

hydrogen production. Increased sun hours and a higher ambient temperature also result in higher culture temperatures, which is more effective for substrate utilisation and cell growth.

Another drawback to an outdoor bioreactor is the variation in temperatures and illumination with the circadian rhythm. Between sunset and sunrise, the lack of illumination would result in poor hydrogen production. In conclusion, when considering that the culture in the bioreactor will acclimatise to the outdoor ambient temperatures as they change with the seasons, it is assumed that the culture would still exhibit cell growth, substrate utilisation and hydrogen production although as suggested, with less than optimal results.

When considering temperature, as this technology is to be applied to glycerol treatment it is important to consider the origin of glycerol to be treated. During biodiesel production, crude glycerol is produced as a by-product during transesterification, at a temperature of 60^{o}C. The output stream is at a higher temperature but cools back down to ambient temperature during the separation of glycerol and methyl, thus the output stream from this process which flows into the bioreactor is at the ambient outside temperature (SRS Biodiesel, no date), which is significantly lower than optimal conditions. A possible design for the piping network between the transesterification process and the photobioreactor is the installation of a water heating jacket, to increase the temperature of the influent to the bioreactor in the winter months for more effective operation. Although would not be required in the other months. This solution would, however, significantly increase capital cost, operational cost, and increased requirements for process control.

Considering the implications of having a higher temperature for operation in the membrane photobioreactor, it is assumed that exposure to high temperatures, such as 50^{o}C where significant cell lysis was observed, was only likely to occur in the summer months when the ambient temperatures and solar illumination would result in such high temperatures. A simple method to prevent such high temperatures is the use of partial shading of the bioreactor. It was assumed that the effect of cell lysis on membrane fouling under processing conditions, can be assumed negligible when the effect of temperature was considered for autumn, spring and winter.

5.1.3 Pressure

Pressure is one of the most concerning factors that could hinder bacterial growth within the membrane photobioreactor system, this is because the membrane system is operated at an elevated pressure by using a back-pressure valve, thus the cells will be exposed to stress from pressure as they are circulated through the system. Pressure is applied on the fluid flowing over the membrane to ensure a permeate flow of fluid over the membrane; without pressure the fluid would simply flow over the membrane and recirculated in the system. This is why as the pressure is increased over the membrane, the permeate flowrate also increases up to the critical flux point, as discussed in section 2.5.2.3(d).

In this investigation a pressure of 82.3 kPa was applied to the cells, as the pressure that could be applied to the culture was limited to the vacuum filter available which had only one negative pressure vacuum line, which resulted in this pressure application. Although, this pressure exceeds the backpressure applied

to the cells in the system under operational conditions which was 35kPa. A much clearer picture could be painted regarding the effect of pressure on the cells, specifically the operating pressure used in this investigation, had it been possible to investigate a range of pressures. Although, due to available equipment limitations it was not possible to do so.

Additionally, there is a significant lack in the literature reporting the effect of pressure on *R. palustris* cells, so the effect of pressure remains largely unknown. In the literature it was observed that elevated pressure resulted in inhibition of metabolic functions as well as premature cell death for other bacterial cultures (Schedler *et al.*, 2014). Therefore, it could be safely assumed that with an increase in pressure, cell death would increase as the peptidoglycan layer is compromised disturbing cellular equilibrium. In the figure below (Figure 42) it was seen that the cells did in fact display significant signs of distress, similar to that seen with the application of 50°C.

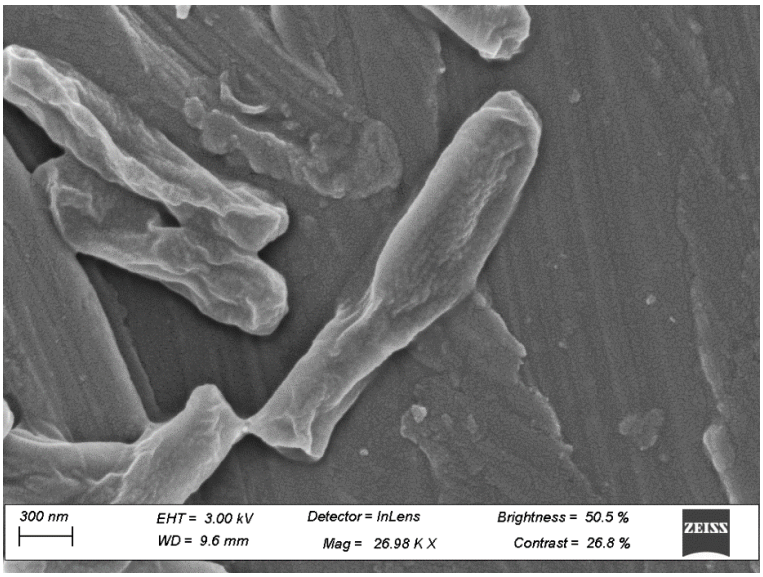

Figure 42: SEM image of an *R. palustris* cell subjected to high pressure (82.3kPa) for ~10 minutes in a Büchner funnel

FCM reported that only 26.2±0.97% of the biomass remained alive; this is a ~65% decrease of live biomass. This supported the assumption that the pressure implied on the bacteria significantly affects cell death in the system, as the amount of cells reported dead after this investigation far exceeded that of elevated temperatures after 30minutes of exposure, as discussed in section 5.1.2.

Table 29: Composition of sample events as found by FCM, of an *R. palustris* culture after exposure to elevated pressure conditions (83.3kPa).

Quadrant	Cell status	Percentage of sample (%)
Q1	Dead	11.2
Q2	Compromised	28.4
Q3	Live	26.2
Q4	Unstained	34.2

From the figure (Figure 42), by observing the cells on the far left in comparison with the cell in the centre of the image it suggests that the FCM results are reliable to a visual extent, and some cells appear to be less compromised than others. To support this suggestion an alternative image with a larger culture sample size is provided below (Figure 43). Another support of the assumption is the characteristic of *R. palustris* to clump when exposed to unfavourable conditions (Pott, 2013), which can be observed in the image below (Figure 43).

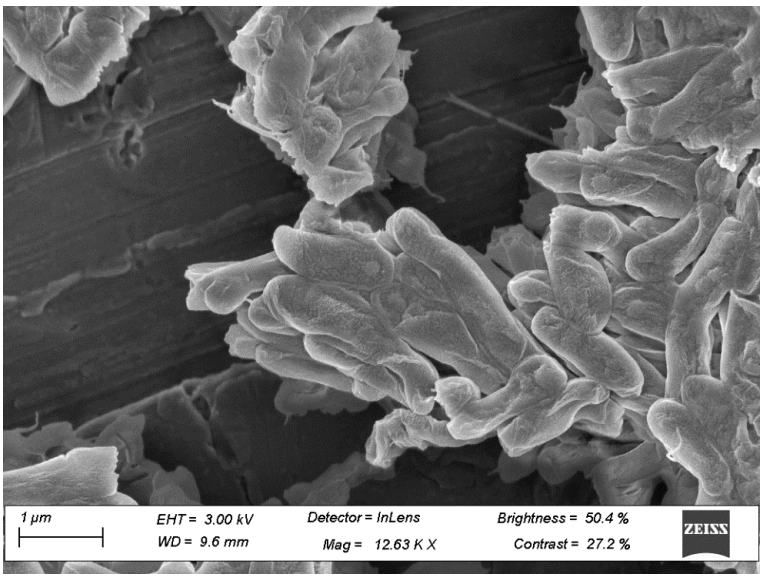

Figure 43: *SEM image of an R. palustris* cell subjected to high pressure (82.3 kPa) for ~10 minutes in a Büchner funnel displaying cell clumping

Under operation, the pressure applied on the bacteria in the system was maintained at around 35 kPa and most likely did not result in the same extensive cell death, which will be discussed in section 5.3.

This is a concerning outcome as cell lysis and bacterial clumping both would severely affect the system. During cell lysis the average particle size distribution changes with an increase in suspended cell debris; this could result in fouling of the membrane, significantly increasing required membrane maintenance and membrane lifespan. Bacterial clumping significantly affects membrane performance as the flocculating cells tend to settle from suspension; the resulting decreased suspended biomass

concentration significantly reduces substrate utilisation efficiency and resulting biohydrogen production. Flocculated cell masses do still participate in substrate utilisation, although due to significant photo-limitation and reduced mass and heat transfer rates for the cells, albeit very ineffectively.

5.1.4 Nutrient limitations

From the investigation conducted by Pott et al. (2013), it was expected that the cellular integrity would not be severely compromised but deliver a simple result; with a lower glycerol concentration, lower biomass concentrations were attained. It must be noted that this statement, however, does not hold true for high substrate concentrations, at which substrate inhibition occurs (Sabourin-Provost and Hallenbeck, 2009; Ghosh, Tourigny and Hallenbeck, 2012). Although not tested in this investigation, *R. palustris* 11774 experiences substrate inhibition at a glycerol concentration of 2720mM (Pott, Howe and Dennis, 2013a).

In the figure below (Figure 44), the images suggest similar behaviour as mentioned in Pott et al. (2013), the cells appear to be externally uncompromised due to the similarities in appearance of these cultures and the control (section 5.1.1). The FCM results (Table 30) indicating the percentage of biomass alive were similar to what was observed in the control culture (section 5.1.1). It is important to remember is that the percentage of cells reported alive is based on the number of events (cells) found in the sample and not an indication of the cell concentration.

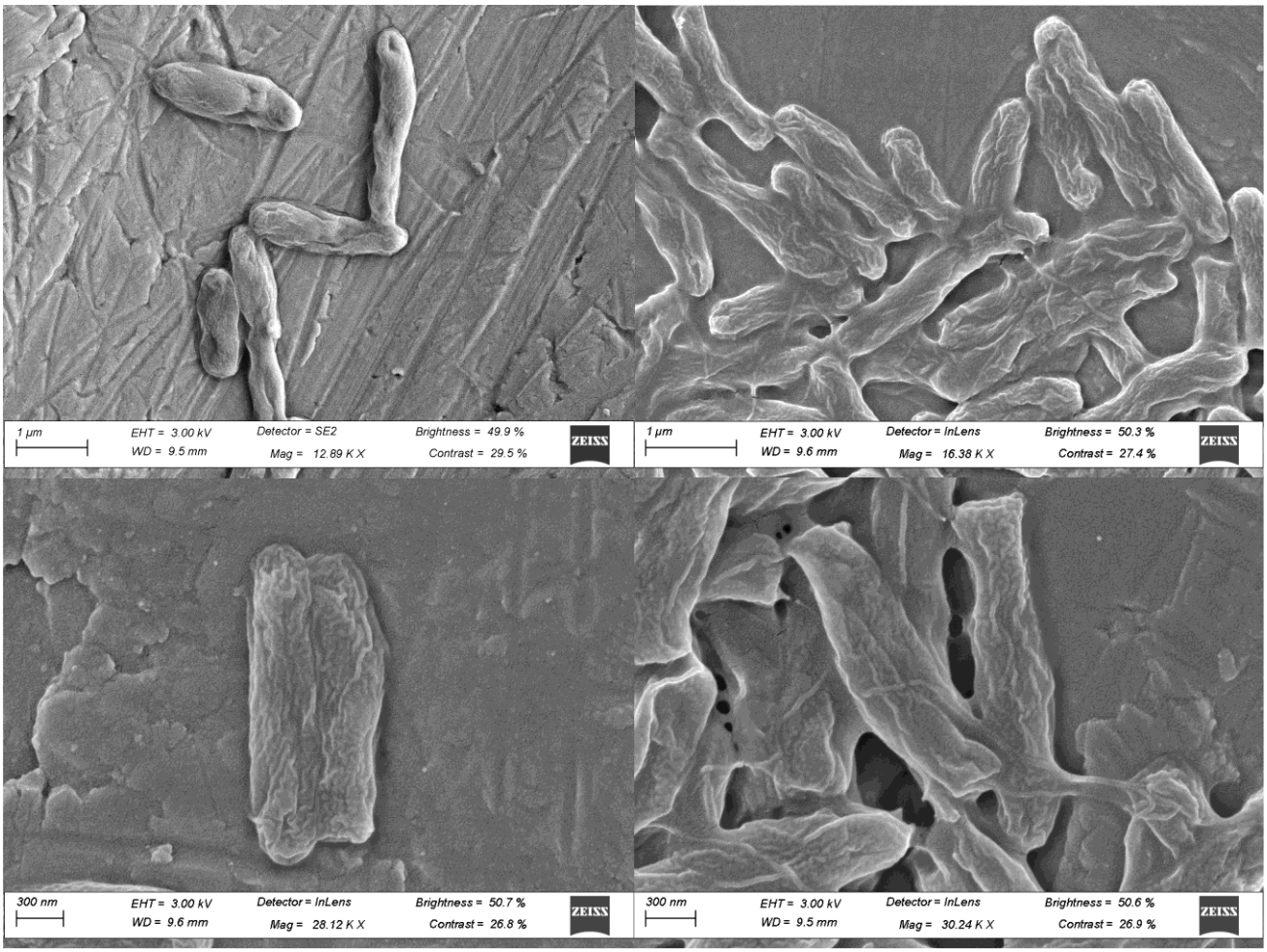

Figure 44: SEM images of *R. palustris* cells under nutrient limitation conditions (different glycerol concentrations), cultured for 240 hours at 35°C (TOP LEFT: 50 mM, TOP RIGHT: 25 mM, BOTTOM LEFT: 10 mM and BOTTOM RIGHT: 5 mM)

There was a significant difference between the final biomass concentrations after 240 hours of growth for the (Table 30)

Table 30: The percentage of biomass reported alive by FCM for each different initial glycerol concentration after 240 hours of growth for the nutrient limitation investigation.

Glycerol concentration (mM)	**% Biomass alive**
0	73.5
5	75.2
10	75.36
25	74.64
50	77.4

Considering that the percentage of biomass alive reported should be the same value to imply that the glycerol concentration does not affect the bacterial culture, it was necessary to statistically prove that there is no significant difference between the percentages of biomass reported alive.

To do this, single-factor ANOVA was used assuming an alpha value of 0.05 (95% confidence) to confirm or reject the null hypothesis, which is that there is no difference between the reported percentages of biomass alive, with 95% confidence. The results can be viewed in the following table (Table 31).

Table 31: Single-factor ANOVA summary on percentage biomass reported alive during nutrient limitation conditions

ANOVA

Source of Variation	*SS*	*df*	*MS*	*F*	*P-value*	*F crit*
Between Groups	12.769	4	3.1923	1.8197	0.2017	3.4781
Within Groups	17.543	10	1.7543			
Total	30.312	14				

The obtained p-value of 0.2017 is larger than the stated significance of 0.05, indicating strong evidence for the null hypothesis; another confirmation is that the F-crit value of 3.478 is larger than the F-value of 1.82. In conclusion, the null hypothesis can be accepted, and it was statistically proven that there is no significant difference between the given percentages of live biomass for different glycerol concentrations. This means that with 95% confidence it can be stated that the nutrient limitation conditions did not affect cell integrity and it is suggested that it solely affects the cell concentration from visual observation, which is the result that was expected from this investigation.

The implication for this result is that when there are lower glycerol concentrations available in the system, which may possibly occur during production downtime, the bacterial culture would not die out but simply grow at a slower rate. In standard industry procedure, most plants schedule plant downtime, where the plant would be fully shut down for maintenance to prevent unplanned plant downtime in the case of process or equipment failure. Due to the large costs associated with plant downtime, as the plant is not generating income during this time, downtime is always kept to a minimum. For this system, this means that the period the culture will be exposed to nutrient limitation conditions will be limited and it can be assumed that the culture will likely not be negatively affected. Another positive assumption that can be drawn from this is that because the cells are not negatively affected by nutrient limitations, the culture death would most likely not decrease for the downtime period.

5.1.5 Shear

From background research, shear stood out as an important parameter to consider during membrane photobioreactor design. In the literature, multiple sources mention the negative effects of high shear in membrane photobioreactors with the application of photosynthetic algae (López-Rosales *et al.*, 2015;

Fortunato, Lamprea and Leiknes, 2020). Vandanjon et al. (1999) conducted an investigation dedicated to determining the effect of shear on algal biomass as contributed by pumps and valves in tangential flow filtration, similar to the design in this project. Similarly, Kim & Lee (2000) and Liao et al. (2012) indicated that shear was a root cause of cell death within a bioreactor setup. In an investigation observed for a bacterial system, it was observed that under elevated shear stress conditions, a decrease in bacterial viability was observed. Also mentioned in this investigation was that viability loss was dependent on both the amount shear stress applied and the exposure time (Lange, Taillandier and Riba, 2001).

Introductory research repeatedly highlighted that the most important physical factor that had to be considered before the operation of this system was the implications of shear on the bacterial cells. For this system, the three components in the MPBR system that contribute to significant shear exposure to the bacterial cells was the ceramic membrane itself, the valve used to create backpressure in the system, and finally the pump. This meant that the effect or extent of shear had to be identified prior to operation of the reactor due to the anticipation of large shear in reactor design.

Therefore, it was assumed that shear would result in significant cell death, and it was necessary to determine the effect of shear over a period of time and this raised to question two things. Firstly, it was asked, does the impact of a constant shear vary for differing times? In other words, when constantly maintaining an elevated shear stress condition, do the effects of shear occur immediately, or does the effect of shear increase during prolonged exposure to shear. Secondly, if the cells are exposed to varying magnitudes of shear for the same period, what would the resulting effect of different shear values be on the culture. The results of these two separate investigations will be discussed in the subsections below.

5.1.5.1 Constant high shear for a varying time

Thus, for this investigation, shear stress was induced on the culture as described in section 4.3.4 by means of a magnetic stirrer and magnetic stirrer bar, using a baffled flask to prevent the formation of a vortex. It was assumed that as the time to shear exposure increased, the number of dead cells would also increase as seen in the investigation by Lange, Taillandier and Riba (2001). It is expected that the high shear conditions emulate the conditions inside the reactor system, which includes mixing in the bioreactor, shear stress over the peristaltic pump and shear stress over the diaphragm valve.

For this investigation, samples were taken in 5-minute intervals up to a time of 15 minutes from the same culture. The culture was subjected to a high velocity gradient of ~5108 s^{-1}. In the figures below (Figure 46, Figure 47 and Figure 48), the effects of shear as time increases can be observed.

As a reference, the control 'healthy' control *R. palustris* cell can also be observed below in Figure 45.

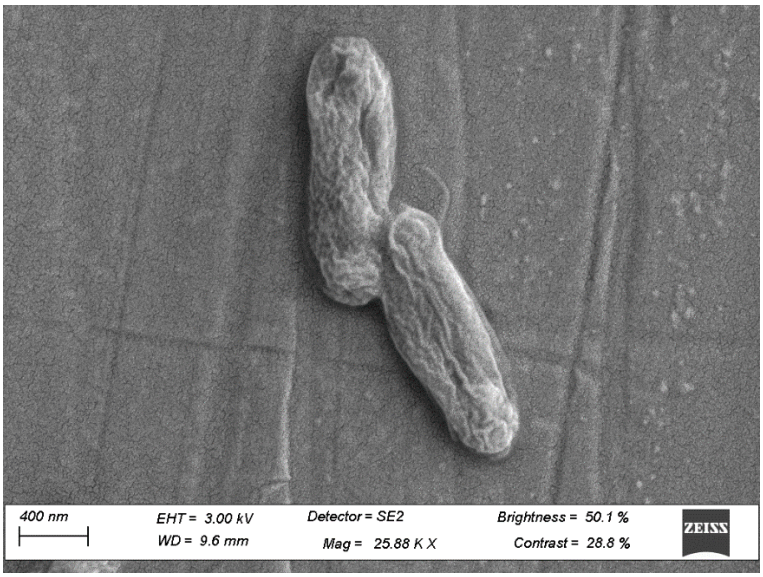

Figure 45: SEM image of an 'Optimal' *R. palustris* cell cultured at 35°C for showing efficient cell growth, substrate utilisation and hydrogen production. This figure is to be used as a control.

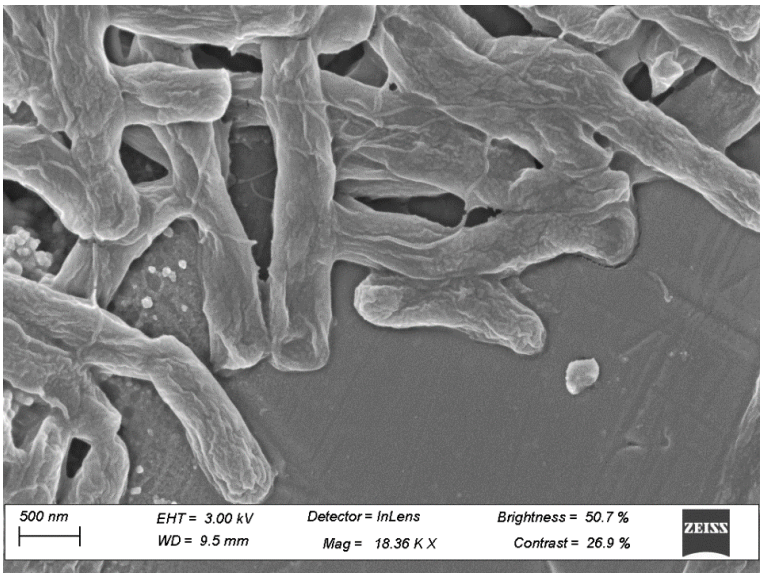

Figure 46: SEM image of *R. palustris* cells subjected to high velocity gradient (~5108 s^{-1}) shear stress for 5 minutes

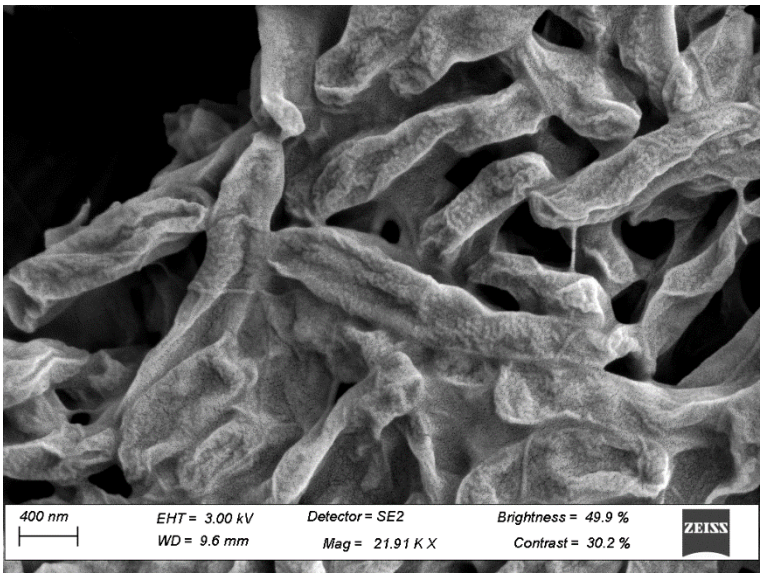

Figure 47: SEM image of *R. palustris* cells subjected to high velocity gradient (~5108 s^{-1}) shear stress for 10 minutes

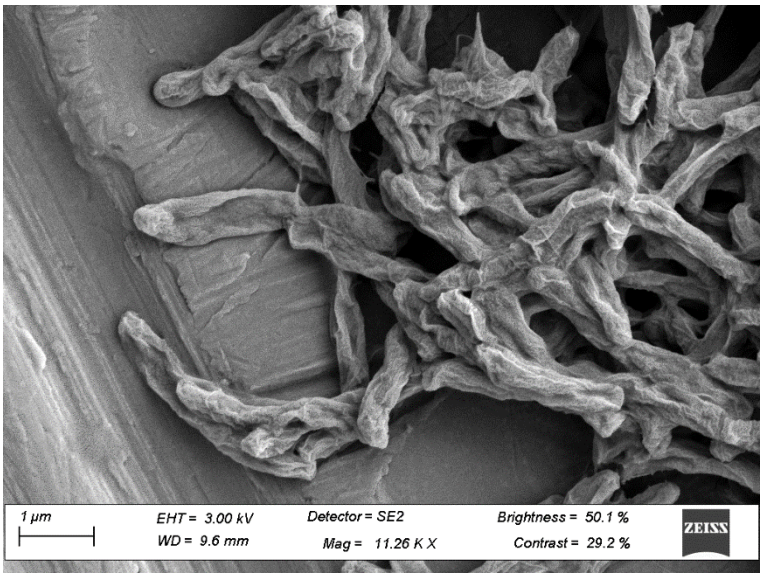

Figure 48: SEM image of *R. palustris* cells subjected to high velocity gradient (~5108 s^{-1}) shear stress for 15 minutes

In Figure 46, the cells display signs of distress although some cells appear relatively uncompromised. In Figure 47, the cell walls appear to indicate that more severe strain was placed on the cells. Finally, for Figure 48, all the cells appear to display signs of significant stress by their collapsed cell walls and overall deformed appearance. Similar to what was seen in the pressure investigation (section 5.1.3), the cells have coagulated which could be due to the characteristic sign of distress seen with *R. palustris*. The increasing appearance of compromised cells suggests the assumption that over time the effects of shear stress increase. To support this assumption the results of FCM were also considered and can be seen in the table (Table 32) below, for each time investigated the duplicate results are also displayed.

Table 32: Reported percentage of biomass alive from FCM after shear exposure for varying times. Shear exposure is related to a velocity gradient of ~5108 s^{-1}.

Time (minutes)	% Live biomass	% Compromised
5	54.5	24.3
10	51.8	25.8
15	45.7	28.3

In order to determine if there is a significant difference between the percentage of live biomass after 5 minutes of shear stress exposure in comparison to 15 minutes of shear stress exposure a t-test was conducted, and the results are displayed in Table 33 below. Assuming a 95% level of confidence in comparing the percentage of live biomass for 5 and 15 minutes of shear stress exposure, the P(T<=t) two-tail value of 0.002 is smaller than the selected significance of 0.05. This means that it was confirmed with 95% confidence that the time exposure to shear did have a significant effect on the resulting percentage of live biomass in the system. Significant breakage of the cells was an indication that the shear stress on the culture could not be sustained.

Table 33: t-Test to determine statistical significance of the difference between 5 and 15 minutes of shear exposure

t-Test: Two-Sample Assuming Equal Variances

	5 minutes	*15 Minutes*
Mean	54.75	45.35
Variance	0.125	0.245
Observations	2	2
Pooled Variance	0.185	
Hypothesized Mean Difference	0	
df	2	
t Stat	21.855	
P(T<=t) one-tail	0.0010	
t Critical one-tail	2.9199	
P(T<=t) two-tail	0.0020	
t Critical two-tail	4.3027	

5.1.5.2 Varying shear for a constant time

For this investigation, five different velocity gradients were implemented, each for a total of 15 minutes on separated liquid cultures from the same large culture volume, to reduce unnecessary variation between results. It was assumed for this investigation that as the magnitude of applied shear increases, in this case, indicated by the percentage of live biomass will decrease. In the following figures (Figure 50,

Figure 51, Figure 52, Figure 53 and Figure 54), the effect of varying shear for a constant time can be observed.

As a reference, the control 'healthy' control *R. palustris* cell can also be observed below in Figure 49.

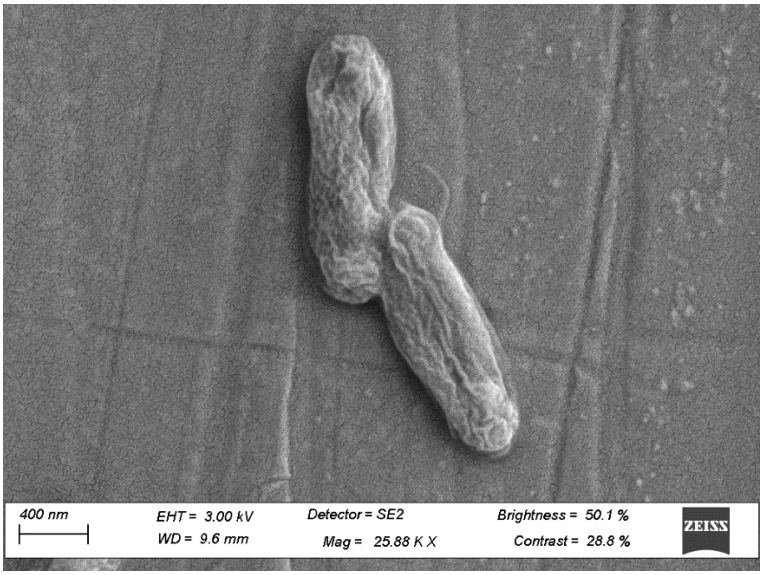

Figure 49: SEM image of an 'Optimal' *R. palustris* cell cultured at 35°C for showing efficient cell growth, substrate utilisation and hydrogen production. This figure is to be used as a control.

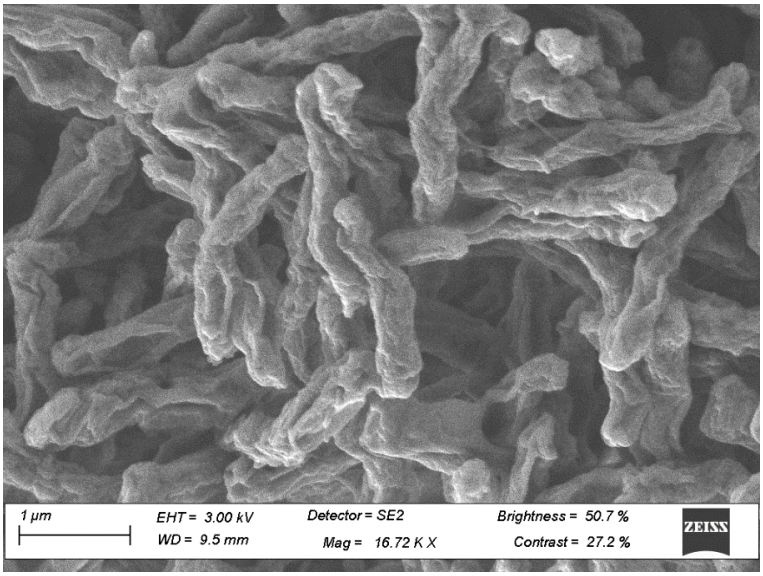

Figure 50: SEM images of *R. palustris* cells under the lowest shear stress setting investigated (~1852 s^{-1}) (named setting 1) for 15 minutes.

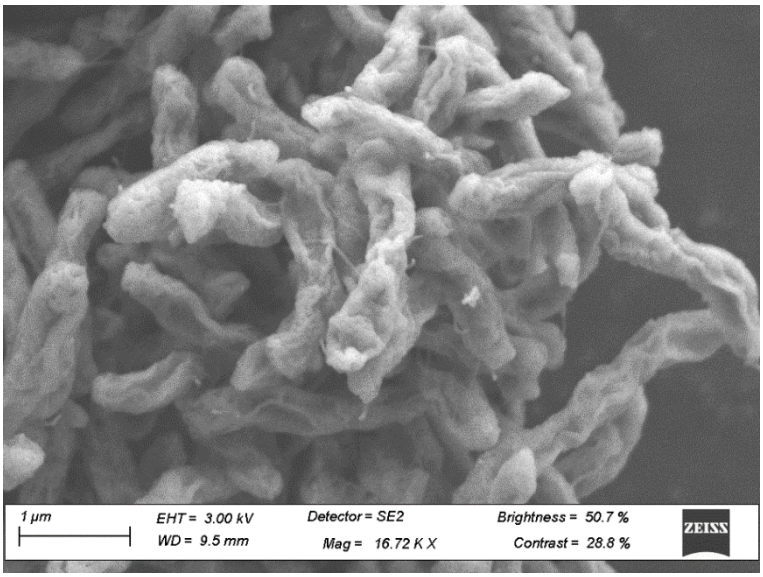

Figure 51: SEM images of *R. palustris* cells under the second lowest shear stress setting investigated (2620 s^{-1}) (named setting 2) for 15 minutes.

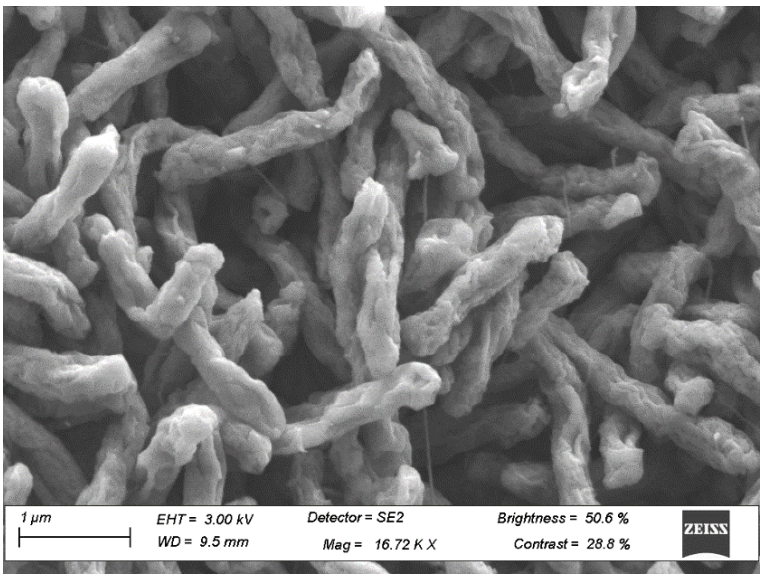

Figure 52: SEM images of *R. palustris* cells under the mid-shear stress setting investigated (3209 s^{-1}) (named shear setting 3) for 15 minutes.

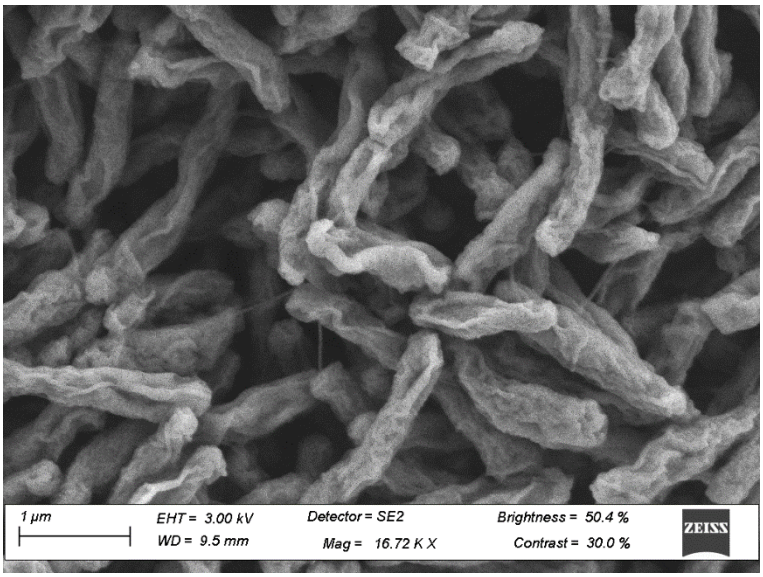

Figure 53: SEM images of *R. palustris* cells under the second highest shear stress setting investigated (3705 s^{-1}) (named setting 4) for 15 minutes.

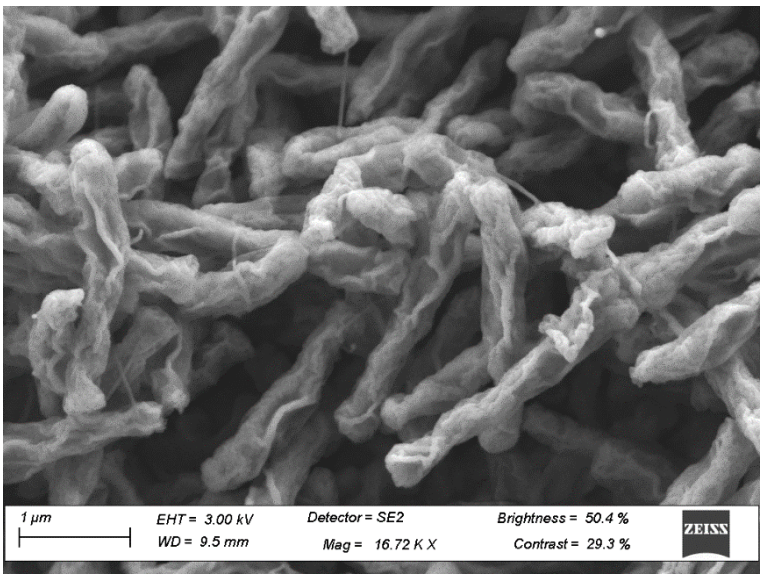

Figure 54: SEM images of *R. palustris* cells under the highest shear stress setting investigated (4143 s^{-1}) (named setting 5) for 15 minutes.

From these images (Figure 50, Figure 51, Figure 52, Figure 53 and Figure 54) in all samples the cells appear to have undergone severe cell lysis, cell walls appear deformed and collapsed; there is no noticeable difference between the appearance of the cells by sole observation from SEM results. In the table below (Table 34), the FCM percentages of biomass alive after shear exposure was reported. At a first glance these results tend to suggest that as the implemented shear was increased, the percentage of biomass increased. To determine if the difference was significant, ANOVA was used as seen in Table 35; the null hypothesis is assuming that there is no difference between the application of different shear magnitudes over an identical period.

Table 34: Each investigated shear value over a period of 15 minutes along with the resulting G-value and remaining live biomass percentage obtained from FCM

Shear Setting	G-value (s^{-1})	% live biomass	% Compromised
1	1852	64.4	25.2
2	2620	60.4	28.7
3	3209	57.5	31.9
4	3705	53.5	36.8
5	4143	48.9	44.2

From Table 35, it can be seen that the P-value is smaller than the assumed significance of 0.05 and the F-value (114.36) is larger than the F-crit value of 3.478. This means that the null hypothesis is rejected in favour of the alternative; the difference in percentage biomass reported alive is significantly different. As the magnitude of shear is increased, this correlates to an increase in cell death under the tested circumstances for the tested period.

Table 35: Single factor ANOVA on different shear magnitudes implemented over a constant time

Source of Variation	*SS*	*df*	*MS*	*F*	*P-value*	*F crit*
Between Groups	270.21	4	67.551	114.3634	2.64E-08	3.4781
Within Groups	5.9067	10	0.5907			
Total	276.11	14				

5.1.5.3 Implications of shear investigation

This investigation suggested two results; firstly, it was seen that the effects of shear, meaning the cell death as the result of shear, did increase with time to exposed shear. Secondly, the magnitude of shear imposed also affects cell death when exposure time to shear is kept at a constant. This implies that the final impact of shear on bacteria in the system will be a factor of both the time the bacteria is exposed to said shear and the magnitude of the shear imposed on the culture.

This is not a positive result when considering the desired use of this organism in the membrane photobioreactor. As mentioned in the introduction to this section, there are three important components in the MPBR system that would contribute shear to the system: the membrane, the pump and the backpressure valve. This means that as the culture is continuously circulated in the system, with each circulation the effects of shear are experienced by the culture and a percentage of the culture would be negatively affected. Another hypothesis is that the energy of the cells would be spent on cell repair rather than cell growth or hydrogen production.

To mitigate the effects of shear, design considerations needed to be made with regard to the physical aspects of these components. As these design considerations needed to be made for investigation, this discussion can be seen in more detail in section 5.2.

5.1.6 Decreasing the effect of shear by increasing fluid viscosity

After observing the severe impact shear had on the cells, it was important to investigate multiple shear mitigation strategies including both design (as discussed in section 5.2.1) and fluid properties. In this investigation, the sole purpose was to observe the effect of an increasing viscosity on the resulting effects of shear on bacterial culture. Although when considering changing the rheology of the culture medium, the impact of this on the culture cells must be investigated. If a thickening agent is used the effect of the substance on mass and heat transfer within the bioreactor, potential photo-limitation and the impact on membrane must be investigated.

In this investigation, guar gum was selected as a thickening agent, as the literature commonly used this inert compound to increase viscosity (Blackburn and Johnson, 1981; Casas, Mohedano and García-Ochoa, 2000), although the application of guar gum in combination with a membrane was not found in the literature. The effect of guar gum on heat and mass transfer, possible photo-limitations, and the effect of the thickener on the guar gum remains unknown as this was not the focus of this investigation.

Unfortunately, the investigation was limited to the results from SEM as FCM could not process these samples due to possible clogging of the FCM column. Results of this experiment can therefore only be suggested from the visual appearance of the cells and not based on a given quantity of cells remaining alive.

5.1.6.1 The effect of increased viscosity on shear

In the images below (Figure 55 to Figure 63), the culture in combination with guar gum can be observed. Figure 55 represents the appearance of the culture without the addition of guar gum with a viscosity of 0.9 cP; this was also assumed to be the viscosity of the culture at any other given point of experimentation. From here the figures are displayed in order of increasing guar gum concentration. For the exact guar gum concentration please refer to Table 19 in section 4.3.6. For this investigation, the mixing energy that was applied to the sample was varied, and the time of shear exposure was kept to a constant. Because the viscosity gradient is a function of viscosity and the relationship between the two parameters will result in a decrease in the viscosity gradient as the viscosity increases for each sample. The viscosity gradient for each sample can be seen in the table (Table 36) below.

It was observed that as the thickening agent concentration increased the cells appear to be caught in a type of gum/cell matrix. Although it is possible that they appear like this due to the methodology used by SEM to spread the cells in a thin layer for observation. So, when solely looking at the cell wall shape, the cell walls at a higher viscosity appear less deformed than those seen at a lower viscosity. This implies that the effect of shear was in fact curbed by changing the rheology of the fluid, which is preliminarily, a positive result.

Table 36: Velocity gradient applied to each sample for each different viscosity tested

Viscosity (cP)	G (s^{-1})
0.9	58594.7
1.9	40327.6
2.5	35156.8
4.1	27452.8
5.9	22885.1
7.5	20297.8
10.2	17405.2
15	14352.7
22.2	11797.8

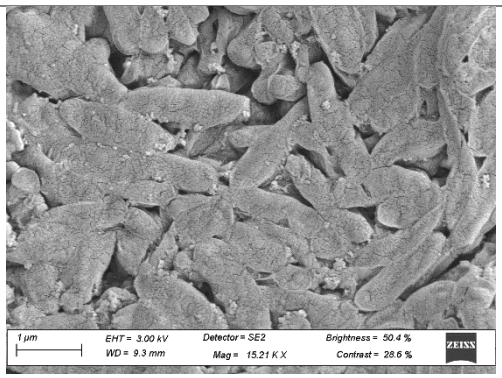

Figure 55: SEM image of *R. palustris* culture with a fluid viscosity of 0.9 cP (No guar gum)

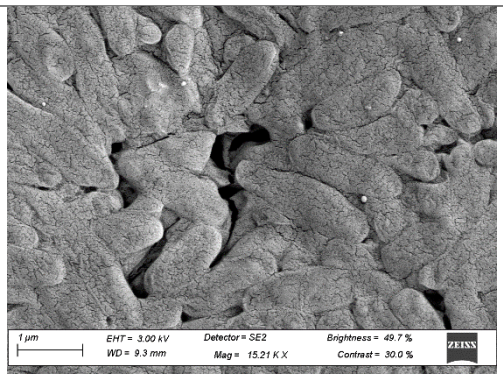

Figure 56: SEM image of *R. palustris* culture with a fluid viscosity of 1.9 cP

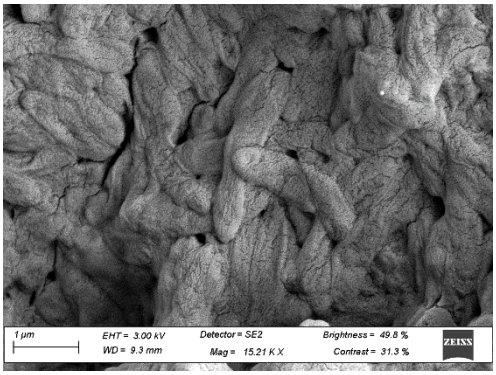

Figure 57: SEM image of *R. palustris* culture with a fluid viscosity of 2.5 cP

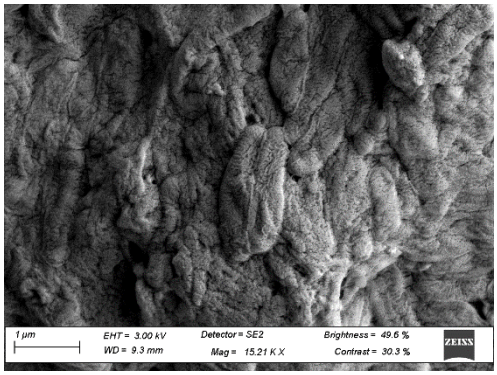

Figure 58: SEM image of *R. palustris* culture with a fluid viscosity of 4.1 cP

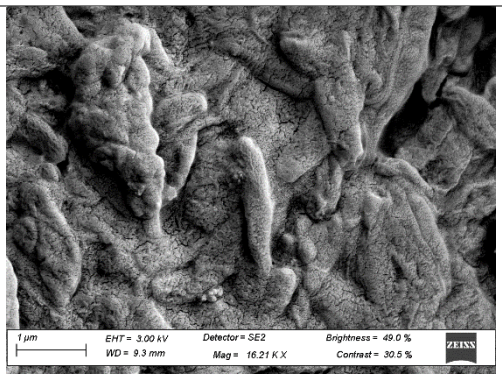

Figure 59: SEM image of *R. palustris* culture with a fluid viscosity of 5.9 cP

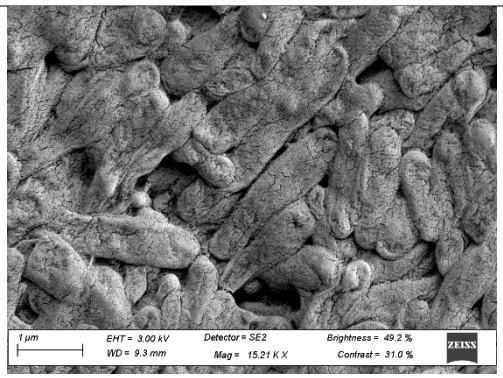

Figure 60: SEM image of *R. palustris* culture with a fluid viscosity of 7.5 cP

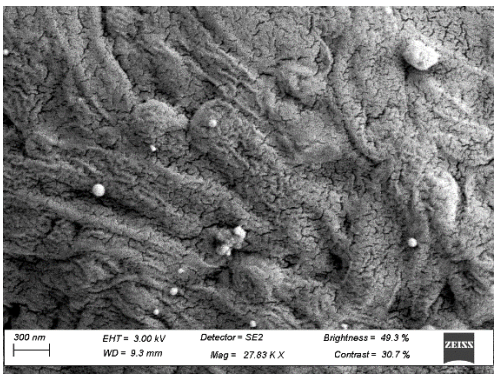

Figure 61: SEM image of *R. palustris* culture with a fluid viscosity of 10.2 cP

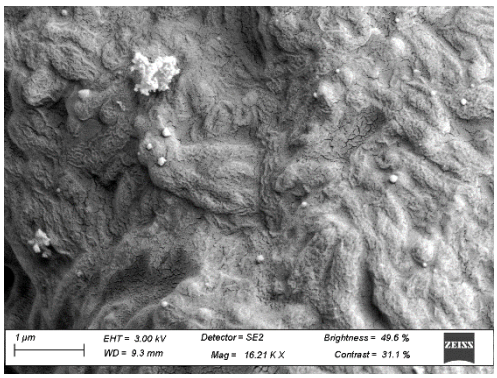

Figure 62: SEM image of *R. palustris* culture with a fluid viscosity of 15 cP

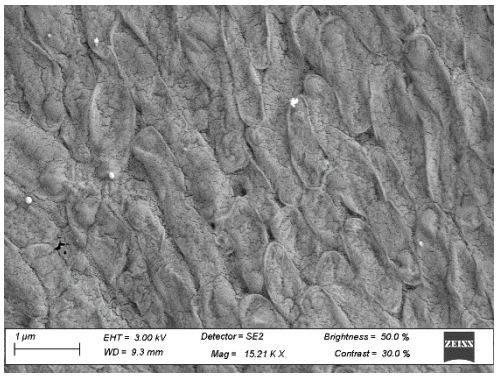

Figure 63: SEM image of *R. palustris* culture with a fluid viscosity of 22.2 cP

5.1.6.2 Implications of increasing viscosity

From this investigation when observing the effect of shear, it is clear that with increasing viscosity, the resulting velocity gradient was decreased. It can only be suggested that with the decrease in the applied

velocity gradient, the effects of shear would also be decreased as seen in the investigation in section (section 5.1.5). Assuming no negate effects are experienced with the application of the thickening agent as mentioned in the previous section, this would mean that the effects of shear could be significantly decreased to aid in increased biomass growth and hydrogen production. The thickening agent is assumed to interfere with membrane operation by depositing onto the membrane in the form of a cake layer, although this is a suspicion and has not been observed in the literature.

5.2 Design, fabrication and operational conditions of the MPBR

From the pathology map, it was deduced that with a suitable design and operational conditions, the effects of shear and pressure could be mitigated to a certain extent to in turn try to improve the performance of the culture, in terms of cell growth and hydrogen production, in the system.

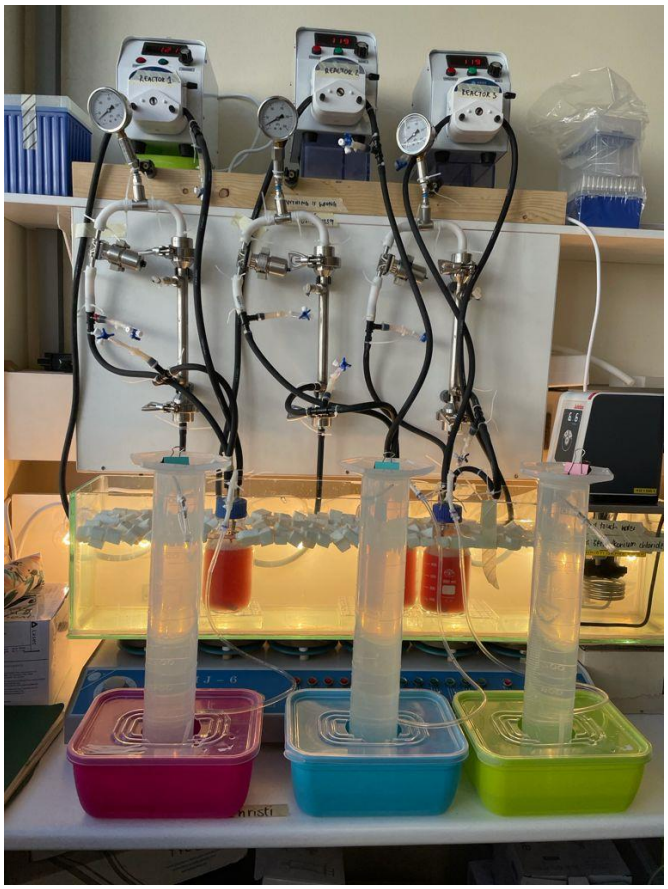

Figure 64: Experimental setup of the MPBR

5.2.1 Photobioreactor design choices

The developed pathology map was used as a guideline in the design process of the MPBR design; this was to ensure that the physical factors that had severe effects on cell integrity were kept to a minimum, as far a design could allow; considering, there are always limitations with the design of any system, be it, capital, space availability or simply physical culture limitations. Vandanjon et al. (1999) dedicated an investigation into the shear effects of valves and pumps in tangential membranes. The influence different

pumps, valves and circulation rates had on the growth of the organism highlighted the importance of the component section in this project.

In the process of designing the MPBR, it was important to ensure that all the physical components were able to withstand exposure to 121°C, as the entire system needed to be autoclaved prior to inoculation to ensure sterility. Sterile operation is essential for experimental investigations in order to be able to compare the results from this investigation to that seen in literature; contamination changes the chemical environment within the reactor which could lead to variation in biological hydrogen production and substrate utilization by *R. palustris.* Simply put, a contaminated culture would deliver different results which would not be repeatable in follow-up investigations.

Considering the use of this system on an industrial scale, a completely sterile system would not be feasible due to extremely high associated costs to sterilise high volumes of fluid or equipment. In industry, steam would be used to sterilise the system, although some contamination would be likely to occur. Thus, completely sterile operation is only a requirement for experimental operation to deliver repeatable results. It is important to note that if sterility is not a requirement, several design changes could be made to both streamline operation and utilise more economic processing equipment (e.g., valves, pumps or piping).

In the following subsections, the major design considerations made for this investigation will be discussed.

5.2.1.1 Back-pressure valve

As mentioned in the introduction to this section, important factors that had to be considered with the selection of the valve were system sterility and shear minimization. This meant that the valve had to adhere to the following requirements: the entire body of the valve must be able to withstand sterilisation temperatures, the shear stress over the valve must be as little as possible and the valve must be able to adjust to a desired position to attain the correct backpressure over the membrane. There are three common types of valves in the industry: block valves, non-return valves and throttle valves (Skousen, 2004). For this application, a manual throttle valve was necessary as it is the only valve type with which the valve position can be changed to achieve the desired effect, in this case backpressure.

When considering the options available within the desired size range for this application, there were needle, globe or diaphragm valves available that complied with the sterility and manual operation requirements. The selected valve must be able to fine-tune to be able to change the resulting backpressure on the membrane, from here the needle valve and diaphragm valve are both a good fit. Considering the significant effect of shear on the bacterial cells, the diaphragm valve was selected to minimize imposed shear in the system. The valve body was constructed from stainless steel and the diaphragm itself is constructed from EPDM to ensure the entire valve body is autoclavable (i.e., able to withstand 121°C and 1 bar) without compromising the valve operation to maintain a sterile environment. The final design specifications of the valve can be seen in Appendix B - Specifications of design choices.

5.2.1.2 Pumps

There were two pumps required for the setup of the system; a main pump to circulate culture to and from the bioreactor, through the membrane and valve and the other pump was required to dose new feed into the bioreactor during continuous operation. Two pump types were considered for operation: a centrifugal or peristaltic pump. Again, both shear and required sterility proved to be the deciding factors. A peristaltic pump is a non-invasive method of pumping to ensure sterility within the piping network. Unfortunately, it was seen in investigations by Kim et al. (2001) and Wang et al. (2017), that the imposed shear stress on cultures in the peristaltic pump was larger than that observed for a centrifugal pump.

Although because sterility was considered the most important factor in this experimental design, peristaltic pumps were selected for both applications. The pump sizes used were significantly different, as a dosing pump needs to pump at a significantly lower flowrate than that of the main piping network. The dosing pump selected obtained from CRpump had a flow range from 0.0015-17.8 mL/min, ideal for the application of low feed flowrates into the bioreactor. The main piping network pump was obtained from Runze Fluid and had a 0-1700 mL/min flow range, which was an ideal application to test a range of pumping speeds to determine a suitable turnover rate for the system The specifications for both pumps can be observed in Appendix B - Specifications of design choices.

As sterility through autoclaving would not be a requirement in an industrial setup, as such an operation would simply not be feasible on such a large scale, a centrifugal pump would be used, which can be sterilised using steam. As seen by Kim et al. (2001) and Wang et al. (2017), this would be beneficial in an industrial setup, as the centrifugal pump imposes less shear stress on the culture.

5.2.1.3 Piping

For this investigation, three different types of piping were required: piping network for culture circulation from the bioreactor through the membrane and back, piping from the bioreactor to the hydrogen collection port and finally the piping required from the feed through the dosing pump into the bioreactor. A summary of the piping specifications can be seen in Appendix B - Specifications of design choices.

Important factors to consider with the selection of the piping required for culture circulation were as follows: resistance to autoclave conditions, prevent light penetration, resistance to use in peristaltic pump and low hydrogen permeability. An opaque pipe was required to limit light exposure outside of the bioreactor, this was to be able to minimize ambient light exposure to draw the conclusion that the illumination of the culture was majority with the light source selected.

The most important factor identified from these requirements is the material the pipe is constructed of. The thickness and opacity of the pipe will affect the light penetration and resistance to pump wear and tear. The piping selected was specifically formulated for low gas permeability, fatigue, abrasion and temperature resistance. Tygon Laboratory (A-60-G) was constructed from industrial grade Norprene in an opaque black colour.

The other type of piping required was the piping network from the bioreactor to the hydrogen collection port. As there is no liquid present in this network, the only major requirement for this piping network is

low hydrogen permeability to ensure that the obtained hydrogen readings were as accurate as possible. This piping section did not need to be subjected to autoclave conditions and could therefore have poor temperature resistance properties to reduce pipe cost. The piping selected was from Tygon Laboratory (S3-E3603) and was seen to have the lowest hydrogen permeability rate from the selections available.

The final piping required was for the feed line into the bioreactor from the feed tank through the dosing pump. The requirements for this pipe selection were: compatibility with the dosing pump selected, resistance to pipe degradation from pump wear and tear, and resistance to autoclave conditions. For this application, piping manufactured from Norprene (A-60-F 06402) was selected. This pipe is also formulated for enhanced abrasion, fatigue, and temperature resistance.

5.2.1.4 Membrane

With membrane selection, the important factor to consider was sterility, this narrowed down the types of membranes that could be used for this application. A single-channel UF ceramic (Al_2O_3) membrane element with a selectivity of 100kDa[10] and an active surface area of 50cm^2 was selected. *R. palustris* cells vary between 0.6 and 0.9μm which places it under ultrafiltration (Imhoff, Hiraishi and Süling, 2005). For this the recommended pore sizes vary between 1 and 500kDa. Thus, for initial testing a 500kDa membrane was used but cells were observed in the permeate, indicating that a smaller pore size might be required. The next pore size selected was the 100kDa, which resulted in the desired filtration with no cells observed in the permeate.

In order to ensure complete sterility, the membrane was placed inside a stainless-steel casing, to reduce handling of the membrane, as this could cause minor fractions that would affect the selectivity of the membrane as well as fouling. The membrane casing and the membrane itself can be seen in the Appendix B - Specifications of design choices.

5.2.2 Operational conditions

In the investigation by Vandanjon et al. (1999), it was found that organism degradation increased with frequency of passes, in this investigation referred to as the turnover rate. This is because at a higher turnover rate the cells experience increased exposure to membrane shear stress, membrane backpressure, shear stress over the valve and shear stress from contact with the pump.

5.2.2.1 Turnover rate

When considering the final goal of the reactor system is sufficient substrate utilisation, hydrogen production, and cell growth, which only occurs optimally with a healthy bacterial culture. From what was observed in the pathology map investigation, this means minimizing shear stress exposure. This was initially mitigated by making design choices that benefit the bacteria, such as the choice of valve or pump, although this can be minimized even further by selecting operation conditions that consider the bacteria as well. One way to do this is to simply limit the exposure time of the bacteria to these components that

[10] Da- Daltons

place shear stress on the culture. By decreasing the flowrate of the culture to the piping, directly relates to the culture spending less time in the piping network and resulting in lower shear stress exposure.

Unfortunately, there is a lack of guidelines in the literature as to the selection of an optimal turnover rate for effective filtration and simultaneous minimization of shear stress exposure. Determining this optimal operating point would, however, be a timely procedure and for the purpose of this investigation, a turnover rate had to be assumed. Considerations that had to be made with regards to the turnover rate were: the average amount of time a bacterial cell would spend in the reactor as an increased reactor residence time would increase light exposure and eventually hydrogen production and from a practical viewpoint, a realistic permeate flow and effluent substrate concentration.

The turnover rate selected was once every six hours, meaning that the entire volume of the bioreactor and fluid in the piping has been circulated once every six hours to ensure that the culture does not spend the majority of the time in the piping where it has no light exposure. A slower turnover rate would result in decreased reactor capacity, slower delivery of a permeate although a faster turnover rate would result in increased stress on the cells and significantly reduced exposure to the light source which is essential for efficient hydrogen production. There was no literature available on ideal turnover rates and it was assumed that a turnover rate of once every six hours is appropriate.

Thus, to calculate the flowrate of the culture in the main piping network, the desired turnover rate and the culture volume was used. This resulted in a crossflow velocity of 0.113 L/h, as applied by peristaltic pump before the membrane.

5.2.2.2 Flux

As mentioned in the background research into membrane operation in section 2.5.2.3, the critical flux of a membrane is a critical parameter to be considered when determining the operating conditions of a membrane. Following the flux-step procedure outlined in section 4.2.2.1, the critical flux value could be obtained for each different pump speed investigated by testing the range of backpressures. In the figure below (Figure 65), a curve was developed that related the critical flux value to membrane cross-flow velocity (in other words different pump speeds).

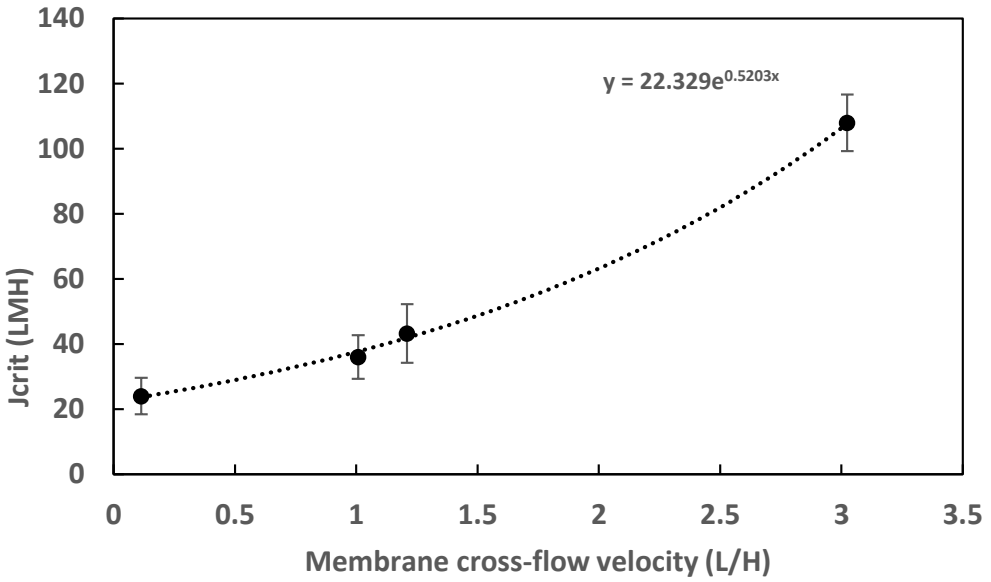

Figure 65: Critical flux as a function of membrane cross-flow velocity. Error is presented by means of standard error bars from triplicate runs.

From this point, the desired cross-flow velocity, which results in a once every six hours turnover rate, can be located on the curve to obtain the resulting critical flux, which is a value of 24 LMH. As mentioned in 2.5.2.3, a good rule of thumb is to operate at a flux value that is 80% of the critical flux, in this case being 19.2 LMH. Thus, when the MPBR was set up for an experimental run, the cross-flow velocity would be set to 0.113 L/h and the valve would be closed to ensure a backpressure of which would result in the desired flux value.

The critical flux curves attained from the flux-step method can be seen in Appendix E – Critical flux.

5.2.3 Summary

In conclusion, this section considered both physical design considerations and operation conditions that were required to attain the required results for this investigation. For physical design considerations, the predominant decisive factors to consider were sterile operation and shear stress mitigation strategies. Operational condition requirements were mostly dependent on membrane fouling and shear stress mitigation strategies for sustainable equipment operation.

5.3 Membrane photobioreactor (MPBR) operation

In the following subsections, the performance of the MPBR can be observed under different operational modes: control, batch and continuous. The results from this investigation give insight into the resulting cell growth, hydrogen production and substrate utilisation profiles for each type of reactor configuration. The possible effects of prolonged exposure to the physical components and operational conditions of the MPBR system as suggested by the pathology map investigation will also be observed.

For the first subsection the control mode operation of the MPBR will be discussed. For this mode of operation, the back-pressure valve was not included in the experimental setup, and the culture was

simply recirculated in the system without permeation through the membrane as backpressure is required for permeation. In batch mode operation of the MPBR, both the permeate and the retentate streams were recycled back into the reactor. Under continuous operation a feed stream was dosed into the bioreactor and the permeate was continuously removed.

The investigated parameters (growth, substrate utilisation and hydrogen production), of the experimental runs will be compared to that of a Schott bottle system as described in section 4.1.4.2.

The starting biomass concentration of experimentation was chosen to be a lower concentration in order to observe both cell growth at the initial stages of experimentation and later for the entire experimentation period, both substrate utilisation and hydrogen production rates over a range of observed biomass concentrations. Data from later stages in experimentation could possibly shed light on changes in substrate utilisation and hydrogen production rates that arise due to photo-limitation at high biomass concentrations. The MPBR was operated under the conditions investigated in section 5.2 and setup as stipulated in section 4.2.3, 4.2.4 and 4.2.5.

5.3.1 Control MPBR operation

The control run was operated to investigate the growth of the culture, hydrogen production and substrate utilisation when culture is circulated through the MPBR system. Thus, for this investigation, the valve was removed from the system. This meant that there was no backpressure in the system and consequently no flux through the membrane. Essentially, the goal was to simply observe the performance of the culture by isolating the effect of constant circulation through the system. The performance parameters of the control run were compared to that of a Schott bottle culture, which means that the only difference between the system is the constant recirculation of the culture. This would then imply that any difference observed in the parameters between the control and Schott bottle experiment is most likely due to the effects of recirculation.

The first parameter in this investigation was the observed biomass concentration for the duration of the experiment. Simply because both hydrogen production and substrate utilisation are obviously heavily dependent on this (Pott, 2013; du Toit and Pott, 2021). The concern for this performance stems from the implications derived from the pathology map investigation, the significant effect of shear, imposed by the peristaltic pump, on the bacterial cells could directly hinder the cell growth in the system. Although, du Toit and Pott (2021) also mention the mistake of assuming that a very high biomass concentration would be a measure of effective hydrogen production, as the ATP energy generated is then favoured by the cell for growth rather than hydrogen production by the hydrogenase enzyme. Additionally, as the biomass concentration in the reactor increases, the effect of mutual shading also increases, which means that the light exposure of an average cell decreases.

In Figure 66 below, it can be seen that the biomass concentration indicated a positive trend, with a positive growth rate, as the culture started with a concentration of 0.74 ± 0.07 g/L, and the experiment was terminated at a concentration of 4.25 ± 0.25 g/L after 240 hours, which compares well to what was observed in the literature (du Toit and Pott, 2021) or as seen in section 2.3.7. Preliminary, this is a positive

result, as increasing biomass concentration implies that the constant circulation of the biomass in the system did not cause overwhelming cell death as suggested by the pathology map. This was assumed due to the colour of the culture.

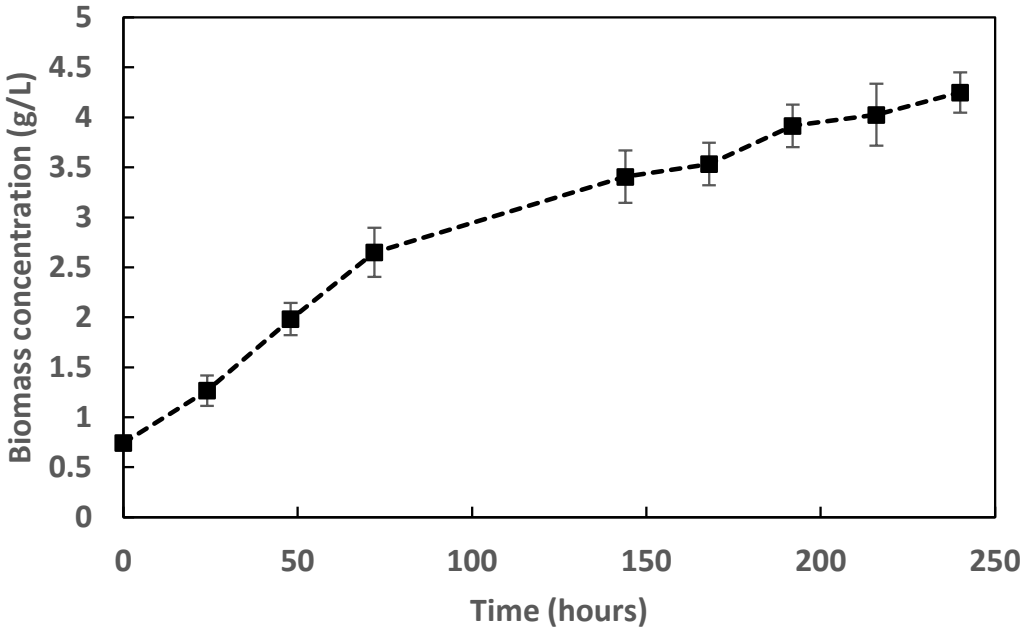

Figure 66: Biomass concentration of *R. palustris* for 240 hours control operation of the MPBR. Error is presented by means of standard error of triplicate runs.

To observe the effect of recirculation on the growth of the culture, the control results were compared to growth observed in a simple Schott bottle reactor setup. In Figure 67, is clear to see that the growth of *R. palustris* is similar for both the control mode operation and Schott bottle growth over a period of 240 hours. This implies that the growth of *R. palustris* is not perceptibly affected by repeated circulation for the investigated time period.

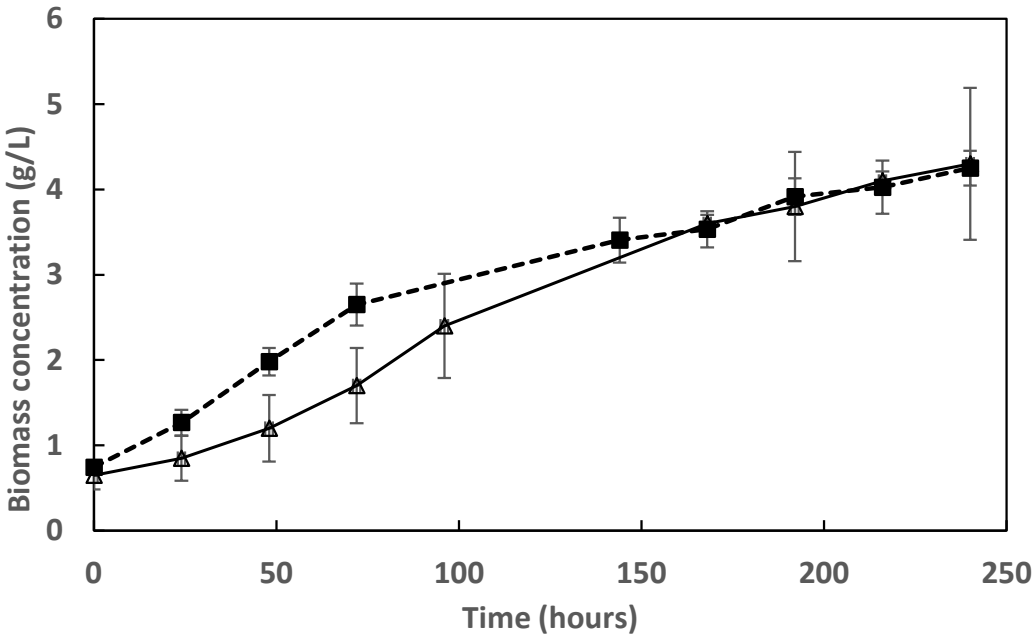

Figure 67: Comparison of *R. palustris* biomass concentration in the MPBR under control mode (--■--) and Schott bottle growth (-Δ-) for a period of 240 hours. Error is represented by means of standard error of triplicate runs.

The substrate concentration for the experimentation period can be seen in Figure 68 below. It was observed that percentage glycerol conversion by *R. palustris* at the end of the 240 hour period was roughly ~74±0.11%. This value is higher than the conversion efficiencies observed in the literature, which were reported to be about 58.06±10.9%. A possible reason for this could be that due to the shear stress experienced by the culture, the rate of substrate uptake in the cells was increased to aid in cell recovery from external physical damage. Another possibility is an increase in efficiency of mass transfer due to better mixing, as the culture is both agitated in the reactor and mixed during circulation. From the shape of the curve (Figure 68), it appears as though the substrate utilisation had not reached a steady state, which suggests that if the system has been operated for a longer period of time, a lower glycerol conversion percentage would have been observed. Despite the system operating in a batch-style configuration with a decreasing glycerol concentration, it was not expected to severely affect the cells as during the pathology map experimentation, the cells that were growing under nutrient deficiency appeared to show no sign of distress.

As the basis of this investigation is wastewater treatment and delivering a wastewater stream with a low substrate concentration is an important requirement, the high glycerol conversion efficiency is preliminarily a positive result. Considering an industry standard for a greasy effluent, as crude glycerol would be, the industrial effluent requirement would be 10 mg/L (National Water Act 36 of 1998, 2013; Krishnan and Balasubramanian, 2014). That means that despite the effective glycerol conversion efficiency observed for this experimentation, the effluent would still be above the industrial effluent standard with a concentration of 0.1 g/L and the effluent would either require additional treatment.

Another option would be to prolong reactor operational time although the effect of extended exposure to stress on the culture remains unknown.

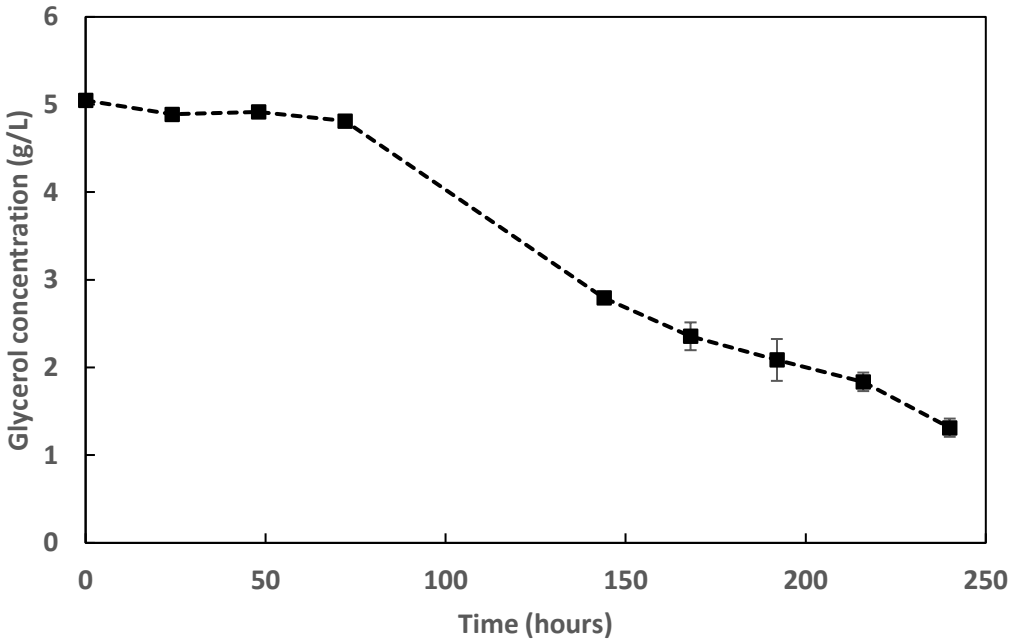

Figure 68: Glycerol concentration as utilized by *R. palustris* for duration of control run experimentation (240 hours). Error is represented by means of standard error of triplicate runs.

When considering hydrogen production over the experimentation period as seen in Figure 69, hydrogen production was negligible for the first 4 days. This maybe be due to the culture that is not yet within the stationary phase, or that there was some hydrogen capture in the system, which had to be displaced back into the reactor volume. After the weekend some hydrogen production was observed, and an increase was recorded for each day up to a cumulative volume of ~262±62.4 mL after 240hours of operation. However, these results compare very poorly with what was observed in the literature for a comparative culture volume, and similarly a significantly poorer production rate. Hydrogen production by the same strain of *R. palustris* and similar conditions was observed to be roughly 1200±100 mL which is almost 5 times higher than what was attained in this investigation (du Toit and Pott, 2021).

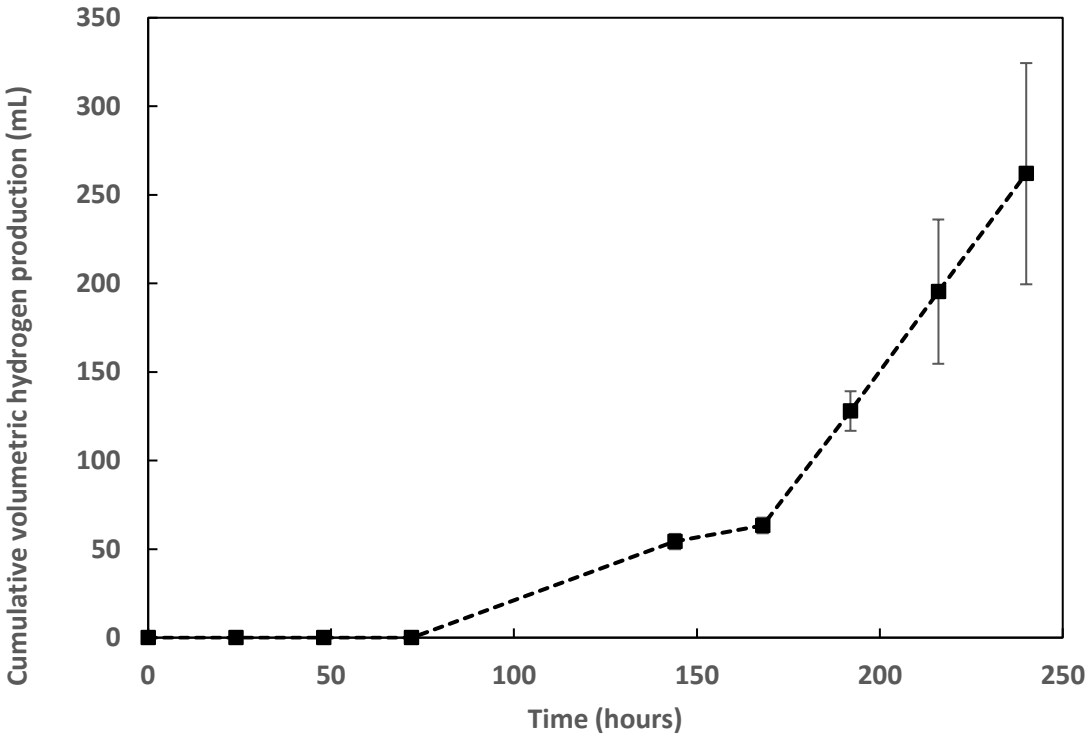

Figure 69: Cumulative volumetric hydrogen production by *R. palustris* for 240 hours operation during control operation of the MPBR. Error is presented by standard error of triplicate runs.

In Figure 70 below, hydrogen production of the control operation of the MPBR is compared to the hydrogen production observed with Schott bottle cultivation, which acts as a control that illustrates the effect of no circulation on bacterial performance. In the figure (Figure 70), there is a perceived difference between hydrogen production for Schott bottle cultivation and hydrogen production in the control mode of operation as the final hydrogen production of the Schott bottle system attained a cumulative hydrogen production of 520±81.3 mL in comparison to the control MPBR hydrogen production of 262±62 mL. Thus, the difference between the two systems suggests being a result of recirculation.

The suspicion of poor hydrogen production was confirmed when referring to Figure 71, where the maximum achieved hydrogen production rate was 0.72±0.2 mL/g_{CDW}/h in comparison to the literature where a maximum of more than 20 mL/g_{CDW}/h was observed. Specific hydrogen production rate is a parameter that provides insight into the hydrogen production of the culture as the culture biomass increases. From this figure it appears that hydrogen production increased as the culture concentration increased, especially closer to the end of the experimental period. This was an anticipated result and hydrogen production occurs in the stationary phase of cell growth.

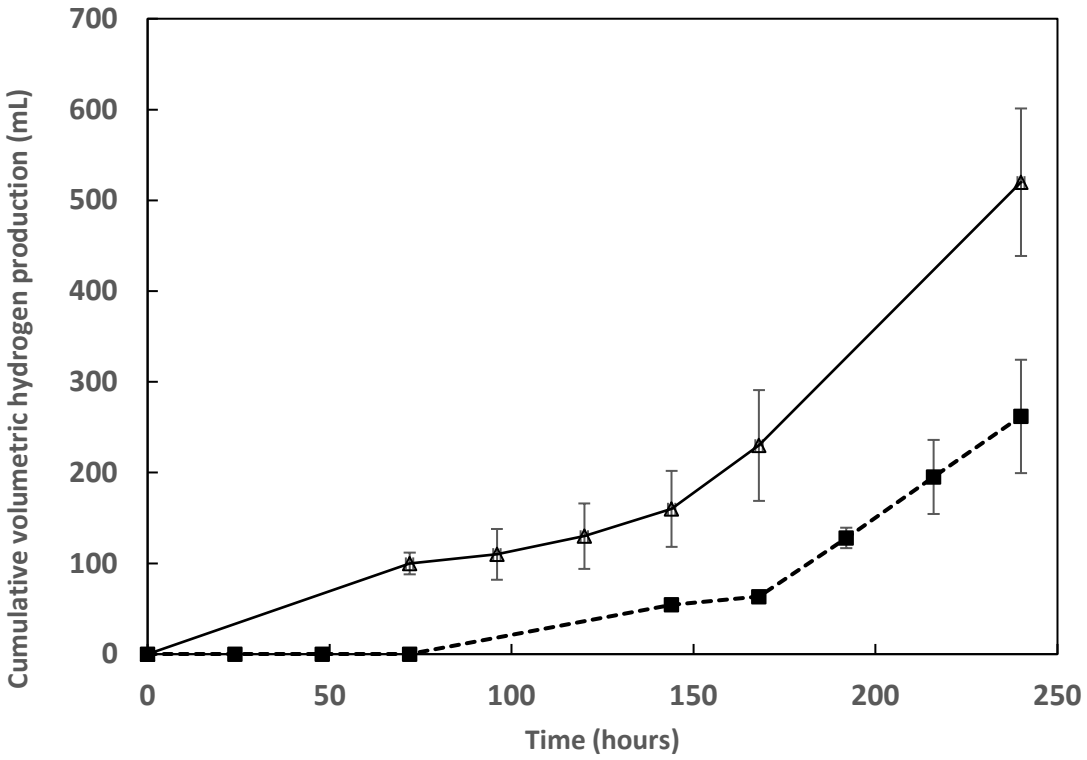

Figure 70: Comparison of *R. palustris* hydrogen production in the MPBR under control mode (--■--) and Schott bottle growth (-Δ-) for a period of 240 hours. Error is represented by means of standard error of triplicate runs.

These poor hydrogen production rates could be attributable to the constant shear stress imposed on the culture by circulation through the system, as the other shear stress-inducing components of the system were removed from this physical setup. It is assumed that as the culture is exposed to the shear stress, ATP energy is redirected to cellular energy demands for cell repair, as suggested by the increasing biomass concentration, rather than ATP being used for hydrogen generation.

The other possibility, as suggested by the difference between hydrogen production in control operation of the MPBR and Schott bottle growth, is the result of the light interaction effect of recirculation. It is assumed that the culture spends ~40% of the total reactor operation time in the dark due to the low flowrate and large piping volume. This would mean that there is significantly less ATP available for hydrogen production as the culture is not sufficiently illuminated, strongly suggesting a light interaction effect. Because the culture spends quite some time in the piping network in the dark and in combination with the stressed condition of the cells, it is likely that the cells are producing polyhydroxybutyrate (PHB) rather than hydrogen. PNSB bacteria produce PHB when placed in a suboptimal environment as an energy-and-carbon-storage compound (Wu, Liou and Lee, 2012). As this is a polymer compound, the presence of this carbon storage compound can be confirmed by microscopic investigation of the sample, although this was not done for this investigation.

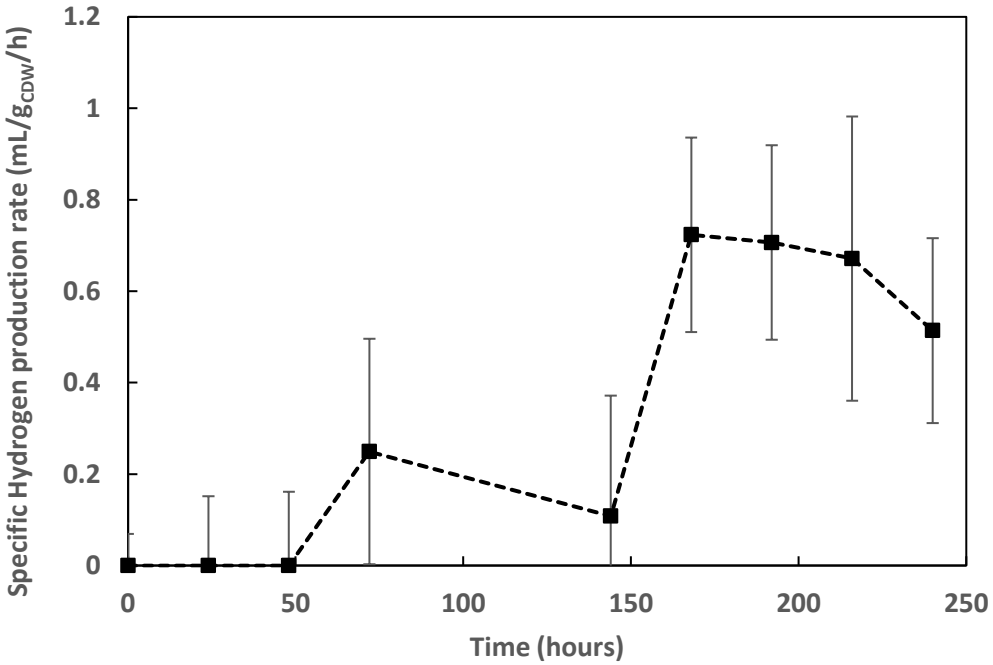

Figure 71: Specific hydrogen production of *R. palustris* under MPBR control mode operation for 240 hours. Error is presented be means of standard error of triplicate runs.

In the figure above, Figure 71, the error bars are relatively large, indicating that the data points may not be trustworthy enough to draw definite assumptions. The jumps in data points are most likely due to the calculation of a specific hydrogen production rate which resulted in a small value being divided by a much smaller value.

From the results in the control investigation, it was anticipated that under both batch operation and continuous operation, hydrogen production would be severely affected. This is because when comparing the growth, substrate utilisation and hydrogen production for the control experimental period to the Schott bottle growth or values observed in the literature for similar culture conditions (as seen in section 2.3.7), poor product production rates were reported.

As more shear stress-inducing components like the valve, flow over a membrane and pressure are introduced, it would be logical to assume that this would impact the bacteria, from assumptions made from the pathology map investigation as an increase in shear stress magnitude was seen to have a significant effect on the culture. Thus, changes in growth, substrate utilisation and hydrogen production were expected.

5.3.2 MPBR under batch operation

From the control MPBR operation investigation it was observed that although the biomass concentration was similar to that observed in the literature for optimal bacterial culturing (du Toit and Pott, 2021), hydrogen production was significantly less than what was stated in the literature, despite similar biomass concentration. As mentioned, this was possibly due to the nature of a batch-style setup MPBR, and the

constant circulation of the culture and the time the culture spends in the dark, it is anticipated that hydrogen production would be even less under the increase of shear stressors in the system. In this system, there is an increase in shear stress from the control by the additional shear stress over the diaphragm valve and the membrane as well as stress due to backpressure over the membrane. For this discussion, some comparisons between the performance of the control experimentation and batch experimentation will be made to draw conclusions regarding the effect of the added shear stress in the system.

In Figure 72, the upwards trajectory of the curve again indicates that despite the physical strain in the system, a positive growth curve was observed for biomass in the system. For this medium, the growth rate observed is similar to that reported in the literature (du Toit and Pott, 2020), and similar to what was observed with the control MPBR operation. The attained cell concentration curve resembles the expected growth curve of the culture as seen in du Toit & Pott (2021) for *R. palustris* grown with a starting substrate concentration of 50 mM glycerol at 35°C. The initial cell concentration at the start of experimentation was 0.75±0.02 g/L and ended at a concentration of 4.3±0.06 g/L after 240 hours of growth. As observed in the literature, the cell population does not tend to increase beyond this observed concentration despite high substrate concentrations. Low sample error could be attributable to the Buglab Biomass Sensor used instead of the simplification used to relate OD to CDW to deliver biomass concentration as described in section 4.4.1, as the multi-step process could have led to a loss in biomass.

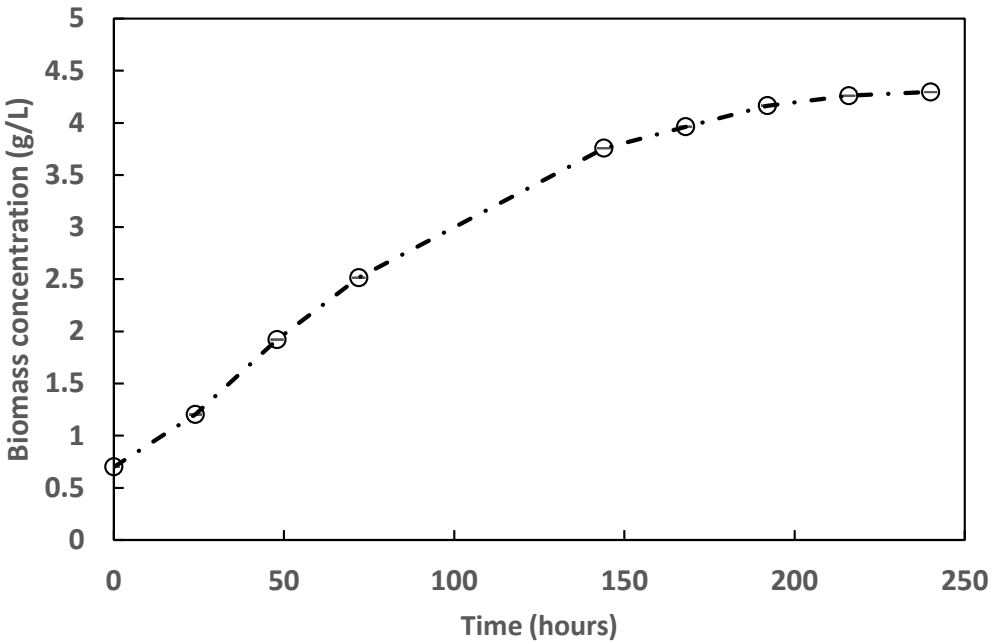

Figure 72: Biomass concentration of *R. palustris* in the MPBR under batch configuration operation for a period of 240 hours. Error is presented by means of standard error of triplicate runs, although not visible, suggesting good repeatability of sampling and readings.

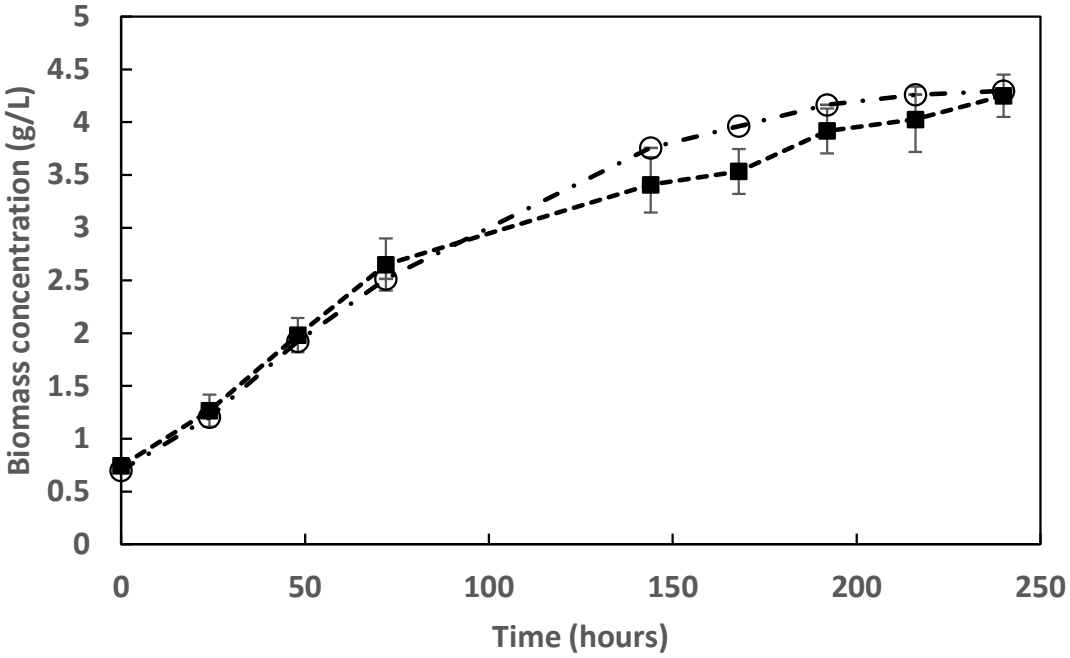

Figure 73: Comparison of *R. palustris* biomass concentration in the MPBR under control mode (--■--) and batch mode (— · O · —) operation for a period of 240 hours. Error is represented by means of standard error of triplicate runs.

From the figure above (Figure 73), the mean data points and associated standard error are close, suggesting that there is no substantial difference in the biomass concentration for the control experimentation and batch operation. This means that the extra shear stress induced on the culture, by the valve, membrane, and backpressure, did not result in any perceptible stunted growth or cell death of the culture. This means that the biomass growth for batch mode operation of the MPBR compares well to Schott bottle and values observed in the literature (du Toit and Pott, 2021)

The next important parameter considered was substrate utilization within the system, as this is the basis of wastewater treatment, and it was expected that the glycerol concentration would decrease over time with increasing cell concentration, as seen with the control run operation. Despite the system operating in a batch configuration with a decreasing glycerol concentration, it was not expected to severely affect the cells. During the pathology map experimentation, the cells that were growing under nutrient deficiency appeared to show no sign of distress. In Figure 74 below, the percentage glycerol conversion was seen to be ~88.72%, again we see a substrate conversion efficiency significantly higher than values reported in the literature. Despite this high conversion efficiency, as mentioned in section 5.3.1, this is not considered sufficient treatment for industrial effluent as the concentration remains above the suggested 10mg/L (National Water Act 36 of 1998, 2013; Krishnan and Balasubramanian, 2014). As mentioned previously, the reactor operation time must either be prolonged, or the effluent must receive additional treatment.

As mentioned in the previous section, this could perhaps be due to the shear stress experienced by the culture and the rate of substrate uptake in the cells was increased to aid in cell recovery from external

damage. The data points below a concentration of 0.1 g/L are not available as the HPLC analysis available is unable to accurately detect the glycerol concentration at this point and is thus not shown. However, this dwindling glycerol concentration coincides with the timepoint at which the biomass concentration curve levels out, both possibly due to limited substrate and reaching the stationary phase of growth.

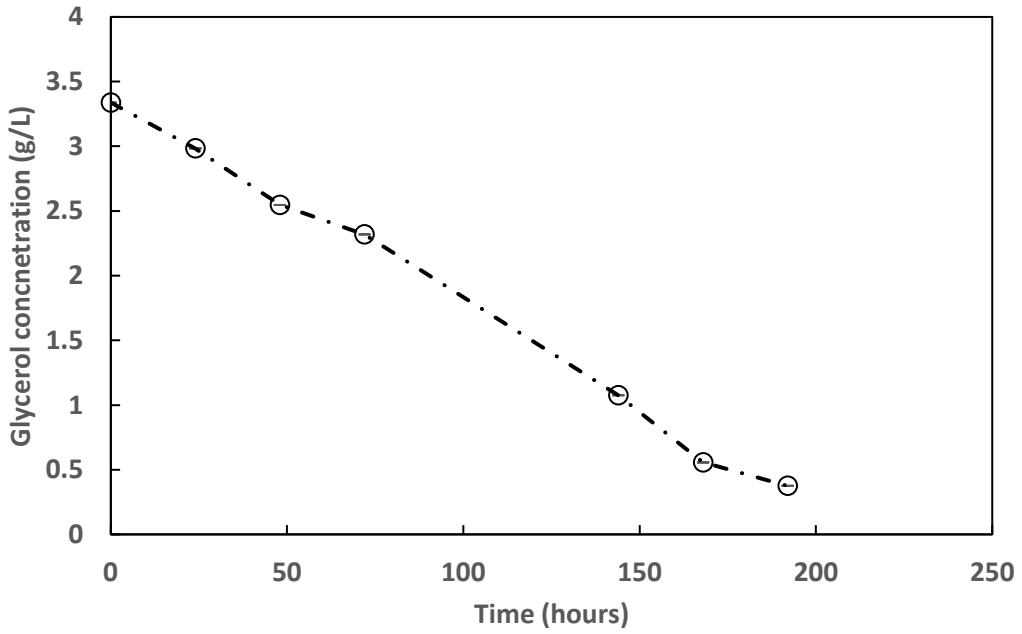

Figure 74: Glycerol concentration in the MPBR system under batch configuration operation for a period of 240 hours. Error is presented by means of standard error of triplicate runs, error bars are present but not visible, indicating good repeatability of sampling and readings.

When considering hydrogen production, from Figure 75 below the hydrogen production for the experimentation period is considerably lower in comparison to hydrogen production by *R. palustris* in other reactor configurations (such as immobilized bacteria in a fluidized or packed bed configuration(du Toit and Pott, 2020; Ross and Pott, 2021a)) or a basic Schott bottle reactor setup for the same period with similar biomass concentrations as seen in section 2.3.7. Similarly, the hydrogen production for batch mode operation even compares poorly to what was observed in the control operation experimentation. The results of cumulative hydrogen production in this system was a full order of magnitude lower with only 106±29.06 mL after 240 hours, to that of du Toit & Pott (2021), which achieved cumulative hydrogen production of 1.2 L for an identical time interval.

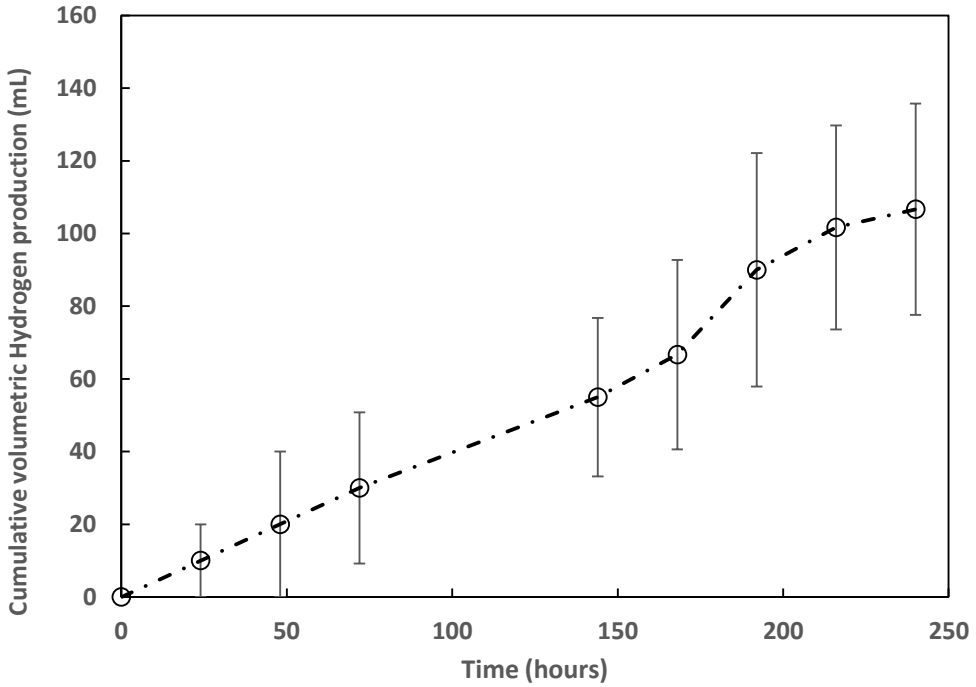

Figure 75: Cumulative volumetric hydrogen production by *R. palustris* in a MPBR system under batch configuration operated under 35°C, with a starting glycerol concentration of 50mM and nitrogen limitation. Error is presented by means of standard error of triplicate runs.

In Figure 76 below, the cumulative hydrogen production volumes for Schott bottle system, control operation and batch operation can be observed. At the 240 hour timepoint, it is apparent that the Schott bottle system had produced the highest cumulative hydrogen production. In comparison to the batch and control system, which had produced similar cumulative hydrogen at the end of the investigative period.

To confirm the significance of the difference, a two-tailed t-test was conducted (selected significance α=0.05), to determine if there is a significant difference between the cumulative volumes of hydrogen gas produced, in the table (Table 37) below. The reported P(T<=t) two-tail value was 0.0017 which is smaller than the selected significance of 0.05. Therefore, with 95% confidence, it can be confirmed that there is a significant difference between the cumulative volumes of hydrogen produced at the selected time point.

Table 37: Summary of two-tailed t-test to determine significance of the difference between cumulative hydrogen production for control run operation and batch operation

t-Test: Two-Sample Assuming Equal Variances

	H_2 control @240h	*H_2 batch @ 240h*
Mean	520	106.6
Variance	6561	2533.3
Observations	3	3
Pooled Variance	4547.2	
Hypothesized Mean Difference	0	
df	4	
t Stat	7.507	
P(T<=t) one-tail	0.001	
t Critical one-tail	2.131	
P(T<=t) two-tail	0.0017	
t Critical two-tail	2.776	

This meant that even for a greater culture volume with similar biomass concentrations, comparing the Schott bottle system of only 500 mL versus batch mode MPBR operation of 680 mL, only a tenth of the volume hydrogen was produced. This was in support of the assumption made at the end of control run experimentation, and that the additional shear stressors in the system were most likely the reason behind poor hydrogen production rates, due to redirection of ATP energy.

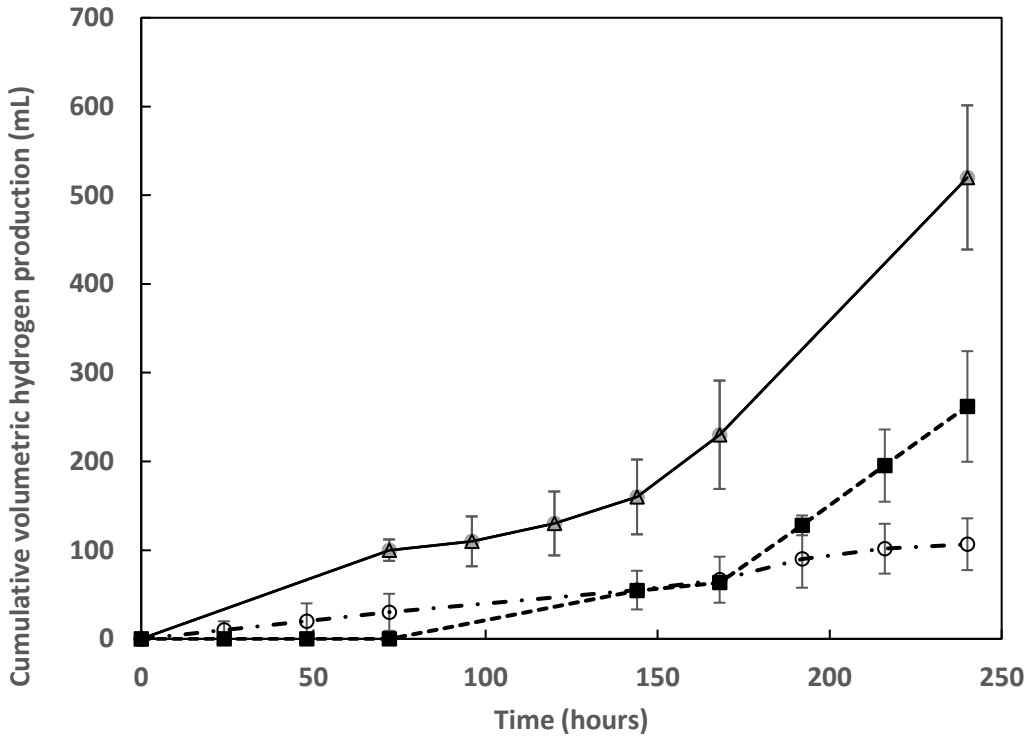

Figure 76: Comparison of *R. palustris* cumulative hydrogen production under Schott bottle growth (-Δ-) control operation (--■--) and batch mode operation (— · O · —) for 240 hours. Error is presented by means of standard error of triplicate runs.

The last parameter to be discussed is the specific hydrogen production of the culture under batch operation. Specific hydrogen production rate is a parameter that provides insight into the hydrogen production of the culture as the culture biomass increases

A maximum specific hydrogen production rate of 0.426±0.008 mL/g_{CDW}/h was observed at the start of experimentation and did not return to this production rate during any observed point in time as seen in Figure 77. A two-tailed t-test was conducted to confirm that there is significance between the maximum and minimum specific hydrogen production rate and the resulting table is below (Table 38). The P(T<=t) two-tailed value obtained was 0.00036 which is lower than the assumed significance of 0.05. This means that it can be stated with 95% confidence that there was a significant difference in specific hydrogen production rates at different points of the experiment. The fact that specific hydrogen production rates showed a decreasing trend for the duration of experimentation was not a surprise and was observed in an investigation by du Toit and Pott (2021), where it was speculated there was deeper light penetration due to lower biomass concentrations. This meant that ATP regeneration was optimised which resulted in high hydrogen production rates.

Table 38: Summary of two-tailed t-test to determine significance of the difference between the maximum and minimum specific hydrogen production rate for batch operation

t-Test: Two-Sample Assuming Equal Variances

	Maximum specific H_2 production rate	*Minimum specific H_2 production rate*
Mean	5	104.17
Variance	150	1964.2
Observations	6	6
Pooled Variance	1057.1	
Hypothesized Mean Difference	0	
df	10	
t Stat	-5.2829	
P(T<=t) one-tail	0.0002	
t Critical one-tail	1.8125	
P(T<=t) two-tail	0.0003	
t Critical two-tail	2.2281	

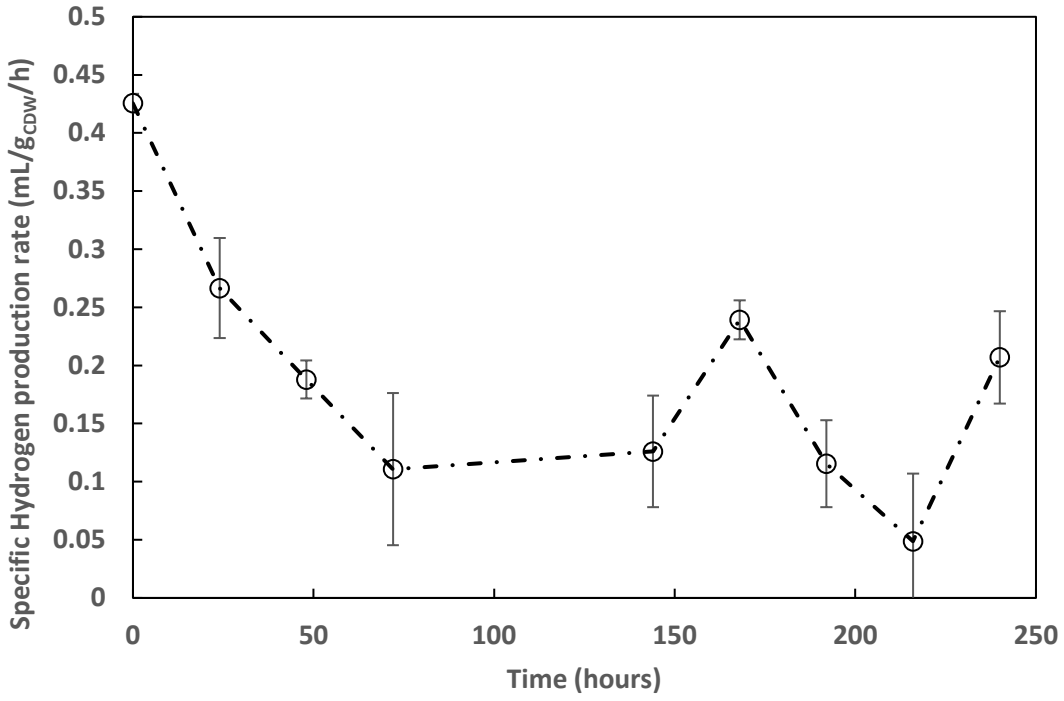

Figure 77: Specific hydrogen production of *R. palustris* for(-Δ-) control operation (--■--) and batch mode operation (— · O · —) for a period of 240hours. Error is presented by means of standard error of triplicate runs.

A photo of the reactor setup can be seen in Figure 79. The system was set up vertically with the Schott bottle reactors in the water bath for temperature control and piping to lead through the pump, into the membrane with permeate and retentate flows back into the reactor. Inverted cylinders acted as a water displacement system for hydrogen collection. It was observed that during operation, there was a build-up of gas at the top of the reactor system by the pressure gauges, this caused an undesired pressure increase and sudden increase in flux; it was also observed that gas build-up disturbance was less prevalent as the culture got older. The system had to be flushed horizontally before the operation could resume. The variation in hydrogen readings is possibly due to this build-up of hydrogen gas as indicated by the problem almost disappearing as hydrogen production from the biomass plateaued, indicating that the gas build-up was most likely hydrogen that was not captured in the water displacement system but rather reverted into the piping network due to physical design.

The design setup and the requirement for regular horizontal flushing also meant that variation between the replicates of the experiment is possibly due to constant manoeuvring of the system and hydrogen production could have occurred at a different time than when it was reported on the graph.

In Figure 78 below, the specific hydrogen production rate between batch and control operation is displayed. It appears as though during initial experimentation, there is difference in specific hydrogen production rates, although during later experimentation, with the onset of the stationary growth phase, the control operation MPBR, suggests having a higher specific hydrogen production rate. This may be due to the higher amount of shear stressors in the batch system in comparison to the control system. It was assumed that with higher stressors the PHB production by the organism increases and hydrogen production decreases. This simply translates to poor specific hydrogen production rates as the time to shear exposure increases as seen with the batch mode operation of the MPBR.

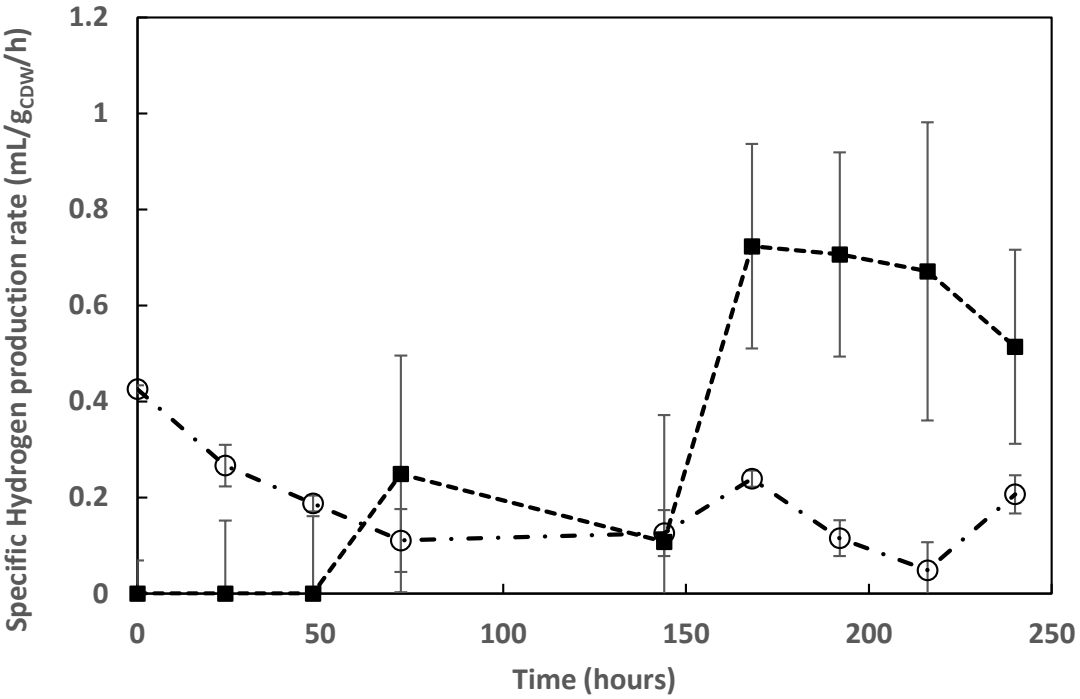

Figure 78: Specific hydrogen production of *R. palustris* for a period of 240hours. Error is presented by means of standard error of triplicate runs.

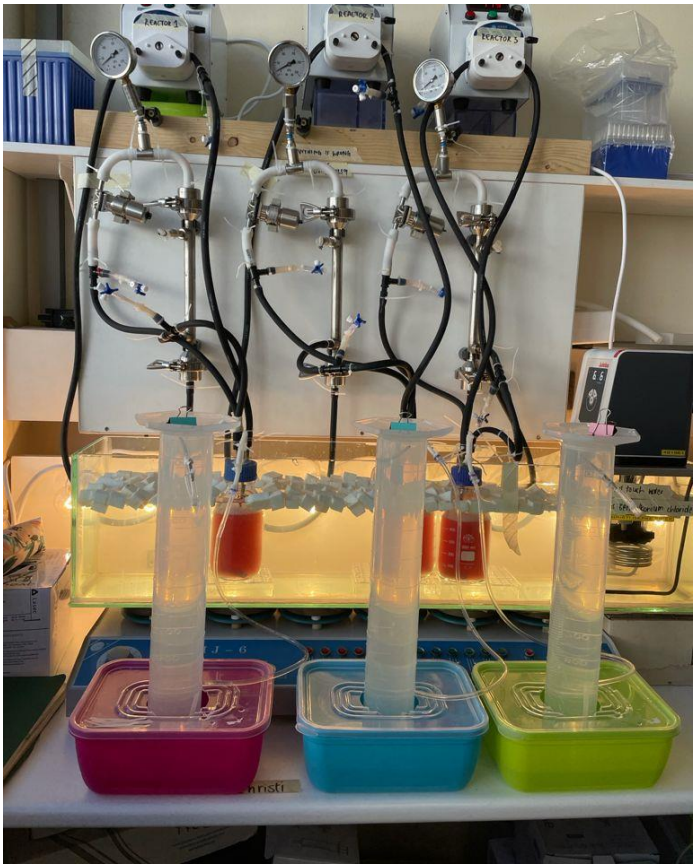

Figure 79: Photograph of the MPBR setup operating under batch configuration.

After experimentation, the pure water flux experiment was conducted to determine whether severe fouling had taken place and it was observed that the critical flux value for the membrane decreased severely. This meant that fouling of the membrane had taken place which could be attributable to cell debris in the system as a result of the severe shear stress on the culture as predicted by the pathology map.

The operation of the membrane photobioreactor under batch conditions was an important first insight into the possible use of this reactor configuration in the industry. The poor hydrogen production rates were definitely a confirmation that this reactor configuration is not ideal if the goal is to produce significant amounts of hydrogen energy by means of waste valorisation. Despite this, positive outcomes were observed with substrate utilisation and biomass concentration, this means that if this was to be applied to biodiesel wastewater for the treatment of crude glycerol as mentioned in section 2.3.6, this could be a possible solution, albeit without a valuable side product. In a large-scale reactor this would be a less prevalent problem, as the piping networks would be designed in manner that prevents gas build-up in in the process network piping. Additionally, transparent piping can be used to increase illumination of the culture as it is being recirculated to and from the reactor. As mentioned in section 5.2, a centrifugal pump would be used in the industry which would most like result in better system performance as the shear stress from recirculation pumping would be less.

The final test for this system is the operation under continuous conditions, considering the issues that arose with operation under batch mode such as gas accumulation in the system and system flushing requirements, it was assumed that this would be amplified under continuous operation.

5.3.3 MPBR under continuous operation

Over a period of 6 months, various attempts were made at successfully operating the MPBR in continuous mode. However, the investigation into the operation of the MPBR under continuous mode resulted in frequent reactor failure for two main observed reasons which will be discussed in the following sections. For the remainder of this discussion, for simplification's sake, each different reason for failure will be referred to as Type 1 and Type 2, which will be discussed in detail in the subsections below. In order to understand the issues experienced with the system setup and operation, the system setup is described below.

Figure 80: Continuous mode setup of the MPBR. Seen on the left window balcony is the minimal media need feed into the bioreactor. The pump on the desk to the right of these bottles is the dosing pump feeding the media into the glass bioreactors. The colourful Tupperware with the upturned measuring cylinders is the water displacement system used to measure volumetric hydrogen production. The white pumps at the top of the image are the main piping network pumps feeding into the membrane. Media is circulated from the glass bioreactor through the main pump into the membrane unit from the bottom; permeate is directed to the glass bottle at the bottom of the image and retentate passes through the valve in the white piping section and back into the bioreactor.

With system setup, after sparging, under sterile conditions, the system was flooded with minimal media to increase culture volume in the system from the 500mL in the bioreactor glass bottle to 680mL, to account for liquid volume present in the piping network. The after flooding the piping network the piping was clipped externally to prevent fluid transfer as the system was moved from a sterile environment to the vertical setup shown in the figure (Figure 80). The valve was fully open and the feed pipe was placed into the main pump, the pump was switched on simultaneously as the external clips were removed. The system was allowed to run for a few minutes to ensure that the air had been pumped from the piping network and then placed in the vertical position as seen in the image. This was to prevent air accumulation at the top of the system, i.e. the piping network by the main pumps and the piping section by the pressure gauge.

It was possible to run this system for a limited amount of time, roughly 5 days at the most, however with regular checks and alterations in the valve position, changes in the dosing flowrate and flooding of the

system. If this was applied to a larger reactor, a control strategy would need to be applied. Using a version of a PI-controller, a change in the pressure over the reactor as well as the permeate flowrate would indicate a required change in the valve position to correct the pressure and permeate flowrate to sustainable operating conditions.

For unattended overnight operation and weekends, severe system failure was observed. Under working conditions, for the limited number of hours the system was operated, hydrogen production was observed, although the hydrogen gas was mixed with the argon gas from sparging, so the exact amount is unknown. This was presumably due to the low biomass concentration in the system, as biomass was constantly pushed from the system due to an increase in liquid level in the reactor, and the continuous high substrate concentration, which was a phenomenon observed in batch mode operation. The observed glycerol concentration in the permeate was also relatively high ($\pm$ 3.67g/L), which indicates that the turnover rate is probably too high and the output stream would be rejected as a waste stream due to high glycerol concentration. The results obtained from continuous mode experimentation were erratic due to loss of biomass through the hydrogen gas collection port and are not displayed in the discussion as they present no value to the argument. The biomass concentration curve can be observed in Appendix F – Continuous mode operation, from the large error visible and erratic style of the curve it is suggests that the results could not be used as an indication of system efficiency as they present no clear trend. There is a large deviation between samples, and they are not statistically viable to draw any conclusions regarding significance.

Additionally, these were not the only issues experienced with the system, the two mentioned occurred the majority of the time, although most of the problems stem from the strict requirement to work sterile which eliminated most of the possible solutions.

5.3.3.1 Reactor failure Type 1

The first problem experienced was the accumulation of gas within the piping network. In Figure 81 below, the piping area in which gas accumulation was observed is indicated by the highlighted green piping. The gas was assumed to be a combination of both hydrogen and Argon gas which was used to sparge the system to remove gaseous nitrogen. As mentioned in section 2.3.3.1, it was required to remove gaseous nitrogen and oxygen from the system to promote hydrogen production by the nitrogenase enzyme. Also seen in the figure are red blocks containing an exclamation mark, these marks indicate the location of actions resulting from air build-up in the system.

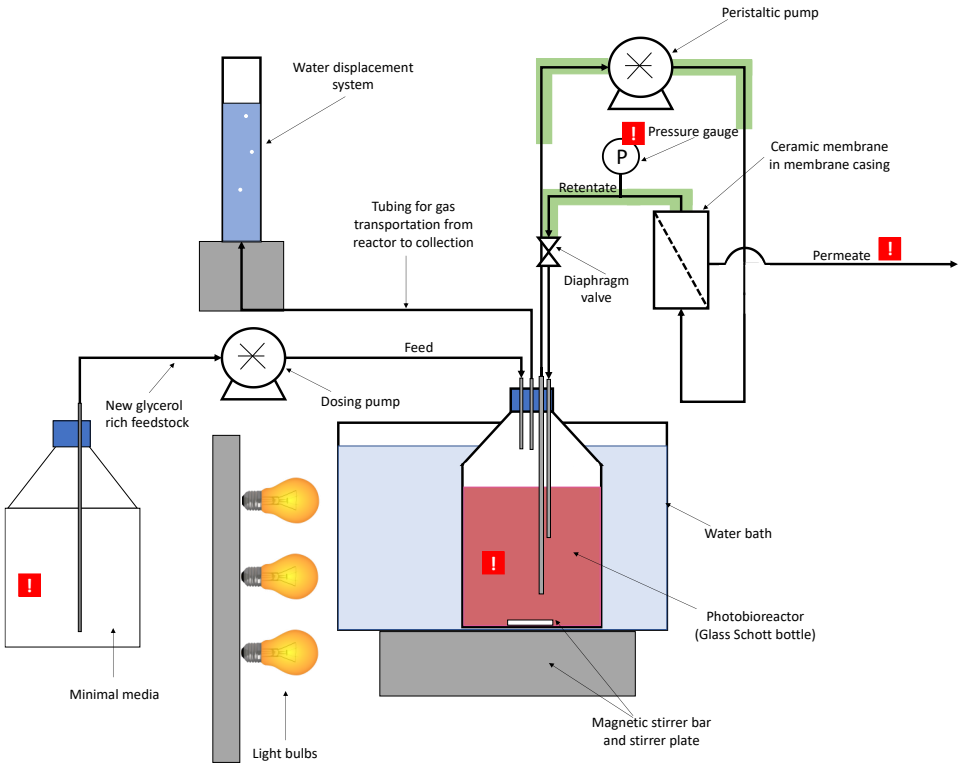

Figure 81: Illustration of the setup for the continuous mode MPBR. Green is used to indicate areas of gas build-up and red blocks containing exclamation marks are used to indicate the locations of events that lead to system failure.

After precautions taken to prevent gas at the top of the bioreactor system, gas accumulation still took place and was usually observed at ~12hours after system initiation, which is the exact point at which the culture is presumed to have circulated the system twice, as the turnover rate is once every six hours. At this point, multiple reactions from the system were observed. There was high pressure present between the pump feeding into the membrane and the backpressure valve, ± 1 bar, in comparison to the 0.35bar operating pressure for desired flux, which meant that significant fouling was taking place in the membrane. This also resulted in a sudden increase in permeate flow. Due to this sudden loss of media through the permeate, the liquid level inside the reactor suddenly dropped. This resulted in negative pressure inside the bioreactor itself and at this point, the inlet feed was drawn into the bioreactor at a high flowrate and the liquid level in the feed tanks suddenly decreased.

A simple solution to the problem would be to remove the piping from the feed to the membrane unit and lift the end of the pipe to ensure that as the pump is working the piping is flooded and when fluid exits the pipe, to quickly reattach the pipe to the membrane feed. Similarly, to flood the piping section between the membrane and the valve, the retentate fed to the bioreactor could be flooded in an identical manner. However, this method could not be employed as this meant that the opened system would be exposed to the environment and result in contamination. This method was not possible to do inside a sterile environment. Further problems that would stem from this solution would be inaccurate hydrogen production results as hydrogen gas would escape to the environment and the introduction of ambient

air into the system. The introduction of ambient air into the system would also result in an immediate stop to hydrogen production as hydrogen production only occurs in a anaerobic state. This meant that the system had to be removed and flooded again horizontally, and erratic pressure variation within the system occurred, which results in membrane fouling as mentioned earlier. This also severely increased changes of system contamination as repeated handling of the complex piping network.

Another solution to the problem would be the introduction of a one-way release valve at the highest point of each of these piping networks, although this would again result in inaccurate hydrogen production readings and was not considered a viable solution for the desired experimental output. In an industrial setup, however, this would not be a fatal issue as accuracy is not as important.

5.3.3.2 Reactor failure Type 2

The other failure type was caused by a liquid build-up in the glass reactor as illustrated in Figure 82. This type of failure usually occurred overnight after the system was set up to operate the previous evening and the effects were observed the next morning, thus to initiation of this type of failure can only be assumed. It was presumed that during the setup of the reactor, significant fouling took place in the membrane. As mentioned in the previous section, as the system is switched on while it is at a horizontal placement, some air bubbles are sometimes stuck due to pipe placement and cause a spike in the pressure reading. Although this fouling is not immediately noticeable and when the system is activated with the fouled membrane and left to operate at the desired flux value severe fouling takes place.

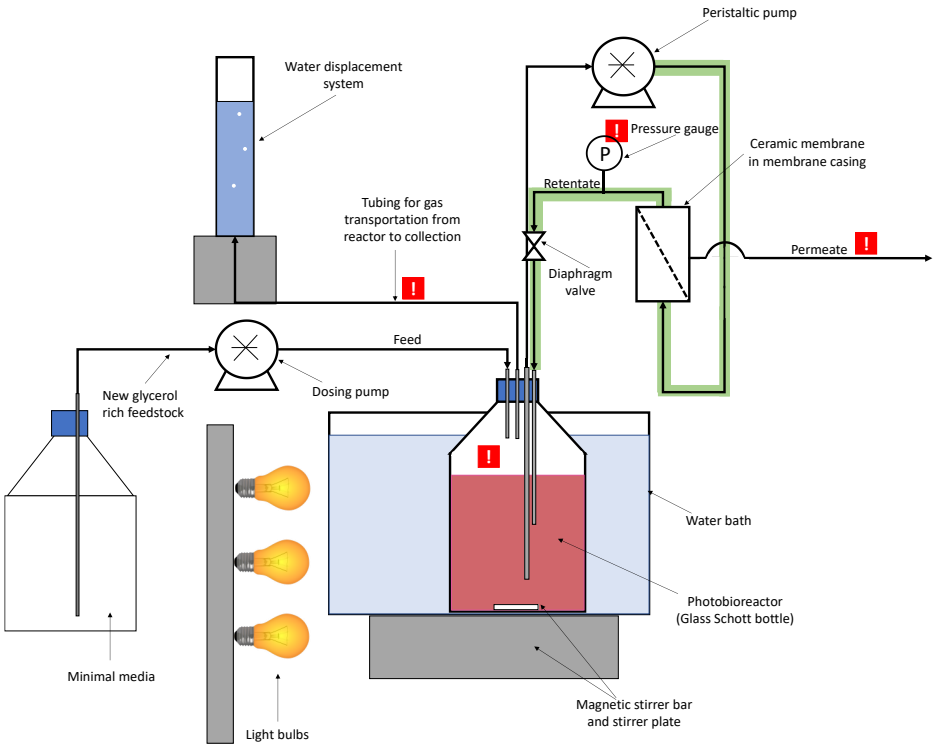

Figure 82: Illustration of the setup for the continuous mode MPBR. Green is used to indicate areas of gas build-up and red blocks containing exclamation marks are used to indicate the locations of events that lead to system failure.

With a fouled membrane there is a severe decrease in permeate flowrate, this is problematic as the feed is still being pumped into the reactor, there is now a rapid accumulation of fluid in the reactor. As the reactor fills up the liquid starts to propagate into the hydrogen collection port and the filter placed between the reactor and hydrogen collection port appears purple due to accumulated bacteria. Due to the pressure increase in the bioreactor, there was a negative pressure between the valve and the main pump which resulted in the piping collapsing and the pressure reading at the gauge read 0 bar. This meant that there was now no flow through the membrane and out of the system.

In the table below, Table 39, the biomass concentrations for the triplicates of the continuous mode MPBR are given. The values highlighted in red indicate the effect of the rising liquid level in the bioreactor, as the liquid level rose up to the point where the reactor volume was completely filled with fluid, the reactor fluid started propagating into the piping networks connected to the reactor cap, specifically the hydrogen collection piping network. The filter between the reactor cap and the rest of the piping network appeared purple as the culture was trapped in the filter and the medium propagated into the hydrogen collection system.

Table 39: Biomass concentration in each replicate of the continuous mode operation of the MPBR.

Day	**Hours**	**Reactor biomass concentration (g/L)**		
		1	2	3
0	0	0.73	0.74	0.74
Day	**Hours**	**Reactor biomass concentration (g/L)**		
		1	2	3
1	24	1.41	1.46	1.24
2	48	0.59	1.86	1.36
3	72	1.11	0.30	2.67
4	96	1.38	0.76	0.23

The reasons for the failure are the unpredictable times at which the system starts to display signs of an increasing liquid level, and the dosing pump was not switched off in time to prevent this from occurring. The only reason it was assumed that fouling due to initial setup was assumed was the purple tinge from the bacteria colour to the membrane when it was removed at this time point.

5.3.3.3 Summary

As mentioned in the discussion hydrogen production was observed under these conditions although the composition of the gas remains unknown, and it is assumed that the gas is a combination of both hydrogen and argon gas. Hydrogen production under the stated conditions was expected considering the biomass concentration was still relatively low for optimal light penetration and there was a constant high concentration of glycerol. As mentioned, the glycerol concentration of the outlet stream was around $\pm$3.67 g/L, which can be considered a loss of valuable substrate for hydrogen production. Additionally, as previously mentioned, this glycerol concentration is also significantly more than the stipulated effluent

specifications. If the system design was streamlined to a working condition, it would be possible to either increase the liquid retention time or place continuous MPBR's in series which would most likely significantly reduce the substrate concentration to desired levels with an increase in hydrogen production.

In conclusion, the continuous mode operation was not a success. The main requirement for the system was sterility to ensure repeatable results, which ruled out the majority of solutions to issues found with the system which led to eventual system failure. For an industry reactor, as sterility would not be a deciding factor as the large scale would allow for slight contamination, several solutions as mentioned in this study can be used to streamline and alter the system to a working condition. In industry, operating at a selected partial pressure to suppress microbial activity of contaminants, preferential inoculation or filtration of inlet streams could all aid in partial sterilisation of the inlet stream to the bioreactor.

It was found with this investigation that continuous mode operation of the MPBR was labour intensive due to system difficulties. If considering the use of this system on a larger scale, significant design alterations would need to be made to bypass the difficulties presented, like gas build-up in the system or severe membrane fouling. Other systems employing the use of glycerol substrate and the same strain of *R. palustris* have obtained significantly more successful waste valorisation results through immobilisation (du Toit and Pott, 2020; Ross and Pott, 2021b). The use of immobilisation technology also eliminates the operational and maintenance requirements of membranes.

6 CONCLUSIONS

The aim of this investigation was to develop and evaluate a membrane photobioreactor (MPBR) for the simultaneous treatment of a glycerol rich wastewater stream and the production of biohydrogen using purple non-sulfur bacteria (PNSB). This investigation aimed to produce a valuable source of energy by the photosynthetic bacterium *Rhodopseudomonas palustris* as a form of waste valorisation. The desired result for this investigation was a bioreactor that could house this bacterium and aid the conversion of the defined waste stream into a treated water stream and usable biohydrogen. The reason for this research and delivered dissertation, stems from the gaps identified in the literature for a useable bioreactor that could be considered a sustainable method of waste valorisation. This study was focused on separating the hydraulic retention time and solids retention time of the system to be used continuously, through the use of a membrane.

This investigation indicated that membrane technology on a continuous scale might not be the best fit for continuous wastewater treatment and simultaneous hydrogen production for *R. palustris* in this designed MPBR reactor configuration. The cell growth and glycerol conversion observed over the study period proved to be comparable to what was observed in the literature and showed positive growth and substrate utilisation efficiency. Although, due to the basic physical components required to operate the system, the cells were placed under severe shear stress, which resulted in poor biohydrogen production. Therefore, this study suggests that this specific system is not ideal to be considered as a method of waste valorisation.

Specific conclusions regarding the stated aims and objectives at the start of this investigation will be discussed in more detail below.

1. Construction of a ‘pathology map’ to understand the effect of certain conditions on the bacterial culture

From the literature study, it was obvious that the literature pertaining to physical effects occurring within a membrane system is severely limited. As mentioned in section 2.5.3, membrane photobioreactors are currently primarily used for photosynthetic algae, and almost no literature utilises alternative photosynthetic bacteria. Investigations that discussed the effects of shear stress, pressure, and temperature on algae within membrane bioreactors were encountered in the literature, which lead to the question being asked, what is the effect of these physical strains on the photosynthetic bacterium in this investigation? After cell lysis occurs in the system, cell debris can be found in suspension in the system, which poses a risk for membrane operation and the change in particle size could accelerate membrane fouling.

It was found that for cultures that have acclimatised to 35°C, a temperature of 40°C or 45°C did not cause severe cell death and only displayed an increase in compromised cells, and only slight variation from the control investigation was observed as seen by both the results from FCM and the visual results from STEM. At 50°C however, it was observed that there was a ~50% decrease in live biomass in the system, indicating that a significant cell death took place at this temperature. As mentioned by du Toit and Pott (2021), an acclimatisation period aids in the temperature resilience of the organism which would

significantly reduce the effect the higher temperatures have on the organism. Considering the desired use for this system in an outdoor bioreactor setup, the controlling factor for hydrogen production is the limitation on light supply during winter months and the standard circadian cycle, during the night or when sun hours are limited and the exposure to elevated temperatures of 50°C during summer and spring months.

The next parameter that was investigated is the effect of pressure on the organism. It was observed that for an applied pressure of 82.3 kPa, which is higher than the pressures that were used during the operation of the MPBR in this investigation, a decrease of ~65% in live biomass was observed. This meant that the effect of pressure in the system would most likely have a significant impact on MPBR operation. With the investigation of limiting the substrate concentration in the system, it was observed that with lower glycerol concentrations the only effect observed was that of a lower biomass concentration at the end of the investigative period and no effect on the cells can be observed on a microscopic level. There was also no significant difference observed in the percentage of live biomass for the range of glycerol concentrations observed.

For the investigation into the effects of shear stress, shear stress under different magnitudes and exposure times were investigated. For a varying exposure time to shear stress when the magnitude of shear stress was kept at a constant, it was observed that the time the organism was subjected to shear stress did have a significant effect on the percentage of live biomass that remained in the system. When the magnitude of shear stress was varied but the exposure time was kept constant it was observed that this too resulted in a significant difference in percentage live biomass. The implications of this investigation are concerning as multiple components in the system impose shear stress on the culture inside the MPBR due to the circulation nature of the system.

This led to the next investigation which was a study into separating the variables of shear stress by means of increasing the viscosity of the fluid. This was conducted for a range of viscosities from 0.9 cP to 22.2 cP. In this study, it was observed that the increase in viscosity did result in a lower resulting G-value imposed on the culture, which implies that the shear stress imposed on the culture was reduced, although the percentage of live biomass could not be confirmed by FCM. The effect of the thickening agent on the membrane remains unknown.

In conclusion, the pathology map found that nutrient limitations and temperatures up to 45°C did not have a severe effect on the bacterial culture and live biomass in the system, meaning that cell lysis as a result of these effects is unlikely. However, with shear stress and pressure, it was found that both the magnitude of the stress and the time the culture was exposed to this stress did lead to significant cell death which was a concerning factor for membrane operation as it could lead to accelerated membrane fouling.

2. Design of the MPBR

The second objective of this investigation was the design of the MPBR system, which was significantly influenced by the findings of the pathology map. As the pressure and shear stress effects on the culture were assumed significant it was necessary to make design choices that mitigate the effect of this stress.

Specific influences to mitigate shear stress was observed in the selection of the pump and valve selection. A major operational consideration was the turnover rate of the culture in the system. By operating at a slower turnover rate, the shear stresses the culture is exposed to over the valve, membrane, and pump as well as exposure to pressure in the system is reduced. The downside to this is, however, a significantly slower permeate (treated wastewater) output.

3. Batch mode operation of the MPBR

Prior to both batch operation and continuous operation of the MPBR, the system was operated under control conditions, with no backpressure applied to observe cell growth, substrate utilisation, and hydrogen production under these conditions. These results were compared to that of the batch mode operation to draw conclusions regarding the effect of the added shear stress of backpressure and shear stress over the valve on the culture, as these additional stressors weren't present in the control mode operation of the MPBR system. Over a period of 240 hours under 35^{o}C conditions and illumination of 200 W/m^{2}, the final biomass concentration, with a starting concentration of 0.74$\pm$0.07 g/L, was observed to be 4.25$\pm$0.25 g/L. The final glycerol concentration in the system was below 0.1 g/L, indicating that glycerol conversation was ~74%. Cumulative hydrogen production for the control mode operation only attained 262$\pm$62mL over the experimental period in comparison to 1200mL observed for the culture conditions in the literature (du Toit and Pott, 2021).

Under batch mode operation, it was observed that the biomass concentration increased, and substrate concentration decreased steadily over the experimentation period. These results correlated with what was observed in the literature for the organism under similar culturing conditions (du Toit and Pott, 2021; Ross and Pott, 2021b). Over a period of 240hours under 35^{o}C conditions and illumination of 200W/m^{2}, the final biomass concentration, with a starting concentration of 0.75$\pm$0.02 g/L, was observed to be 4.3$\pm$0.06 g/L. The final glycerol concentration in the system was below 0.1 g/L, indicating that glycerol conversation was ~88.72%, which was more than what was observed in the literature. It was assumed that the high glycerol conversion rates could be due to the increased energy requirements of the cells for cell repair as the cells were damaged by stress from pressure and shear. This is supported by the increased substrate utilisation of the batch mode operation (~88.72%) of the MPBR in comparison to that of the control mode operation (~74%) of the MPBR, it is assumed as the stressors in the system were increased so did the substrate uptake as the demands for cell repair increase. The assumption that increased stressors in the system during the batch mode operation affect culture performance is supported by the poor cumulative hydrogen production observed in the system, after 240 hours only 106$\pm$29.06 mL was collected in comparison to 1200mL observed for the culture conditions in the literature (du Toit and Pott, 2021) and ~262 mL attained for control mode operation of the MPBR.

In a comparison between control mode and batch mode operation of the MPBR found that there was a negligible difference in biomass concentration over time. The substrate utilisation efficiency was better for the batch operation of the MPBR than for the control mode and it was assumed to be due to the increase in energy required by the cells for cell repair due to the additional stressors present in the system.

The final result from this investigation implied that the use of a MPBR for the treatment of glycerol-rich wastewater into a treated wastewater stream and sustainable source of biohydrogen, was not recommended as the supply of the valuable energy source, biohydrogen, was limited for the operation of this bioreactor.

4. Continuous mode operation of the MPBR

In the final objective of this investigation, the operation of the MPBR under continuous mode operation was investigated. There were crippling difficulties encountered both in the operation procedure itself as well as the factors and two different types of reactor failure were identified. Trapped air in the system, as well as continuous membrane fouling, resulted in a liquid build-up, fluctuating pressures, and varying permeate flowrates which were both difficult to control and required significant daily maintenance which is unsustainable on a larger scale.

It was discussed that for both types of reactor failure observed there are practical solutions, albeit were not applicable to this system due to strict experimental sterility requirements. The results from the batch operation were not positive enough, meaning there is a poor chance of retrieving a reliable valuable by-product, to reinvestigate and redesign the system to an operational condition.

7 RECOMMENDATIONS

This investigation was a success in the way of eliminating questions that arose from the literature. Although some stumbling blocks were encountered within the design and operational conditions, which could be prevented in future research and aid in streamlining future MPBR research. The reason for this is to find applications that can be used continuously to both increase efficiency and operational capacity of a system.

From this study, the pathology map appeared to be useful as a diagnostic tool. In this investigation a one-factor-at-a-time (OFAT) approach was used in terms of each physical stressor and was conducted for temperature, pressure, shear stress and nutrient limitations. In future studies, this could be extended to include interactions between stressors or expanding the ranges investigated. Investigating the effect of prolonged exposure to stressors, with a timeline similar to reactor operation, would give insight into the effect of time on the culture, as observed in the temperature investigation in this study.

During batch operation of the MPBR, the results suggested that the effect of the pump during constant recirculation had a significant effect on both substrate utilization and hydrogen production of the culture. In future studies a solution to this could perhaps be to change the method of sterilization to use a centrifugal pump that would result in less stress on the bacterial culture during recirculation. Another observation made during batch operation of the MPBR, was the effect of light limitation on the culture due to the time the culture spends in the piping network. This was most likely the reason behind poor hydrogen production rates as ATP, and eventual biohydrogen, is limited to the light exposure the culture has. Future studies could benefit from a specialised reactor, designed to optimise illumination of the culture, perhaps by using transparent piping networks and a bioreactor optimised to minimize the effect of mutual shading of the culture.

For continuous mode operation of the MPBR, several design changes need to be made. As the main problems experienced were due to unprecedented liquid build-up in the reactor or air build-up in the piping network, major reconsiderations need to be made with regards to design. The first suggestion would be altering the layout of the piping network, in this study a vertical setup of the MPBR was used, which resulted in air build-up at the top of the reactor. A possible improvement on this would be a venting solution, although would most likely results in a loss of hydrogen. Another consideration would be a simple PI-controller to mange to flowrate of the incoming dosing stream as a function of the permeate out of the reactor and the pressure over the membrane. A specifically designed control system would significantly reduce the labour required to ensure continuous operation.

The poor hydrogen production observed in this investigation tend to suggest studying other methods of separating the HRT and SRT of a system for this specific strain of photosynthetic bacterium and reactor configuration.

Other methods observed in the literature as a method to separate HRT and SRT includes using biofilms as a method of immobilization or the immobilisation of the culture into a matrix. From the literature, it was observed that studies have been conducted using immobilisation matrices as a method of separating HRT and SRT in a system and the results in terms of hydrogen production have been very promising. A

study conducted by Ross and Pott (2021) found that in a fluidised bed photobioreactor hydrogen production rates of up to 15.74 mL/g_{CDW}/h in comparison to results below 1 mL/g_{CDW}/h observed in this study.

8 BIBLIOGRAPHY

Acar, C. and Dincer, I. (2014) 'Comparative assessment of hydrogen production methods from renewable and non-renewable sources', *International Journal of Hydrogen Energy*. Pergamon, pp. 1–12. doi: 10.1016/j.ijhydene.2013.10.060.

Adessi, A. and De Philippis, R. (2014) 'Photobioreactor design and illumination systems for H2 production with anoxygenic photosynthetic bacteria: A review', *International Journal of Hydrogen Energy*. Pergamon, pp. 3127–3141. doi: 10.1016/j.ijhydene.2013.12.084.

AsahiKASEI (2021) *Filtration Modes*. Available at: https://www.asahi-kasei.co.jp/membrane/microza/en/kiso/kiso_3.html (Accessed: 13 November 2021).

Auling, G. *et al.* (1988) 'Phylogenetic Heterogeneity and Chemotaxonomic Properties of Certain Gram-negative Aerobic Carboxydobacteria', *Systematic and Applied Microbiology*, 10(3), pp. 264–272. doi: 10.1016/S0723-2020(88)80011-0.

Baker, R. W. (2012) *Membrane Technology and Applications*, *Membrane Technology and Applications*. John Wiley and Sons. doi: 10.1002/9781118359686.

Ball, M. and Weeda, M. (2016) 'The hydrogen economy—Vision or reality?', *Compendium of Hydrogen Energy*, pp. 237–266. doi: 10.1016/B978-1-78242-364-5.00011-7.

Balster, J. (2013a) 'Plate and Frame Membrane Module', in *Encyclopedia of Membranes*. Springer Berlin Heidelberg, pp. 1–3. doi: 10.1007/978-3-642-40872-4_1584-1.

Balster, J. (2013b) 'Spiral Wound Membrane Module', in *Encyclopedia of Membranes*. Springer Berlin Heidelberg, pp. 1–3. doi: 10.1007/978-3-642-40872-4_1586-1.

Balster, J. (2014) 'Hollow Fiber Membrane Module', in *Encyclopedia of Membranes*. Springer Berlin Heidelberg, pp. 1–2. doi: 10.1007/978-3-642-40872-4_1583-2.

Barbosa, M. J. *et al.* (2001) 'Acetate as a carbon source for hydrogen production by photosynthetic bacteria', *Journal of Biotechnology*, 85(1), pp. 25–33. doi: 10.1016/S0168-1656(00)00368-0.

Basak, N., Kumar Jana, A. and Das, D. (2016) 'CFD modeling of hydrodynamics and optimization of photofermentative hydrogen production by Rhodopseudomonas palustris DSM 123 in annular photobioreactor', *International Journal of Hydrogen Energy*, 41, pp. 7301–7317. doi: 10.1016/j.ijhydene.2016.02.126.

Baykara, S. Z. (2018) 'Hydrogen: A brief overview on its sources, production and environmental impact', *International Journal of Hydrogen Energy*, 43, pp. 10605–10614. doi: 10.1016/j.ijhydene.2018.02.022.

Bergquist, P. L. *et al.* (2009) 'Applications of flow cytometry in environmental microbiology and biotechnology', *Extremophiles*, 13(3), pp. 389–401. doi: 10.1007/s00792-009-0236-4.

Bilad, M. R. *et al.* (2014) 'Coupled cultivation and pre-harvesting of microalgae in a membrane photobioreactor (MPBR)', *Bioresource Technology*, 155, pp. 410–417. doi: 10.1016/j.biortech.2013.05.026.

Bio-Rad (no date) *Flow Cytometry: Cell Analysis vs. Cell Sorting*. Available at: https://www.bio-rad.com/featured/en/flow-cytometer.html (Accessed: 22 September 2021).

Blackburn, N. A. and Johnson, I. T. (1981) 'The effect of guar gum on the viscosity of the gastrointestinal contents and on glucose uptake from the perfused jejunum in the rat', *British Journal of Nutrition*, 46(2), pp. 239–246. doi: 10.1079/BJN19810029.

Britannica (no date) *Africa - Climate*. Available at: https://www.britannica.com/place/Africa/Climate (Accessed: 12 October 2021).

Burris, R. H. (1991) *THE JOURNAL OF BIOLOGICAL CHEMISTRY Nitrogenases**.

Carlozzi, P. (2009) 'The effect of irradiance growing on hydrogen photoevolution and on the kinetic growth in Rhodopseudomonas palustris, strain 42OL', *International Journal of Hydrogen Energy*, 34(19), pp. 7949–7958. doi: 10.1016/j.ijhydene.2009.07.083.

Carlozzi, P. and Sacchi, A. (2001) 'Biomass production and studies on Rhodopseudomonas palustris grown in an outdoor, temperature controlled, underwater tubular photobioreactor', *Journal of Biotechnology*, 88(3), pp. 239–249. doi: 10.1016/S0168-1656(01)00280-2.

Casas, J. A., Mohedano, A. F. and García-Ochoa, F. (2000) 'Viscosity of guar gum and xanthan/guar gum mixture solutions', *Journal of the Science of Food and Agriculture*, 80(12), pp. 1722–1727. doi: 10.1002/1097-0010(20000915)80:12<1722::AID-JSFA708>3.0.CO;2-X.

Chen, C. Y., Lee, C. M. and Chang, J. S. (2006a) 'Feasibility study on bioreactor strategies for enhanced photohydrogen production from Rhodopseudomonas palustris WP3-5 using optical-fiber-assisted illumination systems', *International Journal of Hydrogen Energy*. doi: 10.1016/j.ijhydene.2006.03.007.

Chen, C. Y., Lee, C. M. and Chang, J. S. (2006b) 'Hydrogen production by indigenous photosynthetic bacterium Rhodopseudomonas palustris WP3-5 using optical fiber-illuminating photobioreactors', *Biochemical Engineering Journal*. doi: 10.1016/j.bej.2006.08.015.

Chitapornpan, S. *et al.* (2012) 'Photosynthetic bacteria production from food processing wastewater in sequencing batch and membrane photo-bioreactors', *Water Science and Technology*, 65(3), pp. 504–512. doi: 10.2166/wst.2012.740.

Choi, K. Y. J. *et al.* (2005) 'Bench-scale evaluation of critical flux and TMP in low-pressure membrane filtration', *Journal / American Water Works Association*, 97(7), pp. 134–143. doi: 10.1002/j.1551-8833.2005.tb10939.x.

Clarke, K. G. (2013) *Bioprocess Engineering - An Introductory Engineering and Life Science Approach - Knovel*, *Woodhead Publishing*. Available at: https://app.knovel.com/web/toc.v/cid:kpBEAIELS6/viewerType:toc/ (Accessed: 6 April 2020).

Le Clech, P. *et al.* (2003) 'Critical flux determination by the flux-step method in a submerged membrane bioreactor', *Journal of Membrane Science*, 227(1–2), pp. 81–93. doi: 10.1016/j.memsci.2003.07.021.

Climate-Data.org (2019) *Cape Town climate*. Available at: https://en.climate-data.org/africa/south-africa/western-cape/cape-town-788/ (Accessed: 12 October 2021).

Cunningham, J. H. *et al.* (2008) 'Feasibility of disinfection kinetics and minimum inhibitory concentration determination on bacterial cultures using flow cytometry', *Water Science and Technology*, 58(4), pp. 937–944. doi: 10.2166/wst.2008.619.

Damjanović, A., Ritz, T. and Schulten, K. (1999) 'Energy transfer between carotenoids and bacteriochlorophyll in chromatophores of purple bacteria', *Physical review E*, 59(3). doi: 10.1016/0006-3002(59)90328-2.

Department of Energy USA (2020) *Hydrogen Resources*. Available at: https://www.energy.gov/eere/fuelcells/hydrogen-resources (Accessed: 6 April 2020).

Druz, A. (2008) 'Hollow fibre membrane module image'.

El-Ghaffar, M. A. A. and Tieama, H. A. (2017) 'A Review of Membranes Classifications, Configurations, Surface Modifications, Characteristics and Its Applications in Water Purification', *Http://Www.Sciencepublishinggroup.Com*, 2(2), p. 57. doi: 10.11648/j.cbe.20170202.11.

Faber, M. J. *et al.* (1997) 'Cryopreservation of fluorescent marker-labeled algae (Selenastrum capricornutum) for toxicity testing using flow cytometry', *Environmental Toxicology and Chemistry*, 16(5), pp. 1059–1067. doi: 10.1002/ETC.5620160528.

Field, R. W. *et al.* (1995) 'Critical flux concept for microfiltration fouling', *Journal of Membrane Science*,

100(3), pp. 259–272. doi: 10.1016/0376-7388(94)00265-Z.

Fißler, J., Kohring, G. W. and Giffhorn, F. (1995) 'Enhanced hydrogen production from aromatic acids by immobilized cells of Rhodopseudomonas palustris', *Applied Microbiology and Biotechnology*, 44(1–2), pp. 43–46. doi: 10.1007/BF00164478.

Fortunato, L., Lamprea, A. F. and Leiknes, T. O. (2020) 'Evaluation of membrane fouling mitigation strategies in an algal membrane photobioreactor (AMPBR) treating secondary wastewater effluent', *Science of The Total Environment*, 708, p. 134548. doi: 10.1016/J.SCITOTENV.2019.134548.

Gao, F. *et al.* (2015) 'A novel algal biofilm membrane photobioreactor for attached microalgae growth and nutrients removal from secondary effluent', *Bioresource Technology*, 179, pp. 8–12. doi: 10.1016/j.biortech.2014.11.108.

Ghosh, D., Tourigny, A. and Hallenbeck, P. C. (2012) 'Near stoichiometric reforming of biodiesel derived crude glycerol to hydrogen by photofermentation', *International Journal of Hydrogen Energy*, 37(3), pp. 2273–2277. doi: 10.1016/j.ijhydene.2011.11.011.

González-Camejo, J. *et al.* (2019) 'Optimising an outdoor membrane photobioreactor for tertiary sewage treatment', *Journal of Environmental Management*, 245, pp. 76–85. doi: 10.1016/J.JENVMAN.2019.05.010.

González, E. *et al.* (2017) 'Photosynthetic bacteria-based membrane bioreactor as post-treatment of an anaerobic membrane bioreactor effluent', *Bioresource Technology*, 239, pp. 528–532. doi: 10.1016/j.biortech.2017.05.042.

Guo, C.-L. *et al.* (2011) 'Enhancement of photo-hydrogen production in a biofilm photobioreactor using optical fiber with additional rough surface'. doi: 10.1016/j.biortech.2011.04.075.

Hallenbeck, P. C. (2009) 'Fermentative hydrogen production: Principles, progress, and prognosis', *International Journal of Hydrogen Energy*, 34(17), pp. 7379–7389. doi: 10.1016/j.ijhydene.2008.12.080.

Hallenbeck, P. C. and Ghosh, D. (2009) 'Advances in fermentative biohydrogen production: the way forward?', *Trends in Biotechnology*, 27(5), pp. 287–297. doi: 10.1016/j.tibtech.2009.02.004.

Hallenbeck, P. C. and Liu, Y. (2015) 'Recent advances in hydrogen production by photosynthetic bacteria'. doi: 10.1016/j.ijhydene.2015.11.090.

Heffel, J. W. (2003) 'NOx emission and performance data for a hydrogen fueled internal combustion engine at 1500 rpm using exhaust gas recirculation', *International Journal of Hydrogen Energy*, 28(8), pp. 901–908. doi: 10.1016/S0360-3199(02)00157-X.

Hu, X. *et al.* (1998) *Architecture and mechanism of the light-harvesting apparatus of purple bacteria*, *Computational Biomolecular Science*. Available at: www.pnas.org. (Accessed: 14 April 2020).

Hu, X. *et al.* (2002) *Photosynthetic apparatus of purple bacteria*, *Quarterly Reviews of Biophysics*. doi: 10.1017/S0033583501003754.

Hülsen, T. *et al.* (2020) 'Application of purple phototrophic bacteria in a biofilm photobioreactor for single cell protein production: Biofilm vs suspended growth', *Water Research*, 181, p. 115909. doi: 10.1016/J.WATRES.2020.115909.

Imhoff, J. F., Hiraishi, A. and Süling, J. (2005) 'Anoxygenic Phototrophic Purple Bacteria', in *Bergey's Manual® of Systematic Bacteriology*, pp. 119–132. doi: 10.1007/0-387-28021-9_15.

IPCC (2001) *Future Work Program of the IPCC*, *Intergovernmental Panel on Climate Change*.

Jeison, D. and van Lier, J. B. (2007) 'Thermophilic treatment of acidified and partially acidified wastewater using an anaerobic submerged MBR: Factors affecting long-term operational flux', *Water Research*, 41(17), pp. 3868–3879. doi: 10.1016/j.watres.2007.06.013.

Judd, S. (2008) 'The status of membrane bioreactor technology', *Trends in Biotechnology*, 26(2), pp. 109–116. doi: 10.1016/J.TIBTECH.2007.11.005.

Kalamaras, C. M. *et al.* (2013) 'Hydrogen Production Technologies: Current State and Future Developments', in *Conference Papers in Energy*. Hindawi Publishing Corporation. doi: 10.1155/2013/690627.

Kim, D. H. and Kim, M. S. (2011) 'Hydrogenases for biological hydrogen production', *Bioresource Technology*, 102(18), pp. 8423–8431. doi: 10.1016/j.biortech.2011.02.113.

Kim, J. K. and Lee, B. K. (2000) 'Mass production of Rhodopseudomonas palustris as diet for aquaculture', *Aquacultural Engineering*, 23(4), pp. 281–293. doi: 10.1016/S0144-8609(00)00057-1.

Kim, J. S., Ito, K. and Takashi, H. (1980) 'The relationship between nitrogenase activity and hydrogen evolution in Rhodopseudomonas palustris.', *Agricultural and Biological Chemistry*, 44(4), pp. 827–833. doi: 10.1271/bbb1961.44.827.

Kim, J. S., Lee, C. H. and Chang, I. S. (2001) 'Effect of pump shear on the performance of a crossflow membrane bioreactor', *Water Research*, 35(9), pp. 2137–2144. doi: 10.1016/S0043-1354(00)00495-4.

Koku, H. *et al.* (2002) *Aspects of the metabolism of hydrogen production by Rhodobacter sphaeroides*, *International Journal of Hydrogen Energy*. Available at: www.elsevier.com/locate/ijhydene (Accessed: 10 April 2020).

Koros, W. J., Ma, Y. H. and Shimidzu, T. (1996) 'Terminology for membranes and membrane processes (IUPAC Recommendations 1996)', *Pure and Applied Chemistry*, 68(7), pp. 1479–1489. doi: 10.1351/pac199668071479.

Krishnan, S. S. and Balasubramanian, N. (2014) 'Metallurgical Production Plant—Energy and Environment', *Treatise on Process Metallurgy*, 3, pp. 1193–1247. doi: 10.1016/B978-0-08-096988-6.00032-8.

Kumar Khanal, S. *et al.* (2008) 'Bioenergy and Biofuel Production from Wastes/Residues of Emerging Biofuel Industries', *Source: Water Environment Research*, 80(10), pp. 1625–1647. doi: 10.2175/106143008X328752.

Lange, H., Taillandier, P. and Riba, J. P. (2001) 'Effect of high shear stress on microbial viability', *Journal of Chemical Technology and Biotechnology*, 76(5), pp. 501–505. doi: 10.1002/jctb.401.

Larimer, F. W. *et al.* (2004) 'Complete genome sequence of the metabolically versatile photosynthetic bacterium Rhodopseudomonas palustris', *Nature Biotechnology*, 22(1), pp. 55–61. doi: 10.1038/nbt923.

Lee, H. S., Vermaas, W. F. J. and Rittmann, B. E. (2010) 'Biological hydrogen production: Prospects and challenges', *Trends in Biotechnology*, 28(5), pp. 262–271. doi: 10.1016/j.tibtech.2010.01.007.

Levin, D. B., Pitt, L. and Love, M. (2004) 'Biohydrogen production: Prospects and limitations to practical application', *International Journal of Hydrogen Energy*, 29(2), pp. 173–185. doi: 10.1016/S0360-3199(03)00094-6.

Li, Q. Y. *et al.* (1998) 'Enhancement of ultrafiltration by gas sparging with flat sheet membrane modules', *Separation and Purification Technology*, 14(1–3), pp. 79–83. doi: 10.1016/S1383-5866(98)00062-8.

Liao, Q. *et al.* (2012) 'Improvement of hydrogen production with Rhodopseudomonas palustris CQK-01 by Ar gas sparging', *International Journal of Hydrogen Energy*, 37(20), pp. 15443–15449. doi: 10.1016/J.IJHYDENE.2012.04.107.

Liao, Y. (2006) *Practical Electron Microscopy and Database*. Edited by Northwestern University. Available at: https://www.globalsino.com/EM (Accessed: 9 November 2021).

Lin, J. C. Te, Lee, D. J. and Huang, C. (2010) 'Membrane fouling mitigation: Membrane cleaning', *Separation Science and Technology*, 45(7), pp. 858–872. doi: 10.1080/01496391003666940.

Liu, C. *et al.* (no date) 'Membrane Chemical Cleaning: From Art to Science'.

López-Rosales, L. *et al.* (2015) 'An optimisation approach for culturing shear-sensitive dinoflagellate microalgae in bench-scale bubble column photobioreactors', *Bioresource Technology*, 197, pp. 375–382. doi: 10.1016/J.BIORTECH.2015.08.087.

Luo, Y., Le-Clech, P. and Henderson, R. K. (2018) 'Assessment of membrane photobioreactor (MPBR) performance parameters and operating conditions', *Water Research*, 138, pp. 169–180. doi: 10.1016/J.WATRES.2018.03.050.

McEwan, A. G. (1994) 'Photosynthetic electron transport and anaerobic metabolism in purple non-sulfur phototrophic bacteria', *Antonie van Leeuwenhoek*, 66(1–3), pp. 151–164. doi: 10.1007/BF00871637.

McKinlay, J. B. *et al.* (2014) 'Non-growing rhodopseudomonas palustris increases the hydrogen gas yield from acetate by shifting from the glyoxylate shunt to the tricarboxylic acid cycle', *Journal of Biological Chemistry*, 289(4), pp. 1960–1970. doi: 10.1074/jbc.M113.527515.

McMichael, A. J. (2013) 'Globalization, climate change, and human health', *New England Journal of Medicine*, 368(14), pp. 1335–1343. doi: 10.1056/NEJMra1109341.

Merriam-Webster (no date) *Wild Type*, *Merriam-Webster.com Dictionary*. Available at: https://www.merriam-webster.com/dictionary/wild type (Accessed: 10 October 2021).

Miller, D. J. *et al.* (2014) 'Comparison of membrane fouling at constant flux and constant transmembrane pressure conditions', *Journal of Membrane Science*, 454, pp. 505–515. doi: 10.1016/J.MEMSCI.2013.12.027.

National Water Act 36 of 1998 (2013) 'Wastewater limit values applicable to the irrigation of any land or property up to 50 cubic metres', *Government Gazette No. 19182*, Notice No.(19182), pp. 17–18.

Navaratna, D. and Jegatheesan, V. (2011) 'Implications of short and long term critical flux experiments for laboratory-scale MBR operations', *Bioresource Technology*, 102(9), pp. 5361–5369. doi: 10.1016/j.biortech.2010.12.080.

Okamura, M. Y. and Feher, G. (2006) 'Proton-Coupled Electron Transfer Reactions of QB in Reaction Centers from Photosynthetic Bacteria', in *Anoxygenic Photosynthetic Bacteria*. Kluwer Academic Publishers, pp. 577–593. doi: 10.1007/0-306-47954-0_26.

PALL (no date) *Membralox® SD Sanitary Module image*. Available at: https://shop.pall.com/us/en/food-beverage/food-ingredients/stick-water-from-slautherhouse-fish-processing/zidgri78ln7 (Accessed: 12 November 2021).

Paredes, A. M. (2014) *Microscopy: Scanning Electron Microscopy*. Second Edi, *Encyclopedia of Food Microbiology: Second Edition*. Second Edi. Elsevier. doi: 10.1016/B978-0-12-384730-0.00215-9.

Paulsen, H. (1999) 'Carotenoids and the Assembly of Light-harvesting Complexes', in *The Photochemistry of Carotenoids*. Springer, Dordrecht, pp. 123–135.

Porter, M. C. (1990) *Handbook of Industrial Membrane Technology*. William Andrew Publishing/Noyes. Available at: https://app-knovel-com.ez.sun.ac.za/web/toc.v/cid:kpHIMT0002/viewerType:toc//root_slug:handbook-industrial-membrane/url_slug:synthetic-membranes-their?issue_id=kpHIMT0002&hierarchy= (Accessed: 1 July 2021).

Pott, R., Howe, C. and Dennis, J. (2013a) 'Photofermentation of crude glycerol from biodiesel using Rhodopseudomonas palustris: Comparison with organic acids and the identification of inhibitory compounds', *Bioresource Technology*, 130, pp. 725–730. doi: 10.1016/j.biortech.2012.11.126.

Pott, R., Howe, C. and Dennis, J. (2013b) 'The purification of crude glycerol derived from biodiesel manufacture and its use as a substrate by Rhodopseudomonas palustris to produce hydrogen',

Bioresource Technology, 152, pp. 464–470. doi: 10.1016/j.biortech.2013.10.094.

Pott, R. W. M. (2013) *The Bioconversion of Waste Glycerol into Hydrogen by Rhodopseudomonas palustris*. Cambridge University.

Pugliesi, D. (2008) 'Spiral wound membrane module image'. Available at: https://commons.wikimedia.org/wiki/File:Spiral_flow_membrane_module-en.svg.

Ross, B. S. (2019) *The Effect of Light Intensity and Reactor Configuration on Rhodopseudomonas palustris Growth and Hydrogen Production*. University of Stellenbosch.

Ross, B. S. and Pott, R. W. M. (2021a) 'Hydrogen production by immobilized Rhodopseudomonas palustris in packed or fluidized bed photobioreactor systems', *International Journal of Hydrogen Energy*, 46(2), pp. 1715–1727. doi: 10.1016/j.ijhydene.2020.10.061.

Ross, B. S. and Pott, R. W. M. (2021b) 'Hydrogen production by immobilized Rhodopseudomonas palustris in packed or fluidized bed photobioreactor systems', *International Journal of Hydrogen Energy*, 46(2), pp. 1715–1727. doi: 10.1016/J.IJHYDENE.2020.10.061.

Roszak, A. W. *et al.* (2003) 'Crystal Structure of the RC-LH1 Core Complex from Rhodopseudomonas palustris', *Science*, 302(5652), pp. 1969–1972. doi: 10.1126/science.1088892.

Sabourin-Provost, G. and Hallenbeck, P. C. (2009) 'High yield conversion of a crude glycerol fraction from biodiesel production to hydrogen by photofermentation'. doi: 10.1016/j.biortech.2009.03.027.

SAMCO (2018) *What Are the Different Types of Membrane Fouling and What Causes Them?* Available at: https://www.samcotech.com/types-of-membrane-fouling-and-causes/ (Accessed: 12 November 2021).

Sarangi, P. K., Nanda, S. and Mohanty, P. (2018) *Recent advancements in biofuels and bioenergy utilization*, *Recent Advancements in Biofuels and Bioenergy Utilization*. doi: 10.1007/978-981-13-1307-3.

Schaeffer, R. *et al.* (2011) 'Energy sector vulnerability to climate change: A review', *Energy*, 38, pp. 1–12. doi: 10.1016/j.energy.2011.11.056.

Schedler, M. *et al.* (2014) 'Effect of high pressure on hydrocarbon-degrading bacteria', *AMB Express*, 4(1), pp. 1–7. doi: 10.1186/S13568-014-0077-0/FIGURES/4.

Sharaf, O. Z. and Orhan, M. F. (2014) 'An overview of fuel cell technology: Fundamentals and applications', *Renewable and Sustainable Energy Reviews*, 32, pp. 810–853. doi: 10.1016/j.rser.2014.01.012.

Shimadzu Corporation (no date) *What is HPLC (High Performance Liquid Chromatography) ?* Available at: https://www.shimadzu.com/an/service-support/technical-support/analysis-basics/basic/what_is_hplc.html#1 (Accessed: 25 September 2021).

Shiva Kumar, S. and Himabindu, V. (2019) 'Hydrogen production by PEM water electrolysis – A review', *Materials Science for Energy Technologies*, 2(3), pp. 442–454. doi: 10.1016/j.mset.2019.03.002.

Skousen, P. L. (2004) *Valve Handbook*. 2nd edn. McGraw-Hill. doi: 10.1036/0071437738.

Smith, A. W. (1963) *A Gardener's Handbook of Plant Names: Their Meanings and Origins*. Dover Publications. Available at: https://books.google.co.za/books?id=ahNMkgoNJ7IC&pg=PA258&redir_esc=y#v=onepage&q&f=false (Accessed: 9 April 2020).

Sources of energy - U.S. Energy Information Administration (EIA) (no date). Available at: https://www.eia.gov/energyexplained/what-is-energy/sources-of-energy.php (Accessed: 17 March 2020).

SRS Biodiesel (no date) *Transesterification*. Available at: http://www.srsbiodiesel.com/technologies/transesterification/ (Accessed: 12 October 2021).

Stechemesser, H. and Dobiáš, B. (2005) 'Coagulation and flocculation', *Coagulation and Flocculation, Second Edition*, pp. 1–862. doi: 10.1680/bwtse.63341.061.

Tandori, J. *et al.* (2001) 'Photoinhibition of carotenoidless reaction centers from Rhodobacter sphaeroides by visible light. Effects on protein structure and electron transport', *Photosynthesis Research*, 70(2), pp. 175–184. doi: 10.1023/A:1017907404325.

thewayMembranes (2020) *Air scouring! How is it relevant?* Available at: https://www.thewaymembranes.com/post/air-scouring-how-is-it-relevant (Accessed: 13 November 2021).

Tian, X. *et al.* (2010) 'Characteristics of a biofilm photobioreactor as applied to photo-hydrogen production', *Bioresource Technology*, 101(3), pp. 977–983. doi: 10.1016/j.biortech.2009.09.007.

du Toit, J.-P. and Pott, R. W. M. (2020) 'Transparent polyvinyl-alcohol cryogel as immobilisation matrix for continuous biohydrogen production by phototrophic bacteria', *Biotechnology for Biofuels 2020 13:1*, 13(1), pp. 1–16. doi: 10.1186/S13068-020-01743-7.

du Toit, J. P. and Pott, R. W. M. (2021) 'Heat-acclimatised strains of Rhodopseudomonas palustris reveal higher temperature optima with concomitantly enhanced biohydrogen production rates', *International Journal of Hydrogen Energy*, 46(21), pp. 11564–11572. doi: 10.1016/J.IJHYDENE.2021.01.068.

Tom DiChristoher (2021) *Experts explain why green hydrogen costs have fallen and will keep falling*, *S&P Global Market Intelligence*. Available at: https://www.spglobal.com/marketintelligence/en/news-insights/latest-news-headlines/experts-explain-why-green-hydrogen-costs-have-fallen-and-will-keep-falling-63037203 (Accessed: 1 February 2022).

Touati, K. *et al.* (2017) *Pressure Retarded Osmosis*. Edited by Khaled Touati et al. Available at: https://www.sciencedirect.com/book/9780128121030/pressure-retarded-osmosis (Accessed: 20 September 2021).

Vandanjon, L. *et al.* (1999) 'Effects of shear on two microalgae species. Contribution of pumps and valves in tangential flow filtration systems', *Biotechnology and Bioengineering*, 63(1), pp. 1–9. doi: 10.1002/(SICI)1097-0290(19990405)63:1<1::AID-BIT1>3.0.CO;2-K.

Vezirocjlu, T. N. and Barbir, F. (1992) *HYDROGEN: THE WONDER FUEL*, *Int. J. Hydrogen Energy*.

Vincenzini, M. *et al.* (1982) 'Hydrogen production by immobilized cells-I. light dependent dissimilation of organic substances by Rhodopseudomonas palustris', *International Journal of Hydrogen Energy*, 7(3), pp. 231–236. doi: 10.1016/0360-3199(82)90086-6.

Virtuani, A., Lotter, E. and Powalla, M. (2006) 'Influence of the light source on the low-irradiance performance of Cu(In,Ga)Se2 solar cells', *Solar Energy Materials and Solar Cells*, 90(14), pp. 2141–2149. doi: 10.1016/j.solmat.2005.01.022.

Wang, S. *et al.* (2017) 'Shear contributions to cell culture performance and product recovery in ATF and TFF perfusion systems', *Journal of Biotechnology*, 246, pp. 52–60. doi: 10.1016/J.JBIOTEC.2017.01.020.

Wang, S. and Zhong, J. (2007) 'Chapter 6 . Bioreactor Engineering', in *Science*. Elsevier B.V., pp. 131–161. doi: http://dx.doi.org/10.1016/B978-044452114-9/50007-4.

Wang, Y. Z. *et al.* (2010) 'Characteristics of hydrogen production and substrate consumption of Rhodopseudomonas palustris CQK 01 in an immobilized-cell photobioreactor', *Bioresource Technology*, 101(11), pp. 4034–4041. doi: 10.1016/j.biortech.2010.01.045.

Welander, P. V. *et al.* (2009) 'Hopanoids play a role in membrane integrity and pH homeostasis in Rhodopseudomonas palustris TIE-1', *Journal of Bacteriology*, 191(19), pp. 6145–6156. doi: 10.1128/JB.00460-09.

Westmacott, D. and Primrose, S. (1976) *Synchronous Growth of Rhodopseudomonas palustris from the*

Swarmer Phase, *Journal of General Microbiology*.

Whittenbury, R. and McLee, A. G. (1967) 'Rhodopseudomonas palustris and Rh. viridis-Photosynthetic budding bacteria', *Archiv für Mikrobiologie*, 59(1–3), pp. 324–334. doi: 10.1007/BF00406346.

Wu, S. C., Liou, S. Z. and Lee, C. M. (2012) 'Correlation between bio-hydrogen production and polyhydroxybutyrate (PHB) synthesis by Rhodopseudomonas palustris WP3-5', *Bioresource Technology*, 113, pp. 44–50. doi: 10.1016/J.BIORTECH.2012.01.090.

Wu, X. *et al.* (2010) 'A comparison of hydrogen production among three photosynthetic bacterial strains', in *International Journal of Hydrogen Energy*. Pergamon, pp. 7194–7199. doi: 10.1016/j.ijhydene.2009.12.141.

Xiao, N. (2017) *Use of a Purple Non-Sulphur Bacterium, Rhodopseudomonas palustris, as a Biocatalyst for Hydrogen Production*. University of Cambridge. doi: https://doi.org/10.17863/CAM.16680.

Xu, Z. (2007) 'Bioprocessing for Value-Added Products from Renewable Resources', *Bioprocessing for Value-Added Products from Renewable Resources*, pp. 527–557. doi: 10.1016/B978-044452114-9/50022-0.

Zhang, K., Kurano, N. and Miyachi, S. (1999) 'Outdoor culture of a cyanobacterium with a vertical flat-plate photobioreactor: effects on productivity of the reactor orientation, distance setting between the plates, and culture temperature', *Applied Microbiology and Biotechnology*, 52, pp. 781–786. doi: https://doi.org/10.1007/s002530051591.

APPENDIX A – ANALYTICAL TECHNIQUES

In this section, a short summary will be given on the different analytical techniques used for sample analysis in this investigation; in addition to this, a brief discussion of the operation of the equipment used to perform the analysis will also be given.

High-performance liquid chromatography (HPLC)

HPLC is a process used to separate, quantify, and identify different components in a mixture. This is achieved by passing a liquid sample in combination with a pressurized liquid solvent through a column. This column is filled with a solid adsorbent material; each different component in the initial sample will react differently to the material in the column due to their different chemical nature resulting in the components travelling at a different velocity through the column. As they flow from the column each different component therefore has a different residence time. The final detector converts the quantity of each component into an electrical signal and the final output is graph indicating a spike with regards to different residence times and the quantity of each component that was present in the sample can be observed.

A standard curve must be constructed using glycerol samples of a known concentration; this is then used to find a correlation that relates glycerol concentration to an area under the curve. A simplified diagram of the HPLC process can be seen in the figure (Figure 83) below.

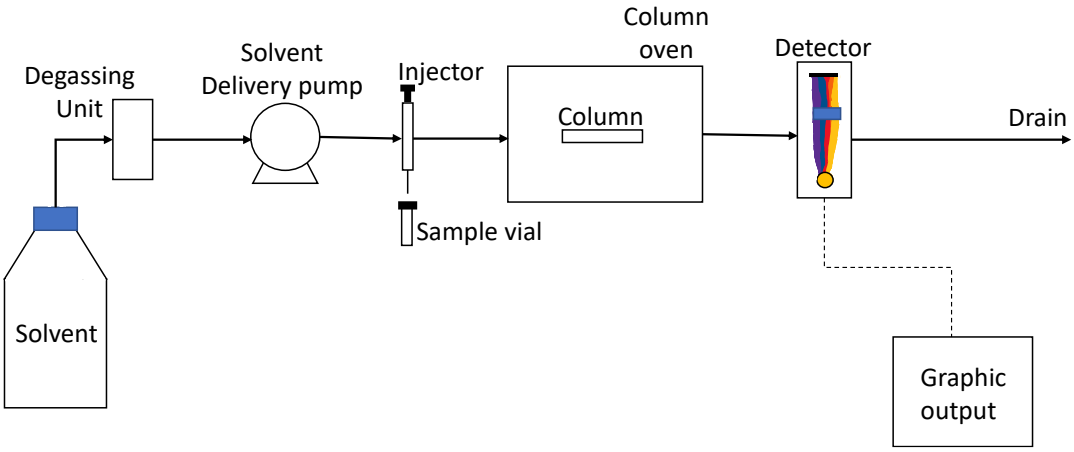

Figure 83: Simplification of an HPLC column (Figure adapted from Shimadzu Corporation (n.d.))

Scanning electron microscope (SEM)

SEM is a microscopic instrument that obtains images of a specimen by scanning with a focused beam of electrons; through this technology it is possible to achieve a significantly higher resolution in comparison to what can be achieved using light microscopy. As the electrons interact with the atoms in the sample, various signals are produced that give information regarding the composition and surface topography of the sample; namely the position of the beam and intensity of the signal which are used to produce the final image (Paredes, 2014).

Flow cytometry (FCM)

Flow cytometry (FCM)is a technique that can simply be defined as the rapid analysis of cells suspended in a stream of fluid. During cell preparation cells are cells are dyed with fluorescent stains that reveal, in this case, the integrity of each individual cell. During cytometry the principles of light scattering, light excitation and emission of fluorescent molecules are used to generate multiparameter data for all cells and particles present (Bergquist *et al.*, 2009).

Previously, FCM was limited to use in medical applications for the analysis of blood samples, however, due to recent developments and an increase in available fluorescent dyes, FCM can now be used in multiple different environmental samples.

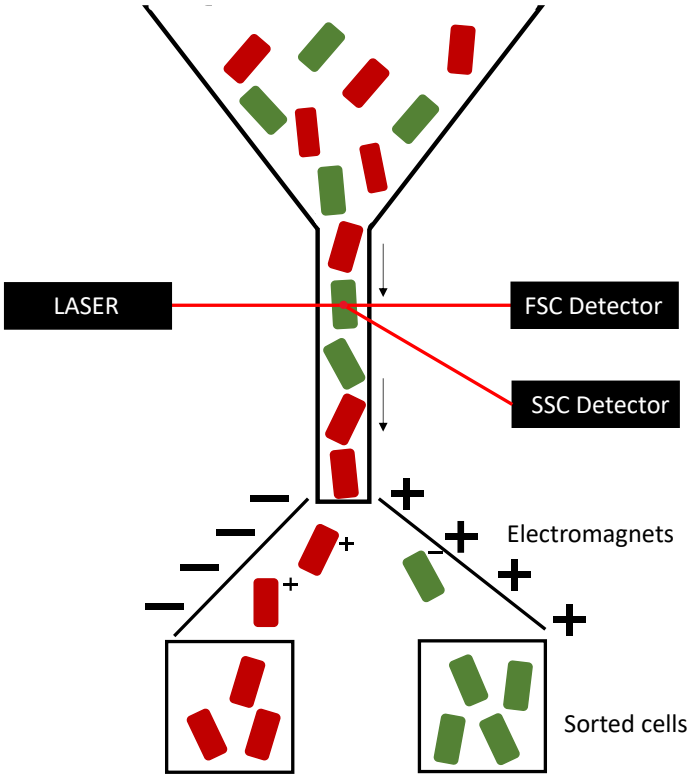

Figure 84: Figure representing the process of sorting dyed cells during flow cytometry (Figure adapted from Bio-Rad (n.d))

APPENDIX B - SPECIFICATIONS OF DESIGN CHOICES

Table 40: Specifications of diaphragm valve, manually operated, stainless steel handwheel electropolished

Nominal diameter	6mm
Body configuration	2/2-way body
Diaphragm size	8mm
Diaphragm material	EPDM[11]
Connection type	Spigot EN 10357 series A / DIN 11866 series A Butt weld spigots 8x1 1.4435, investment casting
Manufacturer	Gemü Valves

Figure 85: Diaphragm valve from Gemü valves

Table 41: Specifications for main piping network tubing

Material	Industrial grade Norprene
Formulation	Tygon A-60-G

[11] Ethylene Propylene Diaphragm

Temperature range (°C)	-60 to 135
Bore size	8mm
Manufacturer	Tygon by Saint-Gobain

Table 42: Specifications for hydrogen gas collection tubing

Formulation	Tygon S3 B-44-3
Temperature range (°C)	-36 to 74
Bore size	3.2mm
Manufacturer	Tygon by Saint-Gobain

Table 43: Specifications for continuous feed dosing line tubing

Material	Norprene
Formulation	A-60-F 06402
Temperature range (°C)	-51 to 135
Manufacturer	CRpump

Table 44: Specification for main piping network pump

Pump type	Peristaltic
Flow range (mL/min)	0-1700
Speed range (rpm)	0-400
Model	SR400-YZ1515X/YZ2515X/SN15/SN25
Manufacturer	Runze Fluid

Figure 86: Main line peristaltic pump from Runze Fluid

Table 45: Specifications for dosing pump

Pump type	Peristaltic
Flow range (mL/min)	0.0015-17.8
Speed range (rpm)	0-100
Model	BT100MH/DG-N(6)
Manufacturer	CRpump

Figure 87: Dosing pump from CRpumps

Table 46: Specifications of the single-channel membrane

Material	Al_2O_3/TiO_2
Selectivity (kD)	100
Active surface (cm^2)	50
Length (mm)	250
Type	Mono channel 10/6
Manufacturer	Atech (supplied by memcon)

Figure 88: Mono channel ceramic membrane

Figure 89: Stainless steel membrane casing

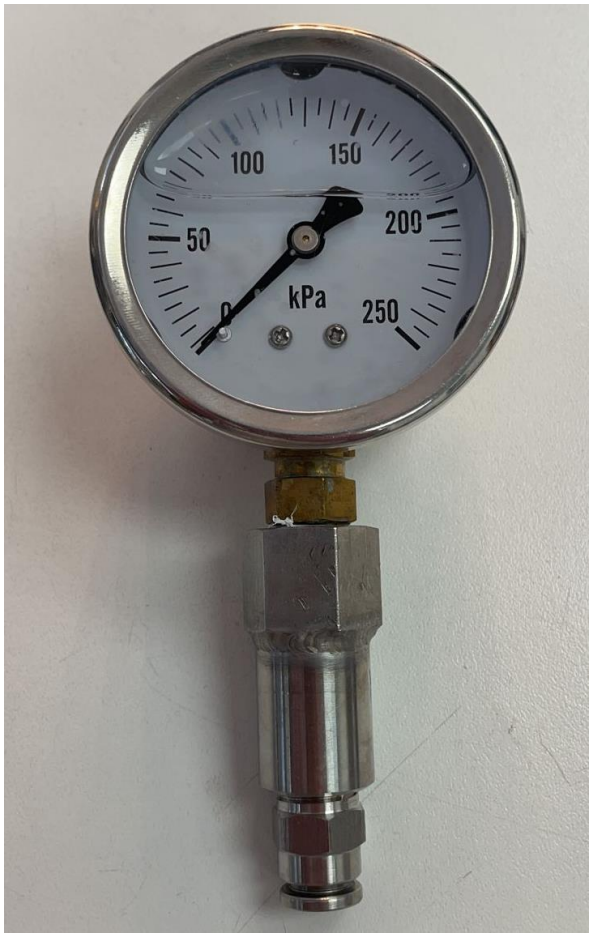

Figure 90: Pressure gauge

APPENDIX C – SEM CONTROL IMAGES

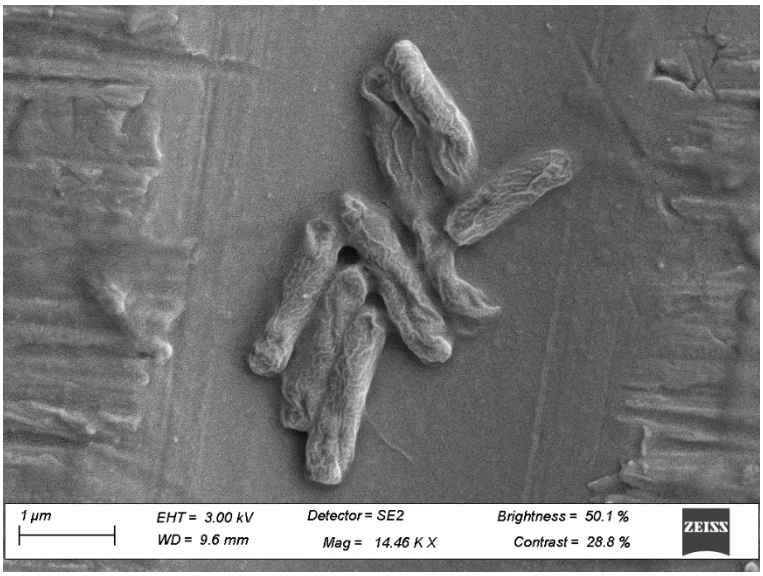

Figure 91: SEM image of an *R. palustris* cell cultured at 35°C. Used as an example of a 'healthy' cell.

APPENDIX D – STEM IMAGES

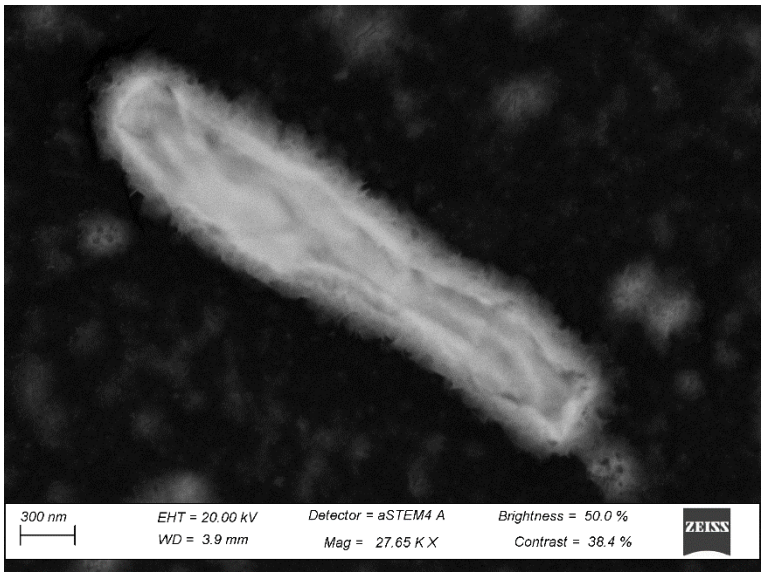

Figure 92: STEM image of an *R. palustris* cell for the investigation on the effect of a temperature of 40^{o}C imposed on the cells for 30minutes

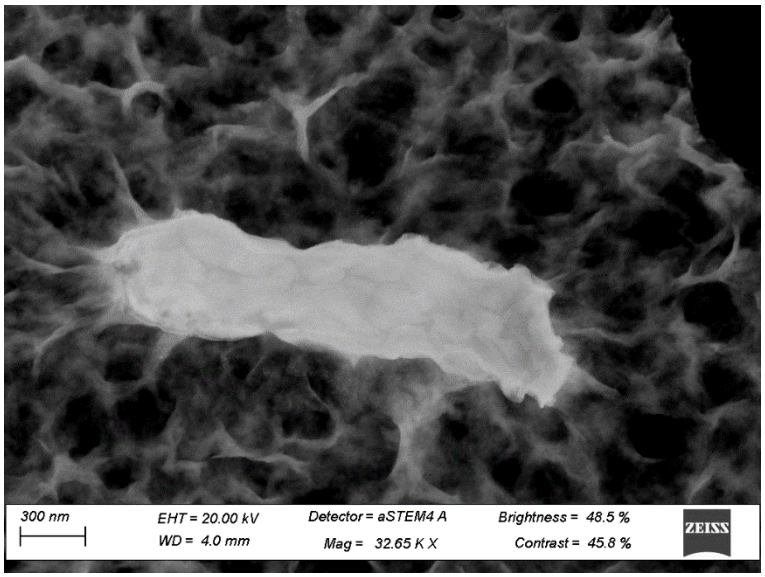

Figure 93: STEM image of an *R. palustris* cell for the investigation on the effect of a temperature of 45^{o}C imposed on the cells for 30minutes

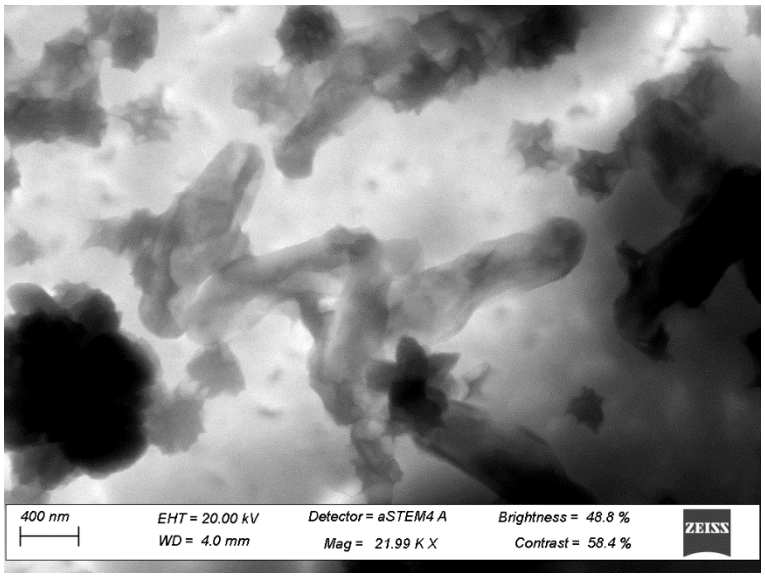

Figure 94: STEM image of an *R. palustris* cell for the investigation on the effect of a temperature of 50°C imposed on the cells for 30minutes

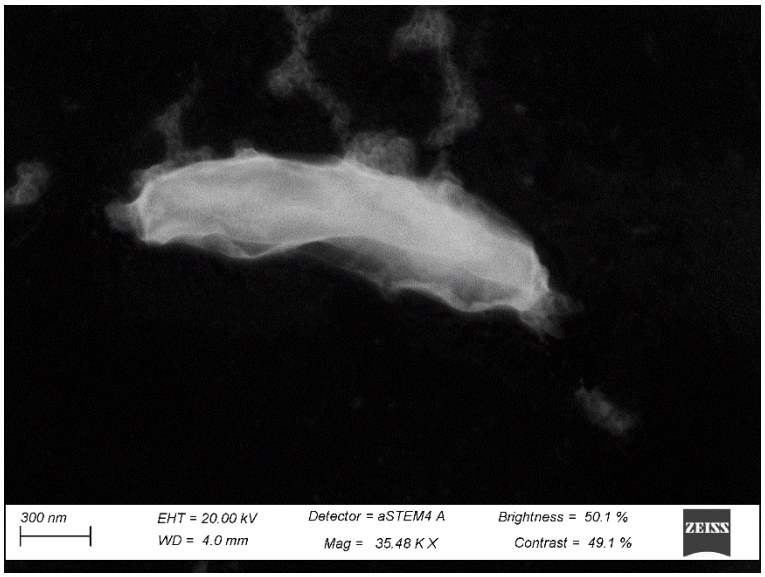

Figure 95 : STEM image of an *R. palustris* cell for the investigation on the effect of an elevated pressure (82.3kPa) imposed on the cells

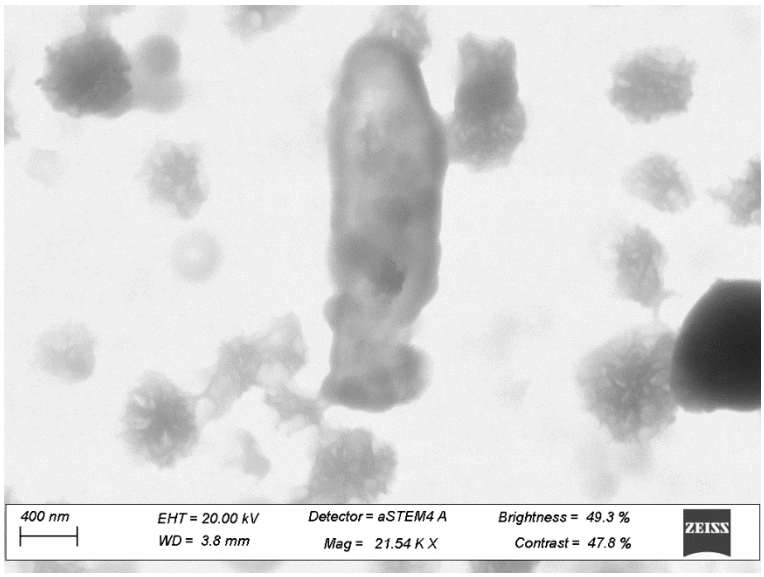

Figure 96: STEM image of an *R. palustris* cell for the investigation on the effect of high shear imposed on the cells for 5 minutes

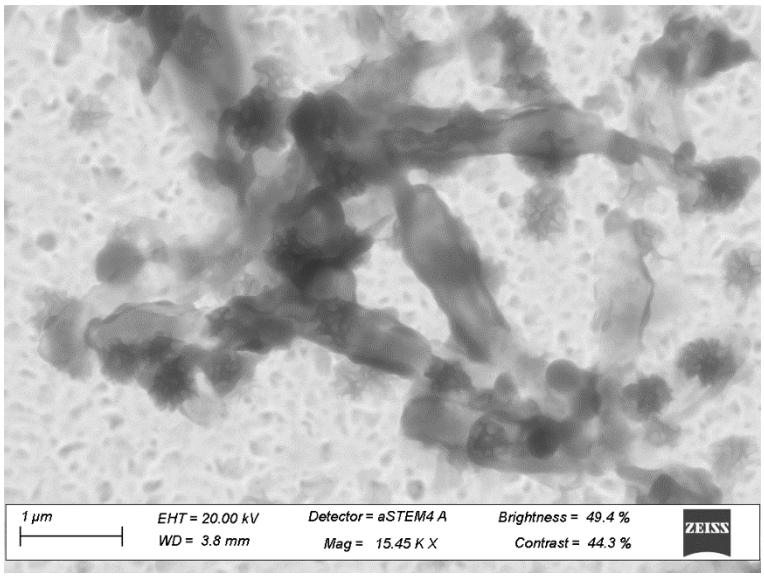

Figure 97: STEM image of an *R. palustris* cell for the investigation on the effect of high shear imposed on the cells for 10 minutes

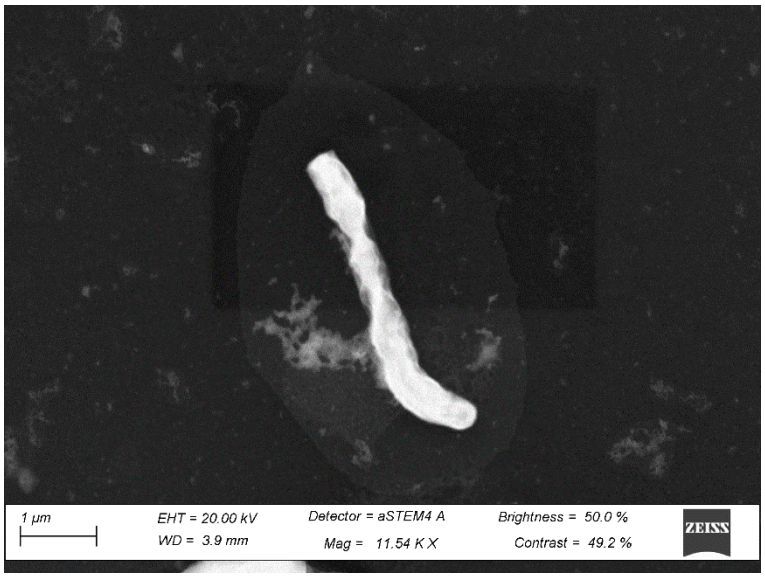

Figure 98: STEM image of an *R. palustris* cell for the investigation on the effect of high shear imposed on the cells for 15 minutes

APPENDIX E – CRITICAL FLUX

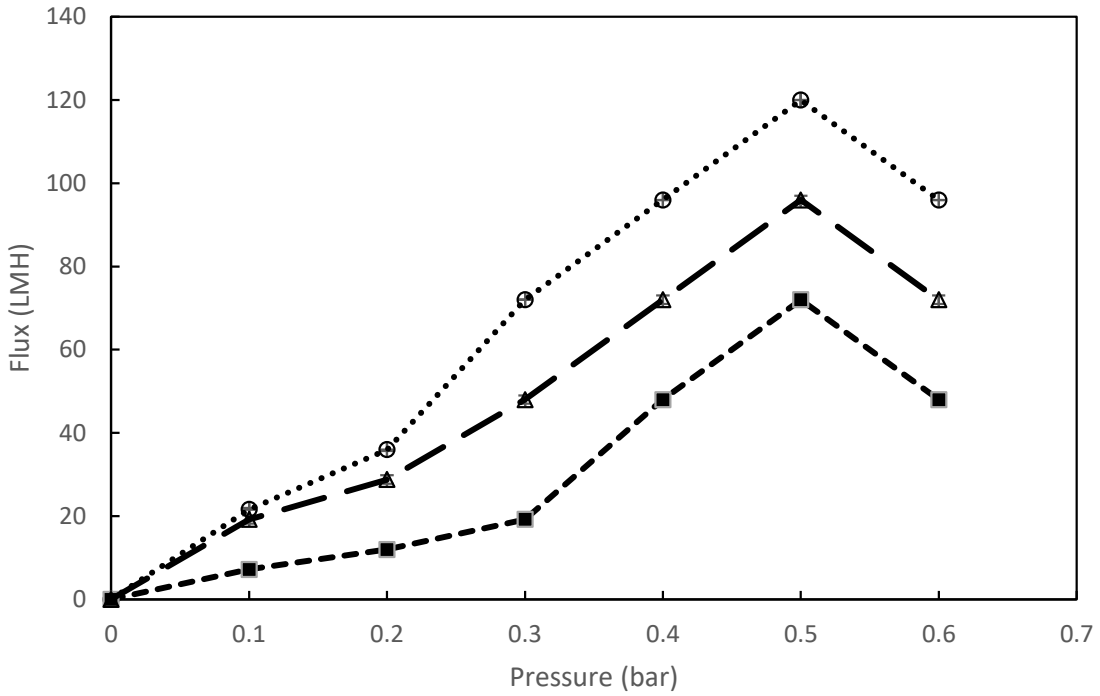

Figure 99: Flux as a function of backpressure over the membrane for three different cross flow velocities. For a culture containing ~3.5g/L of *R. palustris* in minimal medium. 0.113LMH (·· O ··), 0.18LMH (--Δ--) and 0.216LMH (- -■- -). Error is presented by means of standard error bars of triplicate runs.

APPENDIX F – CONTINUOUS MODE OPERATION

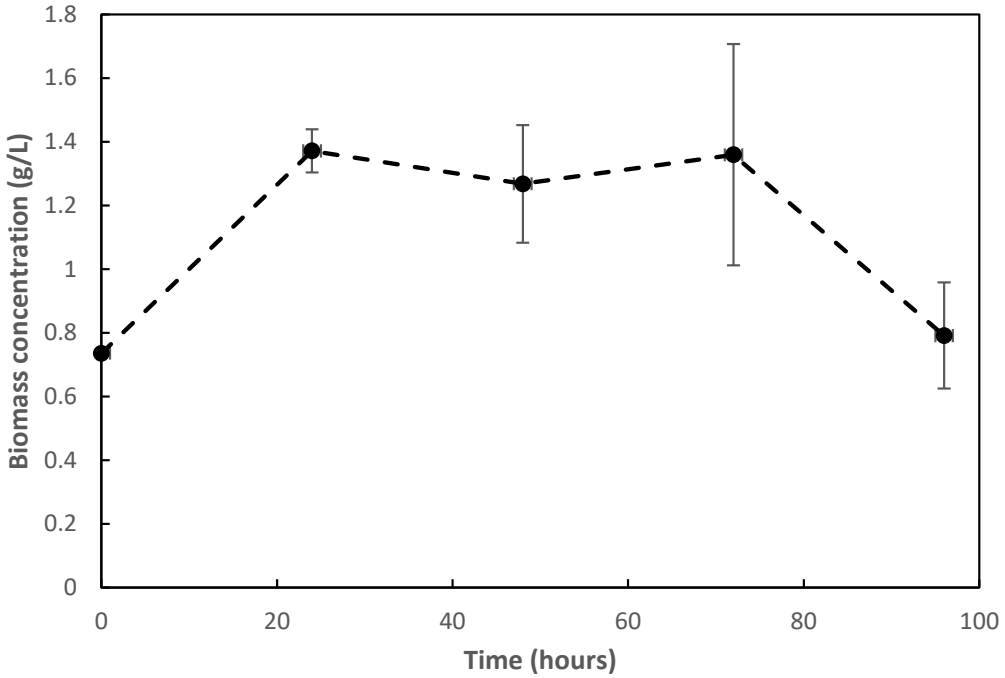

Figure 100: Growth of *R. palustris* in a continuous mode membrane photobioreactor for a period of 96 hours. Error is presented by means of standard error bars of triplicate runs.